2011-04-20

Extension Operators and Finite Elements for Fractal Boundary Value Problems

Emily Jennings Evans
Worcester Polytechnic Institute

Extension Operators and Finite Elements for Fractal Boundary Value Problems

by

Emily J. Evans

A Thesis

Submitted to the Faculty

of

WORCESTER POLYTECHNIC INSTITUTE

In partial fulfillment of the requirements for the

Degree of Doctor of Philosophy

in

Mathematical Sciences

by

April 13, 2011

APPROVED:

Umberto Mosco, Dissertation Advisor WPI Department of Mathematical Sciences	Gilbert Strang Massachusetts Institute of Technology
Maria Rosaria Lancia Università di Roma Sapienza	Bogdan Vernescu WPI Department of Mathematical Sciences
Marcus Sarkis WPI Department of Mathematical Sciences	Maria Agostina Vivaldi Università di Roma Sapienza

To David and Eleanor, with love and gratitude.

Acknowledgements

Although a single name appears as the author of the dissertation, no dissertation could be written without the help and support of others. First and foremost I wish to acknowledge the help of my advisor Umberto Mosco. Through my six years at WPI, he has generously imparted of his expertise while simultaneously guiding me through a dissertation that both interested me and suited my strengths. Without his continued confidence and his patience, I doubt that I could have made it through the process.

I extend my appreciation to my dissertation committee: Professor Mosco, Professor Lancia, Professor Sarkis, Professor Strang, Professor Vernescu, and Professor Vivaldi for taking the time to read this document. I am grateful for the opportunity that I had to collaborate in Rome with Maria Rosaria Lancia, Maria Agostina Vivaldi and Massimo Cefalo. While in Rome they shared their expertise and wisdom with me, and continued to do so after I left. I am thankful for Professor Lancia and Vivaldi's helpful corrections and feedback on much of what appears in Chapters 2-3 and 6 of the dissertation.

I would like to thank the faculty, staff and students at WPI for their help and support during my tenure in the PhD program. I appreciate the friendship of all of the graduate students but especially Rebecca Wasyk and Haodong Liang, my academic siblings, who have so graciously shared portions of their work with me. A thank you also goes out to Ellen Mackin, Rhonda Podell, Debbie Riel and Mike Malone for their help.

Finally I would like to thank my family for their unwavering support through the process. First and foremost, I wish to thank my husband for his love and support over the past six years. He has given so much in order for me to finish this, including quitting his job and taking up mathematics. I also wish to thank my daughter who has seen far too many fractals and finite element meshes for a two year old. I dedicate my work to the two of them with love and gratitude for their sacrifice. I also thank my parents who have always believed that I would get a PhD, and who have sacrificed many things in order for me to get here. Thank you also, to my extended family and network of friends who have continually supported both me and my immediate family throughout this process.

Contents

Chapter 0

Introduction

Our research has focused on both the analytical and computational aspects of domains with prefractal and fractal boundaries. Motivation for this research comes from the intriguing problem of a large surface area or interface versus a comparatively small volume. These types of problems are found in a wide variety of disciplines including engineering, biology, chemistry and physics. One example of such a problem is the catalytic converter where it is desirable to have a large surface area compressed into a small volume so that the maximal amount of toxins may be removed while still maintaining a small enough volume so that the design of a car remains unaffected. A more theoretical example is the problem of a highly conductive material intruding into a material with lower conductivity. The focus of our research are these large surface problems with the additional constraint that the large surfaces have a fractal nature. This allows for additional scaling features and symmetries to be added to the problem while maintaining the characteristics of small volume large surface area problems.

Our research at WPI lies on the border between the analytical and the numerical side of these large surface small volume problems. The first problem considered in the dissertation is the problem of extending a function defined on a fractal set to a larger set. The origin of the idea of analytically extending a function defined on a smaller set to a larger set goes back to the work of Whitney [32], [33], [34] in 1934. Since the publication of Whitney's work, the problem of extending a function to a larger domain has been examined by multiple authors. Of relevance to this dissertation are the work of Jonsson and Wallin [17],[18], [19] who have addressed the question of extending functions defined on special d-sets (of which the fractal Koch curve and Sierpinski gasket are two examples) to larger domains. Their extension results rely on the use of certain trace and

Besov space properties and are abstract. For both the Koch curve and the Sierpinski gasket, we seek to find an extension function from the fractal set constructively so that the use of d-sets can be avoided. The advantage of this new construction will be two fold. First, the functions will be constructed in such a way to facilitate future numerical work. Second, the newly constructed extension functions will allow for simplification of the current theory of certain transmission and boundary value problems. The ideas behind this extension will be presented in Chapters 2-3. At the conclusion of Chapter 3 we will consider an application of our fractal extension operator to a transmission problem with a fractal boundary. This problem was first considered by Lancia and Vivaldi in [21] where they studied the asymptotic behavior of the problem as the prefractal iteration number increased toward infinity. The application of our fractal extension operator will allow their work to be simplified by removing the dependence on d-sets.

The second part of our research, outlined in Part II is the study of transmission and boundary value problems with fractal boundaries. In Chapter 4 we consider the problem of highly conductive thin fibers arranged in such a way to be a Sierpinski type prefractal of a fixed iteration n. We study the asymptotic behavior of the problem as we increase the conductivity of the layer toward infinity while decreasing the thickness of the fiber toward zero. This problem is studied in the framework of homogenization and is joint work with Haodong Liang.

An additional research accomplishment, described in Chapter 6, was the development of a finite element mesh that exploits the self-similarity of the Koch curve for arbitrary rational values of α where $2 < \alpha \leq 4$. Here α is the contraction factor for the Koch curve and the standard Koch curve has value $\alpha = 3$. (Note that as $\alpha \to 2$ the Koch curve becomes space filling in a 2 dimensional domain and as $\alpha \to 4$ the curve approaches a segment.) We have termed this finite element mesh an adaptive mesh because it is adapted to both the fractal iterations and finite element triangulation and is especially suited to the numerical study of problems involving nested sequences of prefractals. Before considering the problem of mesh creation we will provide background information important to understanding the finite element method in Chapter 5. Then in Chapter 7 we will consider the mesh introduced in Chapter 6 with the idea of using it to numerically solve boundary value problems. Specifically we will consider refinements to the mesh that must be made due to the singularities inherent in domains with prefractal boundaries. We will conclude this chapter by using this mesh (with suitable refinements) to solve a transmission type problem.

The dissertation is organized in the following two main parts. *Part I* considers fractal extension operators. In this part we will first consider extending functions which are Hölder continuous on a fractal set to a larger, open domain Ω. We will detail a constructive methodology to perform this extension and show that the extension function is also Hölder continuous. We then consider functions in the domain of the energy form of the fractal and show, using the same methodology in Chapter 2, that the extension function is H^1 on the larger domain. In *Part II*, we will consider transmission and boundary value problems in domains with fractal boundaries. Here we will consider the Sierpinski prefractal and how we might apply the technique of singular homogenization to thin layers constructed on the prefractal. We will also discuss numerical approximation in domains with fractal boundaries, introduce a finite element mesh developed for studying problems in domains with prefractal Koch boundaries, and present sample numerical results for the transmission problem. We also provide an appendix which includes a list of notation.

Chapter 1

Fractal Sets

In this chapter we will introduce two self-similar fractals which belong to a larger class of self-similar fractals studied by Hutchinson in [16]. In this dissertation we restrict ourselves to the study of the von Koch curve (hereafter simply referred to as the Koch curve) and the Sierpinski gasket. For each of these two fractal sets we will introduce notation related to the set and define the set itself. Moreover we will also introduce the energy form of the fractal and define the domain of the energy form.

1.1 The Koch Curve

We define the Koch Curve in the following manner:

Let $\alpha \in (2,4)$ and define $\theta = \cos^{-1}\left(\frac{\alpha}{2} - 1\right)$. We consider the 4 contractive similitudes $\{\psi_1, \psi_2, \psi_3, \psi_4\}$ in $\mathbb{R}^2$:

$$\begin{array}{ll} \psi_1(z) = \frac{z}{\alpha} & \psi_2(z) = \frac{z}{\alpha}e^{i\theta} + \frac{1}{\alpha} \\ \psi_3(z) = \frac{z}{\alpha}e^{-i\theta} + \frac{1}{2} + \frac{i\sin\theta}{\alpha} & \psi_4(z) = \frac{z+\alpha-1}{\alpha} \end{array} \tag{1.1}$$

where $z \in \mathbb{C}$.

For each integer $n > 0$, we will consider arbitrary n-tuples of indices $i|n = (i_1, i_2, \ldots, i_n) \in \{1,2,3,4\}^n$. We then define $\psi_{i|n} = \psi_{i_1} \circ \psi_{i_2} \circ \cdots \circ \psi_{i_n}$ and for any set $\mathcal{G}\,(\subseteq \mathbb{R}^2)$, $\mathcal{G}_{i|n} = \psi_{i|n}(\mathcal{G})$.

Let $V_0 = \{A, B\}$. For every integer $n > 0$, let

$$V^n = \bigcup_{i|n} V_0^{i|n}$$

where $V_0^{i|n} = (V_0)^{i|n}$ in the preceding notation. We put

$$V^\infty = \bigcup_{n=0}^{+\infty} V^n$$

and

$$S = \overline{V}^\infty,$$

the closure being in $\mathbb{R}^2$. The set S is the *Koch curve* in $\mathbb{R}^2$ and has Hausdorff dimension of $\ln 4/\ln \alpha > 1$. We note that $V^n \subset V^\infty \subset S$ and that as n increases the number of points in V^n also increases. We will denote by S^n the prefractal (polygonal) curve of iteration number n created by connecting the points in the set V^n in a prescribed manner. We note that since the dimension of the fractal curve is greater then one, this means that the length of the prefractal curve S^n increases to ∞ as $n \to \infty$.

Remark 1. We note that the prefractal polygonal curves of different iteration number are not nested. That is to say $S^{n-1} \subsetneq S^n \subsetneq S$. For this reason we work with the set of vertices V^n correspondent to each prefractal curve S^n.

Here we make an important distinction. In this dissertation we will refer to the iteration of a prefractal. By this we mean we fix a value of α and iterate n creating a sequence of prefractal curves. See Figure 1.1. Later in the dissertation we will also refer to a family of curves. Here we will consider different values of α and study how the curve changes as α is changed. See Figure 1.2 for a visualization of how the shape of the curve varies with α.

On the Koch curve S, there exists an invariant measure μ that is a positive, regular Borel measure and satisfies the identity

$$\int_S \phi d\mu = \sum_{i=1}^{4} \int_S (\phi \circ \psi_i) d\mu \quad \text{for every } \phi \in C_0(S).$$

After normalization, the measure μ coincides with the restriction to S of the d-dimensional

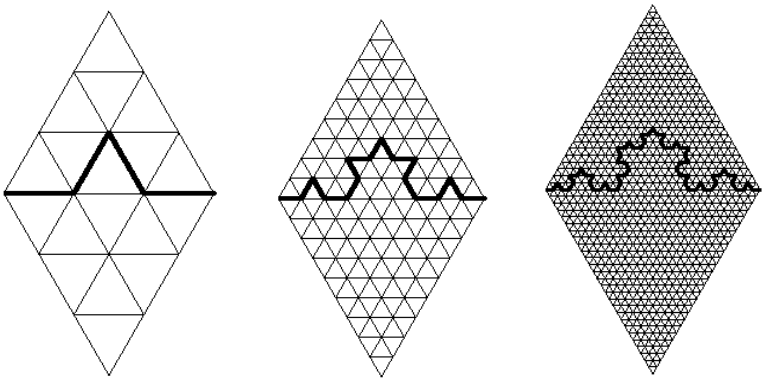

(a) $n = 1$ (b) $n = 2$ (c) $n = 3$

Figure 1.1: Multiple iterations of the fractal curve with $\alpha = 3$

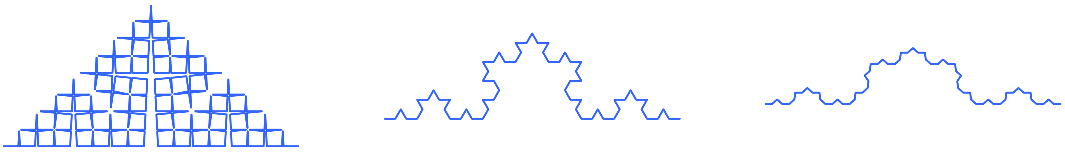

(a) $\alpha = 2.05$, $n = 4$ (b) $\alpha = 3$, $n = 3$ (c) $\alpha = 3.5$, $n = 3$

Figure 1.2: Koch curve for different α

(recall $d = \ln 4 / \ln \alpha$) Hausdorff measure $\mathcal{H}^d$ of $\mathbb{R}^2$:

$$\mu = (\mathcal{H}^d(S))^{-1} \mathcal{H}^d|_S.$$

Energy Form of the Koch Curve

To construct the energy form on the Koch curve we use a finite difference scheme. If the end points of the Koch curve are labeled A and B the energy form is defined as:

$$E^n(u,u) = \rho^n \sum_{i_1 \ldots i_n = 1}^{4} (u(\psi_{i_1 \ldots i_n}(A)) - u(\psi_{i_1 \ldots i_n}(B)))^2, \tag{1.2}$$

where ρ is a renormalization factor and is equal to 4. We know that $E^n(\cdot,\cdot)$ is an increasing sequence and the limit

$$E[u] = E(u,u) = \lim_{n\to\infty} E^n(u,u) < +\infty.$$

We also know that the form $E[u]$ is a closed Dirichlet form in the Hilbert Space $L^2(S,\mu)$ where S is the Koch curve, μ is an invariant measure and the form has dense domain in $L^2(S,\mu)$

$$D_E = \{u \in L^2(S,\mu) : E[u] < +\infty\}.$$

Moreover, we have the following proposition:

Proposition 1.1.1. *The space D_E is continuously embedded in $C^\beta(S)$, the space of Hölder continuous functions with exponent $\beta = d/2$. From this embedding we have the following estimate*

$$|u(X) - u(Y)| \le C\sqrt{E[u]}|X-Y|^\beta \qquad \text{for all } X, Y \in S. \tag{1.3}$$

This result is similar to that given by Kozlov for the Sierpinski Gasket in [20]. We will us the following two properties of the Koch curve

1. There exists a γ where $0 < \gamma \le 1$ and such that $S_{i|m} \cap S_{j|m} = \emptyset$ implies $dist(S_{i|m}, S_{j|m}) \ge \gamma\alpha^{-m}$ for every m.
2. If $i \mid m \ne j \mid m$, then $S_{i|m} \cap S_{j|m} = \Gamma_{i|m} \cap \Gamma_{j|m}$.

Moreover, by $S_{i|m}$ we will denote one of the segments of the polygonal prefractal Koch curve S^m.

Proof. (Proposition 1.1.1)

Let $p, q \in V^\infty \subset S$. Since $V^\infty = \bigcup_{n=0}^{+\infty} V^n$, $p \in S_{i|m}$ and $q \in S_{j|m}$, for some $S_{i|m}$, $S_{j|m} \in S^m$.

Assume $|p-q| < \gamma \le 1$. Then there exists a unique $m \ge 0$ such that

$$\gamma\alpha^{-(m+1)} \le |p-q| < \gamma\alpha^{-m}. \tag{1.4}$$

Therefore, $dist(S_{i|m}, S_{j|m}) \le |p-q| < \gamma\alpha^{-m}$, which implies $S_{i|m} \cap S_{j|m} \ne \emptyset$ by Property 1. Thus, by applying Property 2, $\Gamma_{i|m} \cap \Gamma_{j|m} \ne \emptyset$. This implies there exists

$a \in \Gamma_{i|\,m} \cap \Gamma_{j|\,m}$ such that

$$a = \psi_{i|\,m}(\xi) = \psi_{j|\,m}(\eta)$$

where $\xi, \eta \in \Gamma$

We now consider the case $n \geq m$. There exists a smallest $n \geq m$ such that both $p, q \in V^n$, and hence $p = \psi_{i|\,n}\left(\overline{\xi}\right)$ and $q = \psi_{j|\,n}(\overline{\eta})$, where $\overline{\xi}, \overline{\eta} \in \Gamma$

We now construct a chain of points connecting p to q from "both sides." We start with

$$p = \psi_{i|\,n}\left(\overline{\xi}\right) = \psi_{i_1 \ldots i_m i_{m+1} \ldots i_n}\left(\overline{\xi}\right) =: x_n.$$

Moreover, we let

$$\begin{aligned} x_{n-1} &:= \psi_{i_1 \ldots i_m i_{m+1} \ldots i_{n-1}}\left(\overline{\xi}\right) = \psi_{i|\,n-1}\left(\overline{\xi}\right) \\ x_{n-k} &: = \psi_{i|\,n-k}\left(\overline{\xi}\right) \end{aligned}$$

where $0 \leq k \leq n - m$. We now have a chain of points $x_n, x_{n-1}, \ldots, x_m$, and insert the point a by defining it as $x_{m-1} = a := \psi_{i|\,m}(\xi)$.

We preform a similar procedure for q starting with $y_n = q$. Let $y_{n-k} = \psi_{j|\,n-k}(\overline{\eta})$ where $0 \leq k \leq n - m$ and $y_{m-1} = a = \psi_{j|\,m}(\eta)$

We have now constructed the chain

$$p = x_n, x_{n-1}, \ldots, x_m, x_{m-1} = a = y_{m-1}, y_m, \ldots, y_n = q$$

with the property that any two consecutive points in the chain belong to the same cell.

We check the case when $k = 0$. We let $\overline{\xi}$ be a fixed point of ψ_{i_0}, so $x_{n-1} = \psi_{i_1 \ldots i_{n-1} i_0}\left(\overline{\xi}\right)$. We now have the following two cases:

1. if $i_n = i_0$, then $x_n = x_{n-1}$;
2. if $i_n \neq i_0$, then $\psi_{i_n}\left(\overline{\xi}\right) = \psi_{i_0}\left(\overline{\overline{\xi}}\right)$ for some $\overline{\overline{\xi}} \in \Gamma$.

This means $x_n = \psi_{i_i \ldots i_n}\left(\overline{\xi}\right) = \psi_{i_i \ldots i_{n-1} i_0}\left(\overline{\overline{\xi}}\right)$ which implies $x_n, x_{n-1} \in \Gamma_{i_i \ldots i_{n-1} i_0}$.

We now wish to estimate $|u(p) - u(q)|$. By our chain construction, we have

$$|u(p) - u(q)| \leq \sum_{k=0}^{n-m} \left[|u(x_{n-k}) - u(x_{n-k-1})| + |u(y_{n-k}) - u(y_{n-k-1})| \right].$$

Moreover, since $\overline{\xi} = \psi_{i_0}(\overline{\xi})$ and $\psi_{i_{n-k}}(\overline{\xi}) = \psi_{i_0}(\overline{\overline{\xi}})$, we have

$$\begin{aligned}
|u(x_{n-k}) - u(x_{n-k-1})|^2 &= \left| u\left(\psi_{i|\,n-k-1}\psi_{i_{n-k}}\left(\overline{\xi}\right)\right) - u\left(\psi_{i|\,n-k-1}\psi_{i_0}\left(\overline{\xi}\right)\right)\right|^2 \\
&= \left| u\left(\psi_{i|\,n-k-1}\psi_{i_0}\left(\overline{\overline{\xi}}\right)\right) - u\left(\psi_{i|\,n-k-1}\psi_{i_0}\left(\overline{\xi}\right)\right)\right|^2 \\
&\leq \sum_{i|\,n-k} \left| u\left(\psi_{i|\,n-k}\left(\overline{\overline{\xi}}\right)\right) - u\left(\psi_{i|\,n-k}\left(\overline{\xi}\right)\right)\right|^2 \\
&\leq \sum_{i|n-k} \left\{ \frac{1}{2} \sum_{\xi',\eta'} \left| u\left(\psi_{l|\,n-k}(\xi')\right) - u\left(\psi_{l|\,n-k}(\eta')\right)\right|^2 \right\}.
\end{aligned}$$

We then multiply both sides by ρ^{n-k} to obtain:

$$\rho^{n-k} |u(x_{n-k}) - u(x_{n-k-1})|^2 \leq \rho^{n-k} \sum_{i|n-k} \left\{ \frac{1}{2} \sum_{\xi',\eta'} \left| u\left(\psi_{i|\,n-k}(\xi')\right) - u\left(\psi_{i|\,n-k}(\eta')\right)\right|^2 \right\} = E^{n-k}(u,u).$$

Taking the square root and simplifying we obtain:

$$|u(x_{n-k}) - u(x_{n-k-1})| \leq \rho^{\frac{k-n}{2}} \sqrt{E^{n-k}(u,u)}$$

Clearly, the same holds for terms with y. Thusly:

$$\begin{aligned}
|u(p) - u(q)| &\leq 2 \sum_{k=0}^{n-m} \rho^{\frac{k-n}{2}} \sqrt{E^{n-k}(u,u)} \\
&= 2\rho^{-n/2} \sqrt{E^n(u,u)} \sum_{k=0}^{n-m} \rho^{k/2} \\
&= 2\sqrt{E^n(u,u)} \rho^{-n/2} \frac{\rho^{(n-m+1)/2} - 1}{\rho^{1/2} - 1} \\
&\leq \frac{2}{\rho^{1/2} - 1} \sqrt{E^n(u,u)} \rho^{(1-m)/2}.
\end{aligned}$$

(Since $\rho > 1$ implies $\sum_{k=0}^{n-m} \rho^{k/2} = \frac{\rho^{(n-m+1)/2}-1}{\rho^{1/2}-1}$). Now $\rho^{1-m} = \alpha^{(\log_\alpha \rho)(1-m)}$. We set $\beta = \frac{\ln \rho}{2 \ln \alpha}$, therefore

$$\rho^{1-m} = \alpha^{-(m-1)2\beta}$$

We recall the choice of m from Equation 1.4 which gives

$$\rho^{(-m+1)/2} = \alpha^{-\beta(m+1)} \leq \frac{|p-q|^\beta}{\gamma^\beta}.$$

Therefore,

$$|u(p) - u(q)| \leq \frac{2\rho}{\gamma^\beta}(\rho^{1/2} - 1)\sqrt{E[u]}|p-q|^\beta.$$

We set $C = \dfrac{2\rho}{\gamma^\beta(\rho^{1/2}-1)}$, and thus

$$|u(p) - u(q)| \leq C\sqrt{E[u]}|p-q|^\beta.$$

□

Remark 2. We note that since the space D_E is continuously embedded in $C^\beta(S)$, if $u \in D_E$, then $u \in C(S)$.

We provide one additional lemma

Lemma 1.1.2. *For $u \in D_E$, we have*

$$\sup_S |u| \leq C(\|u\|^2_{L^2(S,\mu)} + E[u])^{1/2} \tag{1.5}$$

Proof. Using the C^β estimate from Proposition 1.1.1 we deduce for all $X, Y \in S$:

$$\begin{aligned} |u(x)| &\leq |u(Y)| + |u(X) - u(Y)| \\ &\leq |u(Y)| + C\sqrt{E[u]}|X-Y|^\beta \\ &\leq |u(Y)| + C\sqrt{E[u]}(diam\ S)^\beta. \end{aligned}$$

Here we note that $diam\ S = 1$ and $\mu(S) = 1$. We then square both sides and integrate

in Y with respect to μ, thus

$$\begin{aligned}|u(X)|^2\mu(S) &\leq 2\int_S (|u(Y)|^2 + C(diam\ S)^{2\beta}E[u])d\mu \\ &\leq 2\int_S u^2 d\mu + 2C(diam\ S)^{2\beta}E[u]\mu(S) \\ &\leq C\left[\int_S u^2 d\mu + E[u]\right] \\ &= C(\|u\|^2_{L^2(S,\mu)} + E[u]).\end{aligned}$$

Therefore

$$\sup_S |u| \leq C(\|u\|^2_{L^2(S,\mu)} + E[u])^{1/2}.$$

□

1.2 The Sierpinski Gasket

We now consider the Sierpinski gasket defined on an equilateral triangle. For contraction factor $\alpha = 2$ we use the 3 contractive similarities defined as

$$\psi_1(z) = \frac{z}{2}, \quad \psi_2(z) = \frac{z}{2} + \frac{1}{2}, \quad \psi_3(z) = \frac{z}{2} + \frac{1}{4} + i\frac{\sqrt{3}}{4} \tag{1.6}$$

here $z \in \mathbb{C}$.

Remark 3. As in the Koch curve the value α refers to the contraction factor, however, for the Sierpinski curve α is restricted to integers greater or equal to 1. In this dissertation, however, we restrict ourselves to the special case of $\alpha = 2$.

For each integer $n > 0$, we will consider arbitrary n-tuples of indices $i|n = (i_1, i_2, \ldots, i_n) \in \{1, 2, 3\}^n$. We then define $\psi_{i|n} = \psi_{i_1} \circ \psi_{i_2} \circ \cdots \circ \psi_{i_n}$ and for any set $\mathcal{G}\,(\subseteq \mathbb{R}^2)$, $\mathcal{G}_{i|n} = \psi_{i|n}(\mathcal{G})$. We set $V_0 = \{A, B, C\}$ and for every integer $n > 0$, let

$$V^n = \bigcup_{i|n} V_0^{i|n}$$

where $V_0^{i|n} = (V_0)^{i|n}$ in the preceding notation. We put

$$V^{\infty} = \bigcup_{n=0}^{+\infty} V^n$$

and

$$S = \overline{V}^{\infty},$$

the closure being in $\mathbb{R}^2$. The set S is the *Sierpinski gasket* in $\mathbb{R}^2$ and has Hausdorff dimension of $\ln 3/\ln 2$ when $\alpha = 2$. We will denote by S^n the prefractal (polygonal) curve of iteration number n created by connecting the points in the set V^n is a prescribed manner.

Remark 4. We observe that the prefractal polygonal curves are nested (i.e. $S^{n-1} \subseteq S^n \subseteq S$). However we will work, as with the Koch curve, with the set of vertices V^n correspondent to each curve S^n.

Similar to the Koch curve we wish to distinguish between a sequence of Sierpinski gaskets (i.e. α fixed) and a family of Sierpinski gaskets (α varies). Figure 1.3 illustrates a sequence of Sierpinski gaskets for $\alpha = 2$ and Figure 1.4 shows a family of Sierpinski gaskets.

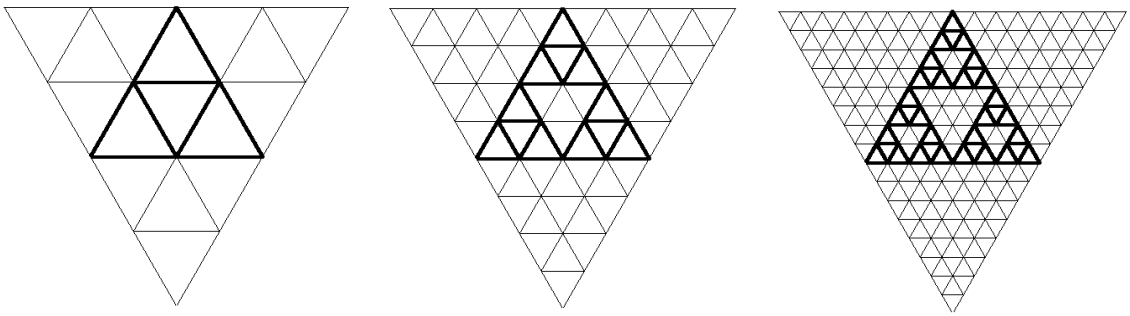

(a) $n = 1$ (b) $n = 2$ (c) $n = 3$

Figure 1.3: A sequence of Sierpinski gaskets for $\alpha = 2$.

On the Sierpinski gasket S, there exists an invariant measure μ that is a positive, regular Borel measure and satisfies the identity

$$\int_S \phi d\mu = \sum_{i=1}^{3} \int_S (\phi \circ \psi_i) d\mu \quad \text{for every } \phi \in C_0(S).$$

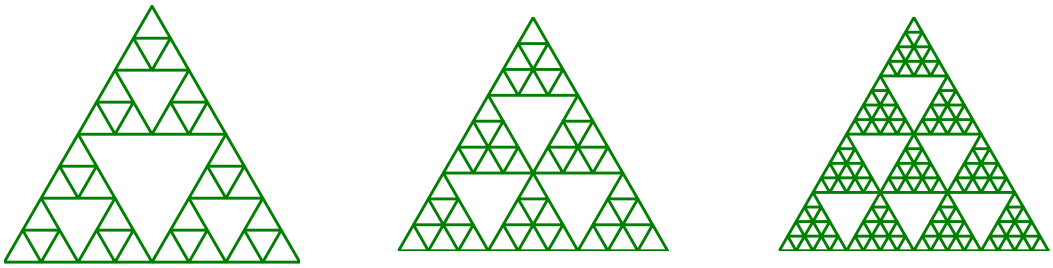

(a) $\alpha = 2$, $n = 3$ (b) $\alpha = 3$, $n = 2$ (c) $\alpha = 4$, $n = 2$

Figure 1.4: Sierpinski Gasket for different α

After normalization, the measure μ coincides with the restriction to S of the d-dimensional (recall $d = \ln 3/\ln 2$) Hausdorff measure $\mathcal{H}^d$ of $\mathbb{R}^2$:

$$\mu = (\mathcal{H}^d(S))^{-1}\mathcal{H}^d|_S.$$

Energy Form of the Sierpinski gasket

In a manner similar to the Koch curve we will construct the energy form on the Sierpinski gasket using a finite difference scheme. If the three vertices of our original triangle are labeled A, B and C the energy form is defined as:

$$\begin{aligned} E^n(u,u) = \rho^n \sum_{i_1\ldots i_n=1}^{3} &(u(\psi_{i_1\ldots i_n}(A)) - u(\psi_{i_1\ldots i_n}(B)))^2 + (u(\psi_{i_1\ldots i_n}(B)) - u(\psi_{i_1\ldots i_n}(C)))^2 \\ &+ (u(\psi_{i_1\ldots i_n}(C)) - u(\psi_{i_1\ldots i_n}(A)))^2, \end{aligned} \tag{1.7}$$

where ρ is a renormalization factor and is equal to 5/3. In the dissertation we will also use the format

$$E^n(u,u) = \rho^n \sum_{i_1\ldots i_n=1}^{3} \left(\sum_{\eta,\xi\in\{A,B,C\}} (u(\psi_{i_1\ldots i_n}(\eta)) - u(\psi_{i_1\ldots i_n}(\xi)))^2 \right) \tag{1.8}$$

We know that $E^n(\cdot,\cdot)$ is an increasing sequence and the limit

$$E[u] = E(u,u) = \lim_{n\to\infty} E^n(u,u) < +\infty.$$

We also know that the form $E[u]$ is a closed Dirichlet form in the Hilbert Space $L^2(S,\mu)$ where S is the Koch curve, μ is an invariant measure and the form has dense domain in $L^2(S,\mu)$

$$D_E = \{u \in L^2(S,\mu) : E[u] < +\infty\}.$$

Clearly Proposition 1.1.1 holds for the Sierpinski gasket with contraction factor $\alpha = 2$ and $\beta = \ln 3/\ln 4$. Moreover Lemma 1.1.2 and Remark 2, also hold for the Sierpinski gasket.

Part I

Fractal Extension Operators

Given a function f defined on a closed subset S of a larger set Ω we wish to extend f to the larger set such that certain characteristics of the original function f are retained. As mentioned in the introduction the origin of this work dates back to Whitney [32], [33], [34] in 1934. Since then, multiple authors have examined the problem of extending a function to a larger domain. Of special consideration to this dissertation is the work by Jonsson and Wallin who studied the problem of extending functions defined on d-sets (i.e. closed non-empty subsets of $\mathbb{R}^n$ with d-measure). Also related to this dissertation, is the work done by Brudnyi and Shvartsman [4], [5] who investigated the existence of general linear extension operators. Finally, most recently, Fefferman has also considered extension of C^m functions on arbitrary sets in Euclidean space, where $m \geq 1$, by linear extension operators [10], [11],[12],[13]. In these works Fefferman also considers the problem of interpolation of data by C^m functions. In the dissertation we consider the extension of a function defined on certain fractal sets (specifically the standard Koch curve or Sierpinski gasket) to a larger domain Ω. The reason why we confine our study to these sets is that they occur as boundaries or layers in the boundary value and transmission problems mentioned in the introduction. As the boundary of a Euclidean domain, these sets become quite interesting as they allow for more general boundaries to be considered than the usual Lipschitz or finite perimeter boundaries common to most of the existing literature.

Our objective is to construct an extension operator adapted to both the fractal iteration and finite element framework. More specifically, we wish our fractal extension operator to be obtained as a limit of a sequence of prefractal extension operators. We create this operator in the following manner:

1. Assume that the fractal set is constructed by iterations (as explained in Chapter 1 and shown in Figure 1.5).

2. For a fixed iteration n we have a triangulation of our domain induced by the prefractal.

3. We extend the function piecewise from the prefractal to the domain using the finite element mesh as scaffolding.

4. We then take the limit in n thus giving an extension operator that is adapted to both fractal iterations and future numerical work using finite element meshes.

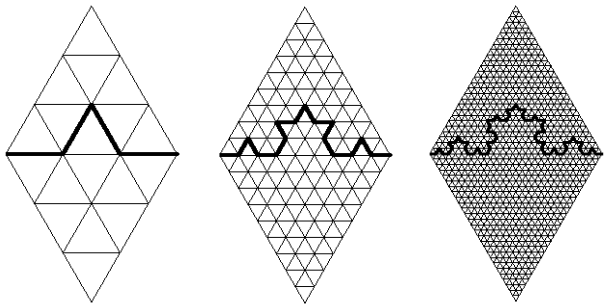

Figure 1.5: The first three iterations of the Koch curve and the first three induced triangulations of a domain ω.

We have produced a extension operator Π such that Π maps a Hölder continuous function from the standard Koch or Sierpinski set to arbitrary open set $\Omega \in \mathbb{R}^2$. This extension operator not only preserves the Hölder exponent, but is constructed in such a way that the extension function for the fractal set is the limit of a sequence of extension functions of the prefractal sets. Moreover, we have an estimate of the convergence of the prefractal extension functions to the extension function itself. If we further restrict the functions to those in the domain of the energy form of the fractal (D_E) the resultant extension function is not only Hölder continuous on Ω but is also in $H^1(\Omega)$. Because the extension operator is adapted to finite elements, the operator is also suitable for numerically approximating prefractal boundary value problems because no re-approximation must occur.

Chapter 2

Hölder Extension using Prefractals

As explained in the introduction our work seeks to exploit both the self-similarity of the fractal, as well as the iterative process used to define the fractal set. We will begin by considering the problem of extending a Hölder continuous function defined on the fractal set to a larger, open domain Ω. We define Π_n as a linear operator that brings functions v defined on V^n to functions v^* defined on Ω according to the methodology detailed in this chapter. (Recall V^n is the set of vertices for the n-th fractal iteration). We use u_n to refer to the restriction of a function u (defined on the fractal) to the prefractal set V^n, that is to say $u_n = u|_{V^n}$. We construct an extension function $\Pi_n u_n$ at every step of the prefractal iteration by considering both the original function u defined at the vertices of the prefractal curve, and the extension function, $\Pi_{n-1}u_{n-1}$, at the previous iteration. We then construct the fractal extension Πu as the limit of the sequence of prefractal extensions $\Pi_n u_n$.

Remark 5. We will use the notation u_n^* to refer to the function $\Pi_n u_n$ and u^* to refer to Πu.

The following theorems are shown in [8] for the Koch curve and [9] for the Sierpinski gasket. Here Ω is an arbitrary domain in $\mathbb{R}^2$ such that the fractal set S (which can be of either the Koch or Sierpinski type) is contained in Ω. We recall a Hölder continuous function u defined on the set S satisfies the estimate

$$|u(x) - u(y)| \leq C_0 |x - y|^\beta$$

for all x, y on S. The constant C_0 is fixed and dependent on u, the minimal value of

which is equal to the Hölder seminorm $|u|_{S,\beta}$. (Here β is constant and $0 < \beta \leq 1$). We indicate by $C^\beta(S)$ the space of Hölder continuous functions defined on S and by $\|u\|_{S,\beta}$ the Hölder norm of u which is equal to $\|u\|_{S,\beta} = |u|_{S,\beta} + \sup_{x \in S} |u(x)|$. We also define $\overline{\Omega}$ as the closure of an open set Ω in $\mathbb{R}^2$ and C_1, C_2 and C_3 to be constants independent of n and β. Moreover we define $u_n := u|_{V^n}$ with $u \in C^\beta(S)$, and $\mathcal{A}_{T_{V^n}}(\Omega)$ the set of piecewise affine functions on the triangulation induced by V^n.

Theorem 2.0.1. *For every n and every $u_n \in C^\beta(V^n)$ we construct a linear extension operator Π_n that brings functions defined on V^n to functions defined on Ω which have the following properties for every $0 < \beta \leq 1$:*

1. $u_n \in C^\beta(V^n) \mapsto u_n^* \in C^\beta(\Omega) \cap \mathcal{A}_{T_{V^n}}(\Omega)$, *($u_n^* := \Pi_n u_n$)*
2. $\|\Pi_n u\|_{\Omega,\beta} \leq C_1 \|u\|_{V^n,\beta}$

Theorem 2.0.2. *Given a fractal set S and a domain Ω we define a linear continuous operator Π such that for all $u \in C^\beta(S)$ the following holds:*

1. $\Pi : C^\beta(S) \mapsto C^\beta(\Omega)$
2. $\|\Pi u\|_{\Omega,\beta} \leq C_2 \|u\|_{S,\beta}$
3. $\Pi u = \lim_{n \to \infty} \Pi_n(u|_{V^n})$ *uniformly in* Ω
4. $\sup_{X \in \Omega} |\Pi_n u_n(X) - \Pi_{n+p} u_{n+p}(X)| \leq C_3 \|u\|_{S,\beta} \alpha^{-n}$ *where* $u_n = u|_{V^n}$ *and* $u_{n+p} = u|_{V^{n+p}}$.

We wish to give a small example that encapsulates the idea of the extension construction. Suppose we are given a triangle $\mathcal{T}$ and a function u defined at the two vertices, X and Y, of the triangle. We extend u to the third vertex, Z, of the triangle, by setting $u^*(Z)$ to the average of the values of the u at the other two vertices of the triangle. That is to say, we set

$$u^*(Z) = \frac{u(X) + u(Y)}{2}.$$

We then set the extension function u^* to be the affine function on the triangle defined by the values of the function at the three vertices. The difficulty in the proofs of these theorems consists of propagating this "extension by averaging" throughout the entire domain while simultaneously maintaining control of the Hölder (and later the H^1) norm.

In this chapter we will first consider extension of functions defined on a Koch curve, and then consider the extension of functions defined on a Sierpinski gasket.

2.1 Koch Curve

First, we will introduce an intermediate domain ω and describe the conformal triangulation of ω induced by the prefractal. Then we will detail the methodology for extending the function u to Ω. Next we will present a few preliminary lemmas and their associated proofs. We then consider the iterative process used to build up the extension function. Finally, we will show Theorem 2.0.2 for the Koch curve.

2.1.1 Induced Triangulation of an Intermediate Domain

We define ω as the polygonal domain with vertices $A = (0,0), B = (1,0), C = \left(\frac{1}{2}, \frac{\sqrt{3}}{2}\right)$, and $D = \left(\frac{1}{2}, \frac{-\sqrt{3}}{2}\right)$, and S the fractal Koch curve with end points A and B. Additionally we will require that the vertices of the prefractal set V^n are nodes of the triangulation T_{V^n} (that is to say the triangulation induced by the prefractals set V^n). We will use the same triangulation defined previously in works by Lancia and Vivaldi [21] and Vacca [30]. We define the initial triangulation T_{V^1} as follows:

We start by constructing the equilateral triangle with vertices $(1/3, 0), (2/3, 0), \left(1/2, \sqrt{3}/6\right)$ and we proceed constructing five other equal triangles such that the union of the six equilateral triangles gives the regular hexagon centered in $\left(1/2, \sqrt{3}/6\right)$. The triangle ABC is the union of 9 congruent equilateral triangles. By proceeding in a symmetric way in the triangle ABD we complete the triangulation of ω.

By proceeding in this regular way we can construct the triangulation $T_{V^{n+1}}$ of ω by subdividing each triangle of T_{V^n} into nine congruent subtriangles. (See Figure 2.1).

2.1.2 A Methodology for the Extension

We construct the extension function on the domain Ω in an iterative manner. We begin by constructing a base extension function $u_0^* = \Pi_0 u_0$ from the function u_0; we then construct the function $u_1^* = \Pi_1 u_1$, using information from both u_1 and u_0^*. We continue

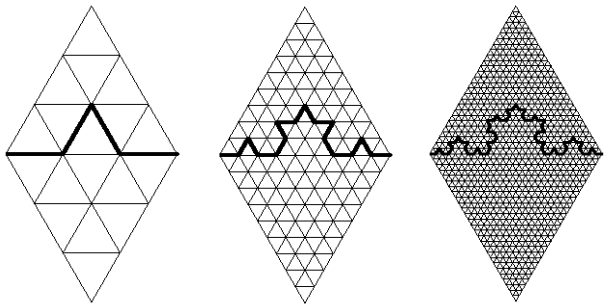

Figure 2.1: The first three iterations of the Koch curve and the first three induced triangulations of a domain ω.

in a step by step manner constructing the extension function u_n^* from u_n and u_{n-1}^*.

Before continuing with our extension methodology we wish to define what we mean when we refer to the *sidecar triangles* of the prefractal set V^n and to the *transition triangles* of the prefractal set V^n.

Definition 1. Given a prefractal set V^n we define the triangles which share one or more vertices with the vertices of the polygonal prefractal curve to be the *sidecar triangles*. See the red triangles in Figure 2.2.

Definition 2. Given a prefractal set V^n we define the triangles which share one or more vertices with the vertices of the sidecar triangles of V^n to be the *transition triangles*. See the white triangles in Figure 2.2.

Extending to ω

For a given set V^n we divide ω into three subdomains: T_{SC}^n, T_{TR}^n and T_{EX}^n. The subdomain T_{SC}^n is composed of the set of sidecar triangles for the set V^n. The subdomain T_{TR}^n is composed of the set of transition triangles of V^n. Finally, the subdomain T_{EX}^n is the set of all the triangles in the domain ω which are neither sidecar triangles nor transition triangles (i.e $T_{EX}^n = \omega \setminus (T_{SC}^n \cup T_{TR}^n)$). This division is illustrated in Figure 2.2 where the red triangles are T_{SC}^n, the white triangles are T_{TR}^n, and the blue triangles are T_{EX}^n. We will consider these three domains separately when constructing u_n^*.

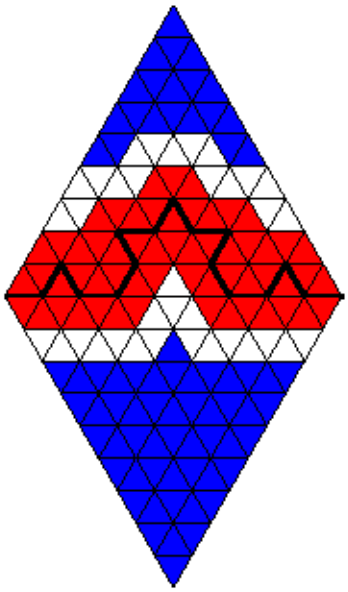

Figure 2.2: The red triangles are the sidecar triangles (T^n_{SC}), the white triangles are the transition triangles (T^n_{TR}) and the blue triangles are external triangles (T^n_{EX}).

The Base Extension

We begin by constructing u^*_0. For this case we do not subdivide ω into three domains, but rather treat ω as the union of two sidecar triangles. To construct u^*_0 we set $u^*_0(C) = u^*_0(D) = \frac{1}{2}(u(A) + u(B))$. We then set u^*_0 to be the affine function determined by the values of u^*_0 at the three vertices of the triangles ABC and ABD respectively; i.e. $u^*_0(x, y) = \dfrac{u(B) - u(A)}{|B - A|}x + u(A)$. (See Figure 2.5).

To construct the extension function u^*_n in ω we use values of u at the vertices of the set V^n and values of u^*_{n-1} from the domain ω. First we obtain the triangulation of ω induced by V^n. We then consider the three subdomains defined earlier and construct the extension as follows:

Extending to T^n_{SC}

First we identify the prefractal set V^n and the sidecar triangles associated with this set. We observe that each triangle in T^n_{SC} has one or more vertices that are elements of V^n and hence have values of u defined at these points. Therefore the value of u^*_n is predetermined at one, two or three vertices of each triangle. We will divide these trian-

gles into three distinct groups. The first group (primary sidecar triangles) will contain those sidecar triangles which have two or three vertices which are elements of V^n. The primary sidecar triangles appear orange in Figure 2.3. The second group (secondary sidecar triangles) will contain those sidecar triangles which have one vertex which is an element of V^n and one or two vertices which are also a vertex of a primary sidecar. The secondary sidecar triangles appear green in Figure 2.3. The third group (tertiary sidecar triangles) will contain those sidecar triangles which have a single vertex in V^n and no vertices shared by a primary sidecar. The tertiary sidecar triangles appear light purple in Figure 2.3.

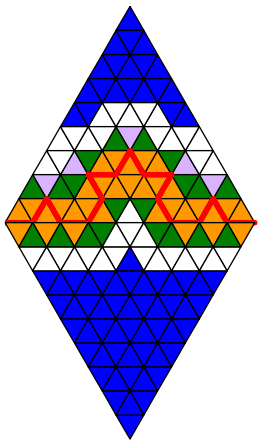

Figure 2.3: In this figure the sidecar triangles are split into three groups. The orange triangles are the primary sidecar triangles, the green triangles are secondary triangles, and the light purple triangles are the tertiary sidecar triangles.

We first extend u to u_n^* in the primary sidecar triangles. We do this by identifying the vertices in the primary sidecar triangles where u_n^* is undetermined. Let J be one of the vertices where u_n^* is undetermined, and $\mathcal{T}_J$ be the set of primary sidecar triangles which have J as a vertex. We set u_n^* at J to be the *average* of the values of u at each element of V^n which is also a vertex of one of the triangles of $\mathcal{T}_J$. (See Figure 2.4 for an

illustration). Now each primary sidecar triangle has u_n^* determined at every vertex and we set the extension function u_n^* to be the affine function on the triangle determined by the values of u_n^* at the three vertices.

We now extend u_n^* to the secondary sidecar triangles. We proceed in a manner similar to that of the primary sidecar triangles by first identifying the vertices in the secondary sidecar triangles where u_n^* is undetermined. Again, we let J be one of the vertices where u_n^* is undetermined, and $\mathcal{T}_J$ be the set of secondary sidecar triangles which have J as a vertex. We set u_n^* at J to be the *average* of the values of u_n^* at each vertex of the triangles $\mathcal{T}_J$ where the value of u_n^* is predetermined. We then set the function u_n^* to be the affine function on the triangle determined by the value of u_n^* at the vertices. Having performed this extension on the secondary sidecar triangles, u_n^* will be predetermined at each vertex of the tertiary sidecar triangles. We set the extension inside these triangles to be the affine function determined by the values of u_n^* at the vertices of the triangle.

Remark 6. We note that the maximum depth of averaging is two. That is to say, in order to find the value of u_n^* at the vertex of a sidecar triangle we may have to perform two averaging steps (one for those in the primary sidecars, and one for the secondary sidecars) but we never perform three averaging steps. This maximum depth is independent of the iteration number n.

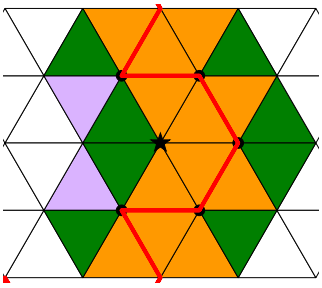

Figure 2.4: The value of u_n^* is predetermined at the nodes with black dots since these are elements of V^n. The value of u_n^* at the node denoted by a star is taken to be the average of the value of u_n^* at each of the nodes with a black dot.

Extending to T_{TR}^n

Prior to this step u has been extended to u_n^* in T_{SC}^n, and hence values for u_n^* are predetermined at every vertex common between T_{SC}^n and T_{TR}^n. Additionally, the function u_{n-1}^* is defined everywhere on the domain ω. Extension to T_{TR}^n is done on a triangle by triangle basis by setting the value of u_n^* to be equal to the value of u_{n-1}^* at any vertex where the value of u_n^* is not predetermined. We then set u_n^* to be the function which is affine on the triangle and determined by the values of u_n^* at the three vertices of the triangle.

Extending to T_{EX}^n
The extension to T_{EX}^n is accomplished by setting u_n^* equal to u_{n-1}^* at every point in T_{EX}^n.

In this manner we proceed in an iterative fashion to construct each function u_n^* on T_{V^n}. We summarize the extension methodology with the following definition

Definition 3. The extension function u_n^* on ω is defined as the function determined by the values of u on V^n and the values of the previous function u_{n-1}^* on ω. The values of u on V^n are used to determine the function u_n^* on the sidecar triangles of ω, the values of u on V^n and the values of u_{n-1}^* are used to determine the function u_n^* on the transition region of ω, and finally only the values of u_{n-1}^* are used to determine the function u_n^* on the region of ω which is neither sidecar or transition region.

This definition is shown visually for steps $0 \to 1$ and $1 \to 2$ in Figures 2.5 and 2.6.

Extending to Ω

We introduce an additional intermediate domain γ where γ is the convex polygonal domain with vertices $E = (-1, 0)$, $F = (0, \sqrt{3})$, $G = (1, \sqrt{3})$, $H = (2, 0)$, $I = (1, -\sqrt{3})$, and $J = (0, -\sqrt{3})$. We subdivide γ into sixteen congruent triangles, two of which are the triangles ABC and ABD, which composed the domain ω. The function v_n^* is constructed on γ by a combination of operations of rotation, reflection and translation applied to the function u_n^* defined on the two triangles ABC and ABD. These operations are shown visually in Figure 2.7. In this figure, the light blue triangles indicate those triangles where the value of v_n^* is obtained by translation and rotation of the function u_n^* defined on ABC and the light green triangles are obtained by translation and rotation of the function u_n^* defined on the triangle ABD. The dark blue triangles

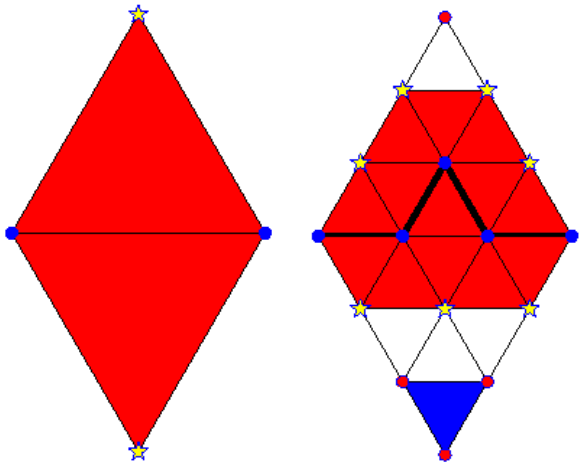

Figure 2.5: u_0^*, and u_1^*. The blue dots are points where u is defined. The values of u_1^* at the pink points come from u_0^*, and the yellow stars are values new to u_1^*.

are obtained by first reflecting the triangle ABC across the x-axis and then translating and rotating the reflected function. Similarly the dark green triangles are obtained by reflecting the function u_n^* in ABD across the x-axis then translating and rotating the function. Clearly if the function $u_n^* \in C^\beta(\omega)$, $v_n^* \in C^\beta(\gamma)$.

We will utilize the standard finite element "hat" function in relationship to the sixteen triangle coarse mesh. The function η_A corresponds to the function with value 1 at point A, zero on the boundary of the hexagon created by the six triangles with A as a vertex, and affine on each of the triangles. In a similar manner we create functions η_B, η_C, and η_D centered at points B, C, and D respectively. We set $\eta = \eta_A + \eta_B + \eta_C + \eta_D$, and observe that $\eta \in H^1(\gamma)$, $\eta(X) = 1$ for all $X \in \omega$, and $\eta(X) = 0$ for all $x \in \partial\gamma$. (See Figure 2.8). We define the function $z_n^*(X) = \eta(X)v_n^*(X)$ for $X \in \gamma$ and $z_n^*(X) = 0$ for $X \in \mathbb{R} \setminus \gamma$. We set the extension function u_n^* to z_n^* and restrict u_n^* to the given domain Ω.

Proposition 2.1.1. *The extension operator* Π_n *is linear*

Proof. Let S be a Koch curve and u, v be two Hölder continuous functions defined at the vertices on the curve that satisfy

$$\frac{|u(X) - u(Y)|}{|X - Y|^\beta} \leq |u|_{S,\beta}$$

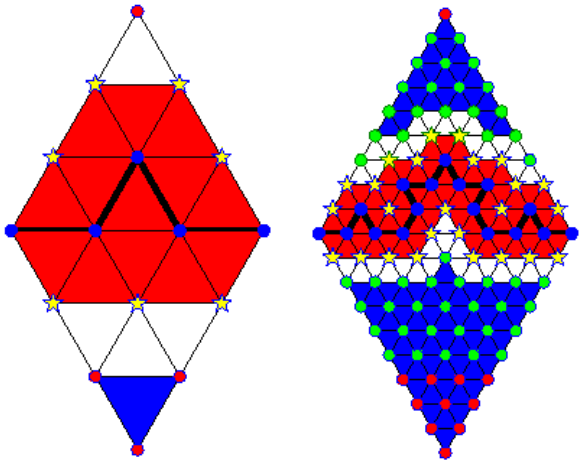

Figure 2.6: u_1^*, and u_2^*. The blue dots are points where u is defined. The values at the pink points come from u_0^*, the values at the green points are from u_1^* , and the yellow stars are values new to u_2^*.

and

$$\frac{|v(X) - v(Y)|}{|X - Y|^\beta} \leq |v|_{S,\beta}$$

for all $X, Y \in V^n$ and for some $\beta \leq 1$. We also let $\kappa, h \in \mathbb{R}$. First, we assume X is an element of ω. By construction the value of $\Pi_n u_n(X)$ is the linear combination of the values of $\Pi_n u_n(X_1)$, $\Pi_n u_n(X_2)$, and $\Pi_n u_n(X_3)$, where X_1, X_2, and X_3 are the vertices of the triangle $\mathcal{T}_X$. Also by construction the value of $\Pi_n u_n(X_i) = \sum_{i=1}^{|V^n|} a_i u(y_i)$ where $y_i \in V^n$, $0 \leq a_i \leq 1$, $\sum a_i = 1$ and the values of a_i are independent of u. Therefore:

$$\begin{aligned}
\kappa \Pi_n u_n(X) + h \Pi_n v_n(X) &= \kappa \sum_{i=1}^{|V^n|} a_i u(y_i) + h \sum_{i=1}^{|V^n|} a_i v(y_i) \\
&= \sum_{i=1}^{|V^n|} a_i (\kappa u(y_i) + h v(y_i)) \\
&= \Pi_n (\kappa u_n(X) + h v_n(X)).
\end{aligned}$$

□

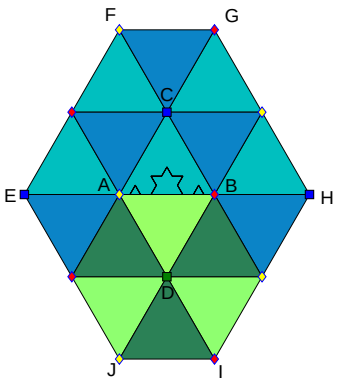

Figure 2.7: An illustration of γ and the sixteen subtriangles. The green triangles are reflections and translations of ABD and the blue triangles are reflections and translations of ABC. The yellow diamonds indicate those points where v_n^* is equal to $u(A)$, the pink diamonds those points where v_n^* is equal to $u(B)$, the blue squares $v_n^* = u_n^*(C)$ and the green square where $v_n^* = u_n^*(D)$.

2.1.3 Preliminary Results

The purpose of this section is to provide a few preliminary results needed for the proof of Theorem 2.0.2 for the Koch curve. The first lemma is specific to the primary sidecar triangles, the second to the secondary sidecar triangles and the third specific to the tertiary sidecar triangles. (Recall, Figure 2.3 gives a visual presentation of this subdivision). Lemmas 4-5 consider the Hölder estimate on two or more triangles.

Lemma 2.1.2. *Given a triangle $\mathcal{T}$ with vertices P, Q, and J, and a function u defined at the vertices of the prefractal V^n such that*

$$\frac{|u(A) - u(B)|}{|A - B|^\beta} \leq |u|_{S,\beta}$$

where $A, B \in V^n$ and $\beta \leq 1$. Moreover $P, Q \in V^n$. Then there exists an extension function u^* defined on $\mathcal{T}$ such that

$$\sup_{X,Y \in \mathcal{T}} \frac{|u^*(X) - u^*(Y)|}{|X - Y|^\beta} \leq 3|u|_{S,\beta}. \tag{2.1}$$

Proof. We consider the case where the value of u^* at point J is determined by the

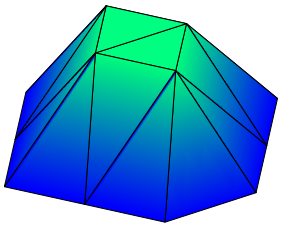

Figure 2.8: The function η on the domain γ. Note that on the subdomain ω, $\eta = 1$.

value of u at five vertices of the prefractal curve. (The case where u^* at point J is determined by two, three or four vertices proceeds in a similar manner, with the right hand side of Equation 2.1 equal to $a|u|_{S,\beta}$, with $a \to 1$ as the number of vertices decreases). We let P, Q, R, S and T be five consecutive vertices along the prefractal curve. (See Figure 2.9 for an illustration of the scenario considered). We begin by constructing the extension function u^*, by prescribing its value at J. We set $u^*(J) = \frac{1}{5}(u(P) + u(Q) + u(R) + u(S) + u(T))$ and let u^* be the affine function defined by these three points. We now check that u^* satisfies the estimate 2.1.

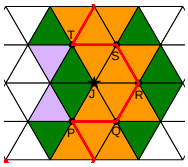

Figure 2.9: The triangle PQJ under consideration

To facilitate our calculations we introduce a reference triangle $\hat{\mathcal{T}}$. The triangle $\hat{\mathcal{T}}$ is the equilateral triangle with $\hat{P}$ located at the origin, $\hat{Q}$ located on the x- axis, and $|\hat{P} - \hat{Q}| = |P - Q|$. With this triangle we associate the map $\tau : \hat{X} \to X$ in $\mathbb{R}^2$ which brings the vertex $\hat{P}$ to P, and the vertex $\hat{Q}$ to Q. Here $\tau\hat{X} = x_0 + B\hat{X}$ where x_0 is a 2×1 vector and B is the rotational matrix with $\theta = -\arctan[(y_Q - y_P)/(x_Q - x_P)]$. We

note that $|X-Y| = |\hat{X}-\hat{Y}|$ and observe that

$$\sup_{X,Y\in\mathcal{T}} \frac{|u^*(X)-u^*(Y)|}{|X-Y|^\beta} = \sup_{\hat{X},\hat{Y}\in\hat{\mathcal{T}}} \frac{|\hat{u}^*(\hat{X})-\hat{u}^*(\hat{Y})|}{|X-Y|^\beta}.$$

Therefore it suffices to show the estimate in $\hat{\mathcal{T}}$. It can easily be checked that the function u^* satisfies

$$\hat{u}^*(\hat{X}) = \frac{u(Q)-u(P)}{|P-Q|}\hat{x} + \frac{2u(J)-u(P)-u(Q)}{\sqrt{3}|P-Q|}\hat{y} + u(P).$$

We also observe that

$$\hat{u}^*(\hat{J}) = \frac{1}{5}(u(P)+u(Q)+u(R)+u(S)+u(T)).$$

Let $\hat{X}_1 = (\hat{x}_1, \hat{y}_1)$ and $\hat{X}_2 = (\hat{x}_2, \hat{y}_2)$ be arbitrary points in $\hat{\mathcal{T}}$.

$$\begin{aligned}
\frac{|\hat{u}^*(\hat{X}_1)-\hat{u}^*(\hat{X}_2)|}{|\hat{X}_1-\hat{X}_2|^\beta} &= \frac{\left|\frac{u(P)-u(Q)}{|P-Q|}(\hat{x}_1-\hat{x}_2) + \frac{2u(J)-u(P)-u(Q)}{\sqrt{3}|P-Q|}(\hat{y}_1-\hat{y}_2)\right|}{|\hat{X}_1-\hat{X}_2|^\beta} \\
&\le \frac{|u(P)-u(Q)|}{|P-Q|^\beta} + \frac{|2(\frac{1}{5}(u(P)+u(Q)+u(R)+u(S)+u(T)) - u(P) - u(Q)|}{\sqrt{3}|P-Q|^\beta} \\
&\le |u|_{S,\beta} + \frac{2}{5\sqrt{3}}\left(\frac{|u(S)-u(P)|}{|P-Q|^\beta} + \frac{|u(R)-u(Q)|}{|P-Q|^\beta}\right) + \\
&\qquad + \frac{1}{5\sqrt{3}}\left(\frac{|u(T)-u(P)|}{|P-Q|^\beta} + \frac{|u(T)-u(Q)|}{|P-Q|^\beta}\right) \\
&\le |u|_{S,\beta} + \frac{2^{(1+\beta)}}{5\sqrt{3}}\frac{|u(S)-u(P)|}{|S-P|^\beta} + \frac{2}{5\sqrt{3}}\frac{|u(R)-u(Q)|}{|R-Q|^\beta} + \\
&\quad + \frac{3^{\beta/2}}{5\sqrt{3}}\frac{|u(T)-u(P)|}{|T-P|^\beta} + \frac{2^\beta}{5\sqrt{3}}\frac{|u(T)-u(Q)|}{|T-Q|^\beta} \\
&\le |u|_{S,\beta} + \frac{2}{5\sqrt{3}}|u|_{S,\beta}\left(2^\beta + 1 + \frac{3^{\beta/2}}{2} + 2^{(\beta-1)}\right) \\
&\le 2.2|u|_{S,\beta} \le 3|u|_{S,\beta}.
\end{aligned}$$

□

Remark 7. We observe that the Hölder seminorm is invariant under translation and rotation. For Lemmas 2-3 and 6-8 we will use this observation and without loss of

generality assume that the triangle under consideration $\mathcal{T}$ is located with one vertex at the origin and a second vertex along the x-axis.

Remark 8. We observe the following relationship between the vertices that are elements of V^n and the vertex J (here $P_i \in V^n$):

$$u_n^*(J) = \sum_{i=1}^{M} u(P_i)$$

and for $2 \leq M \leq 5$ the following estimate holds

$$\frac{|u_n^*(J) - u(P_i)|}{|J - P_i|^\beta} \leq \frac{1}{M} \sum_{k=1}^{M} \frac{|u(P_k) - u(P_i)|}{|J - P_i|^\beta} \leq \frac{1}{M} \sum_{k=1}^{M} \frac{2^\beta |u(P_k) - u(P_i)|}{|P_k - P_i|^\beta} \leq \frac{2(M-1)}{M} |u|_{S,\beta} \leq \frac{8}{5} |u|_{S,\beta}$$

Lemma 2.1.3. *Given a triangle $\mathcal{T}$ with vertices P, Q, and R, and a function u defined at the vertices of the prefractal V^n such that*

$$\frac{|u(A) - u(B)|}{|A - B|^\beta} \leq |u|_{S,\beta}$$

where $A, B \in V^n$ and $\beta \leq 1$. Moreover $P, Q, R \in V^n$. Then there exists an extension function u^* defined on $\mathcal{T}$ such that

$$\sup_{X,Y \in \mathcal{T}} \frac{|u^*(X) - u^*(Y)|}{|X - Y|^\beta} \leq 3|u|_{S,\beta}. \tag{2.2}$$

Proof. We begin by letting u^* be the affine function defined by the value of u at the three vertices of the triangle. We now check that u^* satisfies the estimate (2.2).

By Remark 7 we may assume $\mathcal{T}$ is a triangle with P located at the origin and J is located on the x-axis. It can easily be checked that

$$\hat{u}^*(\hat{X}) = \frac{u(Q) - u(P)}{|P - Q|} \hat{x} + \frac{2u(R) - u(P) - u(Q)}{\sqrt{3}|P - Q|} \hat{y} + u(P).$$

Let $X_1 = (x_1, y_1)$ and $X_2 = (x_2, y_2)$ be arbitrary points in $\mathcal{T}$.

$$\begin{aligned}
\frac{|u^*(X_1) - u^*(X_2)|}{|X_1 - X_2|^\beta} &= \frac{\left|\frac{u(Q)-u(P)}{|P-Q|}(x_1 - x_2) + \frac{2u(R)-u(P)-u(Q)}{\sqrt{3}|P-Q|}(y_1 - y_2)\right|}{|X_1 - X_2|^\beta} \\
&\leq \frac{|u(Q) - u(P)|}{|P-Q|^\beta} \left(\frac{|x_1 - x_2|}{|X_1 - X_2|}\right)^\beta \left(\frac{|x_1 - x_2|}{|P-Q|}\right)^{1-\beta} + \\
&\quad + \frac{|2u(R) - u(P) - u(Q)|}{\sqrt{3}|P-Q|^\beta} \left(\frac{|\hat{y}_1 - \hat{y}_2|}{|\hat{X}_1 - \hat{X}_2|}\right)^\beta \left(\frac{|\hat{y}_1 - \hat{y}_2|}{|P-Q|}\right)^{1-\beta} \\
&\leq \frac{|u(Q) - u(P)|}{|P-Q|^\beta} + \frac{|2u(R) - u(P) - u(Q)|}{\sqrt{3}|P-Q|^\beta} \\
&\leq |u|_{S,\beta} + \frac{1}{\sqrt{3}} \frac{|u(R) - u(P)| + |u(R) - u(Q)|}{|P-Q|^\beta} \\
&\leq |u|_{S,\beta} + \frac{2}{\sqrt{3}}|u|_{S,\beta} \\
&= 3|u|_{S,\beta}.
\end{aligned}$$

Hence $\dfrac{|u^*(X) - u^*(Y)|}{|X-Y|^\beta} \leq 3|u|_{S,\beta}$.

□

The following Lemma holds for any of the secondary sidecar triangles (the green triangles in Figure 2.3).

Lemma 2.1.4. *Let $\mathcal{T}$ be a triangle with with vertices P, J and K and let u be a function defined at P and J. Let us suppose that there exists $\beta \leq 1$ such that*

$$\frac{|u(P) - u(J)|}{|P-J|^\beta} \leq \frac{8}{5}|u|_{S,\beta}$$

holds. Then there exists a function u^* defined for $x \in \mathcal{T}$ such that

$$\sup_{X,Y \in \mathcal{T}} \frac{|u^*(X) - u^*(Y)|}{|X-Y|^\beta} \leq 5|u|_{S,\beta}. \tag{2.3}$$

Proof. First we observe that the secondary sidecar triangles can be classified into four groups as illustrated in Figure 2.10. In the first scenario (see Figure 2.10A), the value of u at point K is predetermined by a primary sidecar triangle. In the second scenario (see Figure 2.10B), the value of u^* at K is set to be $u(K) = \frac{1}{2}(u(P) + u(J))$. In the

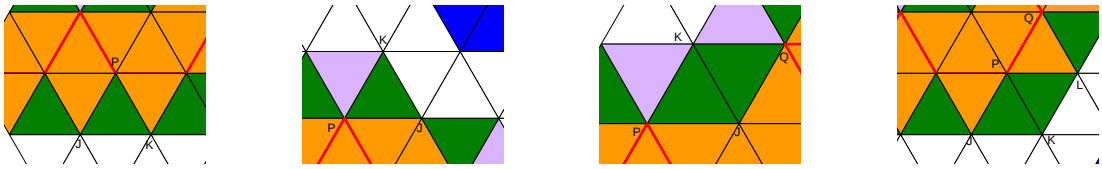

(a) (b) (c) (d)

Figure 2.10: Four sample secondary sidecar triangles.

third scenario (see Figure 2.10C), the value of u at K is set to be $u(K) = \frac{1}{3}(u(P) + u(Q) + u(J))$ where two of these points (P and Q) are elements of V^n and the third point $J \notin V^n$. In the last scenario (see Figure 2.10D), the value of u at K is set to be $u(K) = \frac{1}{3}(u(P) + u(L) + u(J))$ where two of these points (L and J) are sidecar vertices and the third point P is an element of V^n. In all four scenarios we let u^* be the function on $\mathcal{T}$ defined by the values of u at the three vertices. We now check that u^* satisfies the estimate (2.3).

By Remark 7 we may assume $\mathcal{T}$ is a triangle with P located at the origin and J is located on the x-axis. It can easily be checked that

$$u^*(X) = \frac{u(J) - u(P)}{|P - J|}x + \frac{2u(K) - u(P) - u(J)}{\sqrt{3}|P - J|}y + u(P).$$

Let $X_1 = (x_1, y_1)$ and $X_2 = (x_2, y_2)$ be arbitrary points in $\mathcal{T}$.

$$\begin{aligned}\frac{|u^*(X_1) - u^*(X_2)|}{|X_1 - X_2|^\beta} &= \frac{\left|\frac{u(J)-u(P)}{|P-J|}(x_1 - x_2) + \frac{2u(K)-u(P)-u(J)}{\sqrt{3}|P-J|}(y_1 - y_2)\right|}{|X_1 - X_2|^\beta} \\ &\leq \frac{|u(P) - u(J)|}{|P - J|^\beta} + \frac{|2u(K) - u(P) - u(J)|}{\sqrt{3}|P - J|^\beta} \\ &\leq \frac{8}{5}|u|_{S,\beta} + \frac{|2u(K) - u(P) - u(J)|}{\sqrt{3}|P - J|^\beta}\end{aligned}$$

We now consider the term $\dfrac{|2u(K) - u(P) - u(J)|}{\sqrt{3}|P - J|^\beta}$ for each of the scenarios separately.

CASE 1: $u(K)$ was set by a primary sidecar triangle.

$$\begin{aligned}\frac{|2u(K)-u(P)-u(J)|}{\sqrt{3}|P-J|^\beta} &= \frac{|2u(K)-2u(P)+u(P)-u(J)|}{\sqrt{3}|P-J|^\beta}\\ &\le \frac{2|u(K)-u(P)|}{\sqrt{3}|K-P|^\beta}+\frac{|u(P)-u(J)|}{\sqrt{3}|P-J|^\beta}\\ &\le \frac{1}{\sqrt{3}}\left(\frac{16}{5}+\frac{8}{5}\right)|u|_{S,\beta}\\ &\le 2.8|u|_{S,\beta}.\end{aligned}$$

CASE 2: $u(K)=\frac{1}{2}(u(P)+u(J))$.

$$\frac{|2u(K)-u(P)-u(J)|}{\sqrt{3}|P-J|^\beta} = \frac{|u(P)+u(J)-u(P)-u(J)|}{\sqrt{3}|P-J|^\beta} = 0.$$

CASE 3: $u(K)=\frac{1}{3}(u(P)+u(J)+u(Q))$.

$$\begin{aligned}\frac{|2u(K)-u(P)-u(J)|}{\sqrt{3}|P-J|^\beta} &\le \frac{1}{3\sqrt{3}}\frac{|u(Q)-u(P)|+|u(Q)-u(J)|}{|P-J|^\beta}\\ &\le \frac{1}{3\sqrt{3}}\left(\frac{3^{(\beta/2)}|u(Q)-u(P)|}{|Q-P|^\beta}+\frac{|u(Q)-u(J)|}{|P-J|^\beta}\right)\\ &\le \frac{1}{3\sqrt{3}}\left(3^{(\beta/2)}|u|_{S,\beta}+\frac{8}{5}|u|_{S,\beta}\right)\\ &\le |u|_{S,\beta}.\end{aligned}$$

CASE 4: $u(K)=\frac{1}{3}(u(P)+u(J)+u(L))$.

$$\begin{aligned}\frac{|2u(K)-u(P)-u(J)|}{\sqrt{3}|P-J|^\beta} &\le \frac{1}{3\sqrt{3}}\frac{|u(L)-u(P)|+|u(L)-u(J)|}{|P-J|^\beta}\\ &\le \frac{1}{3\sqrt{3}}\frac{2|u(L)-u(P)|+|u(P)-u(J)|}{|P-J|^\beta}\\ &\le \frac{1}{3\sqrt{3}}\left(\frac{2|u(L)-u(P)|}{|L-P|^\beta}+\frac{|u(P)-u(J)|}{|P-J|^\beta}\right)\\ &\le \frac{1}{3\sqrt{3}}\left(\frac{16}{5}|u|_{S,\beta}+\frac{8}{5}|u|_{S,\beta}\right)\\ &\le |u|_{S,\beta}.\end{aligned}$$

In all four cases $\frac{|2u(K)-u(P)-u(J)|}{\sqrt{3}|P-J|^\beta} \leq 2.8|u|_{S,\beta}$ and hence $\frac{|u^*(X)-u^*(Y)|}{|X-Y|^\beta} \leq 5|u|_{S,\beta}$. □

The following Lemma holds for any of the tertiary sidecar triangles (the light purple triangles in Figure 2.3).

Lemma 2.1.5. *Let $\mathcal{T}$ be a triangle with with vertices P, J and K and let u be a function defined at P, J and K. Let us suppose that there exists $\beta \leq 1$ such that*

$$\frac{|u(P)-u(J)|}{|P-J|^\beta} \leq 4|u|_{S,\beta}, \tag{2.4}$$

$$\frac{|u(P)-u(K)|}{|P-K|^\beta} \leq 4|u|_{S,\beta} \tag{2.5}$$

hold. Then there exists a function u^* defined for $x \in \mathcal{T}$ with $u^*(P) = u(P)$, $u^*(J) = u(J)$ and $u^*(K) = u(K)$ such that

$$\sup_{X,Y\in\mathcal{T}} \frac{|u^*(X)-u^*(Y)|}{|X-Y|^\beta} \leq 11|u|_{S,\beta}. \tag{2.6}$$

Remark 9. In Equations 2.4 and 2.5 the right hand side is less then or equal to $4|u|_{S,\beta}$. This may seem in contradiction to the previous lemma which sets the Hölder constant for a secondary sidecar triangle at $5|u|_{S,\beta}$. The reason for this discrepancy is that those secondary sidecar triangles in the first group (i.e. those triangles where the value of u_n^* is predetermined by the primary sidecar triangles at all three vertices) never share a side (and hence two vertices) with a tertiary sidecar triangle. This allows us to use the sharper estimates from secondary sidecar triangles of types 2, 3 and 4.

Proof. We begin by letting u^* be the affine function defined by the value of u at the three vertices of the triangle. We now check that u^* satisfies the estimate (2.6).

By Remark 7 we may assume $\mathcal{T}$ is a triangle with P located at the origin and J is located on the x-axis. It can easily be checked that

$$u^*(X) = \frac{u(J)-u(P)}{|P-J|}x + \frac{2u(K)-u(P)-u(J)}{\sqrt{3}|P-J|}y + u(P).$$

Let $X_1 = (x_1, y_1)$ and $X_2 = (x_2, y_2)$ be arbitrary points in $\mathcal{T}$.

$$\begin{aligned}
\frac{|u^*(X_1) - u^*(X_2)|}{|X_1 - X_2|^\beta} &= \frac{\left|\frac{u(P)-u(J)}{|P-J|}(x_1 - x_2) + \frac{2u(K)-u(P)-u(J)}{\sqrt{3}|P-J|}(y_1 - y_2)\right|}{|X_1 - X_2|^\beta} \\
&\leq \frac{|u(P) - u(J)|}{|P - J|^\beta} + \frac{|2u(K) - u(P) - u(J)|}{\sqrt{3}|P - J|^\beta} \\
&\leq 4|u|_{S,\beta} + \frac{1}{\sqrt{3}} \frac{2|u(K) - u(P)| + |u(P) - u(J)|}{|P - J|^\beta} \\
&\leq 4|u|_{S,\beta} + \frac{1}{\sqrt{3}} \frac{2|u(K) - u(P)|}{|K - P|^\beta} + \frac{1}{\sqrt{3}} \frac{|u(P) - u(J)|}{|P - J|^\beta} \\
&\leq 4|u|_{S,\beta} + \frac{3}{\sqrt{3}} 4|u|_{S,\beta} \\
&= |u|_{S,\beta}(4 + 4\sqrt{3}) \leq 11|u|_{S,\beta}.
\end{aligned}$$

Hence $\dfrac{|u^*(X) - u^*(Y)|}{|X - Y|^\beta} \leq 11|u|_{S,\beta}$. □

The next Lemma considers the case of two triangles each with an affine function defined on them.

Lemma 2.1.6. *Let $\mathcal{T}_V$ and $\mathcal{T}_W$ be two triangles such that $\mathcal{T}_V \cap \mathcal{T}_W \neq \emptyset$. Let v be an affine function defined on $\mathcal{T}_V$ and w an affine function defined on $\mathcal{T}_W$ such that $v|_{\mathcal{T}_V \cap \mathcal{T}_W} = w|_{\mathcal{T}_V \cap \mathcal{T}_W}$. We also require that for some $\beta \leq 1$ there exists constants C_V and C_W such that the following inequalities hold:*

$$\sup_{X,Y \in \mathcal{T}_V} \frac{|v(X) - v(Y)|}{|X - Y|^\beta} \leq C_V,$$

and

$$\sup_{X,Y \in \mathcal{T}_W} \frac{|w(X) - w(Y)|}{|X - Y|^\beta} \leq C_W.$$

Define

$$z(X) = \begin{cases} v(X) & \text{if } X \in \mathcal{T}_V \\ w(X) & \text{if } X \in \mathcal{T}_W \setminus \mathcal{T}_V \end{cases} \tag{2.7}$$

and $C_M = \max(C_V, C_W)$. Then

$$\sup_{X,Y \in \mathcal{T}_V \cup \mathcal{T}_W} \frac{|z(X) - z(Y)|}{|X - Y|^\beta} \leq 2C_M.$$

Proof. For ease of notation we define $\mathcal{W} := \mathcal{T}_V \cup \mathcal{T}_W$. Let X and Y be arbitrary points in $\mathcal{W}$. If X and Y are points in the same triangle the inequality holds trivially. We now consider the case where X and Y are in different triangles and without loss of generality will assume $X \in \mathcal{T}_V$ and $Y \in \mathcal{T}_W$. We note that if $\mathcal{T}_V \cap \mathcal{T}_W \neq \emptyset$ then $\mathcal{T}_V$ and $\mathcal{T}_W$ share either an entire side, or only a single point. In the first case $\overline{XY} \subset \mathcal{W}$ since every triangle is equilateral and we define P as the intersection of $\overline{XY}$ and $\mathcal{T}_V \cap \mathcal{T}_W$. In the second case we define $P = \mathcal{T}_V \cap \mathcal{T}_W$. We also recall that v and w are affine functions on $\mathcal{T}_V$ and $\mathcal{T}_W$ respectively. Clearly

$$\begin{aligned}
\frac{|z(X) - z(Y)|}{|X - Y|^\beta} &\leq \frac{|v(X) - v(P)|}{|X - Y|^\beta} + \frac{|w(P) - w(Y)|}{|X - Y|^\beta} \\
&\leq \frac{C_V |X - P|^\beta}{|X - Y|^\beta} + \frac{C_W |P - Y|^\beta}{|X - Y|^\beta} \\
&= C_V \left(\frac{|X - P|}{|X - Y|} \right)^\beta + C_W \left(\frac{|P - Y|}{|X - Y|} \right)^\beta \\
&\leq C_V + C_W \leq 2C_M.
\end{aligned}$$

Since X and Y were arbitrary

$$\sup_{X,Y \in \mathcal{W}} \frac{|z(X) - z(Y)|}{|X - Y|^\beta} \leq 2C_M.$$

□

Lemma 2.1.7. *Let n be fixed, V^n a prefractal set and given a function u defined on V^n such that*

$$\frac{|u(P) - u(Q)|}{|P - Q|^\beta} \leq |u|_{S,\beta}$$

for all $P, Q \in V^n$ and for some $\beta \leq 1$. Let u_n^* be an extension to the domain ω as defined in Definition 3, then for any X, Y in T_{SC}^n the following holds

$$\frac{|u_n^*(X) - u_n^*(Y)|}{|X - Y|^\beta} \leq 66 |u|_{S,\beta}. \tag{2.8}$$

Proof. We define C_{MSC} as the maximum Hölder constant from Lemmas 2.1.2-2.1.5, therefore $C_{MSC} \leq 11|u|_{S,\beta}$. We also observe that if X and Y are elements of the same triangle $\mathcal{T}$, then inequality 2.8 holds due to those lemmas. Moreover, if X and Y are elements of two triangles that share either an entire side or a single point, inequality 2.8

holds by Lemma 2.1.6. We now consider the case where X and Y are elements of $\mathcal{T}_X$ and $\mathcal{T}_Y$ respectively and that $\mathcal{T}_X \cap \mathcal{T}_Y = \emptyset$.

We let P_X be an element of V^n closest to X, that is to say $|P_X - X| \leq |R - X|$ for all $R \in V^n$ (we know that at least one such element exists). Similarly define P_Y to be the element of V^n closest to Y. Let L be the length of the side of a triangle in our mesh (i.e. $L = 3^{-n}$), therefore we have $|P_X - X| \leq L$, $|P_Y - Y| \leq L$, $|P_X - P_Y| \leq |P_X - X| + |X - Y| + |Y - P_Y|$ and $|X - Y| \geq \frac{\sqrt{3}}{2}L$. We then have,

$$\begin{aligned}
|u_n^*(X) - u_n^*(Y)| &\leq |u_n^*(X) - u_n^*(P_X)| + |u_n^*(P_X) - u_n^*(P_Y)| + |u_n^*(P_Y) - u_n^*(Y)| \\
&\leq C_{\mathcal{T}_X}|X - P_X|^\beta + |u|_{S,\beta}|P_X - P_Y|^\beta + C_{\mathcal{T}_Y}|P_Y - Y|^\beta \\
&\leq C_{MSC}(|X - P_X|^\beta + |P_X - P_Y|^\beta + |P_Y - Y|^\beta) \\
&\leq C_{MSC}\left[\left(\frac{2}{\sqrt{3}}|X - Y|\right)^\beta + \left(\frac{2}{\sqrt{3}} + 1 + \frac{2}{\sqrt{3}}\right)^\beta |X - Y|^\beta + \right. \\
&\qquad \left. + \left(\frac{2}{\sqrt{3}}|X - Y|\right)^\beta\right] \\
&\leq 6C_{MSC}|X - Y|^\beta \\
&\leq 66|u|_{S,\beta}|X - Y|^\beta.
\end{aligned}$$

Hence for $X, Y \in T_{SC}^n$, $\dfrac{|u_n^*(X) - u_n^*(Y)|}{|X - Y|^\beta} \leq 66|u|_{S,\beta}$. □

2.1.4 Iterative Process

The purpose of this section is to provide a few results necessary to show that u_n^* satisfies the Hölder estimate when $n \geq 1$. The first three lemmas consider the Hölder estimate of $\mathcal{T} \in T^n$ where $n \geq 1$. The fourth lemma is similar to Lemma 2.1.7 and shows an estimate for two points in $T_{SC}^n \cup T_{TR}^n$. The fifth lemma gives a Hölder estimate on each triangle $\mathcal{T}$ of the triangulation T^n. Finally we consider the Hölder estimate for the function u_1^* in ω.

This lemma corresponds to those transition triangles where the value for u_n^* is determined by the sidecar triangles at two vertices, and the value at the third vertex is determined by the function u_{n-1}^*. This is shown in Figure 2.11A.

Lemma 2.1.8. *Given a triangle $\mathcal{T}$ with vertices J, K, and L, a function u defined at*

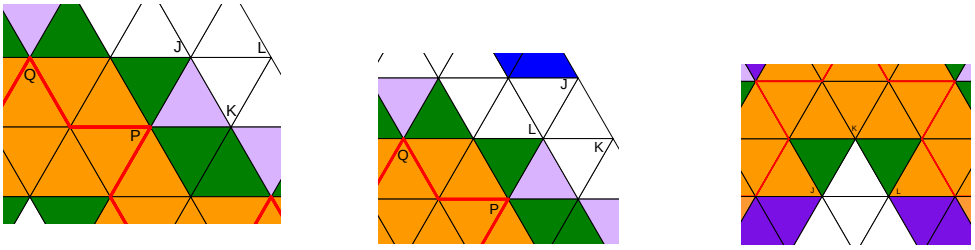

(a) (b) (c)

Figure 2.11: The three types of transition triangles considered in Lemmas 2.1.8 - 2.1.10. (Recall the transition triangles are white).

points J, K and L such that

$$\frac{|u(J)-u(K)|}{|J-K|^\beta} \leq 11|u|_{S,\beta}$$

where $\beta \leq 1$. Suppose we are also given two points P and Q in V^n such that

$$\frac{|u(P)-u(J)|}{|P-J|^\beta} \leq 11|u|_{S,\beta}$$

$$\frac{|u(P)-u(K)|}{|P-K|^\beta} \leq 11|u|_{S,\beta}$$

$$\frac{|u(P)-u(Q)|}{|P-Q|^\beta} \leq |u|_{S,\beta}$$

and

$$\frac{|u(L)-u(Q)|}{|L-Q|^\beta} \leq 11|u|_{S,\beta}.$$

Moreover the following relationships hold: $|J-K| = |P-J| = |P-K|$, $|J-K| \geq \frac{1}{3}|L-Q|$, $|J-K| \geq \frac{1}{\sqrt{3}}|P-Q|$. (Again, see Figure 2.11A for a visual representation). Then, there exists an extension function u^* defined on $\mathcal{T}$ such that

$$\sup_{X,Y\in\mathcal{T}} \frac{|u^*(X)-u^*(Y)|}{|X-Y|^\beta} \leq 65|u|_{S,\beta}. \tag{2.9}$$

Remark 10. In this lemma the value of u at points J and K is determined by the extension function u_n^* in the sidecar region and we therefore have the estimate $|u(J)-u(K)|/|J-K|^\beta \leq 11|u|_{S,\beta}$. The value of u at point L is determined by the previous

extension function u^*_{n-1}. We use this information to determine the relationship between L and a point in V^{n-1} (i.e $|u(L)-u(Q)|/|L-Q|^\beta \leq 11|u|_{S,\beta}$). These relationships drive both the estimates and geometrical assumptions (i.e. the distance between points) in the theorem statement.

Remark 11. For some transition triangles of this type, the scenario will occur that $P \in V^{n-1}$. In this case there is no need for a distinct point Q, so we will set $Q = P$. We observe that all of the estimates and geometrical assumptions are still true in this case.

Proof. We begin by letting u^* be the affine function defined by the value of u at the three vertices of the triangle. We now check that u^* satisfies the estimate (2.9).

By Remark 7 we may assume $\mathcal{T}$ is a triangle with P located at the origin and J located on the x-axis. It can easily be checked that

$$u^*(X) = \frac{u(K)-u(J)}{|K-J|}x + \frac{2u(L)-u(K)-u(J)}{\sqrt{3}|K-J|}y + u(J).$$

Let $X_1 = (x_1, y_1)$ and $X_2 = (x_2, y_2)$ be arbitrary points in $\mathcal{T}$.

$$\begin{aligned}
\frac{|u^*(X_1)-u^*(X_2)|}{|X_1-X_2|^\beta} &= \frac{\left|\frac{u(K)-u(J)}{|K-J|}(x_1-x_2) + \frac{2u(L)-u(K)-u(J)}{\sqrt{3}|K-J|}(y_1-y_2)\right|}{|X_1-X_2|^\beta} \\
&\leq \frac{|u(J)-u(K)|}{|K-J|^\beta} + \frac{|2u(L)-u(J)-u(K)|}{\sqrt{3}|K-J|^\beta} \\
&\leq 11|u|_{S,\beta} + \frac{2|u(L)-u(Q)| + 2|u(Q)-u(P)| + |u(P)-u(J)| + |u(P)-u(K)|}{\sqrt{3}|K-J|^\beta} \\
&\leq 11|u|_{S,\beta} + \frac{1}{\sqrt{3}}\left(\frac{2\cdot 3^\beta |u(L)-u(Q)|}{|L-Q|^\beta} + \frac{2\cdot 3^{\beta/2}|u(Q)-u(P)|}{|Q-P|^\beta}\right. \\
&\qquad \left. + \frac{|u(P)-u(J)|}{|P-J|^\beta} + \frac{|u(P)-u(K)|}{|P-K|^\beta}\right) \\
&\leq 11|u|_{S,\beta} + \frac{1}{\sqrt{3}}\left(66|u|_{S,\beta} + 4|u|_{S,\beta} + 11|u|_{S,\beta} + 11|u|_{S,\beta}\right) \\
&\leq 65|u|_{S,\beta}.
\end{aligned}$$

If $Q = P$ then:

$$\begin{aligned}
\frac{|u^*(X_1) - u^*(X_2)|}{|X_1 - X_2|^\beta} &\leq \frac{|u(J) - u(K)|}{|K - J|^\beta} + \frac{|2u(L) - u(J) - u(K)|}{\sqrt{3}|K - J|^\beta} \\
&\leq 11|u|_{S,\beta} + \frac{2|u(L) - u(P)| + |u(P) - u(J)| + |u(P) - u(K)|}{\sqrt{3}|K - J|^\beta} \\
&\leq 11|u|_{S,\beta} + \frac{1}{\sqrt{3}}\left(\frac{2 \cdot 3^\beta |u(L) - u(P)|}{|L - P|^\beta} + \frac{|u(P) - u(J)|}{|P - J|^\beta} + \frac{|u(P) - u(K)|}{|P - K|^\beta}\right) \\
&\leq 11|u|_{S,\beta} + \frac{1}{\sqrt{3}}\left(66|u|_{S,\beta} + 11|u|_{S,\beta} + 11|u|_{S,\beta}\right) \\
&\leq 62|u|_{S,\beta}.
\end{aligned}$$

Hence $\dfrac{|u^*(X) - u^*(Y)|}{|X - Y|^\beta} \leq 65|u|_{S,\beta}$. □

This lemma corresponds to those transition triangles where the value of u_n^* at two vertices is determined by the function u_{n-1}^*, and the value at the third vertex is determined by the sidecar triangles. See Figure 2.11B.

Lemma 2.1.9. *Given a triangle $\mathcal{T}$ with vertices J, K, and L, and a function u defined at points J, K and L such that*

$$\frac{|u(J) - u(K)|}{|J - K|^\beta} \leq 11|u|_{S,\beta}$$

where $\beta \leq 1$. Suppose we are also given two points P and Q, such that

$$\frac{|u(P) - u(J)|}{|P - J|^\beta} \leq 11|u|_{S,\beta}$$

$$\frac{|u(P) - u(K)|}{|P - K|^\beta} \leq 11|u|_{S,\beta}$$

$$\frac{|u(P) - u(Q)|}{|P - Q|^\beta} \leq |u|_{S,\beta}$$

and

$$\frac{|u(L) - u(Q)|}{|L - Q|^\beta} \leq 11|u|_{S,\beta}.$$

Moreover the following relationships hold $|J - K| = |J - L| = |L - K| = |L - Q|$, $|J - K| \geq \frac{1}{\sqrt{3}}|P - Q|$, $|J - K| \geq \frac{1}{3}|P - K|$, $|J - K| \geq \frac{1}{3}|P - J|$. Then there exists an

extension function u^* defined on $\mathcal{T}$ such that

$$\sup_{X,Y\in\mathcal{T}} \frac{|u^*(X)-u^*(Y)|}{|X-Y|^\beta} \leq 65|u|_{S,\beta}. \tag{2.10}$$

Remark 12. In this Lemma the value of u at L is determined by the extension function u_n^* in the sidecar region. This knowledge drives the assumption $|u(L)-u(Q)|/|Q-L|^\beta \leq 11|u|_{S,\beta}$. The value of u at points J and K are determined by the previous extension function u_{n-1}^* and J and K are both elements of the same triangle $\mathcal{T} \in T_{SC}^{n-1}$. These relationships drive both the estimates and geometrical assumptions (e.g. the distance between points) in the theorem statement.

Remark 13. For some transition triangles of this type, the scenario of Lemma 2.1.8 may also occur where $P \in V^{n-1}$. As in the previous lemma, we set $Q = P$ and observe that the estimates and geometrical constraints still hold.

Proof. The proof of this lemma proceeds in a manner similar to the proof of Lemma 2.1.8. □

This lemma corresponds to those transition triangles where the value for u_n^* is determined by the sidecar triangles at all three vertices. This is shown in Figure 2.11C.

Lemma 2.1.10. *Given a triangle $\mathcal{T}$ with vertices J, K, and L, a function u defined at points J, K and L such that*

$$\frac{|u(J)-u(K)|}{|J-K|^\beta} \leq 11|u|_{S,\beta}$$

and

$$\frac{|u(K)-u(L)|}{|K-L|^\beta} \leq 11|u|_{S,\beta}$$

where $\beta \leq 1$. See Figure 2.11C for a visual representation. Then, there exists an extension function u^* defined on $\mathcal{T}$ such that

$$\sup_{X,Y\in\mathcal{T}} \frac{|u^*(X)-u^*(Y)|}{|X-Y|^\beta} \leq 31|u|_{S,\beta}. \tag{2.11}$$

Proof. We begin by letting u^* be the affine function defined by the value of u at the three vertices of the triangle. We now check that u^* satisfies the estimate (2.11).

By Remark 7 we may assume $\mathcal{T}$ is a triangle with K located at the origin and J located on the x-axis. It can easily be checked that

$$u^*(X) = \frac{u(K) - u(J)}{|K - J|}x + \frac{2u(L) - u(K) - u(J)}{\sqrt{3}|K - J|}y + u(J).$$

Let $X_1 = (x_1, y_1)$ and $X_2 = (x_2, y_2)$ be arbitrary points in $\mathcal{T}$.

$$\begin{aligned}
\frac{|u^*(X_1) - u^*(X_2)|}{|X_1 - X_2|^\beta} &= \frac{\left|\frac{u(K)-u(J)}{|K-J|}(x_1 - x_2) + \frac{2u(L)-u(K)-u(J)}{\sqrt{3}|K-J|}(y_1 - y_2)\right|}{|X_1 - X_2|^\beta} \\
&\leq \frac{|u(K) - u(J)|}{|K - J|^\beta} + \frac{|2u(L) - u(K) - u(J)|}{\sqrt{3}|K - J|^\beta} \\
&\leq 11|u|_{S,\beta} + \frac{2|u(L) - u(K)| + |u(K) - u(J)|}{\sqrt{3}|K - J|^\beta} \\
&\leq 11|u|_{S,\beta} + \frac{1}{\sqrt{3}}\left(\frac{2|u(L) - u(K)|}{|L - K|^\beta} + \frac{|u(K) - u(J)|}{|K - J|^\beta}\right) \\
&\leq 11|u|_{S,\beta} + \frac{1}{\sqrt{3}}\left(22|u|_{S,\beta} + 11|u|_{S,\beta}\right) \\
&\leq 31|u|_{S,\beta}.
\end{aligned}$$

Hence $\dfrac{|u^*(X) - u^*(Y)|}{|X - Y|^\beta} \leq 31|u|_{S,\beta}$. □

We now present a lemma similar to Lemma 2.1.7 except here we consider two points in $T^n_{SC} \cup T^n_{TR}$. (The white and red region in Figure 2.2).

Lemma 2.1.11. *Let n be fixed, V^n a prefractal set and given a function u defined on the set V^n such that*

$$\frac{|u(P) - u(Q)|}{|P - Q|^\beta} \leq |u|_{S,\beta}$$

for all $P, Q \in V^n$ and for some $\beta \leq 1$. Let u^*_n be an extension to the domain ω as defined in Definition 3. Then for any X, Y in $T^n_{SC} \cup T^n_{TR}$ the following holds

$$\frac{|u^*_n(X) - u^*_n(Y)|}{|X - Y|^\beta} \leq 396\,|u|_{S,\beta}\,. \tag{2.12}$$

Proof. We begin by defining C_{MTR} as the maximum Hölder constant for triangles in the transition region, specifically $C_{MTR} = 65|u|_{S,\beta}$. By $\mathcal{T}_X$ and $\mathcal{T}_Y$ we refer to the triangles containing the points X and Y respectively. We observe that if X and Y are elements

of the same triangle (i.e. $\mathcal{T}_X = \mathcal{T}_Y$) the inequality holds due to Lemmas 2.1.2-2.1.5 and 2.1.8-2.1.10. Moreover if X and Y are elements of two triangles that share one or more points, the inequality also holds by application of Lemma 2.1.6. We now consider the case where $\mathcal{T}_X \cap \mathcal{T}_Y = \emptyset$.

We observe that for any two points J and K in the sidecar region the following inequality holds by Lemma 2.1.7

$$\frac{|u_n^*(J) - u_n^*(K)|}{|J-K|^\beta} \leq 66\,|u|_{S,\beta} \tag{2.13}$$

Therefore if $X, Y \in T_{SC}^n$ then the estimate 2.12 holds by Lemma 2.1.7.

We now consider the case with $X, Y \in T_{TR}^n$. We let P_X be the point in $T_{SC}^n \cap \mathcal{T}_X$ closest to X (we know at least one such point exists). Similarly define P_Y to be the point in $T_{SC}^n \cap \mathcal{T}_Y$ closest to Y. Moreover if L is the length of the side of one triangle in our mesh (i.e. $L = 3^{-n}$) we have $|P_X - X| \leq L$, $|P_Y - Y| \leq L$, $|P_X - P_Y| \leq |P_X - X| + |X - Y| + |Y - P_Y|$ and $|X - Y| \geq \frac{\sqrt{3}}{2}L$. We then have,

$$\begin{aligned}
|u_n^*(X) - u_n^*(Y)| &\leq |u_n^*(X) - u_n^*(P_X)| + |u_n^*(P_X) - u_n^*(P_Y)| + |u_n^*(P_Y) - u_n^*(Y)| \\
&\leq C_{\mathcal{T}_X}|X - P_X|^\beta + 66\,|u|_{S,\beta}\,|P_X - P_Y|^\beta + C_{\mathcal{T}_Y}|P_Y - Y|^\beta \\
&\leq \max\{C_{MTR}, 66\,|u|_{S,\beta}\}(|X - P_X|^\beta + |P_X - P_Y|^\beta + |P_Y - Y|^\beta) \\
&\leq 66\,|u|_{S,\beta}\left[\left(\frac{2}{\sqrt{3}}|X - Y|\right)^\beta + \left(\frac{4}{\sqrt{3}} + 1\right)^\beta |X - Y|^\beta + \left(\frac{2}{\sqrt{3}}|X - Y|\right)^\beta\right] \\
&\leq 396\,|u|_{S,\beta}\,|X - Y|^\beta.
\end{aligned}$$

Finally we consider the case with $X \in T_{SC}^n$ and $Y \in T_{TR}^n$. Again we define P_Y to be the point in $T_{SC}^n \cap \mathcal{T}_Y$ closest to Y. (There is no need to define P_X since $X \in T_{SC}^n$). Moreover if L is the length of the side of one triangle in our mesh (i.e. $L = 3^{-n}$) we

have $|P_Y - Y| \leq L$, $|X - P_Y| \leq |X - Y| + |Y - P_Y|$ and $|X - Y| \geq \frac{\sqrt{3}}{2}L$. We then have,

$$\begin{aligned}
|u_n^*(X) - u_n^*(Y)| &\leq |u_n^*(X) - u_n^*(P_Y)| + |u_n^*(P_Y) - u_n^*(Y)| \\
&\leq 66\,|u|_{S,\beta}\,|X - P_Y|^\beta + C_{\mathcal{T}_Y}|P_Y - Y|^\beta \\
&\leq \max\{C_{MTR}, 66\,|u|_{S,\beta}\}(|X - P_Y|^\beta + |P_Y - Y|^\beta) \\
&\leq 66\,|u|_{S,\beta}\left[\left(1 + \frac{2}{\sqrt{3}}\right)^\beta |X - Y|^\beta + \left(\frac{2}{\sqrt{3}}|X - Y|\right)^\beta\right] \\
&\leq 220\,|u|_{S,\beta}\,|X - Y|^\beta.
\end{aligned}$$

Therefore for $X, Y \in T_{SC}^n \cup T_{TR}^n$ estimate 2.12 holds. □

This lemma considers the Hölder estimate on an individual triangle $\mathcal{T}$ of the triangulation T^n of ω.

Lemma 2.1.12. *Let T^n be the induced triangulation of ω for the extension function u_n^*, then for any X, Y in a single triangle $\mathcal{T} \in T^n$ the following holds*

$$\frac{|u_n^*(X) - u_n^*(Y)|}{|X - Y|^\beta} \leq 65\,|u|_{S,\beta}\,. \tag{2.14}$$

Proof. If $\mathcal{T} \in T_{SC}^n \cup T_{TR}^n$ the inequality holds by Lemmas 2.1.2-2.1.5 and 2.1.8-2.1.10. We now consider the case when $\mathcal{T} \in T_{EX}^n$ (the blue region of Figure 2.2). We identify by m the iteration where the value of $u_n^*(\mathcal{T})$ was last set, that is to say $u_m^*(X) \neq u_{m-1}^*(X)$ for some $X \in \mathcal{T}$ but $u_m^*(X) = u_{m+i}^*(X)$ where $1 \leq i \leq n - m$ for all $X \in \mathcal{T}$. We identify by $\mathcal{T}_m$ the triangle from the triangulation T^m which contains $\mathcal{T}$.

By construction of the extension function in ω, $\mathcal{T}_m \in T_{SC}^m \cup T_{TR}^m$. Therefore for $A, B \in \mathcal{T}_m$

$$\frac{|u_m^*(A) - u_m^*(B)|}{|A - B|^\beta} \leq 65|u|_{S,\beta}.$$

Since $\mathcal{T} \subset \mathcal{T}_m$, for X, Y in $\mathcal{T}$ the following holds

$$\frac{|u_m^*(X) - u_m^*(Y)|}{|X - Y|^\beta} \leq 65|u|_{S,\beta}.$$

We therefore have for $X, Y \in \mathcal{T}$

$$\frac{|u_n^*(X) - u_n^*(Y)|}{|X-Y|^\beta} = \frac{|u_m^*(X) - u_m^*(Y)|}{|X-Y|^\beta} \leq 65|u|_{S,\beta}.$$

□

The next Lemma considers the step u_0^* to u_1^* illustrated in Figure 2.5.

Lemma 2.1.13. *Let $n = 1$ and given a function u defined on the prefractal set V^1 such that*

$$\frac{|u(P) - u(Q)|}{|P-Q|^\beta} \leq |u|_{S,\beta}$$

for all $P, Q \in V^1$ and for some $\beta \leq 1$. Let u_1^* be the first extension to the subdomain ω as defined in Definition 3, then for any X, Y in ω the following holds

$$\frac{|u_1^*(X) - u_1^*(Y)|}{|X-Y|^\beta} \leq 820\,|u|_{S,\beta}\,. \tag{2.15}$$

Proof. First we make a few definitions. We define C_{MSC} as the maximum sidecar constant from Lemmas 2.1.2-2.1.5, specifically $C_{MSC} \leq 11|u|_{S,\beta}$. We define C_{MTR} as the maximum transition triangle constant from Lemmas 2.1.8-2.1.10, specifically $C_{MTR} \leq 65|u|_{S,\beta}$. Clearly if X, Y are elements of the same triangle, or if X, Y are in two separate triangles that share one or more points, then estimate 2.15 holds. If $X, Y \in T_{SC}^n \cup T_{TR}^n$ then estimate 2.15 holds by Lemma 2.1.11. We now consider the case where X is in $T_{SC}^n \cup T_{TR}^n$ and Y is in $T_{EX}^n = \omega \setminus (T_{SC}^n \cup T_{TR}^n)$.

We let P_X be the point in $T_{SC}^n \cap \mathcal{T}_X$ such that $|P_X - X|$ is minimized. (Note that if $X \in T_{SC}^n$, than $P_X = X$). Moreover we identify by Q_X the element of V^1 closest to the point P_X and by Q_Y the element of V^0 closest to Y. (We recall that when u_0^* was constructed every point in ω was an element of the sidecar region). We let L be the length of the side of a triangle in induced triangulation T^1. (i.e. $L = |A - B|/3 = 1/3$) and observe that $|X - P_X| \leq L$, $|P_X - Q_X| \leq L$ and $|Q_Y - Y| \leq 3L$. We also observe

that $|X-Y| \geq \frac{\sqrt{3}}{2}L$. We then have:

$$\begin{aligned}
|u_1^*(X) - u_1^*(Y)| &= |u_1^*(X) - u_0^*(Y)| \\
&\leq C_{MTR}|X-P_X|^\beta + C_{MSC}|P_X - Q_X|^\beta + |u|_{S,\beta}|Q_X - Q_Y|^\beta + C_{MSC}|Q_Y - Y|^\beta \\
&\leq \max\{C_{MTR}, C_{MSC}, |u|_{S,\beta}\}(|X-P_X|^\beta + |P_X - Q_X|^\beta + |Q_X - Q_Y|^\beta + |Q_Y - Y|^\beta) \\
&\leq 65|u|_{S,\beta}(|X-P_X|^\beta + |P_X - Q_X|^\beta + |Q_X - Q_Y|^\beta + |Q_Y - Y|^\beta) \\
&\leq 65|u|_{S,\beta}\left[\left(\frac{2}{\sqrt{3}}|X-Y|\right)^\beta + \left(\frac{2}{\sqrt{3}}|X-Y|\right)^\beta + |Q_X - Q_Y|^\beta + \left(\frac{6}{\sqrt{3}}|X-Y|\right)^\beta\right] \\
&\leq 65|u|_{S,\beta}\left[2\left(\frac{2}{\sqrt{3}}\right)^\beta |X-Y|^\beta + \left(2\left(\frac{2}{\sqrt{3}}\right) + 1 + \left(\frac{6}{\sqrt{3}}\right)\right)^\beta |X-Y|^\beta + \right. \\
&\qquad \left. + \left(\frac{6}{\sqrt{3}}\right)^\beta |X-Y|^\beta\right] \\
&\leq 65|u|_{S,\beta}\left[2\left(\frac{2}{\sqrt{3}}\right)^\beta |X-Y|^\beta + \left(2\left(\frac{2}{\sqrt{3}}\right)^\beta + 1^\beta + \left(\frac{6}{\sqrt{3}}\right)^\beta\right)|X-Y|^\beta + \right. \\
&\qquad \left. + \left(\frac{6}{\sqrt{3}}\right)^\beta |X-Y|^\beta\right] \\
&\leq 65|u|_{S,\beta}\left[4\left(\frac{2}{\sqrt{3}}\right)^\beta + 1^\beta + 2\left(\frac{6}{\sqrt{3}}\right)^\beta\right]|X-Y|^\beta \\
&\leq 65|u|_{S,\beta} \cdot 12.6|X-Y|^\beta \\
&\leq 820|u|_{S,\beta}|X-Y|^\beta.
\end{aligned}$$

□

2.1.5 Main Results

Proposition 2.1.14. *Given a prefractal Koch set, V^n, with iteration number $n \geq 1$ and a function u defined at the vertices of the curve that satisfies*

$$\frac{|u(X) - u(Y)|}{|X-Y|^\beta} \leq |u|_{S,\beta}$$

for all $X, Y \in V^n$ and for some $\beta \leq 1$. Let u_n^* be the nth extension to the domain ω. Then for any X, Y in ω the following holds

$$\frac{|u_n^*(X) - u_n^*(Y)|}{|X - Y|^\beta} \leq 1300\,|u|_{S,\beta}\,. \tag{2.16}$$

Remark 14. For any X in $T_{EX}^n = \omega \setminus (T_{SC}^n \cup T_{TR}^n)$ (i.e the blue region in Figure 2.2) $u_n^*(X) = u_{n-1}^*(X)$. This observation will be especially relevant in the proof below.

Proof. By Lemma 2.1.13, estimate 2.16 is true for the extension function u_1^*. Let u_{n-1}^* be the $(n-1)th$ extension to the domain ω and we assume that the following estimate holds for all X, Y in ω

$$\frac{|u_{n-1}^*(X) - u_{n-1}^*(Y)|}{|X - Y|^\beta} \leq 1300\,|u|_{S,\beta}\,. \tag{2.17}$$

We now show that the estimate holds for u_n^* with identical constant on the right hand side.

For ease of notation we set C_{MSC} to be the maximum sidecar constant from Lemmas 2.1.2-2.1.5, specifically $C_{MSC} \leq 11|u|_{S,\beta}$ and C_{MTR} to be the maximum transition triangle constant from Lemmas 2.1.8-2.1.10, specifically $C_{MTR} \leq 65|u|_{S,\beta}$. We also recall the definition of ω as the polygonal domain with vertices $A = (0,0)$, $B = (1,0)$, $C = \left(\frac{1}{2}, \frac{\sqrt{3}}{2}\right)$, $D = \left(\frac{1}{2}, -\frac{\sqrt{3}}{2}\right)$.

By Lemma 2.1.11 for $X, Y \in T_{SC}^n \cup T_{TR}^n$ estimate 2.16 holds. We now consider the case with $X \in T_{SC}^n \cup T_{TR}^n$ and $Y \in T_{EX}^n$. From Lemma 2.1.12, any two points X', Y' in a triangle $\mathcal{T}$ of the triangulation T^n of ω the following estimate

$$\frac{|u_n^*(X') - u_n^*(Y')|}{|X' - Y'|^\beta} \leq 65|u|_{S,\beta}$$

holds. Combining this estimate with Lemma 2.1.6, estimate 2.16 holds for any two triangles in T^n that share one or more points. We now assume that X and Y are in two distinct triangles which do not share any points. See Figure 2.12 for a sample location of the points X and Y.

We begin by observing that the values of u_n^* in T_{EX}^n are historically stratified. This

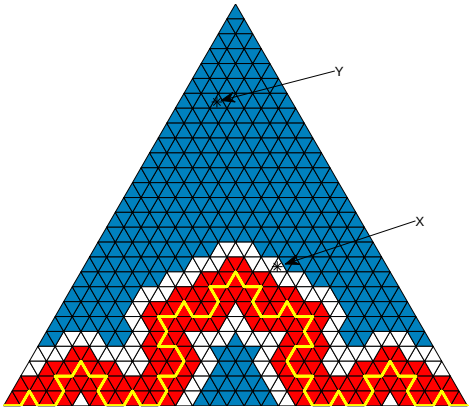

Figure 2.12: A sample location of X and Y, in the extension u_3^*. (Only half the domain is shown, but X and Y could be located anywhere in the domain).

stratification can be observed by noting that the values of u_n^* at points in this region are layered according to when the value of u_n^* was last set. Specifically T_{EX}^n can be broken into subregions where the value of u_n^* was last set at iterations $n-1$,$n-2$, $\ldots, 0$. The stratification for $n = 3$ is shown in Figure 2.13.

We identify by $m_X = n$ the current iteration (recall $X \in T_{SC}^n \cup T_{TR}^n$ so the value of $u_n^*(X)$ is set at this iteration). We identify by $\mathcal{T}_X$ the triangle from T^{m_X} which contains the point X. We let P_X be the point in $T_{SC}^{m_X} \cap \mathcal{T}_X$ such that $|P_X - X|$ is minimized. (We note that if $X \in T_{SC}^{m_X}$ then $P_X = X$). We also identify by Q_X the point in V^{m_X} such that $|Q_X - P_X|$ is minimized. We let L be the length of the side in T^{m_X} (i.e. $L = 3^{-n}$) and observe that $|X - P_X| \leq 3^{(n-m_X)}L = L$ and $|P_X - Q_X| \leq 3^{(n-m_X)}L = L$. (See Figure 2.14).

Similarly for Y, we identify by m_Y the iteration where the value of $u_n^*(Y)$ was last set, that is to say $u_{m_Y}^*(Y) \neq u_{m_Y-1}^*(Y)$ but $u_{m_Y}^*(Y) = u_{m_Y+i}^*(Y)$ where $1 \leq i \leq n - m_Y$. We identify by $\mathcal{T}_Y$ the triangle from T^{m_Y} where the value of Y was last set. We let $P_Y \in T_{SC}^{m_Y} \cap \mathcal{T}_Y$ such that $|P_Y - Y|$ is minimized. (We note that if $Y \in T_{SC}^{m_Y}$ then $P_Y = Y$). We also identify by Q_Y the point in V^{m_Y} that minimizes $|Q_Y - P_Y|$. Using the above definition of L (i.e. $L = 3^{-n}$) we observe that $|Y - P_Y| \leq 3^{(n-m_Y)}L$ and

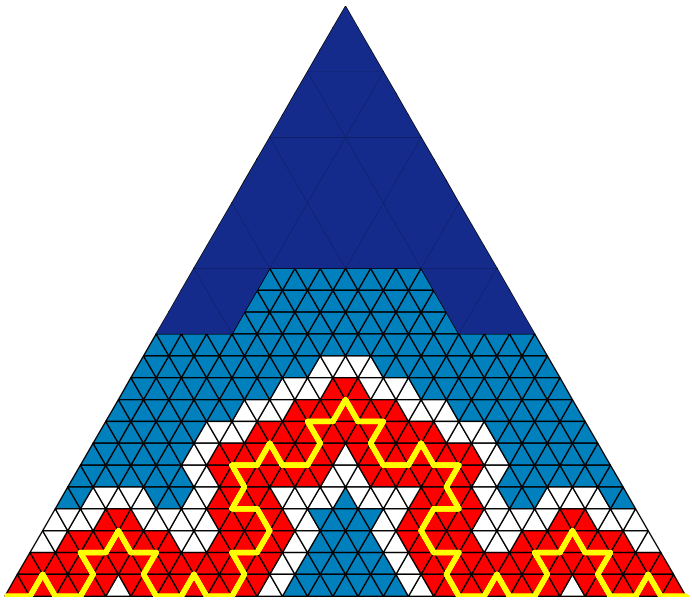

Figure 2.13: In this figure the historical stratification is seen. The value of u_n^* in the dark blue triangles are set by u_1^*, and the value of u_n^* in the light blue triangles are set by u_2^*.

$|P_Y - Q_Y| \leq 3^{(n-m_Y)}L$. (See Figure 2.15).

We note that $V^{m_Y} \subset V^{m_X} = V^n$ and now make an important observation concerning the relationship between $|X - Y|$ and $n - m_Y$:

$$|X - Y| \geq 3^{(n-m_Y-1)}\frac{\sqrt{3}}{2}L.$$

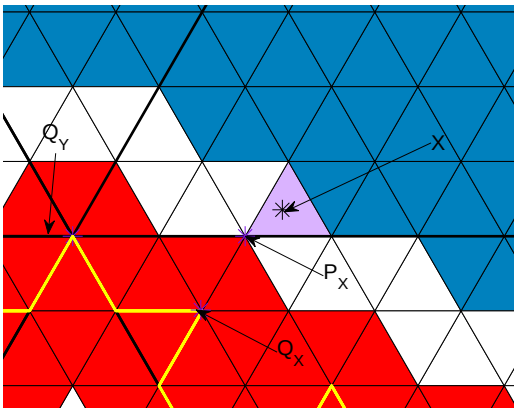

Figure 2.14: The identification of triangle $\mathcal{T}_X$ (the purple triangle) and points P_X and Q_X with respect to X.

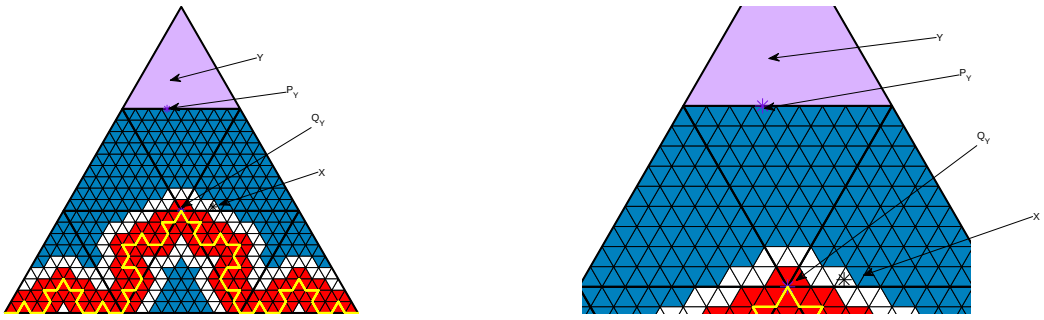

(a) Larger View

(b) Zoomed View

Figure 2.15: The identification of triangle $\mathcal{T}_Y$ (the purple triangle) and points P_Y and Y_Y with respect to Y.

Having made this observation:

$$
\begin{aligned}
|u_n^*(X) - u_n^*(Y)| &= |u_{m_X}^*(X) - u_{m_Y}^*(Y)| \\
&\leq |u_{m_X}^*(X) - u_{m_X}^*(P_X)| + |u_{m_X}^*(P_X) - u_{m_X}^*(Q_X)| + |u_{m_X}^*(Q_X) - u_{m_Y}^*(Q_Y)| \\
&\qquad + |u_{m_Y}^*(Q_Y) - u_{m_Y}^*(P_Y)| + |u_{m_Y}^*(P_Y) - u_{m_Y}^*(Y)| \\
&\leq C_{MTR}|X - P_X|^\beta + C_{MSC}|P_X - Q_X|^\beta + |u|_{S,\beta}|Q_X - Q_Y|^\beta \\
&\qquad + C_{MSC}|Q_Y - P_Y|^\beta + C_{MTR}|P_Y - Y|^\beta \\
&\leq \max\{C_{MTR}, C_{MSC}, |u|_{S,\beta}\}(|X - P_X|^\beta + |P_X - Q_X|^\beta + |Q_X - Q_Y|^\beta \\
&\qquad + |Q_Y - P_Y|^\beta + |P_Y - Y|^\beta) \\
&\leq 65|u|_{S,\beta}(|X - P_X|^\beta + |P_X - Q_X|^\beta + |Q_X - Q_Y|^\beta + |P_Y - Q_Y|^\beta + |P_Y - Y|^\beta) \\
&\leq 65|u|_{S,\beta}\left[\left(\frac{2}{3^{(n-m_Y-1)}\sqrt{3}}|X - Y|\right)^\beta + \left(\frac{2}{3^{(n-m_Y-1)}\sqrt{3}}|X - Y|\right)^\beta + |Q_X - Q_Y|^\beta + \right. \\
&\qquad \left. + \left(\frac{2 \cdot 3^{(n-m_Y)}}{3^{(n-m_Y-1)}\sqrt{3}}|X - Y|\right)^\beta + \left(\frac{2 \cdot 3^{(n-m_Y)}}{3^{(n-m_Y-1)}\sqrt{3}}|X - Y|\right)^\beta\right] \\
&\leq 65|u|_{S,\beta}\left[2\left(\frac{2}{\sqrt{3}}|X - Y|\right)^\beta + |Q_X - Q_Y|^\beta + 2\left(\frac{6}{\sqrt{3}}|X - Y|\right)^\beta\right] \\
&\leq 65|u|_{S,\beta}\left[2\left(\frac{2}{\sqrt{3}}\right)^\beta |X - Y|^\beta + \left(2\left(\frac{2}{\sqrt{3}}\right) + 1 + 2\left(\frac{6}{\sqrt{3}}\right)\right)^\beta |X - Y|^\beta \right. \\
&\qquad \left. + 2\left(\frac{6}{\sqrt{3}}\right)^\beta |X - Y|^\beta\right] \\
&\leq 65|u|_{S,\beta}\left[2\left(\frac{2}{\sqrt{3}}\right)^\beta |X - Y|^\beta + \left(2\left(\frac{2}{\sqrt{3}}\right)^\beta + 1^\beta + 2\left(\frac{6}{\sqrt{3}}\right)^\beta\right)|X - Y|^\beta \right. \\
&\qquad \left. + 2\left(\frac{6}{\sqrt{3}}\right)^\beta |X - Y|^\beta\right] \\
&\leq 65|u|_{S,\beta}\left[4\left(\frac{2}{\sqrt{3}}\right)^\beta + 1^\beta + 4\left(\frac{6}{\sqrt{3}}\right)^\beta\right]|X - Y|^\beta \\
&\leq 65|u|_{S,\beta} \cdot 20|X - Y|^\beta \\
&\leq 1300|X - Y|^\beta.
\end{aligned}
$$

Therefore $\dfrac{|u_n^*(X) - u_n^*(Y)|}{|X - Y|^\beta} \leq 1300|u|_{S,\beta}$ for all $X \in T_{SC}^n \cup T_{TR}^n$, and $Y \in T_{TR}^n$.

One final case remains to be considered, the case with $X, Y \in T_{EX}^n$ (the blue region of Figure 2.2). By Remark 14 we know that for all $X, Y \in T_{EX}^n$ that $u_n^*(X) = u_{n-1}^*(X)$ and $u_n^*(Y) = u_{n-1}^*(Y)$. We then apply our induction assumption (i.e. that the estimate holds for the $(n-1)th$ iteration), thereby giving us $\frac{|u_n^*(X) - u_n^*(Y)|}{|X-Y|^\beta} \leq 1300|u|_{S,\beta}$ for all $X, Y \in T_{EX}^n$. Combining the estimates for each specific case we arrive at $\frac{|u_n^*(X) - u_n^*(Y)|}{|X-Y|^\beta} \leq 1300|u|_{S,\beta}$ for all $X, Y \in \omega$. □

Proposition 2.1.15. *For every n and every $u_n \in C^\beta(V^n)$ we construct a linear extension operator Π_n that brings functions defined on V^n to functions defined on Ω which have the following properties for every $0 < \beta \leq 1$:*

1. $u_n \in C^\beta(V^n) \mapsto u_n^* \in C^\beta(\Omega)$,
2. $\|\Pi_n u_n\|_{\Omega,\beta} \leq 1302 \|u\|_{S,\beta}$.

Proof. By Proposition 2.1.14 we know that for X, Y in ω and u_n^* the following inequality holds:

$$\frac{|u_n^*(X) - u_n^*(Y)|}{|X-Y|^\beta} \leq 1300 \, |u|_{S,\beta} . \tag{2.18}$$

First we recall the definition of the domain γ found in Section 2.1.2 as a convex polygonal domain which contains ω. Section 2.1.2 also details the methodology to extend the function u_n^* to γ and then to Ω. Let X_1 and X_2 be arbitrary points in γ. Then

$$u_n^*(X_1) = v_n^*(X_1)\eta(X_1) = v_n^*(X_1')\eta(X_1)$$

where $X_1' \in \omega$. Similarly,

$$u_n^*(X_2) = v_n^*(X_2)\eta(X_2) = v_n^*(X_2')\eta(X_2)$$

where $X_2' \in \omega$. Moreover $|X_1 - X_2| \geq |X_1' - X_2'|$ and by geometric arguments $\frac{|\eta(X_1) - \eta(X_2)|}{|X_1' - X_2'|} \leq$

$\frac{2}{\sqrt{3}}$. Therefore,

$$\begin{aligned}
\frac{|u_n^*(X_1) - u_n^*(X_2)|}{|X_1 - X_2|^\beta} &= \frac{|v_n^*(X_1')\eta(X_1) - v_n^*(X_2')\eta(X_2)|}{|X_1 - X_2|^\beta} \\
&\leq \frac{|v_n^*(X_1')\eta(X_1) - v_n^*(X_2')\eta(X_2)|}{|X_1' - X_2'|^\beta} \\
&\leq \frac{\eta(X_1)|v_n^*(X_1') - v_n^*(X_2')|}{|X_1' - X_2'|^\beta} + \frac{v^*n(X_2')|\eta(X_1') - \eta(X_2')|}{|X_1' - X_2'|^\beta} \\
&\leq \frac{|v_n^*(X_1') - v_n^*(X_2')|}{|X_1' - X_2'|^\beta} + \sup_{X\in S}|u(X)|\frac{|\eta(X_1') - \eta(X_2')|}{|X_1' - X_2'|^\beta} \\
&\leq 1300\,|u|_{S,\beta} + \sup_{X\in S}|u(X)|\frac{|\eta(X_1') - \eta(X_2')|}{|X_1' - X_2'|}|X_1' - X_2'|^\beta \\
&\leq 1300\,|u|_{S,\beta} + \sup_{X\in S}|u(X)|\frac{2}{\sqrt{3}}(\sqrt{3})^\beta \\
&\leq 1300|u|_{S,\beta} + 2\,\|u\|_{S,\beta} \\
&\leq 1302\,\|u\|_{S,\beta}\,.
\end{aligned}$$

Since u_n^* is identically zero in $\mathbb{R}^2 \setminus \gamma$ we have an extension function u_n^* that is Hölder continuous and satisfies the estimate

$$|u_n^*|_{\overline{\Omega},\beta} \leq 1302\,\|u\|_{S,\beta}\,.$$

□

We now present the proof of the Theorem 2.0.2 for the Koch Curve.

Proof. We claim $\Pi : C^\beta(S) \mapsto C^\beta(\Omega)$. We begin by showing that $\|\Pi u\|_{\Omega,\beta} \leq C_1\,\|u\|_{S,\beta}$ and $\Pi u = \lim_{n\to\infty} \Pi_n(u|_{V^n})$ uniformly in Ω. We let u be a Hölder continuous function defined on the fractal curve S with exponent $\beta \leq 1$ and constant $C_0 = |u|_{S,\beta}$, (i.e. $|u(x) - u(y)| \leq C_0|x - y|^\beta \ \ \forall x, y \in S$). We recall that for a given n, V^n is a subset of the fractal S, and thus given a Hölder continuous function u on S we have $u_n \in C^\beta(V^n)$. From Proposition 2.1.15 we can construct an extension function u_n^* on Ω such that

$$\frac{|u_n^*(X) - u_n^*(Y)|}{|X - Y|^\beta} \leq 1302\,\|u\|_{S,\beta} \tag{2.19}$$

for all $X, Y \in \Omega$. (Here we emphasize that the estimate is independent of n.) Therefore

each extension u_n^* is equicontinuous on Ω. Moreover we know u is bounded on S with $|u(X)| \leq \|u\|_{S,\beta}$ for all $X \in S$. We therefore can say that $|u_n^*(X)| \leq \|u\|_{S,\beta}$ for all $X \in \Omega$. By the Arzelà-Ascoli theorem there exists a subsequence which converges uniformly to a Hölder continuous function u^*. We now easily show that uniform convergence preserves the Hölder exponent β and constant $1302\,\|u\|_{S,\beta}$.

$$\frac{|u^*(X) - u^*(Y)|}{|X - Y|^\beta} \leq \frac{|u^*(X) - u_n^*(X)| + |u_n^*(X) - u_n^*(Y)| + |u_n^*(Y) - u^*(Y)|}{|X - Y|^\beta} \tag{2.20}$$

Since u_n^* converges to u uniformly given $\epsilon > 0$ there exists N such that for all $n \geq N, \quad |u^*(X) - u_n^*(X)| < \epsilon$ for all X in Ω. Therefore equation 2.20 is less then or equal to

$$\frac{2\epsilon + |u_n^*(X) - u_n^*(Y)|}{|X - Y|^\beta}.$$

Since ϵ can be arbitrarily small we have

$$\frac{|u^*(X) - u^*(Y)|}{|X - Y|^\beta} \leq 1302\,\|u\|_{S,\beta}\,.$$

Hence we have a function u^* which is Hölder continuous everywhere in Ω and satisfies the estimate

$$|u^*|_{\overline{\Omega},\beta} \leq 1302\,\|u\|_{S,\beta}\,. \tag{2.21}$$

Moreover, $u^*(X) = u(X)$ for all $X \in V^\infty$ and, due to the density of V^∞ in S, corresponds with u at every point on S.

We now show $\sup_{X\in\Omega} |\Pi_n u_n(X) - \Pi_{n+p} u_{n+p}(X)| \leq C_2\,\|u\|_{S,\beta}\,3^{-n}$. Fix $p > 0$. We observe that by construction, two consecutive extension functions (u_n^* and u_{n+1}^*) differ on ω only in the sidecar and transition triangle regions of the u_{n+1}^* extension. We will assume that $X \in T_{SC}^n \cup T_{TR}^n$ or in the equivalent area of γ. Moreover by Y we denote the element of V^n closest to X.

$$\begin{aligned}
|u_n^*(X) - u_{n+p}^*(X)| &\leq |u_n^*(X) - u(Y)| + |u(Y) - u_{n+p}^*(X)| \\
&\leq 2620\,\|u\|_{S,\beta}\,|X - Y|^\beta \\
&\leq 2620\,\|u\|_{S,\beta}\,3^{-\beta n}.
\end{aligned}$$

□

2.2 Sierpinski Gasket

The organization of this section will closely follow the organization of the previous section. First, we will introduce an intermediate domain ω (specific to the Sierpinski gasket) and describe the conformal triangulation of ω induced by the prefractal. Then we will detail the methodology for extending the function u to Ω. Next we will present a few preliminary Lemmas and their associated proofs. We then consider the iterative process used to build up the extension function. Finally, we will show Theorem 2.0.2 for the Sierpinski gasket.

2.2.1 Induced Triangulation of an Intermediate Domain

We begin by describing the induced triangulation of an intermediate domain ω that will serve as the scaffolding for our extension. In this section, ω is defined as the polygonal domain with vertices D, E, and F where $D = (1/2, -\sqrt{3}/4)$, $E = (3/2, \sqrt{3}/2)$, and $F = (-1/2, \sqrt{3}/2)$. We also define S to be the Sierpinski gasket embedded in ω with vertices $A = (0, 0)$, $B = (1, 0)$ and $C = (1/2, \sqrt{3}/2)$. In order to provide a scaffolding for our extension we use the triangulation induced by the prefractal set ($T_{V^n} = T^n$) on the domain ω. This triangulation, T^n, is composed of equilateral triangles with side length 2^{-n}, and is equivalent to filling the domain ω with $(2^{n+1})^2$ congruent triangles.(See Figure 2.16).

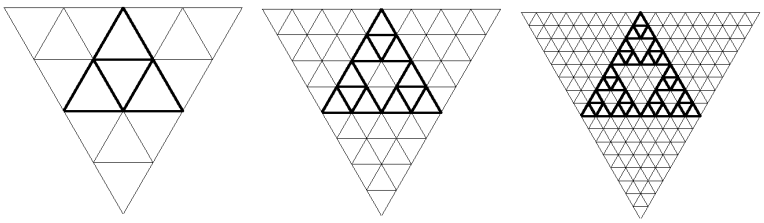

Figure 2.16: The first three iterations of the Sierpinski gasket and the first three induced triangulations of a domain ω.

2.2.2 A Methodology for the Extension

Similar to the Koch curve we will construct the extension function on the domain Ω in an iterative manner. Recall u_n^* refers to the extension function determined by the

prefractal operator Π_n, that is to say $u_n^* = \Pi_n u_n$ (also recall $u_n = u|_{V^n}$). We will also use the same definitions of *sidecar* triangles and *transition* triangles as for the Koch curve (see Definitions 1 and 2). As before we begin by constructing a base extension function u_0^* correspondent to the triangulation T^0; we then construct the function u_1^*, using information from both u_1 and u_0^*. We continue in a step by step manner constructing the extension function u_n^* from u_n and u_{n-1}^*.

Before continuing we will define an operation that will be used frequently, the operation of *completing the triangle.* For this operation we consider a single element of our triangulation and assume that the function u is defined at two of the vertices of the triangle. We extend u to the third vertex of the triangle, by setting $u^*(z)$ to the average of the values of the u at the other two vertices of the triangle x and y. That is to say we set

$$u^*(z) = \frac{u(x) + u(y)}{2}.$$

We then set the extension function u^* to be the affine function on the triangle defined by the values of the function at the three vertices.

Extending to ω

We divide the intermediate domain into three subdomains T_{SC}^n, T_{TR}^n and T_{EX}^n in order to simplify the construction of u_n^*. The subdomain T_{SC}^n is composed of the set of sidecar triangles of a given set V^n. The subdomain T_{TR}^n is composed of the set of transition triangles of V^n. Finally, the subdomain T_{EX}^n is the set of all the triangles in the domain ω which are neither sidecar triangles nor transition triangles (i.e $T_{EX}^n = \omega \setminus (T_{SC}^n \cup T_{TR}^n)$). This division is illustrated in Figure 2.17 for the Sierpinski gasket where the red triangles are elements of T_{SC}^n, the white triangles are elements of T_{TR}^n, and the blue triangles are elements of T_{EX}^n. We will consider these three domains separately when constructing u_n^*.

The Base Extension:

We first consider the special case of constructing u_0^* on ω. For this case we do not subdivide ω into the three subdomains, but rather treat ω as the union of four sidecar triangles. We perform the operation of completing the triangle on three of the triangles: ABD, ACF, and BCE. On the fourth triangle (ABC) we set u_0^* to be the affine func-

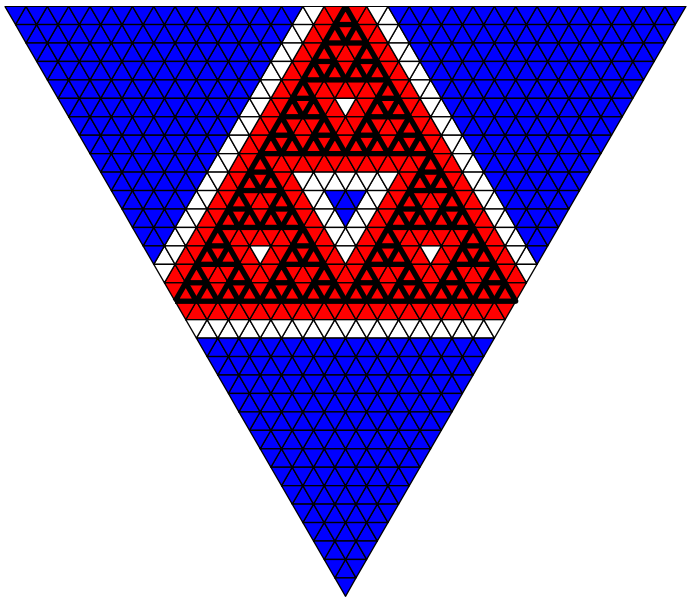

Figure 2.17: The red triangles are the sidecar triangles (T^n_{SC}), the white triangles are the transition triangles (T^n_{TR}) and the blue triangles are external triangles (T^n_{EX}).

tion defined by the value of u at its three vertices. Thus we have determined the value of u^*_0 at every point in ω (see Figure 2.19).

Extending to T^n_{SC}

First we identify the set V^n and the subdomain T^n_{SC}. We observe that each triangle in T^n_{SC} has one or more vertices which are elements of V^n and hence have values of u defined at these points. Therefore, the value of u^*_n is predetermined at one, two or three vertices of each triangle. We divide the sidecar triangles into two groups. The first group (primary sidecar triangles) will contain those sidecar triangles which have two or three vertices which are elements of V^n. The second group (secondary sidecar triangles) will contain those sidecar triangles which have only one vertex which is an element of V^n. (See Figure 2.18). We first extend u_n to u^*_n in the primary sidecar triangles. We do this by identifying the vertices in the primary sidecar triangles where u^*_n is undetermined. Let J be one such vertex, and let $\mathcal{T}_J$ be the set of primary sidecar triangles which have

J as a vertex. If $\mathcal{T}_J$ contains only one triangle we preform the operation of completing the triangle to define the value of u_n^* on that triangle. If $\mathcal{T}_J$ contains more than one triangle we set u_n^* at J to be the *average* of the values of u at each element of V^n which is also a vertex of one of the triangles of $\mathcal{T}_J$. (See Figure 2.22 for an illustration). Once the value of u_n^* has been determined at every vertex we set the extension function u_n^* to be the affine function on the triangle determined by the values of u_n^* at these vertices.

We now extend u_n^* to the secondary sidecar triangles. We observe that the value of u_n^* is predetermined at each vertex of the secondary sidecar triangles. We set the extension u_n^* on these triangles to be the affine function determined by the values of u_n^* at the vertices of the triangle.

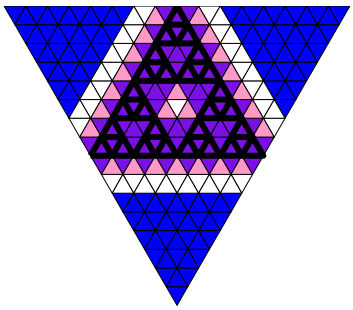

Figure 2.18: In this figure the sidecar triangles are shown. The dark purple triangles are the primary sidecar triangles and the light purple triangles are the secondary sidecar triangles.

Extending to T_{TR}^n

Prior to this step we have extended u_n to u_n^* in T_{SC}^n, and hence values for u_n^* are predetermined at every vertex common between T_{SC}^n and T_{TR}^n. Additionally, the function u_{n-1}^* is defined everywhere on the domain ω. Extension to T_{TR}^n is done on a triangle by triangle basis by setting the value of u_n^* to be equal to the value of u_{n-1}^* at any vertex where the value of u_n^* is not predetermined. We then set u_n^* to be the function which

is affine on the triangle and determined by the values of u_n^* at the three vertices of the triangle.

Extending to T_{EX}^n
The extension to T_{EX}^n is accomplished by setting u_n^* equal to u_{n-1}^* at every point in T_{EX}^n.

In this manner we proceed in an iterative fashion to construct each function u_n^* on ω correspondent to the set V^n. This is shown visually for steps $0 \to 1$ and $1 \to 2$ in Figures 2.19 and 2.20.

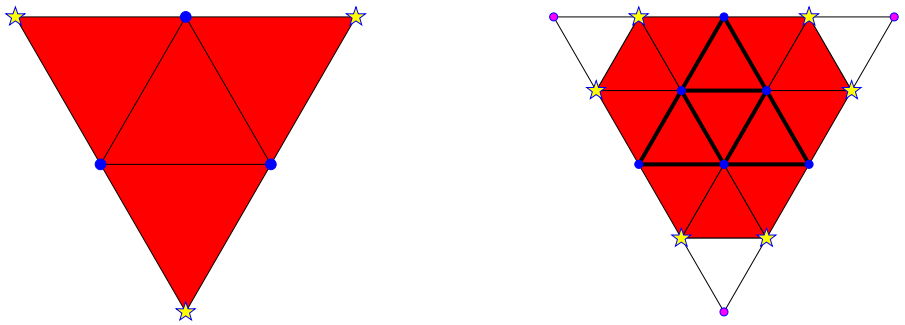

Figure 2.19: u_0^*, and u_1^*. The blue dots are points where u is defined. The values of u_1^* at the pink points come from u_0^*, and the yellow stars are values new to u_1^*.

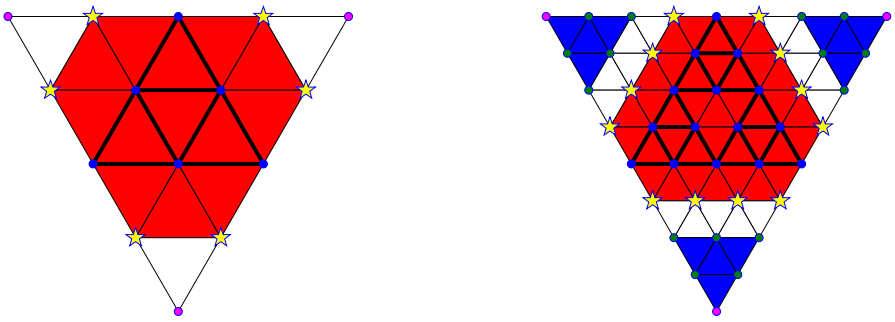

Figure 2.20: u_1^*, and u_2^*. The blue dots are points where u is defined. The values at the pink points come from u_0^*, the values at the green points are from u_1^* , and the yellow stars are values new to u_2^*.

Proposition 2.2.1. *The extension operator Π_n is linear*

Proof. The proof of this proposition for the Sierpinski gasket is identical to the proof of Proposition 2.1.1 for the Koch curve. □

Extending to Ω

We introduce an additional intermediate domain γ, where γ is the convex polygonal domain with vertices $G = (-3/2, \sqrt{3}/2)$, $H = (-(6-\sqrt{3})/4, \sqrt{3})$, $I = ((6+\sqrt{3})/4, \sqrt{3})$, $J = (5/2, \sqrt{3}/2)$, $K = (1, -\sqrt{3})$, and $L = (0, -\sqrt{3})$. We subdivide γ into 22 congruent triangles, four of which composed the domain ω. The function v_n^* is constructed on γ by a combination of operations of rotation, reflection and translation applied to the function u_n^* defined on the four triangles ABC, ABD, ACF, and BCE. These operations are shown visually in Figure 2.21. As in the Koch case if $u_n^* \in C^\beta(\omega)$, $v_n^* \in C^\beta(\gamma)$.

Again we utilize the standard finite element "hat" function in relationship to the 22 triangle coarse mesh. Recall, the function η_A corresponds to the function with value 1 at point A, zero on the boundary of the hexagon created by the six triangles with A as a vertex, and affine on each of the triangles. In a similar manner we create functions $\eta_B, \eta_C, \eta_D, \eta_E$, and η_F centered at points B, C, D, E, and F respectively. We set $\eta = \eta_A + \eta_B + \eta_C + \eta_D + \eta_E + \eta_F$, and observe that $\eta \in H^1(\gamma)$, $\eta(X) = 1$ for all $X \in \omega$, and $\eta(X) = 0$ for all $x \in \partial\gamma$. We define the function $z_n^*(X) = \eta(X) v_n^*(X)$ for $X \in \gamma$ and $z_n^*(X) = 0$ for $X \in \mathbb{R} \setminus \gamma$. We set the extension function u_n^* to z_n^* and restrict u_n^* to the given domain Ω.

2.2.3 Preliminary Results

The purpose of this section is to provide a few preliminary results needed for the proof of the Theorem 2.0.2 for the Sierpinski gasket. The first lemma is an example of the operation of completing the triangle. Lemmas 2.2.2-2.2.5 are related to the Hölder estimate on the four separate types of sidecar triangles in T_{SC}^n. (Figure 2.22 identifies each of these three triangle types). Lemma 2.2.6 considers the Hölder estimate on two or more triangles.

This Lemma corresponds to triangles labeled with a 1 in Figure 2.22 and shows the operation of completing the triangle.

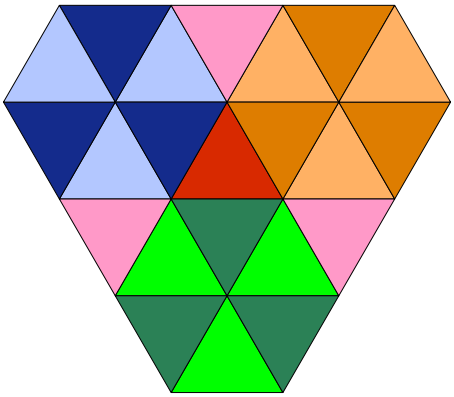

Figure 2.21: An illustration of γ and the 22 subtriangles. The green triangles are reflections and translations of ABD, the blue triangles are reflections and translations of ACF, the orange triangles are reflections and translations of BCE and the pink triangles are reflections and translations of ABC.

Lemma 2.2.2. *Given a triangle $\mathcal{T}$ with vertices P, Q, and J, and a function u defined at points P and Q such that*

$$\frac{|u(P) - u(Q)|}{|P - Q|^\beta} \leq |u|_{S,\beta}$$

where $\beta \leq 1$. Then there exists an extension function u^* defined on $\mathcal{T}$ such that

$$\sup_{X,Y \in \mathcal{T}} \frac{|u^*(X) - u^*(Y)|}{|X - Y|^\beta} \leq |u|_{S,\beta}. \tag{2.22}$$

Proof. We begin by constructing the extension function u^*, by prescribing its value at J. We set $u^*(J) = \frac{1}{2}(u(P) + u(Q))$ and let u^* be the affine function in the triangle defined by these three points. We now check that u^* satisfies the estimate (2.22).

By Remark 7 we may assume $\mathcal{T}$ is a triangle with P located at the origin and J is located on the x-axis. It can easily be checked that the function u^* satisfies

$$u^*(X) = \frac{u(Q) - u(P)}{|P - Q|} x + u(P).$$

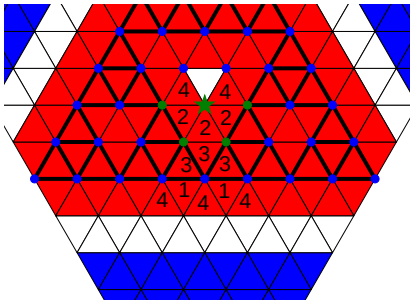

Figure 2.22: This figure illustrates the scenarios considered in Lemmas 2.2.2-2.2.5. The red triangles are the triangles under consideration. The blue (and green) dots are elements of V^n and thus have values of u defined at them. The green star represents a point where the value of the extension function is derived from the averaging the value of u at the four green dots. For reference, the white triangles are transition triangles and are handled in later lemmas.

Let $X_1 = (x_1, y_1)$ and $X_2 = (x_2, y_2)$ be arbitrary points in $\mathcal{T}$.

$$\begin{aligned}\frac{|u^*(X_1) - u^*(X_2)|}{|X_1 - X_2|^\beta} &= \frac{|u(Q) - u(P)||x_1 - x_2|}{|P - Q||X_1 - X_2|^\beta} \\ &\leq \frac{|u(Q) - u(P)|}{|P - Q|^\beta} \left(\frac{|x_1 - x_2|}{|P - Q|}\right)^{1-\beta} \left(\frac{|x_1 - x_2|}{|X_1 - X_2|}\right)^{\beta} \\ &\leq \frac{|u(Q) - u(P)|}{|P - Q|^\beta} \leq |u|_{S,\beta}.\end{aligned}$$

□

The following Lemma holds for any triangle labeled with a 2 in Figure 2.22.

Lemma 2.2.3. *Given a triangle $\mathcal{T}$ with vertices P, Q, and J, and a function u defined at the vertices of the prefractal V^n such that*

$$\frac{|u(A) - u(B)|}{|A - B|^\beta} \leq |u|_{S,\beta}$$

for all $A, B \in V^n$ and $\beta \leq 1$. Moreover $P, Q \in V^n$. Then there exists an extension

function u^* defined on $\mathcal{T}$ such that

$$\sup_{X,Y\in\mathcal{T}} \frac{|u^*(X)-u^*(Y)|}{|X-Y|^\beta} \leq 2|u|_{S,\beta}. \tag{2.23}$$

Proof. For the triangles under consideration (i.e. those in Figure 2.22 labeled with a 2) the value of u^* at point J is set to be the average of four vertices of the fractal curve. We let P, Q, R and S be the four vertices on the prefractal curve determining the value of $u^*(J)$ and set $u^*(J) = \frac{1}{4}(u(P)+u(Q)+u(R)+u(S))$. We then let u^* be the affine function defined by the value of u^* at the three vertices of the triangle.

Remark 15. The geometry that we will use in the proof of this lemma assumes that the following relationships hold $|P-Q| = |P-J| = |Q-R| = |R-S| = \frac{1}{2}|S-P|$. An alternate geometry that exists for triangles of this type is $|P-Q| = |P-J| = |Q-R| = |P-S| = \frac{1}{2}|R-S|$. In the latter case the proof proceeds in the same manner with very little modification.

By Remark 7 we may assume $\mathcal{T}$ is a triangle with P located at the origin and J is located on the x-axis. It can easily be checked that

$$u^*(X) = \frac{u(Q)-u(P)}{|P-Q|}x + \frac{2u(J)-u(P)-u(Q)}{\sqrt{3}|P-Q|}y + u(P).$$

Thus,

$$\begin{aligned}
\frac{|u^*(X_1)-u^*(X_2)|}{|X_1-X_2|^\beta} &= \frac{\left|\frac{u(P)-u(Q)}{|P-Q|}(x_1-x_2) + \frac{2u(J)-u(P)-u(Q)}{\sqrt{3}|P-Q|}(y_1-y_2)\right|}{|X_1-X_2|^\beta} \\
&\leq \frac{|u(P)-u(Q)|}{|P-Q|^\beta} + \frac{|2(\frac{1}{4}(u(P)+u(Q)+u(R)+u(S))-u(P)-u(Q)|}{\sqrt{3}|P-Q|^\beta} \\
&\leq |u|_{S,\beta} + \frac{1}{2\sqrt{3}}\left(\frac{|u(S)-u(P)|}{|P-Q|^\beta} + \frac{|u(R)-u(Q)|}{|P-Q|^\beta}\right) \\
&\leq |u|_{S,\beta} + \frac{2^\beta}{2\sqrt{3}}\frac{|u(S)-u(P)|}{|S-P|^\beta} + \frac{1}{2\sqrt{3}}\frac{|u(R)-u(Q)|}{|R-Q|^\beta} \\
&\leq |u|_{S,\beta} + \frac{1}{2\sqrt{3}}|u|_{S,\beta}\left(2^\beta+1\right) \\
&\leq 2|u|_{S,\beta}.
\end{aligned}$$

□

The following Lemma corresponds to those triangles labeled with a 3 in Figure 2.22.

Lemma 2.2.4. *Let $\mathcal{T}$ be a triangle with with vertices P, Q, and R and let u be a function defined at P, Q and R. Let us suppose that there exists $\beta \leq 1$ such that*

$$\frac{|u(P) - u(Q)|}{|P - Q|^\beta} \leq |u|_{S,\beta},$$

$$\frac{|u(Q) - u(R)|}{|Q - R|^\beta} \leq |u|_{S,\beta}$$

and

$$\frac{|u(P) - u(R)|}{|P - R|^\beta} \leq |u|_{S,\beta}$$

hold. Then there exists a function u^* on $\mathcal{T}$ such that

$$\sup_{X,Y \in \mathcal{T}} \frac{|u^*(X) - u^*(Y)|}{|X - Y|^\beta} \leq 3|u|_{S,\beta}. \tag{2.24}$$

Proof. We begin by letting u^* be the affine function defined by the value of u at the three vertices of the triangle. We now check that u^* satisfies the estimate (2.24).

By Remark 7 we may assume $\mathcal{T}$ is a triangle with P located at the origin and J is located on the x-axis. It can easily be checked that

$$u^*(X) = \frac{u(Q) - u(P)}{|P - Q|} x + \frac{2u(R) - u(P) - u(Q)}{\sqrt{3}|P - Q|} y + u(P).$$

Let $X_1 = (x_1, y_1)$ and $X_2 = (x_2, y_2)$ be arbitrary points in $\mathcal{T}$.

$$\begin{aligned}
\frac{|u^*(X_1) - u^*(X_2)|}{|X_1 - X_2|^\beta} &= \frac{\left| \frac{u(Q)-u(P)}{|P-Q|}(x_1 - x_2) + \frac{2u(R)-u(P)-u(Q)}{\sqrt{3}|P-Q|}(y_1 - y_2) \right|}{|X_1 - X_2|^\beta} \\
&\leq \frac{|u(Q) - u(P)|}{|P - Q|^\beta} + \frac{|2u(R) - u(P) - u(Q)|}{\sqrt{3}|P - Q|^\beta} \\
&\leq |u|_{S,\beta} + \frac{1}{\sqrt{3}} \frac{|u(R) - u(P)| + |u(R) - u(Q)|}{|P - Q|^\beta} \\
&\leq |u|_{S,\beta} + \frac{2}{\sqrt{3}} |u|_{S,\beta} \\
&= |u|_{S,\beta}(1 + 2/\sqrt{3}) \leq 3|u|_{S,\beta}.
\end{aligned}$$

□

The following Lemma corresponds to those triangles labeled with a 4 in Figure 2.22.

Lemma 2.2.5. *Given a triangle $\mathcal{T}$ with vertices P, J, and K. Moreover we are given that*

$$\frac{|u(P) - u(J)|}{|P - J|^\beta} \leq 3|u|_{S,\beta}$$

and

$$\frac{|u(P) - u(K)|}{|P - K|^\beta} \leq 3|u|_{S,\beta}$$

where $\beta \leq 1$.

Then there exists an extension function u^* defined on $\mathcal{T}$ such that

$$\sup_{X,Y \in \mathcal{T}} \frac{|u^*(X) - u^*(Y)|}{|X - Y|^\beta} \leq 9|u|_{S,\beta}. \tag{2.25}$$

Proof. We begin by letting u^* be the affine function defined by the value of u at the three vertices of the triangle. We now check that u^* satisfies the estimate (2.25).

By Remark 7 we may assume $\mathcal{T}$ is a triangle with P located at the origin and J located on the x-axis. It can easily be checked that

$$u^*(X) = \frac{u(J) - u(P)}{|P - J|}x + \frac{2u(K) - u(P) - u(J)}{\sqrt{3}|P - J|}y + u(P).$$

Let $X_1 = (x_1, y_1)$ and $X_2 = (x_2, y_2)$ be arbitrary points in $\mathcal{T}$.

$$\begin{aligned}
\frac{|u^*(X_1) - u^*(X_2)|}{|X_1 - X_2|^\beta} &= \frac{\left|\frac{u(J)-u(P)}{|P-J|}(x_1 - x_2) + \frac{2u(K)-u(P)-u(J)}{\sqrt{3}|P-J|}(y_1 - y_2)\right|}{|X_1 - X_2|^\beta} \\
&\leq \frac{|u(J) - u(P)|}{|P - J|^\beta} + \frac{|2u(K) - u(P) - u(J)|}{\sqrt{3}|P - J|^\beta} \\
&\leq \frac{|u(J) - u(P)|}{|P - J|^\beta} + \frac{2|u(K) - u(P)|}{\sqrt{3}|P - J|^\beta} + \frac{|u(P) - u(J)|}{\sqrt{3}|P - J|^\beta} \\
&\leq 3|u|_{S,\beta} + \frac{9}{\sqrt{3}}|u|_{S,\beta} \\
&\leq 9|u|_{S,\beta}.
\end{aligned}$$

Hence $\dfrac{|u^*(X) - u^*(Y)|}{|X - Y|^\beta} \leq 9|u|_{S,\beta}$.

□

Lemma 2.2.6. *Let n be fixed, V^n the prefractal set and given a function u at the elements of V^n such that*

$$\frac{|u(P) - u(Q)|}{|P - Q|^\beta} \leq |u|_{S,\beta}$$

for all $P, Q \in V^n$ and for some $\beta \leq 1$. Let u_n^* be an extension to the domain ω as defined in this Section, then for any X, Y in the T_{SC}^n the following holds

$$\frac{|u_n^*(X) - u_n^*(Y)|}{|X - Y|^\beta} \leq 54|u|_{S,\beta}. \tag{2.26}$$

Proof. We define C_{MSC} as the maximum Hölder constant from Lemmas 2.2.2-2.2.5, therefore $C_{MSC} \leq 9|u|_{S,\beta}$. We also observe that if X and Y are elements of the same triangle $\mathcal{T}$, then the inequality 2.26 holds due to Lemmas 2.2.2-2.2.5. Moreover, if X and Y are elements of two adjacent triangles that share at least one point then equation 2.26 holds by Lemma 2.1.6. We now consider the case where X and Y are elements of $\mathcal{T}_X$ and $\mathcal{T}_Y$ respectively and that $\mathcal{T}_X \cap \mathcal{T}_Y = \emptyset$.

We let P_X be the element of V^n closest to X, that is to say $|P_X - X| \leq |R - X|$ for all $R \in V^n$ (we know there is at least one). Similarly define P_Y to be the element of V^n closest to Y. Moreover if L is the length of the side of one triangle in T^n (i.e. $L = 2^{-n}$) we know that $|P_X - X| \leq L$, $|P_Y - Y| \leq L$, $|P_X - P_Y| \leq |P_X - X| + |X - Y| + |P_Y - Y|$ and $|X - Y| \geq \frac{\sqrt{3}}{2}L$. We then have,

$$\begin{aligned}
|u_n^*(X) - u_n^*(Y)| &\leq |u_n^*(X) - u_n^*(P_X)| + |u_n^*(P_X) - u_n^*(P_Y)| + |u_n^*(P_Y) - u_n^*(Y)| \\
&\leq C_{\mathcal{T}_X}|X - P_X|^\beta + |u|_{S,\beta}|P_X - P_Y|^\beta + C_{\mathcal{T}_Y}|P_Y - Y|^\beta \\
&\leq C_{MSC}(|X - P_X|^\beta + |P_X - P_Y|^\beta + |P_Y - Y|^\beta) \\
&\leq C_{MSC}\left[\left(\frac{2}{\sqrt{3}}|X - Y|\right)^\beta + \left(\left(1 + \frac{4}{\sqrt{3}}\right)|X - Y|\right)^\beta + \left(\frac{2}{\sqrt{3}}|X - Y|\right)^\beta\right] \\
&\leq 6C_{MSC}|X - Y|^\beta \\
&\leq 54|u|_{S,\beta}|X - Y|^\beta.
\end{aligned}$$

Hence for $X, Y \in T_{SC}^n$, $\dfrac{|u_n^*(X) - u_n^*(Y)|}{|X - Y|^\beta} \leq 54|u|_{S,\beta}$.

□

2.2.4 Iterative Process

This section more closely considers the iterative process used to build up the extension function u_n^* from a function u defined on the Sierpinski gasket. The first five lemmas will consider the five types of transition triangles for the extension u_n^* where $n \geq 1$. (See Figure 2.23). Next we will show a lemma similar to Lemma 2.2.6, except here we will consider the case when $X, Y \in T_{SC}^n \cup T_{TR}^n$. The seventh lemma gives a Hölder estimate on each triangle $\mathcal{T}$ of the triangulation T^n. Finally we prove a proposition showing the extension u_1^* has certain properties.

Remark 16. In the lemmas that follow we will make assumptions in the theorem statement about the value of u defined at certain points of the triangle, as well as the geometrical relationships between points in the triangle and other points in ω. The basis for these assumptions is the fact that we are considering transition triangles where the value of the extension function u_n^* is fixed by the sidecar triangles at one, two or three vertices of the triangle under consideration and the value of u_n^* at the remaining (if any) vertices are determined by the function u_{n-1}^*.

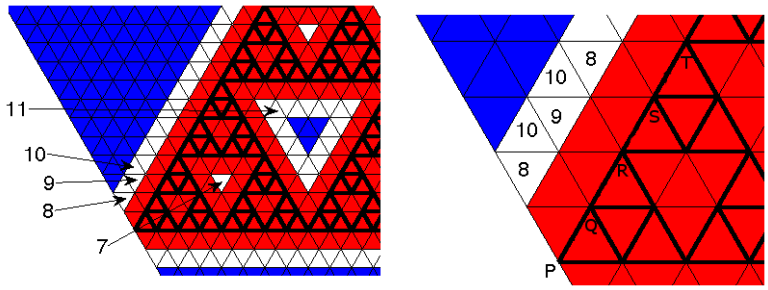

Figure 2.23: These figure illustrates the scenarios considered in Lemmas 2.2.7-2.2.11. The first figure labels each of the transition triangles considered in Lemmas 2.2.7-2.2.11. The second figure illustrates more specifically the triangles considered in Lemmas 2.2.8-2.2.10.

Lemma 2.2.7. *Let $\mathcal{T}$ be a triangle with with vertices J, K, and L and let u be a function*

defined at J, K and L. Let us suppose that there exists $\beta \leq 1$ such that

$$\frac{|u(J) - u(K)|}{|J - K|^\beta} \leq 9|u|_{S,\beta},$$

$$\frac{|u(K) - u(L)|}{|K - L|^\beta} \leq 9|u|_{S,\beta}$$

and

$$\frac{|u(J) - u(L)|}{|J - L|^\beta} \leq 9|u|_{S,\beta}$$

hold. Then there exists a function u^* defined for $X \in \mathcal{T}$ with $u^*(J) = u(J)$, $u^*(K) = u(K)$ and $u^*(L) = u(L)$ such that

$$\sup_{X,Y \in \mathcal{T}} \frac{|u^*(X) - u^*(Y)|}{|X - Y|^\beta} \leq 20|u|_{S,\beta}. \tag{2.27}$$

Proof. We begin by letting u^* be the affine function defined by the value of u at the three vertices of the triangle. We now check that u^* satisfies the estimate (2.27).

By Remark 7 we may assume $\mathcal{T}$ is a triangle with J located at the origin and J is located on the x-axis. It can easily be checked that

$$u^*(X) = \frac{u(K) - u(J)}{|J - K|}x + \frac{2u(L) - u(J) - u(K)}{\sqrt{3}|J - K|}y + u(J).$$

Let $X_1 = (x_1, y_1)$ and $X_2 = (x_2, y_2)$ be arbitrary points in $\mathcal{T}$.

$$\begin{aligned}
\frac{|u^*(X_1) - u^*(X_2)|}{|X_1 - X_2|^\beta} &= \frac{\left|\frac{u(K)-u(J)}{|J-K|}(x_1 - x_2) + \frac{2u(L)-u(J)-u(K)}{\sqrt{3}|J-K|}(y_1 - y_2)\right|}{|X_1 - X_2|^\beta} \\
&\leq \frac{|u(K) - u(J)|}{|J - K|^\beta} + \frac{|2u(L) - u(J) - u(K)|}{\sqrt{3}|J - K|^\beta} \\
&\leq 9|u|_{S,\beta} + \frac{1}{\sqrt{3}} \frac{|u(L) - u(J)| + |u(L) - u(K)|}{|J - K|^\beta} \\
&\leq 9|u|_{S,\beta} + \frac{18}{\sqrt{3}}|u|_{S,\beta} \\
&\leq 20|u|_{S,\beta}.
\end{aligned}$$

Hence $\dfrac{|u^*(X) - u^*(Y)|}{|X - Y|^\beta} \leq 20|u|_{S,\beta}$.

□

Lemma 2.2.8. *Given a triangle $\mathcal{T}$ with vertices J, K and L, and three additional points P,Q,R such that $u(J) = \frac{1}{2}(u(P) + u(Q))$, $u(K) = \frac{1}{2}(u(Q) + u(R))$ and $u(L) = \frac{1}{2}(u(P) + u(R))$. Moreover we know the following relationships hold $|J - K| = |P - Q| = |Q - R| = \frac{1}{2}|P - R|$ and also the estimate*

$$\frac{|u(X) - u(Y)|}{|X - Y|^\beta} \leq |u|_{S,\beta}$$

for $X, Y \in \{P, Q, R\}$ and $\beta \leq 1$.

Then there exists an extension function u^* defined on $\mathcal{T}$ such that

$$\sup_{X,Y \in \mathcal{T}} \frac{|u^*(X) - u^*(Y)|}{|X - Y|^\beta} \leq 2|u|_{S,\beta}. \tag{2.28}$$

Proof. We begin by letting u^* be the affine function defined by the value of u at the three vertices of the triangle. We now check that u^* satisfies the estimate (2.28).

By Remark 7 we may assume $\mathcal{T}$ is a triangle with P located at the origin and J located on the x-axis. It can easily be checked that

$$u^*(X) = \frac{u(K) - u(J)}{|J - K|}x + \frac{2u(L) - u(J) - u(K)}{\sqrt{3}|J - K|}y + u(J).$$

Let $X_1 = (x_1, y_1)$ and $X_2 = (x_2, y_2)$ be arbitrary points in $\mathcal{T}$.

$$\begin{aligned}
\frac{|u^*(X_1)-u^*(X_2)|}{|X_1-X_2|^\beta} &= \frac{\left|\frac{u(K)-u(J)}{|J-K|}(x_1-x_2)+\frac{2u(L)-u(J)-u(K)}{\sqrt{3}|P-J|}(y_1-y_2)\right|}{|X_1-X_2|^\beta} \\
&\leq \frac{|u(J)-u(K)|}{|J-K|^\beta}+\frac{|2u(L)-u(J)-u(K)|}{\sqrt{3}|J-K|^\beta} \\
&\leq \frac{|u(P)-u(R)|}{2|J-K|^\beta}+\frac{|u(P)+u(R)-2u(Q)|}{2\sqrt{3}|J-K|^\beta} \\
&\leq \frac{2^\beta|u(P)-u(R)|}{2|P-R|^\beta}+\frac{|u(P)-u(Q)|}{2\sqrt{3}|P-Q|^\beta}+\frac{|u(R)-u(Q)|}{2\sqrt{3}|R-Q|^\beta} \\
&\leq |u|_{S,\beta}+\frac{1}{2\sqrt{3}}\left(|u|_{S,\beta}+|u|_{S,\beta}\right) \\
&\leq 2|u|_{S,\beta}.
\end{aligned}$$

Hence $\dfrac{|u^*(X)-u^*(Y)|}{|X-Y|^\beta} \leq 2|u|_{S,\beta}$. □

Lemma 2.2.9. *Given a triangle $\mathcal{T}$ with vertices J, K and L, and five additional points P,Q,R,S and T such that $u(J)=\frac{1}{2}(u(Q)+u(R))$, $u(K)=\frac{1}{2}(u(R)+u(S))$ and $u(L)=\frac{1}{4}(u(P)+2u(R)+u(T))$. Moreover the following relationships hold $|J-K|=|P-Q|=|Q-R|=|R-S|=|S-T|=\frac{1}{2}|Q-S|$ as well as the estimate*

$$\frac{|u(X)-u(Y)|}{|X-Y|^\beta} \leq |u|_{S,\beta}$$

for $X,Y \in \{P,Q,R,S,T\}$ and $\beta \leq 1$.

Then there exists an extension function u^* defined on $\mathcal{T}$ such that

$$\sup_{X,Y\in\mathcal{T}} \frac{|u^*(X)-u^*(Y)|}{|X-Y|^\beta} \leq 2|u|_{S,\beta}. \tag{2.29}$$

Proof. We begin by letting u^* be the affine function defined by the value of u at the three vertices of the triangle. We now check that u^* satisfies the estimate (2.29).

By Remark 7 we may assume $\mathcal{T}$ is a triangle with P located at the origin and J located on the x-axis. It can easily be checked that

$$u^*(X)=\frac{u(K)-u(J)}{|J-K|}x+\frac{2u(L)-u(J)-u(K)}{\sqrt{3}|J-K|}y+u(J).$$

Let $X_1 = (x_1, y_1)$ and $X_2 = (x_2, y_2)$ be arbitrary points in $\mathcal{T}$.

$$\begin{aligned}
\frac{|u^*(X_1) - u^*(X_2)|}{|X_1 - X_2|^\beta} &= \frac{\left|\frac{u(K)-u(J)}{|J-K|}(x_1 - x_2) + \frac{2u(L)-u(J)-u(K)}{\sqrt{3}|P-J|}(y_1 - y_2)\right|}{|X_1 - X_2|^\beta} \\
&\leq \frac{|u(J) - u(K)|}{|J-K|^\beta} + \frac{|2u(L) - u(J) - u(K)|}{\sqrt{3}|J-K|^\beta} \\
&\leq \frac{|u(Q) - u(S)|}{2|J-K|^\beta} + \frac{|u(P) + u(T) - u(Q) - u(S)|}{2\sqrt{3}|J-K|^\beta} \\
&\leq \frac{2^\beta |u(Q) - u(S)|}{2|Q-S|^\beta} + \frac{|u(P) - u(Q)|}{2\sqrt{3}|P-Q|^\beta} + \frac{|u(T) - u(S)|}{2\sqrt{3}|T-S|^\beta} \\
&\leq |u|_{S,\beta} + \frac{1}{2\sqrt{3}}\left(|u|_{S,\beta} + |u|_{S,\beta}\right) \\
&\leq 2|u|_{S,\beta}.
\end{aligned}$$

Hence $\dfrac{|u^*(X) - u^*(Y)|}{|X-Y|^\beta} \leq 2|u|_{S,\beta}$. □

Lemma 2.2.10. *Given a triangle $\mathcal{T}$ with vertices J, K and L, and four additional points P,Q,R and T such that $u(J) = \frac{1}{2}(u(R) + u(Q))$, $u(K) = \frac{1}{2}(u(P) + u(R))$ and $u(L) = \frac{1}{4}(u(P) + 2u(R) + u(T))$. Moreover, $|J-K| = |P-Q| = \frac{1}{3}|Q-T|$ and*

$$\frac{|u(X) - u(Y)|}{|X-Y|^\beta} \leq |u|_{S,\beta}$$

for $X, Y \in \{P, Q, R, T\}$ and $\beta \leq 1$.

Then there exists an extension function u^* defined on $\mathcal{T}$ such that

$$\sup_{X,Y \in \mathcal{T}} \frac{|u^*(X) - u^*(Y)|}{|X-Y|^\beta} \leq \frac{3}{2}|u|_{S,\beta}. \tag{2.30}$$

Proof. We begin by letting u^* be the affine function defined by the value of u at the three vertices of the triangle. We now check that u^* satisfies the estimate (2.30).

By Remark 7 we may assume $\mathcal{T}$ is a triangle with P located at the origin and J located on the x-axis. It can easily be checked that

$$u^*(X) = \frac{u(K) - u(J)}{|J-K|}x + \frac{2u(L) - u(J) - u(K)}{\sqrt{3}|J-K|}y + u(J).$$

Let $X_1 = (x_1, y_1)$ and $X_2 = (x_2, y_2)$ be arbitrary points in $\mathcal{T}$.

$$\begin{aligned}
\frac{|u^*(X_1) - u^*(X_2)|}{|X_1 - X_2|^\beta} &= \frac{\left|\frac{u(K)-u(J)}{|J-K|}(x_1 - x_2) + \frac{2u(L)-u(J)-u(K)}{\sqrt{3}|P-J|}(y_1 - y_2)\right|}{|X_1 - X_2|^\beta} \\
&\leq \frac{|u(J) - u(K)|}{|J-K|^\beta} + \frac{|2u(L) - u(J) - u(K)|}{\sqrt{3}|J-K|^\beta} \\
&\leq \frac{|u(Q) - u(P)|}{2|J-K|^\beta} + \frac{|u(T) - u(Q)|}{2\sqrt{3}|J-K|^\beta} \\
&\leq \frac{|u(Q) - u(P)|}{2|P-Q|^\beta} + \frac{3^\beta|u(T) - u(Q)|}{2\sqrt{3}|T-Q|^\beta} \\
&\leq \frac{|u|_{S,\beta}}{2} + \frac{3|u|_{S,\beta}}{2\sqrt{3}} \\
&\leq \frac{3}{2}|u|_{S,\beta}.
\end{aligned}$$

Hence $\dfrac{|u^*(X) - u^*(Y)|}{|X-Y|^\beta} \leq \dfrac{3}{2}|u|_{S,\beta}$.

□

Lemma 2.2.11. *Given a triangle $\mathcal{T}$ with vertices J, K, and L, a function u defined at points J, K, L, P and Q such that*

$$\frac{|u(P) - u(J)|}{|P-J|^\beta} \leq 9|u|_{S,\beta},$$

$$\frac{|u(P) - u(K)|}{|P-K|^\beta} \leq 9|u|_{S,\beta},$$

$$\frac{|u(P) - u(Q)|}{|P-Q|^\beta} \leq |u|_{S,\beta},$$

and

$$\frac{|u(Q) - u(L)|}{|Q-L|^\beta} \leq 9|u|_{S,\beta}$$

where $\beta \leq 1$. Moreover we have $|J-K| = |K-P| = |L-Q| = \frac{1}{2}|P-Q| = \frac{1}{2}|P-J|$. Then there exists an extension function u^* defined on $\mathcal{T}$ such that

$$\sup_{X,Y\in\mathcal{T}} \frac{|u^*(X) - u^*(Y)|}{|X-Y|^\beta} \leq 56|u|_{S,\beta}. \tag{2.31}$$

Proof. We begin by letting u^* be the affine function defined by the value of u at the

three vertices of the triangle. We now check that u^* satisfies the estimate (2.31).

By Remark 7 we may assume $\mathcal{T}$ is a triangle with P located at the origin and J located on the x-axis. It can easily be checked that

$$u^*(X) = \frac{u(K)-u(J)}{|J-K|}x + \frac{2u(L)-u(K)-u(J)}{\sqrt{3}|J-K|}y + u(J).$$

Let $X_1 = (x_1, y_1)$ and $X_2 = (x_2, y_2)$ be arbitrary points in $\mathcal{T}$.

$$\begin{aligned}
\frac{|u^*(X_1)-u^*(X_2)|}{|X_1-X_2|^\beta} &= \frac{\left|\frac{u(K)-u(J)}{|J-K|}(x_1-x_2) + \frac{2u(L)-u(K)-u(J)}{\sqrt{3}|J-K|}(y_1-y_2)\right|}{|X_1-X_2|^\beta} \\
&\leq \frac{|u(J)-u(K)|}{|J-K|^\beta} + \frac{|2u(L)-u(K)-u(J)|}{\sqrt{3}|J-K|^\beta} \\
&\leq \frac{|u(P)-u(J)|}{|J-K|^\beta} + \frac{|u(P)-u(K)|}{|J-K|^\beta} + \frac{2|u(L)-u(Q)|}{\sqrt{3}|J-K|^\beta} + \\
&\quad + \frac{2|u(Q)-u(P)|}{\sqrt{3}|J-K|^\beta} + \frac{|u(P)-u(K)|}{\sqrt{3}|J-K|^\beta} + \frac{|u(P)-u(J)|}{\sqrt{3}|J-K|^\beta} \\
&\leq \frac{2^\beta|u(P)-u(J)|}{|P-J|^\beta} + \frac{|u(P)-u(K)|}{|P-K|^\beta} + \frac{2|u(L)-u(Q)|}{\sqrt{3}|L-Q|^\beta} + \\
&\quad + \frac{2^{(1+\beta)}|u(Q)-u(P)|}{\sqrt{3}|Q-P|^\beta} + \frac{|u(P)-u(K)|}{\sqrt{3}|P-K|^\beta} + \frac{2^\beta|u(P)-u(J)|}{\sqrt{3}|P-J|^\beta} \\
&\leq 9(2^\beta+1)|u|_{S,\beta} + \frac{(18+2^{\beta+1}+9+9\cdot 2^\beta)}{\sqrt{3}}|u|_{S,\beta} \\
&\leq 27|u|_{S,\beta} + 29|u|_{S,\beta} \\
&\leq 56|u|_{S,\beta}.
\end{aligned}$$

Hence $\dfrac{|u^*(X)-u^*(Y)|}{|X-Y|^\beta} \leq 56|u|_{S,\beta}$.

□

We now present a lemma similar to Lemma 2.2.6 except here we consider two points in $T^n_{SC} \cup T^n_{TR}$. (The white and red triangles in Figure 2.17).

Lemma 2.2.12. *Let n be fixed, V^n the prefractal set and given a function u defined on*

V^n such that

$$\frac{|u(P)-u(Q)|}{|P-Q|^\beta} \leq |u|_{S,\beta}$$

for all $P, Q \in V^n$ and for some $\beta \leq 1$. Let u_n^* be an extension to the domain ω as defined in this Section. Then for any X, Y in $T_{SC}^n \cup T_{TR}^n$ the following holds

$$\frac{|u_n^*(X)-u_n^*(Y)|}{|X-Y|^\beta} \leq 336\,|u|_{S,\beta}\,. \tag{2.32}$$

Proof. We begin by defining C_{MTR} as the maximum Hölder constant for triangles in the transition triangles, specifically $C_{MTR} = 56|u|_{S,\beta}$. By $\mathcal{T}_X$ and $\mathcal{T}_Y$ we refer to the triangles containing the points X and Y respectively. We observe that if X and Y are elements of the same triangle (i.e. $\mathcal{T}_X = \mathcal{T}_Y$) the inequality holds due to Lemmas 2.2.2-2.2.5, and 2.2.7 -2.2.11. Moreover if X and Y are elements of two triangles that share one or more points, the inequality also holds by Lemma 2.1.6. We now consider the case where $\mathcal{T}_X \cap \mathcal{T}_Y = \emptyset$.

If J and K are two points in T_{SC}^n then the following inequality holds by Lemma 2.2.6

$$\frac{|u_n^*(J)-u_n^*(K)|}{|J-K|^\beta} \leq 54\,|u|_{S,\beta} \tag{2.33}$$

We now consider the case with $X, Y \in T_{TR}^n$. We let P_X be the point in the sidecar triangles closest to X, that is to say $|P_X - X| \leq |R - X|$ for all R in the sidecar triangles. Similarly define P_Y to be the point in the sidecar triangles closest to Y. Moreover if L is the length of the side of one triangle in our mesh (i.e. $L = 2^{-n}$) we have $|P_X - X| \leq L$, $|P_Y - Y| \leq L$, $|P_X - P_Y| \leq |P_X - X| + |X - Y| + |Y - P_Y|$ and $|X - Y| \geq \frac{\sqrt{3}}{2}L$. We then have,

$$\begin{aligned}
|u_n^*(X) - u_n^*(Y)| &\leq |u_n^*(X) - u_n^*(P_X)| + |u_n^*(P_X) - u_n^*(P_Y)| + |u_n^*(P_Y) - u_n^*(Y)| \\
&\leq C_{\mathcal{T}_X}|X - P_X|^\beta + 54|u|_{S,\beta}|P_X - P_Y|^\beta + C_{\mathcal{T}_Y}|P_Y - Y|^\beta \\
&\leq \max\{C_{MTR}, 54|u|_{S,\beta}\}(|X - P_X|^\beta + |P_X - P_Y|^\beta + |P_Y - Y|^\beta) \\
&\leq 56|u|_{S,\beta}\left[\left(\frac{2}{\sqrt{3}}|X-Y|\right)^\beta + \left(\left(1+\frac{4}{\sqrt{3}}\right)|X-Y|\right)^\beta + \left(\frac{2}{\sqrt{3}}|X-Y|\right)^\beta\right] \\
&\leq 336|u|_{S,\beta}|X - Y|^\beta.
\end{aligned}$$

Finally we consider the case with $X \in T^n_{SC}$ and $Y \in T^n_{TR}$. Again we define P_Y to be the point in the sidecar triangles closest to Y. (There is no need to define P_X since $X \in T^n_{SC}$). Moreover if L is the length of the side of one triangle in our mesh (i.e. $L = 2^{-n}$) we have $|P_Y - Y| \leq L$, $|X - P_Y| \leq |X - Y| + |Y - P_Y|$ and $|X - Y| \geq \frac{\sqrt{3}}{2}L$. We then have,

$$\begin{aligned}
|u^*_n(X) - u^*_n(Y)| &\leq |u^*_n(X) - u^*_n(P_Y)| + |u^*_n(P_Y) - u^*_n(Y)| \\
&\leq 54\,|u|_{S,\beta}\,|X - P_Y|^\beta + C_{\mathcal{T}_Y}|P_Y - Y|^\beta \\
&\leq \max\{C_{MTR}, 54\,|u|_{S,\beta}\}(|X - P_Y|^\beta + |P_Y - Y|^\beta) \\
&\leq 56\,|u|_{S,\beta}\left[\left(\frac{2}{\sqrt{3}} + 1\right)^\beta |X - Y|^\beta + \left(\frac{2}{\sqrt{3}}|X - Y|\right)^\beta\right] \\
&\leq 224\,|u|_{S,\beta}\,|X - Y|^\beta.
\end{aligned}$$

Therefore for $X, Y \in T^n_{SC} \cup T^n_{TR}$ estimate 2.32 holds.

□

This lemma considers the Hölder estimate on any individual triangle $\mathcal{T}$ of the triangulation T^n of ω.

Lemma 2.2.13. *Let T^n be the induced triangulation for the extension function u^*_n, then for any X, Y in a single triangle $\mathcal{T} \in T^n$ the following holds*

$$\frac{|u^*_n(X) - u^*_n(Y)|}{|X - Y|^\beta} \leq 56\,|u|_{S,\beta}\,. \tag{2.34}$$

Proof. If $\mathcal{T} \in T^n_{SC} \cup T^n_{TR}$ the inequality holds by Lemmas 2.2.2-2.2.5 and 2.2.7-2.2.11. We now consider the case when $\mathcal{T} \in T^n_{EX}$ (the blue triangles of Figure 2.17). We identify by m the iteration where the value of $u^*_n(\mathcal{T})$ was last set, that is to say $u^*_m(X) \neq u^*_{m-1}(X)$ for some $X \in \mathcal{T}$ but $u^*_m(X) = u^*_{m+i}(X)$ where $1 \leq i \leq n - m$ for all $X \in \mathcal{T}$. We identify by $\mathcal{T}_m$ the triangle from the triangulation T^m which contains $\mathcal{T}$.

By construction of the extension function in ω, $\mathcal{T}_m \in T^n_{SC} \cup T^n_{TR}$ for the triangulation T^m. Therefore for $A, B \in \mathcal{T}_m$

$$\frac{|u^*_m(A) - u^*_m(B)|}{|A - B|^\beta} \leq 56|u|_{S,\beta}.$$

Since $\mathcal{T} \subset \mathcal{T}_m$, for X, Y in $\mathcal{T}$ the following holds

$$\frac{|u_m^*(X) - u_m^*(Y)|}{|X - Y|^\beta} \leq 56|u|_{S,\beta}.$$

We therefore have for $X, Y \in \mathcal{T}$

$$\frac{|u_n^*(X) - u_n^*(Y)|}{|X - Y|^\beta} = \frac{|u_m^*(X) - u_m^*(Y)|}{|X - Y|^\beta} \leq 56|u|_{S,\beta}.$$

□

The next Lemma considers the step from u_0^* to u_1^* illustrated in Figure 2.5.

Lemma 2.2.14. *Let $n = 1$, u be a function defined on the Sierpinski gasket and u_1 be the restriction of u to the elements of V^1 such that*

$$\frac{|u(P) - u(Q)|}{|P - Q|^\beta} \leq |u|_{S,\beta}$$

for all $P, Q \in V^1$ and for some $\beta \leq 1$. Let u_1^* be the first extension to the domain ω for the Sierpinski gasket, then for any X, Y in ω the following holds

$$\frac{|u_1^*(X) - u_1^*(Y)|}{|X - Y|^\beta} \leq 336|u|_{S,\beta}. \tag{2.35}$$

Proof. For u_1^*, $\omega = T_{SC}^n \cup T_{TR}^n$, therefore inequality 2.35 holds trivially by Lemma 2.2.12. □

2.2.5 Main Results

Proposition 2.2.15. *Given a prefractal Sierpinski gasket, V^n, with iteration number $n \geq 1$ and a function u defined at the elements of the set that satisfies*

$$\frac{|u(X) - u(Y)|}{|X - Y|^\beta} \leq |u|_{S,\beta}$$

for all $X, Y \in V^n$ and for some $\beta \leq 1$. Let u_n^* be the nth extension to the domain ω. Then for any X, Y in ω the following holds

$$\frac{|u_n^*(X) - u_n^*(Y)|}{|X - Y|^\beta} \leq 840|u|_{S,\beta}. \tag{2.36}$$

Remark 17. For any X in $T^n_{EX} = \omega \setminus (T^n_{SC} \cup T^n_{TR})$ (i.e the blue triangles in Figure 2.17) $u^*_n(X) = u^*_{n-1}(X)$. This observation will be especially relevant in the proof below.

Proof. By Lemma 2.2.14 we know that estimate 2.36 holds for the extension function u^*_1. Let u^*_{n-1} be the $(n-1)th$ extension to the domain ω and we assume that the following estimate holds

$$\frac{|u^*_{n-1}(X) - u^*_{n-1}(Y)|}{|X-Y|^\beta} \leq 840|u|_{S,\beta} \tag{2.37}$$

for all $X, Y \in \omega$. We now show the estimate holds for u^*_n with identical constant on the right hand side.

We define C_{MSC} as the maximum sidecar constant from Lemmas 2.2.2-2.2.5, specifically $C_{MSC} \leq 9|u|_{S,\beta}$. We also define C_{MTR} as the maximum Hölder constant for the transition triangles, specifically $C_{MTR} = 56|u|_{S,\beta}$. We recall the definition of ω as the polygonal domain with vertices D, E, and F defined as $D = (1/2, -\sqrt{3}/4)$, $E = (3/2, \sqrt{3}/2)$, and $F = (-1/2, \sqrt{3}/2)$.

By Lemma 2.2.12 we know that for any two points in $X, Y \in T^n_{SC} \cup T^n_{TR}$ estimate 2.36 holds. We now consider the case where $X \in T^n_{SC} \cup T^n_{TR}$ and $Y \in T^n_{EX} = \omega \setminus (T^n_{SC} \cup T^n_{TR})$. From Lemma 2.2.13 if X', Y' are in a single triangle $\mathcal{T} \in T^n$ the following estimate holds

$$\frac{|u^*_n(X') - u^*_n(Y')|}{|X'-Y'|^\beta} \leq 54|u|_{S,\beta}.$$

Combining this estimate with Lemma 2.1.6 we can say that estimate 2.36 holds for any two triangles in T^n that share one or more points. We now show the estimate holds when X and Y are in two distinct triangles which do not share any points. See Figure 2.24 for an idea of where points X and Y may be located.

We begin by observing that the values of u^*_n in T^n_{EX} are historically stratified. We observe this stratification by noting that the values of u^*_n at points in this region are layered according to when the value of u^*_n was last set. Specifically T^n_{EX} can be broken into subregions where the value of u^*_n was last set at iterations $n-1$,$n-2$, $\ldots, 0$. This stratification for $n = 4$ is seen in Figure 2.25.

We identify by $m_X = n$ the current iteration (recall $X \in T^n_{SC} \cup T^n_{TR}$ so the value of

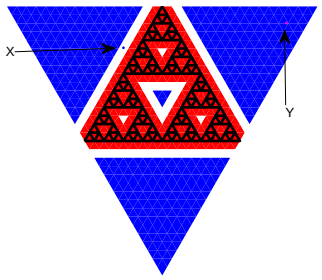

Figure 2.24: A sample location of X and Y, in the extension u_4^*.

$u_n^*(X)$ is set at this iteration). We identify by $\mathcal{T}_X$ the triangle from T^{m_X} which contains the point X. We let P_X be the point in the sidecar region of $T^{m_X} \cap \mathcal{T}_X$ which minimizes $|P_X - X|$. (We note that if X is in the sidecar region of T^{m_X} then $P_X = X$). We also identify by Q_X the point in V^{m_X} closest to P_X. We let L be the length of the side in our original mesh (i.e. $L = 2^{-n}$) and observe that $|X - P_X| \leq 2^{(n-m_X)}L = L$ and $|P_X - Q_X| \leq 2^{(n-m_X)}L = L$. (See Figure 2.26).

Similarly for Y, we identify by m_Y the iteration where the value of $u_n^*(Y)$ was last set, that is to say $u_{m_Y}^*(Y) \neq u_{m_Y-1}^*(Y)$ but $u_{m_Y}^*(Y) = u_{m_Y+i}^*(Y)$ where $1 \leq i \leq n - m_Y$. We identify by $\mathcal{T}_Y$ the triangle from T^{m_Y} where the value of Y was last set. We let P_Y be the point in the sidecar region of $T^{m_Y} \cap \mathcal{T}_Y$ such that $|P_Y - Y|$ is minimized. (We note that if Y is in a sidecar triangle of T^{m_Y} then $P_Y = Y$). We also identify by Q_Y the point in V^{m_Y} closest to P_Y. Using the above definition of L (i.e. $L = 2^{-n}$) we observe that $|Y - P_Y| \leq 2^{(n-m_Y)}L$ and $|P_Y - Q_Y| \leq 2^{(n-m_Y)}L$. (See Figure 2.27).

We note that $V^{m_Y} \subset V^{m_X} = V^n$ and now make an important observation concerning the relationship between $|X - Y|$ and $n - m_Y$:

$$|X - Y| \geq 2^{(n-m_Y-1)}\frac{\sqrt{3}}{2}L.$$

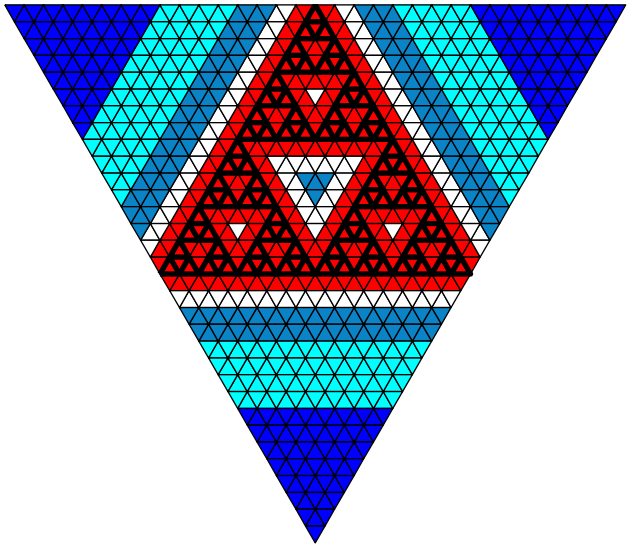

Figure 2.25: In this figure the historical stratification is seen. The value of u_n^* in the dark blue triangles are set by u_1^*, the value of u_n^* in the turquoise triangles are set by u_2^* and the value of u_n^* in the blue gray triangles are set by u_3^*

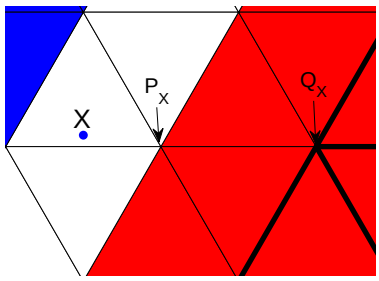

Figure 2.26: The identification P_X and Q_Y with respect to X.

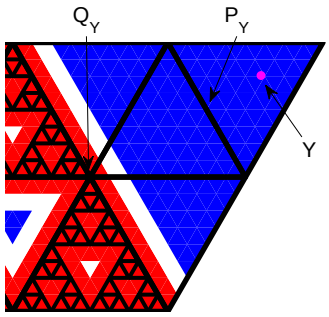

Figure 2.27: The identification points P_Y and Q_Y with respect to Y.

Having made this observation:

$$
\begin{aligned}
|u_n^*(X) - u_n^*(Y)| &= |u_{m_X}^*(X) - u_{m_Y}^*(Y)| \\
&\leq |u_{m_X}^*(X) - u_{m_X}^*(P_X)| + |u_{m_X}^*(P_X) - u_{m_X}^*(Q_X)| + |u_{m_X}^*(Q_X) - u_{m_Y}^*(Q_Y)| \\
&\qquad + |u_{m_Y}^*(Q_Y) - u_{m_Y}^*(P_Y)| + |u_{m_Y}^*(P_Y) - u_{m_Y}^*(Y)| \\
&\leq C_{MTR}|X - P_X|^\beta + C_{MSC}|P_X - Q_X|^\beta + |u|_{S,\beta}|Q_X - Q_Y|^\beta \\
&\qquad + C_{MSC}|Q_Y - P_Y|^\beta + C_{MTR}|P_Y - Y|^\beta \\
&\leq \max\{C_{MTR}, C_{MSC}, |u|_{S,\beta}\}(|X - P_X|^\beta + |P_X - Q_X|^\beta + |Q_X - Q_Y|^\beta \\
&\qquad + |Q_Y - P_Y|^\beta + |P_Y - Y|^\beta) \\
&\leq 56|u|_{S,\beta}(|X - P_X|^\beta + |P_X - Q_X|^\beta + |Q_X - Q_Y|^\beta + |P_Y - Q_Y|^\beta + |P_Y - Y|^\beta) \\
&\leq 56|u|_{S,\beta}\left[\left(\frac{2}{2^{(n-m_Y-1)}\sqrt{3}}|X - Y|\right)^\beta + \left(\frac{2}{2^{(n-m_Y-1)}\sqrt{3}}|X - Y|\right)^\beta + |Q_X - Q_Y|^\beta + \right. \\
&\qquad \left. + \left(\frac{2 \cdot 2^{(n-m_Y)}}{2^{(n-m_Y-1)}\sqrt{3}}|X - Y|\right)^\beta + \left(\frac{2 \cdot 2^{(n-m_Y)}}{2^{(n-m_Y-1)}\sqrt{3}}|X - Y|\right)^\beta\right] \\
&\leq 56|u|_{S,\beta}\left[2\left(\frac{2}{\sqrt{3}}|X - Y|\right)^\beta + |Q_X - Q_Y|^\beta + 2\left(\frac{4}{\sqrt{3}}|X - Y|\right)^\beta\right] \\
&\leq 56|u|_{S,\beta}\left[2\left(\frac{2}{\sqrt{3}}\right)^\beta |X - Y|^\beta + \left(2\left(\frac{2}{\sqrt{3}}\right) + 1 + 2\left(\frac{4}{\sqrt{3}}\right)\right)^\beta |X - Y|^\beta \right. \\
&\qquad \left. + 2\left(\frac{4}{\sqrt{3}}\right)^\beta |X - Y|^\beta\right] \\
&\leq 56|u|_{S,\beta}\left[2\left(\frac{2}{\sqrt{3}}\right)^\beta |X - Y|^\beta + \left(2\left(\frac{2}{\sqrt{3}}\right)^\beta + 1^\beta + 2\left(\frac{4}{\sqrt{3}}\right)^\beta\right) |X - Y|^\beta \right. \\
&\qquad \left. + 2\left(\frac{4}{\sqrt{3}}\right)^\beta |X - Y|^\beta\right] \\
&\leq 56|u|_{S,\beta}\left[4\left(\frac{2}{\sqrt{3}}\right)^\beta + 1^\beta + 4\left(\frac{4}{\sqrt{3}}\right)^\beta\right] |X - Y|^\beta \\
&\leq 56|u|_{S,\beta} \cdot 15|X - Y|^\beta \\
&\leq 840|X - Y|^\beta.
\end{aligned}
$$

Therefore $\dfrac{|u_n^*(X) - u_n^*(Y)|}{|X - Y|^\beta} \leq 840|u|_{S,\beta}$ for all $X \in T_{SC}^n \cup T_{TR}^n$, and $Y \in T_{EX}^n$.

One final case remains to be considered, the case with $X, Y \in T^n_{EX}$ (the blue triangles of Figure 2.17). By Remark 17 we know for all $X, Y \in T^n_{EX}$ that $u^*_n(X) = u^*_{n-1}(X)$ and $u^*_n(Y) = u^*_{n-1}(Y)$. We then apply our induction assumption (i.e. that the estimate holds for the $(n-1)th$ iteration), thereby giving us $\frac{|u^*_n(X) - u^*_n(Y)|}{|X-Y|^\beta} \leq 840|u|_{S,\beta}$ for all $X, Y \in T^n_{EX}$.

Combining the estimates for each specific case we arrive at $\frac{|u^*_n(X) - u^*_n(Y)|}{|X-Y|^\beta} \leq 840|u|_{S,\beta}$ for all $X, Y \in \omega$. □

Proposition 2.2.16. *For every n and every $u_n \in C^\beta(V^n)$ we construct a linear extension operator Π_n that brings functions defined on V^n to functions defined on Ω which have the following properties for every $0 < \beta \leq 1$:*

1. $u_n \in C^\beta(V^n) \mapsto u^*_n \in C^\beta(\Omega) \cap \mathcal{A}_{T_{V^n}}(\Omega)$,
2. $\|\Pi_n u_n\|_{\Omega,\beta} \leq 850 \|u\|_{S,\beta}$.

Here $\mathcal{A}_{T_{V^n}}$ is the set of affine functions on the triangulation induced by the prefractal set at iteration n.

Proof. By the construction detailed in Section 2.2.2 we have our first result, i.e. $u_n \in C^\beta(V^n) \mapsto u^*_n \in C^\beta(\Omega) \cap \mathcal{A}_{T_{V^n}}(\Omega)$. We now show the second result.

By Proposition 2.2.15 we know that for X, Y in ω and $\Pi_n u_n = u^*_n$ the following inequality holds:

$$\frac{|u^*_n(X) - u^*_n(Y)|}{|X-Y|^\beta} \leq 840 \, |u|_{S,\beta}. \tag{2.38}$$

We recall the definition of the domain γ found in Section 2.2.2 as a convex polygonal domain which contains ω. Section 2.2.2 also details the methodology to extend the function u^*_n to γ and then to Ω. Let X_1 and X_2 be arbitrary points in γ. Then,

$$u^*_n(X_1) = v^*_n(X_1)\eta(X_1) = v^*_n(X'_1)\eta(X_1)$$

where $X'_1 \in \omega$. Similarly,

$$u^*_n(X_2) = v^*_n(X_2)\eta(X_2) = v^*_n(X'_2)\eta(X_2)$$

where $X_2' \in \omega$. Moreover $|X_1 - X_2| \geq |X_1' - X_2'|$ and by geometric arguments $\dfrac{|\eta(X_1) - \eta(X_2)|}{|X_1' - X_2'|} \leq \dfrac{2}{\sqrt{3}}$. Therefore,

$$\begin{aligned}
\frac{|u_n^*(X_1) - u_n^*(X_2)|}{|X_1 - X_2|^\beta} &= \frac{|v_n^*(X_1')\eta(X_1) - v_n^*(X_2')\eta(X_2)|}{|X_1 - X_2|^\beta} \\
&\leq \frac{|v_n^*(X_1')\eta(X_1) - v_n^*(X_2')\eta(X_2)|}{|X_1' - X_2'|^\beta} \\
&\leq \frac{\eta(X_1)|v_n^*(X_1') - v_n^*(X_2')|}{|X_1' - X_2'|^\beta} + \frac{v^*n(X_2')|\eta(X_1') - \eta(X_2')|}{|X_1' - X_2'|^\beta} \\
&\leq \frac{|v_n^*(X_1') - v_n^*(X_2')|}{|X_1' - X_2'|^\beta} + \sup_{X\in S}|u(X)|\frac{|\eta(X_1') - \eta(X_2')|}{|X_1' - X_2'|^\beta} \\
&\leq 840\,|u|_{S,\beta} + \sup_{X\in S}|u(X)|\frac{|\eta(X_1') - \eta(X_2')|}{|X_1' - X_2'|}|X_1' - X_2'|^\beta \\
&\leq 840\,|u|_{S,\beta} + \sup_{X\in S}|u(X)|\frac{2}{\sqrt{3}}(\sqrt{3})^\beta \\
&\leq 840|u|_{S,\beta} + 2\,\|u\|_{S,\beta} \\
&\leq 842\,\|u\|_{S,\beta}\,.
\end{aligned}$$

Since u_n^* is identically zero in $\mathbb{R}^2 \setminus \gamma$ we have an extension function u_n^* that is Hölder continuous and satisfies the estimate

$$|u_n^*|_{\overline{\Omega},\beta} \leq 850\,\|u\|_{S,\beta}\,.$$

Therefore $\|\Pi_n u_n\|_{\Omega,\beta} \leq 850\,\|u\|_{S,\beta}\,.$ □

Before showing the Theorem 2.0.2 for the Sierpinski gasket we give one more result that gives an estimate as to the speed of convergence of u_n^* to u^* in Ω.

Proposition 2.2.17. *Given the Sierpinski gasket S and a function u defined on the gasket that satisfies*

$$\frac{|u(X) - u(Y)|}{|X - Y|^\beta} \leq |u|_{S,\beta}$$

for all $X, Y \in S$, for some $\beta \leq 1$. Then the sequence of extension functions $\{u_n^*\}$ defined on Ω is uniformly Cauchy and

$$\sup_{X\in\Omega}|u_n^*(X) - u_{n+p}^*(X)| \leq C\left(\frac{1}{2}\right)^{\beta n}$$

where C is equal to $1700\,\|u\|_{S,\beta}$.

Proof. Fix $p > 0$. We observe that by construction two consecutive extension functions (u_n^* and u_{n+1}^*) differ on ω only in the sidecar and transition triangles of the $u_{n+1}^* th$ extension. These differences are also seen in the 22 subtriangles that compose the domain γ. Without loss of generality, we will assume that $X \in T_{SC}^n \cup T_{TR}^n$. Moreover by Y we denote the element of V^n closest to X.

$$\begin{aligned}|u_n^*(X) - u_{n+p}^*(X)| &\leq |u_n^*(X) - u(Y)| + |u(Y) - u_{n+p}^*(X)| \\ &\leq 2 \cdot 850\,\|u\|_{S,\beta}\,|X-Y|^\beta \\ &\leq 1700\,\|u\|_{S,\beta}\left(\frac{1}{2}\right)^{\beta n}.\end{aligned}$$

□

We now present the proof of Theorem 2.0.2 for the Sierpinski gasket.

Proof. We claim by construction $\Pi : C^\beta(S) \mapsto C^\beta(\Omega)$. We now show that $\|\Pi u\|_{\Omega,\beta} \leq C_1\,\|u\|_{S,\beta}$ and $\Pi u = \lim_{n\to\infty} \Pi_n(u|_{V^n})$ uniformly in Ω.

We let u be a Hölder continuous function defined on the fractal curve S with exponent $\beta \leq 1$ and constant $C_0 = |u|_{S,\beta}$, (i.e. $|u(x) - u(y)| \leq C_0|x-y|^\beta \ \ \forall x, y \in S$). We recall that for a given n, V^n is a subset of the fractal S. This allows us to say that given a Hölder continuous function u on S then $u_n \in C^\beta(V^n)$. From Proposition 2.2.16 we have a prefractal extension operator Π_n such that $u_n \in C^\beta(V^n) \mapsto u_n^* \in C^\beta(\Omega)$ and $\|\Pi_n u_n\|_{\Omega,\beta} \leq 850\,\|u\|_{S,\beta}$. We note that the right hand side is independent of n. Therefore each extension $\Pi_n u_n$ is equicontinuous on Ω. Moreover we know u is bounded on S with $|u(X)| \leq \|u\|_{S,\beta}$ for all $X \in S$. We therefore can say that $|\Pi_n u_n(X)| \leq \|u\|_{S,\beta}$ for all $X \in \Omega$. By the Arzelà-Ascoli theorem there exists a subsequence which converges uniformly to a Hölder continuous function Πu. We now easily show that uniform convergence preserves the Hölder exponent β and constant $850\|u\|_{S,\beta}$.

$$\frac{|\Pi u(X) - \Pi u(Y)|}{|X-Y|^\beta} \leq \frac{|\Pi u(X) - \Pi_n u_n(X)| + |\Pi_n u_n(X) - \Pi_n u_n(Y)| + |\Pi_n u_n(Y) - \Pi u(Y)|}{|X-Y|^\beta} \tag{2.39}$$

Since $\Pi_n u_n$ converges to Πu uniformly given $\epsilon > 0$ there exists N such that for all $n \geq N$, $\quad |\Pi u(X) - \Pi_n u_n(X)| < \epsilon$ for all X in Ω. Therefore equation 2.39 is less then or

equal to

$$\frac{2\epsilon + |\Pi_n u_n(X) - \Pi_n u_n(Y)|}{|X-Y|^\beta}.$$

Since ϵ can be arbitrarily small we therefore have

$$\frac{|\Pi u(X) - \Pi u(Y)|}{|X-Y|^\beta} \leq 850\|u\|_{S,\beta}.$$

Hence we have a function Πu is Hölder continuous everywhere in Ω and satisfies the estimate

$$|\Pi u|_{\overline{\Omega},\beta} \leq 850\|u\|_{S,\beta}. \tag{2.40}$$

The final property $\sup_{X\in\Omega} |\Pi_n u_n(X) - \Pi_{n+p} u_{n+p}(X)| \leq C_2 \|u\|_{S,\beta} \alpha^{-n}$ $(\alpha = 2)$ is given by Proposition 2.2.17. □

Chapter 3

H^1 Extension using Prefractals

In the previous chapter we studied the extension of a Hölder continuous function defined on either the fractal Koch curve or Sierpinski gasket to a larger open domain Ω. Recall that Π_n was defined as a linear operator that extended Hölder continuous functions v defined on V^n (the prefractal set) to Hölder continuous functions v^* defined on Ω. In this chapter of the dissertation we wish to show that the extension operator Π defined in Theorem 2.0.2 has the additional characteristic of mapping a function in the domain of the energy form of the fractal, to an $H^1(\Omega)$ function defined on any larger domain Ω. We recall the definition of the H^1 as the Hilbert space with inner product $(u,v)_{H^1(\Omega)} = \int_\Omega uv + \sum_{i=1}^{2} \int \frac{\partial u}{\partial x_i}\frac{\partial v}{\partial x_i}$ and norm $\|u\|_{H^1(\Omega)} = \left(\|u\|^2_{L^2(\Omega)} + \sum_{i=1}^{2} \left\| \frac{\partial u}{\partial x_i} \right\|^2_{L^2(\Omega)} \right)^{1/2}$. Moreover, we also recall that the energy form $E[u]$ has domain D_E in $L^2(S,\mu)$ where μ is a normalized Hausdorff measure on S and $D_E \hookrightarrow C^\beta(S)$. (See Chapter 1 for further details). We will show the following theorem (with the same notation as in Theorems 2.0.1 and 2.0.2).

Theorem 3.0.18. *Given a fractal set S and an open domain $\Omega \subseteq \mathbb{R}^2$ containing S the linear continuous operator introduced in Theorem 2.0.2 has the following additional characteristics:*

1. $\Pi : D_E \mapsto H^1(\Omega)$
2. $\Pi_n u|_{V^n}$ *converges weakly to* Πu *in* $H^1(\Omega)$ *and strongly in* $L^2(\Omega)$.
3. $\|\Pi u\|_{H^1(\Omega)} \leq C\sqrt{E[u] + \|u\|^2_{L^2(S,\mu)}}$ *where C is a numerical constant independent of u.*

4. $\varphi \circ \Pi u = u$ *for all* $u \in D_E$ *and where* φ *is* $\Pi u|_S$.

The format of this chapter is as follows. First we will provide some preliminary lemmas that will be common between the Koch curve and the Sierpinski gasket. We will then consider the two fractals separately. For each fractal we will introduce the idea of the domain of influence for a single difference term in the energy form, show a few preliminary lemmas, and finally show Theorem 3.0.18.

3.1 Preliminaries

We begin with a few preliminary lemmas that will be common to both the Koch curve and the Sierpinski gasket. The first lemma considers the H^1 seminorm of an affine function defined on an equilateral triangle. The second lemma presented is a elementary iteration lemma that is used in the proof of Theorem 3.0.18 for both fractals.

Lemma 3.1.1. *Given an equilateral triangle* $\mathcal{T}$ *with vertices* A, B *and* C *with an affine function* u *defined on it then,* $|u|^2_{H^1(\mathcal{T})} = \dfrac{\sqrt{3}}{4}\left[(u(B)-u(A))^2 + \dfrac{1}{3}(2u(C)-u(A)-u(B))^2\right]$

Proof. Without loss of generality we may assume that A is located at the origin and B lies on the positive x-axis. The function $u(x,y)$ for $x, y \in \mathcal{T}$ is then

$$u(x,y) = \frac{u(B)-u(A)}{|A-B|}x + \frac{2u(C)-u(A)-u(B)}{\sqrt{3}|A-B|}y + u(A).$$

Then

$$\begin{aligned}
|u|^2_{H^1(\mathcal{T})} &= \iint_{\mathcal{T}} u_x^2 + u_y^2 \, dx\, dy \\
&= \iint_{\mathcal{T}} \left[\left(\frac{u(B)-u(A)}{|A-B|}\right)^2 + \left(\frac{2u(C)-u(A)-u(B)}{\sqrt{3}|A-B|}\right)^2\right] dx\, dy \\
&= \left(\frac{1}{|A-B|}\right)^2 \left((u(B)-u(A))^2 + \frac{1}{3}(2u(C)-u(A)-u(B))^2\right) \iint_{\mathcal{T}} dx\, dy \\
&= \left(\frac{1}{|A-B|}\right)^2 \left((u(B)-u(A))^2 + \frac{1}{3}(2u(C)-u(A)-u(B))^2\right) \left(\frac{\sqrt{3}}{4}|A-B|^2\right) \\
&= \frac{\sqrt{3}}{4}\left[(u(B)-u(A))^2 + \frac{1}{3}(2u(C)-u(A)-u(B))^2\right].
\end{aligned}$$

□

We now prove the following elementary iteration lemma.

Lemma 3.1.2. *Let $c_0 > 0$, $\rho > 1$, $e(n)$, $g(n)$ exist for $n \geq 0$. Moreover $e(n)$ and $g(n)$ satisfy*

$$e(n) \leq e(n+1) \tag{3.1}$$

$$g(n) \leq g(n-1) + c_0(\rho^{-n}e(n))^{1/2} \tag{3.2}$$

for all $n \geq 1$. Then

$$g(n) \leq g(0) + c_0 \frac{\rho^{1/2} - \rho^{-n/2}}{\rho^{1/2} - 1} \sup_n (e(n))^{1/2}. \tag{3.3}$$

In particular

$$\limsup_{n \to +\infty} g(n) \leq g(0) + M \sup_n (e(n))^{1/2}. \tag{3.4}$$

Proof. We have

$$\begin{aligned}
g(1) &\leq g(0) + c_0(\rho^{-1}e(1))^{1/2}, \\
g(2) &\leq g(1) + c_0(\rho^{-2}e(2))^{1/2} \\
&\leq g(0) + c_0(\rho^{-1}e(1))^{1/2} + c_0(\rho^{-2}e(2))^{1/2} \\
&\leq g(0) + c_0\left(\rho^{-1/2} + \rho^{-1}\right)(e(2))^{1/2}.
\end{aligned}$$

More precisely for $n \geq 1$

$$g(n) \leq g(0) + c_0 \left(\sum_{k=1}^{n} \rho^{-k/2} \right) (e(n))^{1/2},$$

thus

$$\begin{aligned}
g(n) &\leq g(0) + c_0 \left(\sum_{k=1}^{n} \rho^{-k/2} \right) \sup_n (e(n))^{1/2} \\
&\leq g(0) + c_0 \left(\frac{1 - (\rho^{-1/2})^{n+1}}{1 - \rho^{-1/2}} \right) \sup_n (e(n))^{1/2} \\
&\leq g(0) + c_0 \left(\frac{\rho^{1/2} - \rho^{-n/2}}{\rho^{1/2} - 1} \right) \sup_n (e(n))^{1/2}.
\end{aligned}$$

□

3.2 Koch curve

3.2.1 Domain of Influence

We now introduce a scheme for classifying triangles which are elements of T^n_{SC}. Before beginning we note that when the prefractal is iterated, the induced triangulation is also iterated. This iteration subdivides each triangle into nine congruent subtriangles. We classify the triangles in T^n_{SC} according to how the nth extension function (u^*_n) is obtained on the triangles (i.e. which vertices are elements of V^n and which are averages) as well as how the $n+1$th extension function (u^*_{n+1}) is obtained on the subtriangles. The classification allows us to determine whether the resultant subtriangles are sidecar, transition, or external triangles. Moreover, if one of the subtriangles is a sidecar triangle the classification of that triangle can be determined. This classification is shown visually in Figures 3.3-3.4 with the original triangle on the left and the subdivided triangle on the right. By circles we denote the elements of V^{n+1} and by stars we denote those points where u^*_n is obtained by averaging. Associated with each star is a string of numbers. The first number denotes the number of points used when averaging, the remaining numbers denote the number of points used to determine the value of u^*_n at the points used in averaging. For example, $3[1,1,1]$ denotes a point where the value of u^*_n was derived from the average of u^*_n at three points each of which is an element of V^n, whereas $3[2,1,2]$ again denotes a point where u^*_n was obtained as an average of u^*_n at three points but value of u^*_n at two of these points was obtained by averaging. Vertices with neither a star nor a circle maintain their value from the previous iteration. The numbers appearing in the sidecar (red) triangles on the right denote the classification of each of those triangles.

Proof that only sixteen triangles types exist is obtained by studying the classification of the subtriangles. Although each refinement produces additional triangles, by considering the mappings between original and refined subtriangles it is clear that no additional subtriangle types are introduced.

We now consider the H^1 seminorm of u^*_n restricted to a triangle, $\mathcal{T} \in T^n_{SC}$ classified as type 3, and wish to relate this seminorm to the energy form of the fractal. In Figure 3.1, we illustrate the original triangle (abc), the subtriangles (labeled T_1-T_9), and the prefractal curve S^{n+1}. We note that vertices $a, b, c \in V^n$ and $a, b, c, g, h, j, k, l, m \in V^{n+1}$.

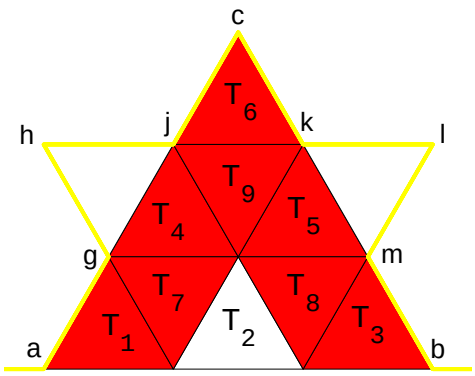

Figure 3.1: The identification of points and triangles. We note that the yellow curve is the prefractal curve S^{n+1}

By Lemma 3.1.1:

$$|u_n^*|^2_{H^1(\mathcal{T})} \leq \frac{\sqrt{3}}{4}\left[(u(a)-u(b)^2+\frac{1}{3}(2u(c)-u(a)-u(b))^2\right].$$

In order to relate this to the energy form of the fractal all terms must be in the form $(u(x)-u(y))^2$ where x and y are two consecutive points on the prefractal curve (more specifically x and y belong to the same *cell*). We therefore have

$$|u_n^*|^2_{H^1(\mathcal{T})} \leq \frac{\sqrt{3}}{4}\left[\frac{8}{3}(u(a)-u(c))^2+\frac{8}{3}(u(b)-u(c))^2\right].$$

We will refer to the H^1 seminorm in this format as the *adjusted* H^1 seminorm. The differences in consecutive points are the differences $(u(\psi_{i_1\ldots i_n}(A))-u(\psi_{i_1\ldots i_n}(B)))^2$ that occur in the energy form.

Additionally we wish to determine the adjusted H^1 seminorm of u_{n+1}^* restricted to those subtriangles of $\mathcal{T}$ which are transition triangles. For triangles classified as type 3, there is only a single transition subtriangle which we will denote by $\mathcal{T}_R$. The adjusted seminorm is:

$$|u^*_{n+1}|^2_{H^1(\mathcal{T}_R)} \leq \frac{\sqrt{3}}{4}\left[\frac{8}{3}(u(a)-u(g))^2+\frac{26}{3}(u(g)-u(h))^2+\frac{26}{3}(u(h)-u(j)^2+\frac{32}{3}(u(j)-u(c))^2+\right.$$
$$\left.+\frac{32}{3}(u(c)-u(k))^2+\frac{26}{3}(u(k)-u(l))^2+\frac{26}{3}(u(l)-u(m))^2+\frac{8}{3}(u(m)-u(c))^2\right].$$

We perform similar calculations for each of the sixteen triangle types and record the largest coefficient in H^1 seminorm sum in Table 3.1 (we omit the factor of $\frac{\sqrt{3}}{4}$ shared by all). We emphasize that the coefficients in Table 3.1 are all independent of n.

We now consider what we will term *the domain of influence* for a single difference pair $(u(\psi_{i_1\ldots i_n}(A))-u(\psi_{i_1\ldots i_n}(B)))^2$ in the energy form sum.

Lemma 3.2.1. *A single difference term, $(u(\psi_{i_1\ldots i_n}(A))-u(\psi_{i_1\ldots i_n}(B)))^2$ in the energy form occurs in the adjusted H^1 seminorm of u^*_n in at most 20 sidecar triangles.*

Proof. We consider two cases separately.
Case 1 - Above the prefractal curve

From the description of the extension methodology for triangles in T^n_{SC} found in Section 2.1.2 we observe that any point where u^*_n is obtained by averaging is at most two deep. That is to say, in order to find the value of u^*_n at a vertex we may have to perform two averaging steps (one for those in the primary sidecars, and one for the secondary sidecars) but we never perform three averaging steps. This maximum depth is independent of the iteration number n. We consider those averages where both point $\psi_{i_1\ldots i_n}(A)$ and point $\psi_{i_1\ldots i_n}(B)$ appear. The requirement that both points must appear in the average, along with the depth requirement, restrict us to a maximum of two averaged points that contain our two original points. Each of these averaged points is a vertex of at most 6 triangles, however since one of these averaged points contains the second averaged point in its average, the maximal number of triangles containing one or more of these averaged points is 10. Therefore the difference, $(u(\psi_{i_1\ldots i_n}(A))-u(\psi_{i_1\ldots i_n}(B)))^2$, occurs in the adjusted H^1 seminorm of at most 10 triangles above the prefractal curve.

Case 2 - Below the prefractal curve

Similar to the domain above the fractal curve, any point where u^*_n is obtained by averaging is at most two deep. By an identical argument this restricts the maximal

number of triangles where the difference term occurs in the adjusted seminorm to 10. The geometry of the domain below the curve requires us to consider an additional scenario where both terms do not appear in the average, however both terms appear in the adjusted seminorm. (See Figure 3.2 or the previous example of the refinement of triangles of type 3). The geometry of this special case restricts the occurrence of the difference term, $(u(\psi_{i_1\ldots i_n}(A)) - u(\psi_{i_1\ldots i_n}(B)))$, to at most 6 adjusted H^1 seminorms.

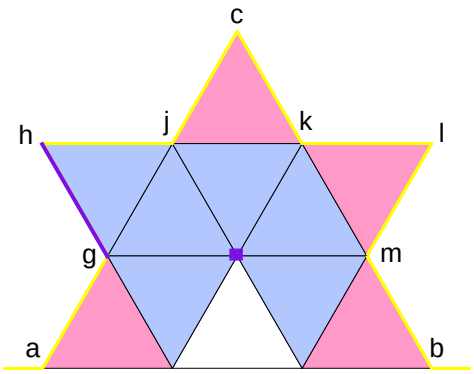

Figure 3.2: An illustration of the domain of influence of the difference term $(u(g)-u(h))^2$. The purple triangles contain the difference term in the adjusted H^1 seminorm of u_n^*, whereas the pink sidecar triangles do not contain the difference term. Note that the purple square denotes an average which contains only $u(g)$, but not $u(h)$.

Summing the number of triangles above and below the curve, we find that the difference term, $(u(\psi_{i_1\ldots i_n}(A)) - u(\psi_{i_1\ldots i_n}(B)))^2$, occurs in the adjusted H^1 seminorm of u_n^* at most 20 sidecar triangles. □

Lemma 3.2.2. *A single difference term, $(u(\psi_{i_1\ldots i_n}(A)) - u(\psi_{i_1\ldots i_n}(B)))^2$ in the energy form occurs in the adjusted H^1 seminorm of u_n^* in at most 100 transition triangles.*

Proof. By Lemma 3.2.1 we know that the domain of influence of a single difference term, $(u(\psi_{i_1\ldots i_n}(A)) - u(\psi_{i_1\ldots i_n}(B)))^2$ in the energy form is at most 20 sidecar triangles. From our triangle characterization scheme (see Figure 3.3-3.4) we know that a refinement of

a sidecar triangle results in at most five transition triangles. Therefore the domain of influence of a single difference term is at most $20 \cdot 5 = 100$ transition triangles. □

Lemma 3.2.3. *Let u be a function in D_E defined on the fractal set S and let $u_n^* = \Pi_n u_n$ be the nth extension to the domain Ω. Then*

$$|u_n^*|_{H^1(T_{SC}^n \cup T_{TR}^n)} \leq \left(D \sum_{i_1 \ldots i_n = 1}^{4} (u(\psi_{i_1 \ldots i_n}(A)) - u(\psi_{i_1 \ldots i_n}(B)))^2 \right)^{1/2}$$

where $D \leq 651$ and is independent of n.

Proof. From Lemma 3.2.1 the domain of influence of a single difference term, $(u(\psi_{i_1 \ldots i_n}(A)) - u(\psi_{i_1 \ldots i_n}(B)))^2$ is at most 20 sidecar triangles. Moreover, by Lemma 3.2.2 the domain of influence of the same difference term is at most 100 transition triangles. The largest coefficient occurring in the adjusted H^1 seminorm of a sidecar triangle is $\dfrac{2048}{675}$, and the largest coefficient occurring in the adjusted H^1 seminorm of a transition triangle is $\dfrac{9728}{675}$, hence the largest coefficient on any one difference, $(u(\psi_{i_1 \ldots i_n}(A)) - u(\psi_{i_1 \ldots i_n}(B)))^2$, is

$$20 \cdot \frac{2048}{675} + 100 \cdot \frac{9728}{675} \leq 1502.$$

Hence

$$|u_n^*|_{H^1(T_{SC}^n \cup T_{TR}^n)} \leq \left(D \sum_{i_1 \ldots i_n = 1}^{4} (u(\psi_{i_1 \ldots i_n}(A)) - u(\psi_{i_1 \ldots i_n}(B)))^2 \right)^{1/2}$$

where $D \leq 1502 \cdot \frac{\sqrt{3}}{4} = 651$. □

3.2.2 Main results for Koch curve

The first lemma considers the H^1 seminorm of u_0^* on ω. We next give two additional lemmas which study the H^1 seminorm of u_n^*. The first lemma considers triangles in the extension region of two consecutive prefractal iterations. The second lemma relates the H^1 seminorm of u_n^* in two consecutive iterations. Finally we show Theorem 3.0.18 for the Koch curve.

Lemma 3.2.4. *With the extension methodology defined in Section 2.1.2 $|u_0^*|^2_{H^1(\omega)} = \frac{\sqrt{3}}{2}(u(A) - u(B))^2$.*

Proof. As stated when describing the extension for the base case, $u_0^* = \dfrac{u(B)-u(A)}{|A-B|}x + u(A)$. Therefore

$$\begin{aligned}
|u_0^*|^2_{H^1(\omega)} &= \iint_\omega u_x^2 + u_y^2 \, dx \, dy \\
&= \iint_{\mathcal{T}_1} u_x^2 + u_y^2 \, dx \, dy + \iint_{\mathcal{T}_2} u_x^2 + u_y^2 \, dx \, dy \\
&= \frac{\sqrt{3}}{4}(u(B)-u(A))^2 + \frac{\sqrt{3}}{4}(u(B)-u(A))^2 \\
&= \frac{\sqrt{3}}{2}\left[(u(B)-u(A))^2\right]
\end{aligned}$$

□

Lemma 3.2.5. *Let $\mathcal{T}$ be a triangle in $T^n_{EX} \cup T^n_{TR}$, and let $\mathcal{T}_1 \dots \mathcal{T}_9$ be the nine congruent triangles in T^{n+1} such that $\bigcup_{i=1}^{9} \mathcal{T}_i = \mathcal{T}$ then $\mathcal{T}_i \in T^{n+1}_{EX}$ for $1 \le i \le 9$.*

Proof. If $\mathcal{T} \in T^n_{EX}$ then clearly $\mathcal{T}_1 \dots \mathcal{T}_9 \in T^{n+1}_{EX}$. Assume that $\mathcal{T} \in T^n_{TR}$. By construction the sidecar triangles of a triangulation T^{n+1} are those triangles with at least one vertex in V^{n+1}, and the transition triangles are those triangles which share one (or more) vertices with the sidecar triangles. We may therefore say that the transition triangles are *one triangle away* from the vertices V^{n+1}. Since the triangles in T^n_{SC} were refined to 9 congruent subtriangles in T^{n+1}, those triangles which are one triangle away from the set V^{n+1} are also a subset of T^n_{SC}. Hence $T^{n+1}_{SC} \cup T^{n+1}_{TR} \subseteq T^n_{SC}$. □

Lemma 3.2.6. *Let $u \in D_E$ be a function defined on the fractal set S. Then the following recursive estimate holds:*

$$|u_n^*|_{H^1(\omega)} \le |u_{n-1}^*|_{H^1(\omega)} + \left(D \sum_{i_1 \dots i_n = 1}^{4} (u(\psi_{i_1 \dots i_n}(A)) - u(\psi_{i_1 \dots i_n}(B)))^2 \right)^{1/2} \tag{3.5}$$

for every $n \ge 1$, in particular

$$|u_1^*|_{H^1(\omega)} \le |u_0^*|_{H^1(\omega)} + \left(D \sum_{i_1=1}^{4} (u(\psi_{i_1}(A)) - u(\psi_{i_1}(B)))^2 \right)^{1/2}.$$

Here D is the constant from Lemma 3.2.3 and is independent of n.

Proof. We begin with $u_0^* = \Pi_0 u_0$. By Lemma 3.2.4,

$$|u_0^*|_{H^1(\omega)} = \left(\frac{\sqrt{3}}{2}|u(A) - u(B)|^2\right)^{1/2} = \left(\frac{\sqrt{3}}{2}E^0[u,u]\right)^{1/2}.$$

We now prove that for every $n \geq 1$, estimate 3.5 holds. We observe that in the external triangles (i.e. T_{EX}^n), $u_n^* = u_{n-1}^*$. We therefore have

$$\begin{aligned}
|u_n^*|_{H^1(\omega)} &= |u_n^*|_{H^1(T_{EX}^n)} + |u_n^*|_{H^1(T_{SC}^n \cup T_{TR}^n)} \\
&= |u_{n-1}^*|_{H^1(T_{EX}^n)} + |u_n^*|_{H^1(T_{SC}^n \cup T_{TR}^n)} \\
&\leq |u_{n-1}^*|_{H^1(\omega)} + |u_n^*|_{H^1(T_{SC}^n \cup T_{TR}^n)} \\
&\leq |u_{n-1}^*|_{H^1(\omega)} + \left(D \sum_{i_1 \ldots i_n = 1}^{4} (u(\psi_{i_1 \ldots i_n}(A)) - u(\psi_{i_1 \ldots i_n}(B)))^2\right)^{1/2}.
\end{aligned}$$

□

We now recall the definition of the intermediate domain γ introduced in Section 2.1.2 as the convex polygonal domain with vertices $E = (-1, 0)$, $F = (0, \sqrt{3})$, $G = (1, \sqrt{3})$, $H = (2, 0)$, $I = (1, -\sqrt{3})$, and $J = (0, -\sqrt{3})$. We recall the construction of v_n^* by first subdividing γ into sixteen congruent triangles then using the operations of rotation, reflection and translation to extend the function u_n^* defined on ω to γ. (See Figure 2.7). Clearly if the function $u_n^* \in H^1(\omega)$, $v_n^* \in H^1(\gamma)$. We also recall the utilization of "hat" functions to create a function z_n^* which is equal to zero on the boundary of γ and equal to u_n^* in ω. We set the extension function u_n^* to z_n^* and restrict u_n^* to the given domain Ω. We now present the following lemma which gives a relationship between $\|u_n^*\|_{H^1(\omega)}$ and $\|u_n^*\|_{H^1(\Omega)}$.

Lemma 3.2.7. *Suppose there exists a function u_n^* defined on ω such that $u_n^* \in H^1(\omega)$ and $\|u_n^*\|_{H^1(\omega)} \leq C$, then $z_n^* \in H^1(\Omega)$ and $\|z_n^*\|_{H^1(\Omega)} \leq 70C$.*

Proof. We begin by observing $0 \leq \eta(X) \leq 1$ for all $X \in \gamma$, $\eta_x \leq 2/\sqrt{3}$ and $\eta_y \leq 2/\sqrt{3}$. By the process used in creating the function v_n^* we note that $\|v_n^*\|_{H^1(\gamma)} \leq 10\,\|u_n^*\|_{H^1(\omega)}$.

We also recall that $z_n^* \equiv 0$ for all $X \in \mathbb{R}^2 \setminus \gamma$.

$$\begin{aligned}
\|z_n^*\|_{H^1(\Omega)} &= \left(\|z_n^*\|^2_{L^2(\Omega)} + \sum_{i=1}^{2} \left\| \frac{\partial z_n^*}{\partial x_i} \right\|^2_{L^2(\Omega)} \right)^{1/2} \\
&= \left(\int_\Omega (v_n^*\eta)^2 dx\, dy + \int_\Omega (v_n^*\eta)_x^2 + (v_n^*\eta)_y^2 dx\, dy \right)^{1/2} \\
&= \left(\int_\gamma (v_n^*\eta)^2 dx\, dy + \int_\gamma (v_n^*\eta)_x^2 + (v_n^*\eta)_y^2 dx\, dy \right)^{1/2} \\
&\leq \left(\int_\gamma (v_n^*)^2 dx\, dy + \int_\gamma (v_n^*\eta_x + (v_n^*)_x\eta)^2 + (v_n^*\eta_y + (v_n^*)_y\eta)^2 dx\, dy \right)^{1/2} \\
&\leq \left(\|v_n^*\|^2_{L^2(\gamma)} + 2\int_\gamma (v_n^*\eta_x)^2 + ((v_n^*)_x\eta)^2 + (v_n^*\eta_y)^2 + ((v_n^*)_y\eta)^2 dx\, dy \right)^{1/2} \\
&= \left(\|v_n^*\|^2_{L^2(\gamma)} + 2\int_\gamma \eta^2((v_n^*)_x^2 + (v_n^*)_y^2) dx\, dy + 2\int_\gamma (v_n^*)^2(\eta_x^2 + \eta_y^2) dx\, dy \right)^{1/2} \\
&\leq \left(\|v_n^*\|^2_{L^2(\gamma)} + 2\int_\gamma ((v_n^*)_x^2 + (v_n^*)_y^2) dx\, dy + \frac{16}{3}\int_\gamma (v_n^*)^2 dx\, dy \right)^{1/2} \\
&= \left(\|v_n^*\|_{L^2(\gamma)} + 2\sum_{i=1}^{2} \left\| \frac{\partial v_n^*}{\partial x_i} \right\|^2_{L^2(\Omega)} + \frac{16}{3}\|v_n^*\|_{L^2(\gamma)} \right)^{1/2} \\
&\leq 7\|v_n^*\|_{H^1(\gamma)} \\
&\leq 70\|u_n^*\|_{H^1(\omega)}
\end{aligned}$$

□

We now present the proof of Theorem 3.0.18

Proof. We claim by construction: $\Pi : D_E \mapsto H^1(\omega)$.

We apply Lemma 3.1.2 with $\rho = 4$, $g(n) = |u_n^*|_{H^1(\omega)}$, $c_0 = D^{1/2}$ and

$$e(n) = \rho^n \sum_{i_1 \ldots i_n = 1}^{4} (u(\psi_{i_1 \ldots i_n}(A)) - u(\psi_{i_1 \ldots i_n}(B)))^2 = E^n(u,u).$$

We note that D is the constant from Lemma 3.2.3 and is independent of n. We also recall from the definition of the energy form in Chapter 1, that $E^n(u,u) \leq E^{n+1}(u,u)$

and for $u \in D_E$

$$E[u] := \sup_n E^n(u,u) < +\infty.$$

Moreover $g(0) = |u_0^*|_{H^1(\omega)} = \left(\frac{\sqrt{3}}{2}(u(A) - u(B))^2\right)^{.1/2}$ Thus

$$\limsup_{n\to\infty} |u_n^*|_{H^1(\omega)} \leq |u_0^*|_{H^1(\omega)} + D^{1/2}\frac{2-2^{-n}}{2-1}(E[u])^{1/2} \leq |u_0^*|_{H^1(\omega)} + M(E[u])^{1/2}$$

which implies there exists $C_5 > 0$ such that

$$|u_n^*|_{H^1(\omega)} \leq C_5(E[u])^{1/2}. \tag{3.6}$$

We now calculate the H^1 norm of u_n^* on ω, By construction, and Remark 2

$$\sup_\omega (u_n^*)^2 \leq \sup_{V^n} u_n^2 \leq \sup_{V^\infty} u_\infty^2 \leq \sup_S u^2.$$

Moreover we apply Lemma 1.1.2 to get:

$$\|u_n^*\|^2_{L^2(\omega)} \leq |\omega| \sup_\omega (u_n^*)^2 \leq |\omega| \sup_S (u)^2 \leq C_6(\|u\|^2_{L^2(S,\mu)} + E[u]), \tag{3.7}$$

where C_6 is a constant independent of n. Combining 3.6 and 3.7 we have

$$\|u_n^*\|_{H^1(\omega)} = \left(|u_n^*|^2_{H^1(\omega)} + \|u_n^*\|^2_{L^2(S,\mu)}\right)^{1/2} \leq C_7\sqrt{E[u] + \|u\|^2_{L^2(S,\mu)}},$$

where C_7 is independent of n.

Since $\|u_n^*\|_{H^1(\omega)}$ is bounded, $\|u_n^*\|_{H^1(\Omega)}$ is also bounded by Lemma 3.2.7 with

$$\|u_n^*\|_{H^1(\Omega)} = \left(|u_n^*|^2_{H^1(\Omega)} + \|u_n^*\|^2_{L^2(S,\mu)}\right)^{1/2} \leq C\sqrt{E[u] + \|u\|^2_{L^2(S,\mu)}},$$

where $C = 70C_7$ and is independent of n.

Since $\|u_n^*\|_{H^1(\Omega)} \leq C\sqrt{E[u] + \|u\|^2_{L^2(S,\mu)}}$, by the (sequentially) weak compactness of the unit ball of $H^1(\Omega)$, there exists a subsequence that converges weakly in $H^1(\Omega)$. Moreover by the Rellich Theorem, there exists a subsequence that converges strongly in

$L^2(\Omega)$. Therefore, there exists a subsequence of $\{u_n^*\}$ that converges to some $z \in H^1(\Omega)$ weakly in $H^1(\Omega)$ and strongly in $L^2(\Omega)$. We now prove that for any such subsequence, $z = u^*$ where $u^* = \Pi u$. By Theorem 2.0.2, $u_n^*(x) \to u^*(x)$ uniformly on Ω, hence also strongly in $L^2(\Omega)$. Therefore, as $z \in H^1(\Omega) \hookrightarrow L^2(\Omega)$, by the uniqueness of the limit in $L^2(\Omega)$ we get $z = u^*$. This also implies the whole sequence $\{u_n^*\}$ converges to u^*, strongly in $L^2(\Omega)$ and weakly in $H^1(\Omega)$. Clearly, $z(x) = u^*(x)$ almost everywhere for $x \in \Omega$. Finally, by the lower semi-continuity of a Hilbert norm under weakly convergent sequences as $u_n^* \rightharpoonup u^*$ in $H^1(\Omega)$ we get

$$\|u^*\|_{H^1(\Omega)} \leq \liminf_{n\to\infty} \|u_n^*\|_{H^1(\Omega)} \leq C\sqrt{E[n] + \|u\|^2_{L^2(S,\mu)}}.$$

□

We end with a proposition that shows that the restriction of our extension function to the fractal set S is the original function.

Proposition 3.2.8. *Let $u \in D_E$ be a function defined on S, and Πu the extension function defined on Ω by the operator Π, then $\varphi_S \circ \Pi u = u$, where φ_S is the pointwise restriction of a continuous function on Ω to the set $S \subset \Omega$.*

Proof. We recall from Theorem 2.0.2 that Πu is continuous on $\overline{\Omega}$. Therefore, $\varphi_S \circ \Pi u$ is well defined for all $Y \in S$. We now prove that $\varphi_S \circ \Pi u(Y) = u(Y)$ for all $Y \in S$.
We recall that the set

$$V^\infty := \bigcup_{n=1}^{\infty} V^n$$

is dense in S (see Chapte 1). Therefore, (since both u and $\varphi_S \circ \Pi u$ are continuous), it suffices to show that

$$\varphi_S \circ |\Pi u(X) = u(X)$$

for all $X \in V^\infty$. We have that $V^m \subset V^n$ for all $n > m$. Moreover, by the construction of Π_n, we know that for every $n \geq m$:

$$\Pi_n u|_{V^n}(X) = \Pi_m u|_{V^m}(X) = u(X), \tag{3.8}$$

for all $X \in V^m$. Let $X \in V^\infty$ be fixed. Then $X \in V^m$ for some m therefore identity (3.8) holds. Moreover

$$\lim_{n\to\infty} \Pi_n u|_{V^n}(X) = \Pi u(X)$$

for all $X \in \Omega$. We therefore take the limit in equation (3.8) as $n \to \infty$ to arrive at

$$\Pi u(X) = u(X)$$

for all $X \in S$. □

3.3 Sierpinski Gasket

3.3.1 Domain of Influence

As with the Koch curve we introduce a scheme for classifying triangles which are elements of T^n_{SC}. Before beginning, we note that when the prefractal is iterated, the induced triangulation is also iterated. This iteration subdivides each triangle into four congruent subtriangles. We classify the triangles in T^n_{SC} according to how the nth extension function (u^*_n) is obtained on the triangles (i.e. which vertices are elements of V^n and which are averages) as well as how the $n+1$th extension function (u^*_{n+1}) is obtained on the subtriangles. The classification allows us to determine whether the resultant subtriangles are sidecar, transition, or external triangles. Moreover, if one of the subtriangles is a sidecar triangle the classification of that triangle can be determined. This classification is shown visually in Figure 3.6 with the original triangle on the left and the subdivided triangle on the right. The notation used in these figures is similar to the notation used in the Koch figures (see 3.3). By circles we denote the elements of V^{n+1} and stars denote those points where u^*_n is obtained by averaging. Associated with each star is a number that indicates the number of points used when in avergaing. Vertices with neither a star nor a circle maintain their value from the previous iteration. The numbers appearing in the sidecar (red) triangles on the right denote the classification of each of those triangles.

Proof that only ten triangles types exist is obtained by studying the classification of the subtriangles. Although each refinement produces additional triangles, by considering the mappings between original and refined subtriangles it is clear that no additional subtriangle types are introduced.

We now consider the H^1 seminorm of u^*_n restricted to a triangle, $\mathcal{T} \in T^n_{SC}$ classified as type 2, and wish to relate this seminorm to the energy form of the fractal. In Figure 3.5, we illustrate the original triangle (abc), the subtriangles, and the prefractal curve

S^{n+1}. We note that vertices $a, c \in V^n$ and $a, b, c \in V^{n+1}$.

By Lemma 3.1.1:

$$|u_n^*|^2_{H^1(\mathcal{T})} \leq \frac{\sqrt{3}}{4}\left[(u(a)-u(b))^2 + \frac{1}{3}(2u(c)-u(a)-u(b))^2\right]$$
$$= \frac{\sqrt{3}}{4}(u(a)-u(b))^2.$$

As for the Koch curve case we wish to determine the adjusted H^1 seminorm of u_{n+1}^* restricted to those subtriangles of $\mathcal{T}$ which are transition triangles. For triangles classified as type 2, there is only a single transition subtriangle which we will denote by $\mathcal{T}_R$. The adjusted seminorm is: By Lemma 3.1.1:

$$|u_{n+1}^*|^2_{H^1(\mathcal{T}_R)} \leq \frac{\sqrt{3}}{4}\left[\frac{1}{4}(u(a)-u(c))^2 + \frac{1}{3}\left(\frac{1}{2}u(a)+\frac{1}{2}u(c)-u(b)\right)^2\right].$$

In order to relate this to the energy form of the fractal all terms must be in the form $(u(x)-u(y))^2$ where x and y are two consecutive points on the prefractal curve (more specifically x and y belong to the same *cell*). We therefore have

$$|u_{n+1}^*|^2_{H^1(\mathcal{T}_R)} \leq \frac{\sqrt{3}}{4}\left[\frac{2}{3}(u(a)-u(b))^2 + \frac{2}{3}(u(b)-u(c))^2\right].$$

We will refer to the H^1 seminorm in this format as the *adjusted* H^1 seminorm. The differences in consecutive points are the differences $(u(\psi_{i_1\ldots i_n}(A)) - u(\psi_{i_1\ldots i_n}(B)))^2$ that occur in the energy form.

We perform similar calculations for each of the ten triangle types and record the largest coefficient in H^1 seminorm sum in Table 3.2 (we omit the factor of $\frac{\sqrt{3}}{4}$ shared by all). We emphasize that the coefficients in Table 3.2 are all independent of n.

We now consider what we will term *the domain of influence* for a single difference pair $(u(\psi_{i_1\ldots i_n}(A)) - u(\psi_{i_1\ldots i_n}(B)))^2$ in the energy form sum.

Lemma 3.3.1. *A single difference term, $(u(\psi_{i_1\ldots i_n}(A)) - u(\psi_{i_1\ldots i_n}(B)))^2$ in the energy form occurs in the adjusted H^1 seminorm of u_n^* in at most 7 sidecar triangles.*

Proof. By the properties of the energy form each difference term corresponds to one seg-

ment in the Sierpinski gasket and, by construction of our scaffolding, the side of exactly two triangles in the triangulation T^n. Suppose we choose one of these triangles with vertices A, B and C. Moreover let A and B be two vertices in the difference term. The value of u_n^* at the third vertex C is determined in one of three ways: completing the triangle, averaging the value of u at four points, or predetermined since $C \in V^n$. We consider the domain of influence in each of these three cases separately.

Case 1: Completing the Triangle
For this case the difference term appears in all sidecar triangles which have C as a vertex. Since $u(C)$ was determined by completing the triangle, this means C must be the vertex of at most three sidecar triangles (triangle ABC, triangle ACD and triangle BCE where D and E are nodes in our triangulation).

Case 2: Average of Four
In this case the value at vertex C is determined by the value of u at four vertices. Moreover the value of $u(C)$ appears in the seminorm of six triangles five of which are sidecar triangles. Hence the domain of influence in this case is five sidecar triangles.

Case 3: $C \in V^n$
For this case we must consider two subcases:
Case 3a: AC, AB and BC are all consecutive points on the gasket In this case the domain of influence is 1 triangle.

Case 3b: AB and BC are all consecutive points on the gasket but AC is not
Because of the geometry of the gasket this implies that $u(A)$ and $u(C)$ are used to determine the value at a point D where $u(D)$ is the average of u at four nodes. By the arguments for Case 2, this implies the domain of influence equals the five sidecar triangles containing $u(D)$ plus the triangle ABC for a total of six.

The same case arguments can be made for triangle ABG which is the other triangle containing the segment AB. However, due to the construction of the gasket either ABC or ABG must be the triangle considered in Case 3a. Hence the domain of influence for a single difference term is 1+max(Case 1, Case 2, Case 3) = 7.

□

Lemma 3.3.2. *A single difference term,* $(u(\psi_{i_1 \ldots i_n}(A)) - u(\psi_{i_1 \ldots i_n}(B)))^2$ *in the energy form occurs in the adjusted* H^1 *seminorm of* u_n^* *in at most 21 transition triangles.*

Proof. By Lemma 3.3.1 we know that the domain of influence of a single difference term, $(u(\psi_{i_1\ldots i_n}(A)) - u(\psi_{i_1\ldots i_n}(B))^2$ in the energy form is at most 7 sidecar triangles. From our triangle characterization scheme (see Figure 3.6) we know that a refinement of a sidecar triangle results in at most three transition triangles. Therefore the domain of influence of a single difference term is at most $7 \cdot 3 = 21$ transition triangles. □

Lemma 3.3.3. *Let u be a function in D_E defined on the fractal set S and let $u_n^* = \Pi_n u_n$ be the nth extension to the domain Ω. Then*

$$|u_n^*|_{H^1(T_{SC}^n \cup T_{TR}^n)} \leq \left(D \sum_{i_1\ldots i_n=1}^{3} \left(\sum_{\eta,\xi\in\{A,B,C\}} (u(\psi_{i_1\ldots i_n}(\eta)) - u(\psi_{i_1\ldots i_n}(\xi)))^2 \right) \right)^{1/2}$$

where $D \leq 94$ and is independent of n.

Proof. From Lemma 3.3.1 the domain of influence of a single difference term, $(u(\psi_{i_1\ldots i_n}(A)) - u(\psi_{i_1\ldots i_n}(B)))^2$ is at most 7 sidecar triangles. Moreover, by Lemma 3.3.2 the domain of influence of the same difference term is at most 21 transition triangles. The largest coefficient occurring in the adjusted H^1 seminorm of a sidecar triangle is 6, and the largest coefficient occurring in the adjusted H^1 seminorm of a transition triangle is $\frac{25}{3}$, hence the largest coefficient on any one difference, $(u(\psi_{i_1\ldots i_n}(A)) - u(\psi_{i_1\ldots i_n}(B)))^2$, is

$$7 \cdot 6 + 21 \cdot \frac{25}{3} \leq 217.$$

Hence

$$|u_n^*|_{H^1(T_{SC}^n \cup T_{TR}^n)} \leq \left[D \sum_{i_1\ldots i_n=1}^{3} \left(\sum_{\eta,\xi\in\{A,B,C\}} (u(\psi_{i_1\ldots i_n}(\eta)) - u(\psi_{i_1\ldots i_n}(\xi)))^2 \right) \right]^{1/2}$$

where $D \leq 217 \cdot \frac{\sqrt{3}}{4} = 94$. □

3.3.2 Main results for Sierpinski gasket

Lemma 3.3.4. *With the extension methodology defined in Section 2.2.2*

$$|u_0^*|_{H^1(\omega)}^2 \leq \frac{\sqrt{3}}{2} \left[(u(A) - u(B))^2 + (u(B) - u(C))^2 + (u(A) - u(C))^2 \right].$$

Proof. Using Lemma 3.1.1

$$\begin{aligned}
|u_0^*|^2_{H^1(\omega)} &= \iint_\omega u_x^2 + u_y^2 \, dx \, dy \\
&= \iint_{\mathcal{T}_1} u_x^2 + u_y^2 \, dx \, dy + \iint_{\mathcal{T}_2} u_x^2 + u_y^2 \, dx \, dy + \iint_{\mathcal{T}_3} u_x^2 + u_y^2 \, dx \, dy + \iint_{\mathcal{T}_4} u_x^2 + u_y^2 \, dx \, dy \\
&= \frac{\sqrt{3}}{4}(u(B) - u(A))^2 + \frac{\sqrt{3}}{4}(u(B) - u(C))^2 + \frac{\sqrt{3}}{4}(u(A) - u(C))^2 + \\
&\qquad + \frac{\sqrt{3}}{4}\left((u(B) - u(A))^2 + \frac{1}{3}(2u(C) - u(A) - u(B))^2\right) \\
&\leq \frac{\sqrt{3}}{4}\left[(u(B) - u(A))^2 + (u(B) - u(C))^2 + (u(A) - u(C))^2 + (u(B) - u(A))^2 + \right. \\
&\qquad \left. + \frac{2}{3}(u(C) - u(A))^2 + \frac{2}{3}(u(C) - u(B))^2\right] \\
&\leq \frac{\sqrt{3}}{2}\left[(u(B) - u(A))^2 + (u(B) - u(C))^2 + (u(C) - u(A))^2\right].
\end{aligned}$$

□

Lemma 3.3.5. *Let $u \in D_E$ be a function defined on the fractal set S. Then the following recursive estimate holds:*

$$|u_n^*|_{H^1(\omega)} \leq |u_{n-1}^*|_{H^1(\omega)} + \left(D \sum_{i_1 \ldots i_n = 1}^{3} \left(\sum_{\eta, \xi \in \{A,B,C\}} (u(\psi_{i_1 \ldots i_n}(\eta)) - u(\psi_{i_1 \ldots i_n}(\xi)))^2 \right) \right)^{1/2} \tag{3.9}$$

for every $n \geq 1$, in particular

$$|u_1^*|_{H^1(\omega)} \leq |u_0^*|_{H^1(\omega)} + \left(D \sum_{i_1 = 1}^{3} \left(\sum_{\eta, \xi \in \{A,B,C\}} (u(\psi_{i_1}(\eta)) - u(\psi_{i_1}(\xi)))^2 \right) \right)^{1/2}$$

Here D is the constant from Lemma 3.3.3 and is independent of n.

Proof. We begin with $u_0^* = \Pi_0 u_0$. By Lemma 3.3.4,

$$|u_0^*|_{H^1(\omega)} \leq \left(\frac{\sqrt{3}}{2}\left((u(A) - u(B)^2 + (u(B) - u(C))^2 + (u(A) - u(C))^2)\right)\right)^{1/2}.$$

We now prove that for every $n \geq 1$, the estimate 3.9 holds. We observe that in the

external triangles (i.e. T^n_{EX}), $u^*_n = u^*_{n-1}$. We therefore have

$$\begin{aligned}
|u^*_n|_{H^1(\omega)} &= |u^*_n|_{H^1(T^n_{EX})} + |u^*_n|_{H^1(T^n_{SC}\cup T^n_{TR})} \\
&= |u^*_{n-1}|_{H^1(T^n_{EX})} + |u^*_n|_{H^1(T^n_{SC}\cup T^n_{TR})} \\
&\leq |u^*_{n-1}|_{H^1(\omega)} + |u^*_n|_{H^1(T^n_{SC}\cup T^n_{TR})} \\
&\leq |u^*_{n-1}|_{H^1(\omega)} + \left(D \sum_{i_1\dots i_n=1}^{3} \left(\sum_{\eta,\xi\in\{A,B,C\}} (u(\psi_{i_1\dots i_n}(\eta)) - u(\psi_{i_1\dots i_n}(\xi)))^2 \right) \right)^{1/2}.
\end{aligned}$$

□

We now present the proof of Theorem 3.0.18 for the Sierpinski gasket.

Proof. We claim by construction $\Pi : D_E \mapsto H^1(\omega)$.

We apply Lemma 3.1.2 with $\rho = 5/3$, $g(n) = |u^*_n|_{H^1(\omega)}$, $c_0 = D^{1/2}$ and

$$\begin{aligned}
e(n) =& \rho^n \sum_{i_1\dots i_n=1}^{3} \left(\sum_{\eta,\xi\in\{A,B,C\}} (u(\psi_{i_1\dots i_n}(\eta)) - u(\psi_{i_1\dots i_n}(\xi)))^2 \right) \\
=& E^n[u,u].
\end{aligned}$$

We note that D is the constant from Lemma 3.3.3 and is independent of n. We also recall from the definition of the energy form in Chapter 1, that $E^n[u,u] \leq E^{n+1}[u,u]$ and for $u \in D_E$

$$E[u,u] := \sup_n E^n[u,u] < +\infty.$$

Moreover $g(0) = |u^*_0|_{H^1(\omega)} \leq [\frac{\sqrt{3}}{2}\left((u(A)-u(B))^2 + (u(B)-u(C))^2 + (u(A)-u(C))^2\right)]^{1/2}$. We get

$$\limsup_{n\to\infty} |u^*_n|_{H^1(\omega)} \leq |u^*_0|_{H^1(\omega)} + D^{1/2}\frac{\left(\frac{5}{3}\right)^{1/2} - \left(\frac{5}{3}\right)^{-n/2}}{\left(\frac{5}{3}\right)^{1/2} - 1}(E[u,u])^{1/2} \leq |u^*_0|_{H^1(\omega)} + M(E[u,u])^{1/2}$$

which implies there exists $C_5 > 0$ such that

$$|u^*_n|_{H^1(\omega)} \leq C_5(E[u,u])^{1/2}. \tag{3.10}$$

We now calculate the H^1 norm of u_n^* on ω, By construction, and Remark 2

$$\sup_{\omega}(u_n^*)^2 \leq \sup_{V^n} u_n^2 \leq \sup_{V^\infty} u_\infty^2 \leq \sup_{S} u^2.$$

Moreover we apply Lemma 1.1.2 to get:

$$\|u_n^*\|^2_{L^2(\omega)} \leq |\omega| \sup_{\omega}(u_n^*)^2 \leq |\omega| \sup_{S}(u)^2 \leq C_6(\|u\|^2_{L^2(S,\mu)} + E[u]), \tag{3.11}$$

where C_6 is a constant independent of n. Combining 3.10 and 3.11 we have

$$\|u_n^*\|^2_{H^1(\omega)} = \left(|u_n^*|^2_{H^1(\omega)} + \|u_n^*\|_{L^2(S,\mu)}\right)^{1/2} \leq C_7\sqrt{E[u,u] + \|u\|^2_{L^2(S,\mu)}},$$

where C_7 is independent of n.

Since $\|u_n^*\|_{H^1(\omega)}$ is bounded, $\|u_n^*\|_{H^1(\Omega)}$ is also bounded with

$$\|u_n^*\|_{H^1(\Omega)} = \left(|u_n^*|^2_{H^1(\Omega)} + \|u_n^*\|^2_{L^2(S,\mu)}\right)^{1/2} \leq C\sqrt{E[u,u] + \|u\|^2_{L^2(S,\mu)}},$$

where C is independent of n.

Since $\|u_n^*\|_{H^1(\Omega)} \leq C\sqrt{E[u,u] + \|u\|^2_{L^2(S,\mu)}}$, by the (sequentially) weak compactness of the unit ball of $H^1(\Omega)$, there exists a subsequence that converges weakly in $H^1(\Omega)$. Moreover by the Rellich Theorem, there exists a subsequence that converges strongly in $L^2(\Omega)$. Therefore, there exists a subsequence of $\{u_n^*\}$ that converges to some $z \in H^1(\Omega)$ weakly in $H^1(\Omega)$ and strongly in $L^2(\Omega)$. We now prove that for any such subsequence, $z = u^*$ where $u^* = \Pi u$. By Theorem 2.0.2, $u_n^*(x) \to u^*(x)$ uniformly on Ω, hence also strongly in $L^2(\Omega)$. Therefore, as $z \in H^1(\Omega) \hookrightarrow L^2(\Omega)$, by the uniqueness of the limit in $L^2(\Omega)$ we get $z = u^*$. This also implies the whole sequence $\{u_n^*\}$ converges to u^*, strongly in $L^2(\Omega)$ and weakly in $H^1(\Omega)$. Clearly, $z(x) = u^*(x)$ almost everywhere for $x \in \Omega$. Finally, by the lower semi-continuity of a Hilbert norm under weakly convergent sequences as $u_n^* \rightharpoonup u^*$ in $H^1(\Omega)$ we get

$$\|u^*\|_{H^1(\Omega)} \leq \liminf_{n\to\infty} \|u_n^*\|^2_{H^1(\Omega)} \leq C\sqrt{E[n] + \|u\|^2_{L^2(S,\mu)}}.$$

□

We end with a proposition that shows that the restriction of our extension function to the fractal set S is the original function.

Proposition 3.3.6. *Let $u \in D_E$ be a function defined on S, and Πu the extension function defined on Ω by the operator Π, then $\varphi_S \circ \Pi u = u$, where φ_S is the pointwise restriction of a continuous function on Ω to the set $S \subset \Omega$.*

Proof. The proof of this proposition is identical to Proposition 3.2.8 □

Triangle	Largest Coefficient for $\mathcal{T}$	Largest Coefficient for Transition Triangles
1	1	$\frac{29}{27}$
2	$\frac{29}{27}$	$\frac{28}{27}$
3	$\frac{8}{3}$	$\frac{32}{3}$
4	$\frac{8}{9}$	$\frac{2912}{675}$
5	$\frac{16}{27}$	$\frac{364}{243}$
6	$\frac{224}{75}$	$\frac{7936}{675}$
7	$\frac{1568}{675}$	$\frac{8192}{2025}$
8	$\frac{144}{75}$	$\frac{9728}{675}$
9	$\frac{79}{75}$	$\frac{360}{75}$
10	1	$\frac{52}{27}$
11	6	$\frac{32}{3}$
12	$\frac{26}{3}$	8
13	2	8
14	$\frac{2048}{675}$	$\frac{8192}{2025}$
15	$\frac{4}{3}$	$\frac{16}{9}$
16	$\frac{11}{27}$	$\frac{224}{243}$

Table 3.1: Coefficients in the adjusted H^1 seminorms

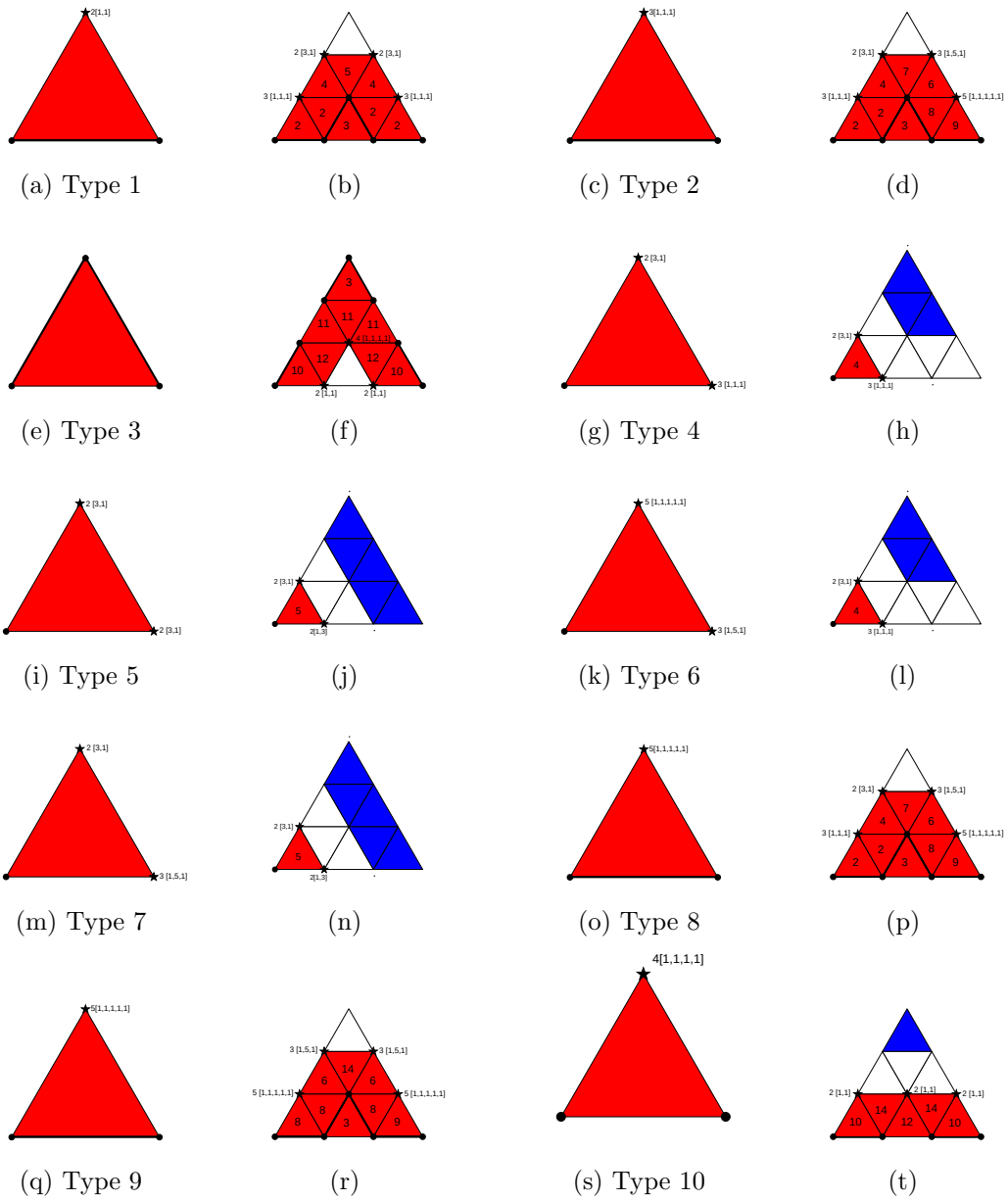

(a) Type 1 (b) (c) Type 2 (d)

(e) Type 3 (f) (g) Type 4 (h)

(i) Type 5 (j) (k) Type 6 (l)

(m) Type 7 (n) (o) Type 8 (p)

(q) Type 9 (r) (s) Type 10 (t)

Figure 3.3: Classification of triangle types 1-10.

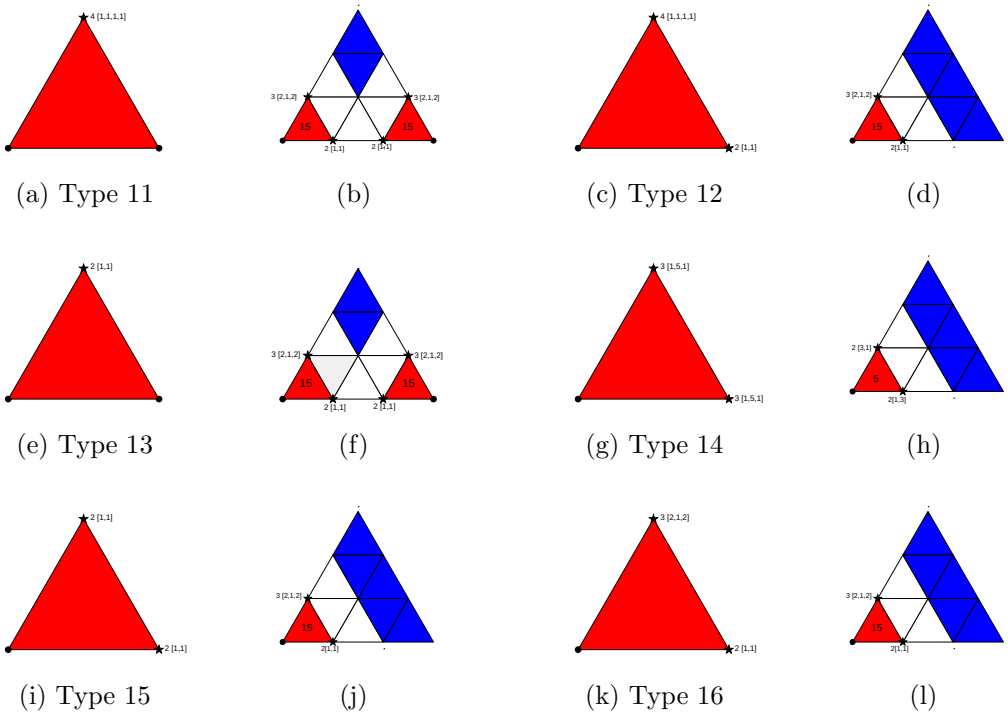

(a) Type 11 (b) (c) Type 12 (d)

(e) Type 13 (f) (g) Type 14 (h)

(i) Type 15 (j) (k) Type 16 (l)

Figure 3.4: Classification of triangle types 11-16.

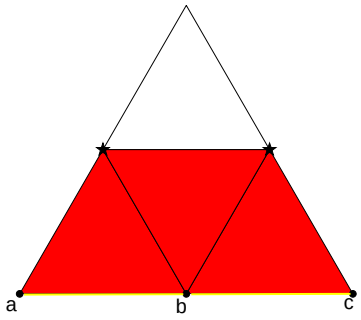

Figure 3.5: The identification of points and triangles. We note that the yellow curve is the prefractal curve S^{n+1}

Triangle	Largest Coefficient for $\mathcal{T}$	Largest Coefficient for Transition Triangles
1	1	N/A
2	1	$\frac{2}{3}$
3	1	N/A
4	$\frac{2}{3}$	1
5	$\frac{8}{3}$	N/A
6	2	6
7	$\frac{4}{3}$	$\frac{8}{3}$
8	2	$\frac{25}{3}$
9	6	$\frac{9}{2}$
10	6	$\frac{9}{2}$

Table 3.2: Coefficients in the adjusted H^1 seminorms

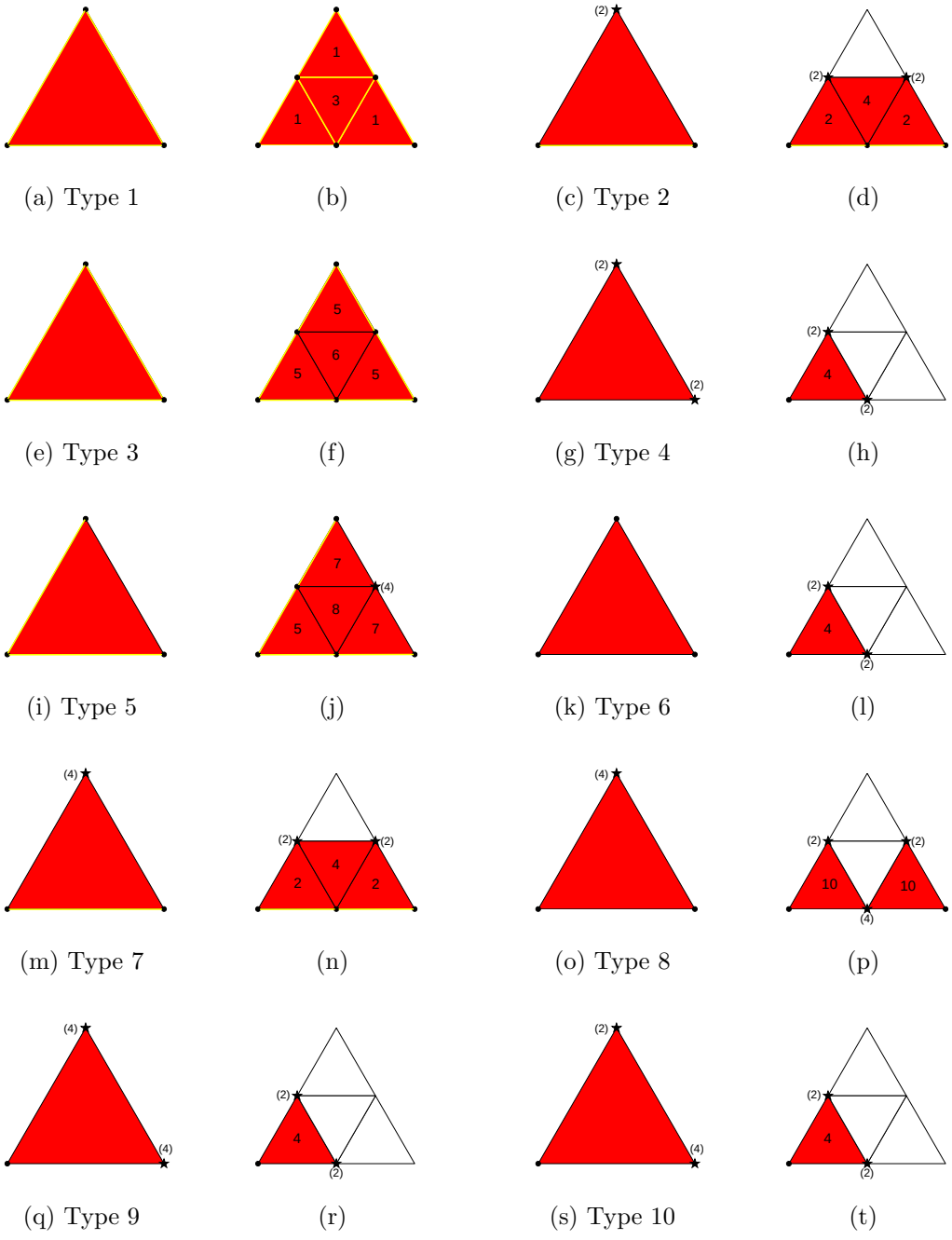

Figure 3.6: Classification of triangle types 1-10.

3.4 An Application of the Extension Operator

This section we will study one possible application of the fractal extension operator presented in this chapter. We consider a paper by Lancia and Vivaldi titled "Asymptotic Convergence of Transmission Energy Forms" with the expectation that the application of the fractal extension operator will both clarify and simplify the paper. The paper considers two transmission problems on a given parallogram domain Ω, the first is the prefractal transmission problem:

$$\begin{cases} -\Delta u_h = f & \text{in } \Omega_h^i,\ i = 1, 2 \\ -\rho_h \Delta_t u_h = \left[\frac{\partial u_h}{\partial \nu}\right] & \text{on } K_h \\ [u] = 0 & \text{across } K_h \\ u = 0 & \text{on } \partial\Omega. \end{cases} \tag{3.12}$$

Here K_h is the prefractal Koch curve (denoted by S^n elsewhere in the dissertation) and divides the domain Ω into two subsets Ω_h^1 and Ω_h^2. Moreover Δ_t denotes the tangential Laplacian on K_h, $[u_h]$ denotes the jump of u_h across the prefractal curve, and $\left[\dfrac{\partial u_h}{\partial \nu}\right]$ the jump of the normal derivatives of u_h across the prefractal curve and ρ_h is a positive constant. We also require that $f \in L^2(\Omega)$ be given.

The second problem considered is the fractal transmission problem:

$$\begin{cases} -\Delta u = f & \text{in } \Omega^i,\ i = 1, 2 \\ -c_h \Delta_K u = \left[\frac{\partial u}{\partial \nu}\right] & \text{on } K \\ [u] = 0 & \text{across } K \\ u = 0 & \text{on } \partial\Omega. \end{cases} \tag{3.13}$$

Similarly K is the fractal Koch curve (denoted by S elsewhere in the dissertation) and divides the domain Ω into two subsets Ω^1 and Ω^2. Here Δ_K denotes the Laplace operator defined on K, $[u]$ denotes the jump of u across the fractal curve, and $\left[\dfrac{\partial u}{\partial \nu}\right]$ the jump of the normal derivatives of u across the fractal curve in a suitable sense.

Remark 18. We retain the notation originally used by Lancia and Vivaldi in this section of the dissertation.

In the paper by Lancia and Vivaldi the asymptotic behavior of problem 3.12 is studied with the expectation that the asymptotic behavior is actually the problem 3.13. The convergence of solutions of the prefractal problem to the solution of the fractal problem is not obvious, and is the focus of the paper. The primary theorem shown is the convergence of the energy form

$$a_n(u_n, u_n) = \int_\Omega |\nabla u_n|^2 dx\ dy + \rho_n \int_{K_h} |\nabla_t u_n|^2 ds, \tag{3.14}$$

defined on the domain

$$V(\Omega, K_h) = \{u_n \in H_0^1(\Omega) : \gamma_0 u_n \in H_0^1(K_h)\} \tag{3.15}$$

to the form

$$a(u, u) = \int_\Omega |\nabla u|^2 dx\ dy + E(u, u) \tag{3.16}$$

defined on the domain

$$V(\Omega, K) = \{u \in H_0^1(\Omega) : \gamma_0 u \in D_0(K)\} \tag{3.17}$$

in the Mosco sense. Here $H_0^1(K_h)$ is the trace space and $\gamma_0 u_n$ is the trace of u_n on K_h. Moreover ∇_t denotes the tangential derivative on K_h, ds is the one-dimensional measure on K_h and ρ_n is a positive constant. In Equation 3.16, $E(u, u)$ is the energy form of the Koch curve, K is the fractal Koch curve and $\gamma_0 u$ is the restriction of u to K. Moreover, $D_0(K) = z \in D_E : z = 0$ on ∂K.

More specifically they show the following theorem (for a definition of M-convergence see Section 4.1)

Theorem 3.4.1. *Let $\rho_h = c_0 3^{(d-1)h}$, then the sequence of forms $a_h(\cdot, \cdot)$ defined in 3.14 M-converges to the form $a(\cdot, \cdot)$ defined in 3.16.*

The proof that the sequence of forms $\{a_n(\cdot, \cdot)\}$ M-converge to the form $a(\cdot, \cdot)$ requires the knowledge that K is a d-set. In the paper Lancia and Vivaldi use this knowledge to show that $u|_K \in B^{2,2}_{1-\epsilon}(K)$. Here $B^{2,2}_{1-\epsilon}$(K) is the Besov space defined as the class functions on K with finite norm

$$\|f\|_{B^{2,2}_{1-\epsilon}} = \|f\|_{2,\mu} + \left(\sum_{n=0}^{\infty} 3^{n(d+2(1-\epsilon))} \int\int_{|x-y|<3^{-n}} |f(x) - f(y)|^2 d\mu(x) d\mu(y) \right)^{1/2}.$$

(See [18] and [21]). From here they show they use the results of Theorem 1 of [17] to show that the function u can be extend to the domain Ω such that the resultant function u^* is in $H^1(\Omega)$ and $C^\beta(\Omega)$ using fractional Sobolev spaces.

In contrast we will be able to apply the extension operator of Chapters 2-3 directly. In particular given a function $u \in V(\Omega, K)$ and $v = u|_K$ we can extend v to a function $v^* \in H^1(\Omega)$. We then proceed as in the paper by Lancia and Vivaldi. Although the use of the fractal extension operator will not improve the results of the paper, it will greatly simplify the paper. Moreover, the numerical investigation of these problems will be easier to accomplish since the extension operator eliminates the need to re-approximate in the prefractal case.

Part II

Fractal Boundary Value Problems

In this section we will consider both transmission problems and boundary value problems with the added constraint that the boundary is a fractal. The presence of a fractal boundary adds complexity to the problem because the boundary is so irregular that derivatives must be defined in the sense of limits of derivatives on prefractal curves. As mentioned in the introduction, this contrasts with most of the existing literature which considers a much smoother boundary.

We will consider two problems in this part of the dissertation. The first is the problem of a domain with a highly conductive internal layer and is joint work with Haodong Liang. Here we arrange the thin fibers in the form a Sierpinski prefractal with fixed iteration n, and study the behavior of the problem as the conductivity increases and the width of the layer decreases. Second, we will consider the numerical solution to both boundary value and transmission problems with fractal boundaries. We will begin with an overview of finite element theorey and then introduce a mesh specifically designed for use with prefractal boundaries. We will also present an analysis of this mesh from the standpoint of numerical approximation. With this analysis we will present a scheme for refining the mesh around sinular points in the domain. We then use the mesh to solve a sample transmission problem.

Chapter 4

Singular Homogenization for Sierpinski Prefractals

This work considers the problem of a domain with a highly conductive internal layer and is joint work with Haodong Liang. This problem has been previously studied in a general sense by Cannon and Meyer [6], Pham Huy and Sanchez Palencia [15] and Attouch [1]. In their work the problem of an infinitely conductive layer is studied from the perspective of homogenization. They replace the layer Σ by a very thin layer of thickness ϵ. They then let the conductivity of the layer increase towards infinity as the thickness of the layer decreases towards zero. In the limit, the layer is a smooth lower dimensional subsection of the original domain. Lancia and Vivaldi have expanded on this study by considering the case when the layer Σ is actually a fractal Koch set. By allowing Σ to be a fractal set an additional scaling parameter is added which increases the complexity of the model. This increase in complexity is balanced by the fact that the problem can now better model actual applications by allowing surface energy to play a role as well as providing additional flexibility to the dimension of the thin layer.

This section of the dissertation considers an open problem not yet consider by Lancia, Mosco and Vivaldi. In [22] Lancia, Mosco, and Vivaldi consider the problem of homogenization for conductive layers when the conductive thin layers are of prefractal Koch curve type. They allow the value of α to vary thus allowing for an entire family of fractal curves each with different Hausdorff dimension. In [22] the infinitely conductive layer is replaced by thin layers with increasing conductivity, thus allowing the problem to be considered from a homogenization perspective.

In [27] Mosco and Vivaldi consider the Sierpinski gasket, however in this paper the thickness ϵ of the layer Σ was made dependent on the iteration number n. Mosco and Vivaldi then undertook a study of the convergence as the iteration number $n \to \infty$. In this paper we also consider the Sierpinski gasket, however we fix n at an arbitrary number. We then study the homogenization-type asymptotic as the thickness of the layer vanishes and the conductivity of the layer approaches infinity.

The main result of this portion of the dissertation is the M-convergence of the energy functionals as stated in Theorem 4.1.1. As in [22] and [27] we will introduce a weight function w_ϵ which consolidates both the geometric and physical characteristics of the thin layer into a single function. As in the previous works this function is singular at the angular boundary points between subdomains. We will work with weighted second-order elliptic equations on a triangular planar domain Ω and show that the energy functionals related to these equations M-converge to an energy functional that is both supported within the prefractal layer and singular. Our work in this section is a natural progression from the earlier work done by Lancia, Mosco and Vivaldi.

4.1 Problem Definition and Results

We let Ω be the equilateral triangle with vertices D, E, and F defined as $D = (1/2, -\sqrt{3}/4)$, $E = (3/2, \sqrt{3}/2)$, and $F = (-1/2, \sqrt{3}/2)$ and embed a smaller equilateral triangle with vertices A, B and C defined as $A = (0, 0)$, $B = (1, 0)$ and $C = (1/2, \sqrt{3}/2)$ into the domain. In this embedded triangle we will construct the Sierpinski gasket in the usual manner with contraction factor 2^{-1}. (We refer the reader to the definition of the Sierpinski gasket found in Section 1.2).

We will denote by S_0 the collection of three segments $\overline{AB}$, $\overline{BC}$, and $\overline{CA}$, and by S^n we will denote the nth prefractal Sierpinski gasket.

By K_l, $l = 0, 1, 2$ we denote the segments with end points A and B, B and C, and C and A respectively. We now define the ϵ-neighborhood of the segment K_0, denoted

by $\Sigma_{0,\epsilon}$, as the polygon whose vertices are the points A, P_1, P_2, B, P_3 P_4, where

$$P_1 := \left(\tfrac{\epsilon}{c_1}, \tfrac{\epsilon}{2}\right) \qquad P_2 := \left(1 - \tfrac{\epsilon}{c_1}, \tfrac{\epsilon}{2}\right)$$
$$P_3 := \left(1 - \tfrac{\epsilon}{c_1}, -\tfrac{\epsilon}{2}\right) \quad P_4 := \left(\tfrac{\epsilon}{c_1}, -\tfrac{\epsilon}{2}\right).$$

Here $c_1 = \tan(\pi/12)$ and $0 < \epsilon \leq c_1/2$.

We also subdivide $\Sigma_{0,\epsilon}$ into the union of three parts: a rectangle $\mathcal{R}_{0,\epsilon}$ and two triangles $\mathcal{T}_{0,j,\epsilon},\ j = 1, 2$. Here, $\mathcal{R}_{0,\epsilon}$ is the rectangle with vertices P_1, P_2, P_3, and P_4; $\mathcal{T}_{0,1,\epsilon}$ is the triangle with vertices A, P_1, and P_4 and $\mathcal{T}_{0,2,\epsilon}$ is the triangle with vertices B, P_2, and P_3. For $l = 1, 2$ we construct similar ϵ-neighborhoods $\Sigma_{l,\epsilon}$ of K_l and subdivide $\Sigma_{l,\epsilon}$ in a similar manner as for $\Sigma_{0,\epsilon}$.

We now define the larger set

$$S_0 = \bigcup_{l=0,1,2} K_l$$

and its associated ϵ- neighborhood of S_0:

$$\Sigma_\epsilon = \bigcup_{l=0,1,2} \Sigma_{l,\epsilon}.$$

For every n we consider the polygonal curve

$$S^n = \bigcup_{i|n} S_0^{i|n}$$

and the ϵ-neighborhood

$$\Sigma_\epsilon^n = \bigcup_{i|n} \Sigma_\epsilon^{i|n}$$

With our domain Ω and the embedded layer Σ_ϵ^n (given n and ϵ) in mind we now define a weight w_ϵ^n, as follows. For some $i|n$ and some l, let P be a point on the boundary $\partial\left(\sum_{l,\epsilon}^{i|n}\right)$ of $\sum_{l,\epsilon}^{i|n}$ and let $P^\perp$ be the orthogonal projection of P on $H_l^{i|n}$. Let c_0 be a fixed positive constant and let $\left|P - P^\perp\right|$ the (Euclidean) distance between P and $P^\perp$ in $\mathbb{R}^2$. If (ξ, η) belongs to the segment with end points P and $P^\perp$, we set with our current

notation:

$$w_\epsilon^n(\xi,\eta)=\begin{cases}\frac{2+c_1^2}{4\left|P-P^\perp\right|}c_0 & \text{if } (\xi,\eta)\in\mathcal{T}_{l,j,\epsilon}^{i|n},\ j=1,2\\ \frac{1}{2\left|P-P^\perp\right|}c_0 & \text{if } (\xi,\eta)\in\mathcal{R}_{l,\epsilon}^{i|n}\\ 1 & \text{if } (\xi,\eta)\notin\sum_\epsilon^n\end{cases}\tag{4.1}$$

where c_0 is a fixed positive constant.

Given the weight w_ϵ^n, the associated Sobolev spaces are

$$H^1(\Omega,w_\epsilon^n)=\left\{u\in L^2(\Omega):\int_\Omega|\nabla u|^2\,w_\epsilon^n d\xi d\eta<+\infty\right\}\tag{4.2}$$

and $H_0^1(\Omega,w_\epsilon^n)$, the latter being the completion of $C_0^\infty(\Omega)$ in the norm

$$\|u\|_{H^1(\Omega,w_\epsilon^n)}:=\left\{\int_\Omega|u|^2\,d\xi d\eta+\int_\Omega|\nabla u|^2\,w_\epsilon^n d\xi d\eta\right\}^{1/2}.$$

We now define the associated weighted energy functionals in $L^2(\Omega)$

$$F_\epsilon^n([u])=\begin{cases}\int_\Omega w_\epsilon^n(\xi,\eta)\,|\nabla u|^2\,d\xi d\eta & \text{if } u\in D_0[F_\epsilon^n]\\ +\infty & \text{if } u\in L^2\setminus D_0[F_\epsilon^n],\end{cases}\tag{4.3}$$

where $D_0[F_\epsilon^n]=H_0^1(\Omega,w_\epsilon^n)$. From [22] we know that $D_0[F_\epsilon^n]$ is a Hilbert space with respect to the norm

$$||u||_{D_0[F_\epsilon^n]}=\sqrt{F_\epsilon^n[u]}.$$

For a given n we now consider the polygonal curve generated by the prefractal S^n. We define the Sobolev space $H_0^1(S^n)$ as

$$H_0^1(S^n)=\{v\in C_0^0(S^n):v|_{S_0^{i|n}}\in H^1(S_0^{i|n})\}\quad\text{for all sets } S_0^{i|n}\in S^n.\tag{4.4}$$

We also denote by $\nabla_\tau u$ the tangential derivative of u along each segment of S^n.

Before stating our main result we familiarize the reader with the definition of *M-convergence* of functionals, first introduced in [26], see also [25].

Definition 4. A sequence of functionals $F^m:H\to(-\infty,+\infty]$ is said to M-converge to a functional $F:H\to(-\infty,+\infty]$ in a Hilbert space H if:

1. for every $u \in H$ there exists v_m converging strongly in H such that

$$\overline{\lim} F^m [v_m] \leq F(u), \text{as } m \to \infty. \tag{4.5}$$

2. For every v_m converging weakly to u in H

$$\underline{\lim} F^m [v_m] \geq F[u], \text{ as } m \to \infty. \tag{4.6}$$

The result is the following

Theorem 4.1.1. *For every fixed n, the functionals F_ϵ^n M-converge in L^2 to the functional F^n as $\epsilon \to 0$, where*

$$F^n[u] = \begin{cases} \int_\Omega |\nabla u|^2 \, d\xi d\eta + c_0 \int_{S^n} |\nabla_\tau u|^2 ds & \text{if } u \in D_0[F^n] \\ +\infty & \text{if } u \in L^2(\Omega) \setminus D_0[F^n] \end{cases} \tag{4.7}$$

where

$$D_0[F^n] = \left\{ v \in H_0^1(\Omega) : v_{|S^n} \in H_0^1(S^n) \right\}. \tag{4.8}$$

4.2 Proof of Theorem 4.1.1

4.2.1 Proof of "lim sup" condition

We begin by constructing a reference domain $\mathcal{D}$ as a subset of Ω. We also construct a larger layer $\Sigma_{2\epsilon}$, which contains Σ_ϵ and is contained in $\mathcal{D}$, see Figure 4.1. By $\mathcal{D}_0$ we will denote the domain with vertices A, G, B, H where A and B are as defined previously and

$$G = (1/2, \sqrt{3}/6), \quad \text{and } H = (1/2, -\sqrt{3}/6).$$

For every $0 < \epsilon \leq \frac{c_1}{2}$, (recall $c_1 = \tan(\pi/12)$), we define the set $\Sigma_{0,2\epsilon}$ to be the quadrilateral domain with vertices A, Q_1, Q_2, B, Q_3, Q_4. Here:

$$\begin{array}{ll} Q_1 := \left(\frac{\epsilon}{c_1}, \epsilon\right) & Q_2 := \left(1 - \frac{\epsilon}{c_1}, \epsilon\right) \\ Q_3 := \left(1 - \frac{\epsilon}{c_1}, -\epsilon\right) & Q_4 := \left(\frac{\epsilon}{c_1}, -\epsilon\right) \end{array}$$

We define the sets $\mathcal{D}_1$, $\mathcal{D}_2$, $\Sigma_{1,2\epsilon}$, $\Sigma_{2,2\epsilon}$ in a similar way by replacing K_0 with K_1 and K_2.

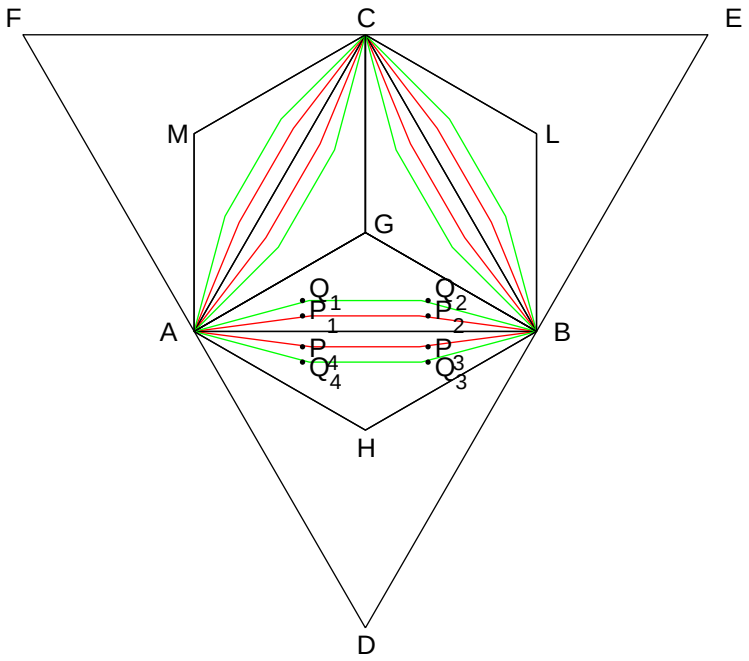

Figure 4.1: ϵ, 2ϵ, and $\mathcal{D}$

Moreover we define a larger domain $\mathcal{D}$ to be the hexagonal domain defined by the points A, H, B, L, C, M where $L = (1, 1/\sqrt{3})$, and $M = (0, 1/\sqrt{3})$. We also define

$$\Sigma_{2\epsilon} = \bigcup_{l=0,1,2} \Sigma_{l,2\epsilon}.$$

Obviously, $G_0 \subset \Sigma_\epsilon \subset \Sigma_{2\epsilon} \subset \mathcal{D} \subset \Omega$. (See figure 4.1.)

For a given l the segment K_l divides both the set $\Sigma_{l,\epsilon}$ and the set $\Sigma_{l,2\epsilon}$ into two pieces. The first piece lies within the triangle A, B, C and will be denoted by $\Sigma^+_{l,\epsilon}$ ($\Sigma^+_{l,2\epsilon}$), and the second lies external to this triangle and will be denoted by $\Sigma^-_{l,\epsilon}$ ($\Sigma^-_{l,2\epsilon}$). For every point (x, y) in $\overline{\Sigma}_{l,2\epsilon}$ we call (x_l, y_l) the orthogonal projection of (x, y) onto K_l. By $P_{l,\pm} = P_{l,\pm}(x, y) = (\hat{x}_{l,\pm}, \hat{y}_{l,\pm}) \in \partial\Sigma_{l,\epsilon}$ the point where the straight line connecting (x, y)

to (x_l, y_l) intersects the boundary of $\Sigma_{l,\epsilon}$, likewise by $Q_{l,\pm} = Q_{l,\pm}(x,y) = (\tilde{x}_{l,\pm}, \tilde{y}_{l,\pm}) \in \partial\Sigma_{l,2\epsilon}$ the point where the straight line connecting (x,y) to (x_l, y_l) intersects the boundary of $\Sigma_{l,2\epsilon}$. As before the $+$ sign refers to points internal to the triangle A, B, C and the $-$ sign refers to points external to this triangle.

We define the operator $G_\epsilon : C^1\left(\overline{\mathcal{D}}\right) \to Lip(\overline{\mathcal{D}})$ by setting for a given function $g \in C^1(\overline{\mathcal{D}}), g_\epsilon = G_\epsilon(g)$ where the function $g_\epsilon(x,y)$ is defined for $(x,y) \in \mathcal{D}$ as follows.

$$g_\epsilon(x,y) = \begin{cases} g(x,y) & \text{if } (x,y) \in \overline{\mathcal{D}} \setminus \Sigma_{2\epsilon} \\ g(x_l, y_l) & \text{if } (x,y) \in \overline{\Sigma}_{l,\epsilon} \\ g(x_l, y_l)\, b_{l,\pm} + g(Q_{l,\pm})(1 - b_{l,\pm}) & \text{if } (x,y) \in \overline{\Sigma}_{l,2\epsilon} \setminus \Sigma_{l,\epsilon} \end{cases} \tag{4.9}$$

where:

$$b_{l,\pm} = \frac{|\tilde{y}_{l,\pm} - y| + |\tilde{x}_{l,\pm} - x|}{|\tilde{y}_{l,\pm} - \hat{y}_{l,\pm}| + |\tilde{x}_{l,\pm} - \hat{x}_{l,\pm}|}.$$

By construction g_ϵ is equal to g in $\mathcal{D} \setminus \Sigma_{2\epsilon}$, and on each segment S_l, defined as the segment obtained as the intersection of $\overline{\Sigma}_{l,2\epsilon}$ with the orthogonal line to K_l at the point (x_l, y_l), g_ϵ is a piecewise affine function which is equal to $g(x_l, y_l)$ on $S \cap \overline{\Sigma}_{l,\epsilon}$ and equal to g at the intersection of S_l and $\partial\Sigma_{l,2\epsilon}$. Using the notation of the first section we put $\mathcal{D}^{i|n} = \psi_{i|n}(\mathcal{D})$ and

$$\mathcal{D}^n = \bigcup_{i|n} \mathcal{D}^{i|n}.$$

Finally for every function $u \in C_0^1(\Omega)$ and each n and ϵ, we define:

$$u_\epsilon^n(\xi,\eta) = \begin{cases} u(\xi,\eta) & \text{if } (\xi,\eta) \in \Omega \setminus \mathcal{D}^n \\ G_\epsilon\left(u \circ \psi_{i|n}\right) \circ \psi_{i|n}^{-1}(\xi,\eta) & \text{if } (\xi,\eta) \in \mathcal{D}_{i|n} \end{cases} \tag{4.10}$$

where G_ϵ is the operator defined before.

Remark 19. We note that $u_\epsilon^n(P) = u(P)$ for every $P \in V^n$. Moreover we note that since $u \in C_0^1(\Omega)$ by construction u_ϵ^n is continuous on Ω.

Step 1: We suppose $u \in C_0^1(\Omega)$.

Proposition 4.2.1. *With the assumptions of the Theorem 4.1.1 we have that for every*

$u \in C_0^1(\Omega)$,

$$\overline{\lim}_{\epsilon\to 0} F_\epsilon^n\left[u_\epsilon^n\right] \le F^n\left[u\right] \tag{4.11}$$

where u_ϵ^n is defined as in (4.10). Moreover, u_ϵ^n converges to u in $L^2(\Omega)$ as $\epsilon \to 0$.

Proof. We begin by observing that at any step n, two hexagonal domains $\mathcal{D}^{i|n}$ and $\mathcal{D}^{j|n}$ with different n-addresses (i.e $i|n \neq j|n$), may share vertices or entire sides but the interior of the domains never overlap. Moreover two distinct quadrilateral domains $\psi_{i|n}(\mathcal{D}_l), \psi_{j|n}(\mathcal{D}_m)$ (where $l \neq m$ or $i|n \neq j|n$) also do not share interiors. A similar observation holds true for $K_l^{i|n}$ and $K_m^{j|n}$ for these two copies intersect only at most vertices (and these vertices belong to the larger set V^n, and also the sets $\Sigma_{l,2\epsilon}^{i|n}$ and $\Sigma_{m,2\epsilon}^{j|n}$ (with $l \neq m$) meet at most at vertices in V^n.)

As a consequence of these intersection properties, the functions u_ϵ^n belong to $Lip(\overline{\Omega})$. We split the integral $F_\epsilon^n[u_\epsilon^n]$ into three terms according to the definition of the weight function w_ϵ^n.

$$F_\epsilon^n\left[u_\epsilon^n\right] = \int_{\Omega\setminus\Sigma_{2\epsilon}^n} |\nabla u|^2\, d\xi d\eta + \int_{\Sigma_\epsilon^n} |\nabla u_\epsilon^n|^2\, w_\epsilon^n d\xi d\eta + \int_{\Sigma_{2\epsilon}^n\setminus\Sigma_\epsilon^n} |\nabla u_\epsilon^n|^2\, d\xi d\eta$$

Since the 2-dimensional Lebesgue measure of $\Sigma_{2\epsilon}^n$ goes to zero as $\epsilon \to 0$, we conclude that

$$\lim_{\epsilon\to 0} \int_{\Omega\setminus\Sigma_{2\epsilon}^n} |\nabla u|^2\, d\xi d\eta = \int_\Omega |\nabla u|^2\, d\xi d\eta. \tag{4.12}$$

Then in order to prove Proposition 4.2.1 we must only show that:

$$\lim_{\epsilon\to 0} \int_{\Sigma_{2\epsilon}^n\setminus\Sigma_\epsilon^n} |\nabla u_\epsilon^n|^2\, d\xi d\eta = 0 \tag{4.13}$$

and

$$\overline{\lim}_{\epsilon\to 0} \int_{\Sigma_\epsilon^n} |\nabla u_\epsilon^n|^2\, w_\epsilon^n d\xi d\eta = c_0 \int_{S^n} |\nabla_\tau u|^2 ds. \tag{4.14}$$

Moreover we will also show that $u_\epsilon^n \in H^1\left(\Omega; w_\epsilon^n\right)$ for every ϵ and n.

We have

$$\int_{\Sigma_{2\epsilon}^n\setminus\Sigma_\epsilon^n} |\nabla u_\epsilon^n|^2 d\xi d\eta = \sum_{i|n} \int_{(\Sigma_{2\epsilon})^{i|n}\setminus(\Sigma_\epsilon)^{i|n}} |\nabla u_\epsilon^n|^2 d\xi d\eta.$$

(Note that the number of elements on the right hand side is equal to 3^n.) For a fixed n-

address $i|n$ the domain $(\Sigma_{2\epsilon})^{i|n}\backslash(\Sigma_{\epsilon})^{i|n}$ can be decomposed into the union of six rectangles and twelve triangles. We split the integral (4.13) according to this decomposition, and write

$$\int_{\Sigma_{2\epsilon}^{i|n}\backslash\Sigma_{\epsilon}^{i|n}} |\nabla u_{\epsilon}^{n}|^{2}\, d\xi d\eta \equiv \sum_{l=0}^{2} R_{l}^{+} + \sum_{l=0}^{2} R_{l}^{-} + \sum_{l=0}^{2}\sum_{j=3}^{6} X_{l,j}$$

where

$$R_{l}^{+} = \int_{\psi_{i|n}\left(\mathcal{R}_{l,\epsilon}^{+}\right)} |\nabla u_{\epsilon}^{n}|^{2}\, d\xi d\eta,$$

$$R_{l}^{-} = \int_{\psi_{i|n}\left(\mathcal{R}_{l,\epsilon}^{-}\right)} |\nabla u_{\epsilon}^{n}|^{2}\, d\xi d\eta$$

and

$$X_{l,j} = \int_{\psi_{i|n}\left(\mathcal{T}_{l,j,\epsilon}\right)} |\nabla u_{\epsilon}^{n}|^{2}\, d\xi d\eta, \quad j = 3,4,5,6 \quad \text{and} \quad l = 0,1,2.$$

Here $\mathcal{R}_{0,\epsilon}^{+}$ is the rectangle of vertices P_1, P_2, Q_2, Q_1, $\mathcal{R}_{0,\epsilon}^{-}$ the rectangle of vertices Q_4, P_4, P_3, Q_3, X_j the triangle of vertices A, P_h, Q_h for $j = 3,6$ and X_h the triangle of vertices P_h, Q_h, B for $j = 4,5$ and $h = j-2$. The rectangles $\mathcal{R}_{1,\epsilon}^{+}$, $\mathcal{R}_{1,\epsilon}^{-}$, $\mathcal{R}_{2,\epsilon}^{+}$, $\mathcal{R}_{2,\epsilon}^{-}$, and the triangles $\mathcal{T}_{1,j,\epsilon}$, $\mathcal{T}_{2,j,\epsilon}$ are defined in a like manner.
We prove that

$$\lim_{\epsilon\to 0} R_{l}^{\pm} = 0 \quad l = 0,1,2. \tag{4.15}$$

We will prove the equality for R_0^+, the proof for the other rectangles being analogous. By using an appropriate change of coordinates $(\xi,\eta) = \psi_{i|n}(x,y)$ we get

$$R_{0}^{+} = \int_{\mathcal{R}_{0,\epsilon}^{+}} |\nabla g_{\epsilon}|^{2} dx dy. \tag{4.16}$$

We recall that $g(x,y) = u \circ \psi_{i|n}(x,y)$ and on $\mathcal{R}_{0,\epsilon}^{+}$, $\hat{y}_{0,+}(x) = \frac{\epsilon}{2}$, $\tilde{y}_{0,+}(x) = \epsilon$, $\hat{x}_{0,+}(x) = \tilde{x}_{0,+}(x) = x$ $P_{0,+} = \left(x, \frac{\epsilon}{2}\right)$, $Q_{0,+} = (x,\epsilon)$ and hence

$$b_{0,+} = \frac{|\tilde{y}_{0,+} - y| + |\tilde{x}_{0,+} - x|}{|\tilde{y}_{0,+} - \hat{y}_{0,+}| + |\tilde{x}_{0,+} - \hat{x}_{0,+}|} = \frac{|\epsilon - y|}{\frac{\epsilon}{2}}.$$

Thereby we obtain

$$g_{\epsilon}(x,y)dx\, dy = \frac{2y}{\epsilon}(g(x,\epsilon) - g(x,0)) + 2g(x,0) - g(x,\epsilon) \tag{4.17}$$

and

$$\begin{aligned}\int_{\mathcal{R}_\epsilon^+}(g_\epsilon)_y^2 &= \frac{4}{\epsilon^2}\int_{\frac{\epsilon}{c_1}}^{1-\frac{\epsilon}{c_1}} dx \int_{\frac{\epsilon}{2}}^{\epsilon}(g(x,\epsilon)-g(x,0))^2 dy \\ &\leq \frac{4}{\epsilon^2}\frac{\epsilon^2}{2}\int_{\frac{\epsilon}{c_1}}^{1-\frac{\epsilon}{c_1}} dx \int_0^{\epsilon} g_t^2(x,t)dt \to 0\end{aligned} \tag{4.18}$$

as $g \in H^1(\mathcal{D})$ and the Lebesgue measure of $\mathcal{R}_{0,\epsilon}^+ \to 0$ as $\epsilon \to 0$.
Similarly we consider the term $\int_{\mathcal{R}_{0,\epsilon}^+}(g_\epsilon)_x^2 dx\, dy$ (as $\frac{\epsilon}{2} < y < \epsilon$) that has behavior of the type

$$c\frac{\epsilon}{2}\int_{\frac{\epsilon}{c_1}}^{1-\frac{\epsilon}{c_1}}(g_x^2(x,0)+g_x^2(x,\epsilon))dx \to 0 \text{ as } \epsilon \to 0.$$

Hence we have shown 4.15 (since $g \in C^1(\overline{\mathcal{D}})$).

Now we show that

$$X_{l,j} = 0 \qquad j = 3,4,5,6 \qquad l = 0,1,2 \tag{4.19}$$

We consider only the term $X_{0,3}$, since the other $X_{l,j}$'s are analogous. By a suitable change of coordinates $(\xi,\eta) = \psi_{i|n}(x,y)$ we get

$$X_{0,3} = \int_{\mathcal{T}_{0,3,\epsilon}} |\nabla g_\epsilon|^2 dxdy,$$

where $g(x,y) = u \circ \psi_{i|n}(x,y)$ and g_ϵ is defined in 4.9. On the triangle $\mathcal{T}_{0,3,\epsilon}$, we have $\hat{y}_{0,+} = \frac{c_1 x}{2}$, $\tilde{y}_{0,+} = c_1 x$, $P_{0,+} = (x, \frac{c_1 x}{2})$, $Q_{0,+} = (x, c_1 x)$ and

$$b_{0,+} = \frac{|\tilde{y}_{0,+} - y| + |\tilde{x}_{0,+} - x|}{|\tilde{y}_{0,+} - \hat{y}_{0,+}| + |\tilde{x}_{0,+} - \hat{x}_{0,+}|} = \frac{|c_1 x - y|}{\frac{c_1 x}{2}}.$$

Thereby we obtain

$$g_{\epsilon(x,y)} = \frac{2y}{c_1 x}(g(x,c_1 x) - g(x,0)) + 2g(x,0) - g(x,c_1 x) \tag{4.20}$$

and

$$\begin{aligned}\int_{\mathcal{T}_{0,3\epsilon}} (g_\epsilon)_y^2 &= \frac{4}{c_1^2}\int_0^{\frac{\epsilon}{c_1}} dx \int_{\frac{c_1 x}{2}}^{c_1 x} \frac{(g(x,c_1x)-g(x,0))^2}{x^2}dy \\ &\leq \frac{4}{c_1^2}\frac{c_1^2}{2}\int_0^{\frac{\epsilon}{c_1}} dx \int_0^{c_1 x} g_t^2(x,t)dt \to 0\end{aligned} \tag{4.21}$$

since the measure of $\mathcal{T}_{l,j,\epsilon} \to 0$ as $\epsilon \to 0$. In a similar manner the integral $\int_{\mathcal{T}_{0,3,\epsilon}} (g_\epsilon)_x^2 dxdy$ contains terms either of the type

$$c\int_0^{\frac{\epsilon}{c_1}} dx \int_{\frac{c_1 x}{2}}^{c_1 x} \frac{(g(x,c_1x)-g(x,0))^2}{x^2}dy$$

that can be calculated as above, or of the type

$$c\int_0^{\frac{\epsilon}{c_1}} \frac{c_1 x}{2}(g_x^2(x,c_1x)+g_y^2(x,c_1x)+g_x^2(x,0))dx \to 0 \text{ as } \epsilon \to 0$$

(as $g \in C^1(\overline{\mathcal{D}})$). By combining the estimates we arrive as the proof of Equation 4.13.

We now turn our attention to Equation 4.14.

As before we split the integral on Σ_ϵ^n in the same of the 3^n integrals on the copies of the n-generation $\sum_\epsilon^{i|n}$. These copies we split into the union of three rectangles and six triangles and we evaluate the corresponding integrals by means of an appropriate coordinate change. We write

$$\int_{\Sigma_\epsilon^{i|n}} |\nabla u_\epsilon^n|^2 w_\epsilon^n d\xi d\eta \equiv \sum_{l=0}^{2} R_l + \sum_{l=0}^{2}\sum_{j=1}^{2} X_{l,j}$$

where

$$R_l = \int_{\psi_{i|n}(\mathcal{R}_{l,\epsilon})} |\nabla u_\epsilon^n|^2 w_\epsilon^n d\xi d\eta,$$

and

$$X_l, j = \int_{\psi_{i|n}(\mathcal{T}_{l,j,\epsilon})} |\nabla u_\epsilon^n|^2 w_\epsilon^n d\xi d\eta, \quad j=1,2 \quad \text{and} \quad l=0,1,2.$$

Here $\mathcal{R}_{0,\epsilon}$ is the rectangle with vertices P_1, P_2, P_3, P_4; $\mathcal{T}_{0,\epsilon,1}$ is the triangle with vertices A, P_1, P_4 and $\mathcal{T}_{0,\epsilon,2}$ is the triangle with vertices B, P_2, P_3. The rectangles $\mathcal{R}_{1,\epsilon}, \mathcal{R}_{2,\epsilon}$

and the four triangles $\mathcal{T}_{1,j,\epsilon}, \mathcal{T}_{2,j,\epsilon}$ $(j = 1, 2)$ are defined analogously.

We note that for $(\xi, \eta) \in \Sigma_\epsilon^{i|n}$, $(\xi, \eta) = \psi_{i|n}(x, y)$ and $w_\epsilon^n(\xi, \eta) = 2^n \ell_\epsilon^{-1}(x)\, c_0$ where

$$\ell_\epsilon(x) = \begin{cases} \epsilon & \text{if } \frac{\epsilon}{c_1} < x < 1 - \frac{\epsilon}{c_1} \\ \frac{2(c_1 - c_1 x)}{2 + c_1^2} & \text{if } 1 - \frac{\epsilon}{c_1} < x < 1 \\ \frac{2c_1 x}{2 + c_1^2} & \text{if } 0 < x < \frac{\epsilon}{c_1} \end{cases}.$$

We continue the calculation in terms of R_0 and $X_{0,1}$. By taking 4.9 into account (and with $g(x, y) = u^n \circ \psi_{i|n}(x, y)$) we have

$$R_0 = \frac{2^n c_0}{\epsilon} \int_{\frac{\epsilon}{c_1}}^{1 - \frac{\epsilon}{c_1}} dx \int_{-\frac{\epsilon}{2}}^{\frac{\epsilon}{2}} g_x^2(x, 0) dy = 2^n c_0 \int_{\frac{\epsilon}{c_1}}^{1 - \frac{\epsilon}{c_1}} g_x^2(x, 0) dx$$

here the last term

$$2^n c_0 \int_{\frac{\epsilon}{c_1}}^{1 - \frac{\epsilon}{c_1}} g_x^2(x, 0) dx \to 2^n c_0 \int_0^1 g_x^2(x, 0) dx$$

as $\epsilon \to 0$ and

$$2^n c_0 \int_0^1 g_x^2(x, 0) dx = \frac{2^n}{2^n} c_0 \int_{\psi_{i|n}(K_0)} |\nabla_\tau u_\epsilon^n|^2 ds.$$

Suppose now that $(\xi, \eta) \in \mathcal{T}_{1,\epsilon}^{i|n}$, then the weight $w_\epsilon^n(\xi, \eta)$ is equal to $c_0 2^n \frac{(2 + c_1^2)}{2c_1}$ and

$$\begin{aligned} X_1 &= \frac{c_0 2^n (2 + c_1^2)}{2c_1} \int_0^{\frac{\epsilon}{c_1}} \frac{dx}{x} \cdot \int_{-\frac{c_1 x}{2}}^{\frac{c_1 x}{2}} g_x^2(x, 0) dy \\ &= \frac{c_0 2^n (2 + c_1^2)}{2} \int_0^{\frac{\epsilon}{c_1}} g_x^2(x, 0) dx \quad \text{as } \epsilon \to 0 \end{aligned}$$

since $g \in H^1(S_0)$. All of the other terms X_l, j $(l = 0, 1, 2$ and $j = 1, 2)$ can be evaluated in an analogous way the proof of proposition 4.2.1 is complete. □

Remark 20. In this dissertation the index n is arbitrary but fixed. The behavior as ϵ goes to 0 and n goes to infinity is simultaneously is studied in [28].

Step 2. The goal of this step is to remove the previous assumption that $u \in C_0^1(\Omega)$

Proposition 4.2.2. *For any function $u \in D_0[F]$ there exists a family of functions $u_\epsilon^* \in H_0^1(\Omega)$, such that*

$$\begin{cases} u_\epsilon^* \to u \quad in\ L^2(\Omega) \\ and \\ \lim_{\epsilon\to 0} F_\epsilon[u_\epsilon^*] \leq F[u]. \end{cases} \tag{4.22}$$

Proof. From the density results there exists a sequence of functions $u_m \in C_0^1(\Omega)$ such that

$$F[u] = \lim_{m\to\infty} F[u_m]$$

By proceeding as in Step 1, we prove that for each fixed m

$$F[u_m] = \lim_{\epsilon\to 0} F_\epsilon[u_{m,\epsilon}].$$

We now proceed by applying the diagonal formula of Corollary 1.16 in [1]. This Corollary shows that there exists a strictly increasing mapping $\epsilon \to m(\epsilon) = +\infty$. If we denote by $u_\epsilon^* = u_{m(\epsilon),\epsilon}$ we arrive at proof of 4.22 and of Proposition 4.2.2. □

4.2.2 Proof of "lim inf" condition

Step 1: We suppose $v_\epsilon \in C_0^1(\Omega)$.

Proposition 4.2.3. *Let $v_\epsilon \in C_0^1(\Omega)$, $v_\epsilon \rightharpoonup u$ in $L^2(\Omega)$, then*

$$F[u] \leq \underline{\lim}_{\epsilon\to 0} F_\epsilon[v_\epsilon]. \tag{4.23}$$

Proof. In order to prove the inequality (4.23), it is not restrictive to assume that $\underline{\lim}_{\epsilon\to 0} F_\epsilon[v_\epsilon] < +\infty$. We can also assume that

$$v_\epsilon \to u \tag{4.24}$$

in $L^2(\Omega)$ strongly. Moreover, up to passing to a subsequence, which we still denote by

v_ϵ, we can also suppose that for every ϵ

$$\begin{cases} \lim_{\epsilon\to 0} ||v_\epsilon||^2_{H^1_0(\Omega)} \leq c^*, \\ \lim_{\epsilon\to 0} F_\epsilon[v_\epsilon] = c^*. \end{cases} \tag{4.25}$$

for a constant c^* independent from ϵ.

If $(\xi,\eta) \in S^n$, then $(\xi,\eta) = \psi_{i|n}(x_l, y_l)$ with $(x_l, y_l) \in K_l$, for some index $l = 0, 1, 2$ and some n-address $i|n$. We then set

$$\tilde{v}_\epsilon(\xi,\eta) = \mathcal{M}_\epsilon(v_\epsilon \circ \psi_{i|n}) \circ \psi^{-1}_{i|n}(\xi,\eta), \tag{4.26}$$

where the operator $\mathcal{M}_\epsilon : C^1(\overline{\Sigma}_\epsilon) \to Lip(G_0)$ is defined in the following way: for $h \in C^1(\overline{\Sigma}_\epsilon)$, let $\tilde{h}_\epsilon = \mathcal{M}_\epsilon(h)$ be the function which we now describe. In the same notation of the previous section, for each $l = 0, 1, 2$, let $S_{l,\epsilon}$ denote the segment obtained as the intersection of $\overline{\Sigma}_{l,\epsilon}$ with the straight line orthogonal to K_l at the point $(x_l, y_l) \in K_l$. Let $\gamma_{l,\epsilon}$ be the length of $S_{l,\epsilon}$. If $(x_l, y_l) \in K_l \backslash V_0$, define

$$\tilde{h}_{l,\epsilon}(x_l, y_l) = \frac{1}{\gamma_{l,\epsilon}} \int_{S_{l,\epsilon}} h(x,y)ds. \tag{4.27}$$

Then for every $(x,y) \in G_0$, we put

$$\tilde{h}_\epsilon(x,y) = \begin{cases} \tilde{h}_{l,\epsilon}(x,y), \quad \text{if } (x,y) \in K_l \backslash V_0, \\ \tilde{h}_{0,\epsilon}(A) = \tilde{h}_{1,\epsilon}(A) = h(A), \\ \tilde{h}_{0,\epsilon}(B) = \tilde{h}_{2,\epsilon}(B) = h(B), \\ \tilde{h}_{1,\epsilon}(C) = \tilde{h}_{2,\epsilon}(C) = h(C). \end{cases} \tag{4.28}$$

Clearly, $\tilde{h}_\epsilon \in Lip(G_0)$.

By $\nabla_\tau \tilde{v}_\epsilon$ we denote the tangential derivative on each side of the polygonal curve S^n,

then we have

$$
\begin{aligned}
c_0 \sum_{i|n} \int_{S_0^{i|n}} |\nabla_\tau \tilde{v}_\epsilon|^2 ds &= c_0 \int_{S^n} |\nabla_\tau \tilde{v}_\epsilon|^2 ds \\
&\leq \int_{\Sigma_\epsilon^n} |\nabla v_\epsilon|^2 w_\epsilon^n d\xi d\eta \\
&= \sum_{i|n} \int_{\Sigma_\epsilon^{i|n}} |\nabla v_\epsilon|^2 w_\epsilon^n d\xi d\eta \qquad (4.29)
\end{aligned}
$$

Recall that $S_0^{i|n} = \bigcup_{l=0}^{2} K_l^{i|n}$. First, we estimate the term relative to $K_0^{i|n}$. Our aim is to prove that

$$
c_0 \int_{K_0^{i|n}} |\nabla_\tau \tilde{v}_\epsilon|^2 ds \leq \int_{\Sigma_{0,\epsilon}^{i|n}} |\nabla v_\epsilon|^2 w_\epsilon^n d\xi d\eta \qquad (4.30)
$$

By changing coordinates $(\xi, \eta) = \psi_{i|n}(x, y)$, and setting $\alpha = 2$, we find

$$
\frac{1}{\alpha^n} \int_{K_0^{i|n}} |\nabla_\tau \tilde{v}_\epsilon|^2 ds = \int_{K_0} |\nabla_x \tilde{h}_\epsilon(x, 0)|^2 dx \qquad (4.31)
$$

where $\tilde{h}_\epsilon(x, y)$ for $(x, y) \in K_0$ is defined according to (4.28). To simplify notaion, we put $h(x, y) = (v_\epsilon \circ \psi_{i|n})(x, y)$. Then we have

$$
\begin{aligned}
\int_{K_0} |\nabla_x \tilde{h}_\epsilon(x, 0)|^2 dx = &\int_0^{\epsilon/c_1} \left(\frac{1}{c_1 x} \int_{-c_1 x/2}^{c_1 x/2} h(x, y) dy \right)_x^2 dx \\
&+ \int_{\epsilon/c_1}^{1-\epsilon/c_1} \left(\frac{1}{\epsilon} \int_{-\epsilon/2}^{\epsilon/2} h(x, y) dy \right)_x^2 dx \\
&+ \int_{1-\epsilon/c_1}^{1} \left(\frac{1}{c_1(1-x)} \int_{(c_1 x - c_1)/2}^{(c_1 - c_1 x)/2} h(x, y) dy \right)_x^2 dx \\
= &X_1 + X_2 + X_3 \qquad (4.32)
\end{aligned}
$$

where X_1, X_2, X_3 are the integrals on the intervals $[0, \epsilon/c_1]$, $[\epsilon/c_1, 1-\epsilon/c_1]$ and $[1-\epsilon/c_1, 1]$ respectively. We first evaluate X_2. For $x \in (\epsilon/c_1, 1 - \epsilon/c_1)$, $\hat{x}_{0,+} = x$ and $\hat{y}_{0,+} = \epsilon/2$.

Moreover, on $\psi_{i|n}(\mathcal{R}_{0,\epsilon})$ we have $w_\epsilon^n = \alpha^n c_0/\epsilon$. Therefore,

$$X_2 \leq \frac{1}{\epsilon}\int_{\mathcal{R}_{0,\epsilon}} h_x^2(x,y)dxdy \leq \frac{1}{\alpha^n c_0}\int_{\mathcal{R}_{0,\epsilon}^{i|n}} |\nabla v_\epsilon|^2 w_\epsilon^n d\xi d\eta. \tag{4.33}$$

Now we evaluate X_1 (X_3 can be evaluated in an analogous way). W have $\hat{x}_{0,+} = x$ and $\hat{y}_{0,+} = c_1 x/2$ and thus

$$\begin{aligned} X_1 &\leq \int_0^{\epsilon/c_1} \frac{1 + c_1^2/2}{c_1 x} dx \int_{-c_1 x/2}^{c_1 x/2} [h_x^2(x,y) + h_y^2(x,y)]dy \\ &\leq \frac{1}{\alpha^n c_0}\int_{\mathcal{T}_{1,\epsilon}^{i|n}} |\nabla v_\epsilon|^2 w_\epsilon^n d\xi d\eta. \end{aligned} \tag{4.34}$$

The desired inequality follows. The terms relative to the sets $K_l^{i|n}$ for $l = 1, 2$ can be estimated similarly. Therefore, we find

$$c_0 \int_{S_0^{i|n}} |\nabla_\tau \tilde{v}_\epsilon|^2 ds \leq \int_{\Sigma_\epsilon^{i|n}} |\nabla v_\epsilon|^2 w_\epsilon^n d\xi d\eta \tag{4.35}$$

and so the inequality (4.29) follows by summing up the 3^n terms. We deduce from (4.29) and (4.25) that

$$\lim_{\epsilon \to 0} \int_{S^n} |\nabla_\tau \tilde{v}_\epsilon|^2 ds \leq c^*/c_0. \tag{4.36}$$

Up to extracting a subsequence, which we still denoted by $\tilde{v}_\epsilon$, we have that

$$\tilde{v}_\epsilon \to v^* \text{ in } H_0^1(S^n) \text{ weakly.} \tag{4.37}$$

We now prove that

$$v^* = u|_{S^n}. \tag{4.38}$$

By trace results, we get

$$v_\epsilon|_{S^n} \to u|_{G^n} \text{ in } L^2(S^n) \text{ strongly} \tag{4.39}$$

and then we only need to show that

$$\lim_{\epsilon\to 0}||v_\epsilon|_{S^n}-\tilde{v}_\epsilon||_{L^2(S^n)}=0. \tag{4.40}$$

In fact,

$$\alpha^n\int_{K_0^{i|n}}|v_\epsilon-\tilde{v}_\epsilon|^2ds=\int_{K_0}(h(x,0)-\tilde{h}_\epsilon(x))^2dx=X_1+X_2+X_3 \tag{4.41}$$

where X_1, X_2, X_3 are integrals on the intervals $[0,\epsilon/c_1], [\epsilon/c_1, 1-\epsilon/c_1]$ and $[1-\epsilon/c_1, 1]$ respectively. We have

$$X_2\le\frac{\epsilon}{2}\int_{\epsilon/c_1}^{1-\epsilon/c_1}dx\int_{-\epsilon/2}^{\epsilon/2}h_y^2(x,y)dy\to 0,\quad \epsilon\to 0. \tag{4.42}$$

Similarly, we have

$$X_1\le\frac{\epsilon}{2}\int_{0}^{\epsilon/c_1}dx\int_{-c_1x/2}^{c_1x/2}h_y^2(x,y)dy\to 0,\quad \epsilon\to 0. \tag{4.43}$$

The term X_3 can be evaluated analogously as X_1. Note that same results for $K_1^{i|n}$ and $K_2^{i|n}$ can be proved. Then we have

$$\lim_{\epsilon\to 0}\alpha^n\int_{S_0^{i|n}}|v_\epsilon-\tilde{v}_\epsilon|^2ds=0 \tag{4.44}$$

It follows that (4.40) is achieved by summing up all 3^n terms and hence (4.38) is proved. From (4.24),(4.25),(4.37) and (4.38), we have

$$c_0\int_{S^n}|\nabla_\tau u|^2ds\le\underline{\lim}_{\epsilon\to 0}c_0\int_{S^n}|\nabla_\tau\tilde{v}_\epsilon|^2ds\le\underline{\lim}_{\epsilon\to 0}\int_{\Sigma_\epsilon^n}w_\epsilon|\nabla v_\epsilon|^2d\xi d\eta \tag{4.45}$$

and

$$\int_\Omega|\nabla u|^2d\xi d\eta\le\underline{\lim}_{\epsilon\to 0}\int_{\Omega\setminus\Sigma_\epsilon^n}|\nabla v_\epsilon|^2d\xi d\eta \tag{4.46}$$

Then we accomplish the proof.

□

Step 2: We remove the assumption $v_\epsilon \in C_0^1(\Omega)$.

Proposition 4.2.4. *For any v_ϵ converging to a function u in $L^2(\Omega)$, we have*

$$F[u] \leq \underline{\lim}_{\epsilon\to 0} F_\epsilon[v_\epsilon]. \tag{4.47}$$

Proof. Up to extracting a subsequence which we still denote by v_ϵ, we can still suppose that (4.24) and (4.25) hold and in particular: $c^* = \underline{\lim}_{\epsilon\to 0} F_\epsilon[v_\epsilon]$. Combining the weak convergence of $v_\epsilon \to u$ in $H_0^1(\Omega)$ and the density of $C_0^1(\Omega)$ in $H_0^1(\Omega; w_\epsilon^n)$, we construct a sequence $v_\epsilon^* \in C_0^1(\Omega)$ by a diagonalization procedure such that

$$v_\epsilon^* \to u$$

weakly in $H_0^1(\Omega)$ as $\epsilon \to 0$ and

$$\underline{\lim}_{\epsilon\to 0} F_\epsilon[v_\epsilon^*] \leq c^*.$$

By proceeding as in Step 1 with respect to the functions v_ϵ^*, we obtain:

$$F[u] \leq \underline{\lim}_{\epsilon\to 0} F_\epsilon[v_\epsilon^*] = \underline{\lim}_{\epsilon\to 0}(F_\epsilon[v_\epsilon^*] - F_\epsilon[v_\epsilon]) + \lim_{\epsilon\to 0} F_\epsilon[v_\epsilon] \leq \underline{\lim}_{\epsilon\to 0} F_\epsilon[v_\epsilon].$$

□

Chapter 5

Finite Element Theory

The purpose of this chapter is two-fold, first to present some well-known finite element error estimates for H^2-regular problems and the second is to present some lesser-known results for domains with singularities. The presentation of the error estimates for the H^2-regular case can be found in multiple books, for example [2], [3], [7], and [29], with our presentation following most closely the presentation found in [2]. We present these results so that the results in the second half of the chapter, which gives error estimates for domains with singular points, can be better understood. Since the problems we are interested in are those with prefractal boundaries, we must account for singular points. We will follow the presentation of [14], when presenting these error estimates. Those readers who are familiar with finite element theory, may wish to ship to the proceeding chapter and refer to this chapter as needed for notation or as theorems are referenced.

5.1 An introduction to some important spaces

Before defining the Sobolev spaces $H^1(\Omega)$ and $H^2(\Omega)$ we first define some preliminary spaces in Ω. Let Ω be an open subset of $\mathbb{R}^n$ (later we restrict Ω to be a domain relevant to finite element problems, but for now we keep the more general domain.) We now make the following definitions.

Definition 5. Let $f : \Omega \to \mathbb{R}$. Then supp$f$ is the smallest closed set in $\overline{\Omega}$ such that $f = 0$ on its open complement.

We now define what we mean when we say the space of continuous functions.

Definition 6. Let $0 \leq m \leq \infty$. Then $C^m(\Omega)$ denotes the space of functions that are m times continuously differentiable on Ω. Moreover let $C_0^m(\Omega)$ denote the subspace of $C^m(\Omega)$ consisting of functions with compact support, that is to say $\text{supp} f \subset\subset \Omega$.

We also recall the definition of an L^p space.

Definition 7. Let $L^p(\Omega) = \left\{ f \,:\, \left(\int_\Omega |f|^p dx\right)^{1/p} < \infty \right\}$, where $1 < p < \infty$ and integration is taken in respect to the n-dimensional Lebesgue measure. The norm on $L^p(\Omega)$ is defined as $\|f\|_{L^p(\Omega)} := \left(\int_\Omega |f|^p dx\right)^{1/p}$. Moreover
$L^p_{loc}(\Omega) = \left\{ f \in L^p(\Omega) | \, \|f\|_{L^p(K)} \leq \infty \text{ for every compact set } K \subset \Omega \right\}$.

Definition 8. Given two function space A and B we write $A \hookrightarrow B$ or $A \subset\subset B$ to mean that A is compactly imbedded in B.

We now wish to introduce the idea of distributions

Definition 9. We denote by $\mathcal{D}(\Omega)$ the space of all C^∞ functions with compact support in Ω. This space is occasionally referred to as the space of test functions.

Definition 10. A distribution T is a continuous linear functional on $\mathcal{D}(\Omega)$. The space of all distributions is denoted by $\mathcal{D}'(\Omega)$.

Convergence in $\mathcal{D}'(\Omega)$ is then defined as follows: if $\{T_n\} \subset \mathcal{D}'(\Omega)$, then $T_n \to T \in \mathcal{D}'(\Omega)$ if $T_n(\phi) \to T(\phi)\ \forall \phi \in \mathcal{D}(\Omega)$. We now define the distributional derivative.

Definition 11. Let α be a multi-index and $T \in \mathcal{D}'(\Omega)$. Then $D^\alpha T \in \mathcal{D}'(\Omega)$ defined by $(D^\alpha T)(\phi) := (-1)^{|\alpha|} T(D^\alpha \phi)$ is the distributional derivative of T.

By the above definition, we immediately see that partial distributional derivatives of all orders are defined for every distribution. Also, since

$$(D^\alpha T_f)(\phi) = (-1)^{|\alpha|} T_f(D^\alpha \phi) = (-1)^{|\alpha|} \int_\Omega f D^\alpha \phi \, dx,$$

if f has the weak derivative $D^\alpha f \in L^1_{\text{loc}}(\Omega)$, then

$$(D^\alpha T_f)(\phi) = (-1)^{|\alpha|} \int_\Omega f D^\alpha \phi \, dx = (-1)^{|\alpha|} \int_\Omega D^\alpha f \phi \, dx.$$

Thus, identifying a function $f \in L^1_{\text{loc}}(\Omega)$ with the distribution T_f defined above, and the weak derivative of f with the distribution $T_{D^\alpha f}$, we see that the when f has a weak

derivative, it coincides with the distributional derivative. For more information about the distributional derivative, see [23].

We now wish to consider the Sobolev Spaces. For completeness we begin with the definition of the Sobolev space on the whole Euclidean space. We will then turn to Sobolev Spaces on subdomains relevant to our study.

Definition 12. (Grisvard 1.3.1.1)
We denote by $W^{s,p}(\mathbb{R}^n)$ the space of all distributions defined in $\mathbb{R}^n$, such that

$$D^\alpha u \in L^p(\mathbb{R}^n), \text{ for } |\alpha| \leq m \text{ where } s = m \text{ is a nonnegative integer.}$$

Moreover we define the norm on $W^{s,p}(\mathbb{R}^n)$ by

$$\|u\|_{W^{s,p}(\mathbb{R}^n)} = \left\{ \sum_{|\alpha| \leq m} \int_{\mathbb{R}^n} |D^\alpha u|^p dx \right\}^{1/p}.$$

Now we consider Ω, an open subset of $\mathbb{R}^n$.

Definition 13. (Grisvard 1.3.2.1)
We denote by $W^{s,p}(\Omega)$ the space of all distributions u defined in Ω, such that

$$D^\alpha u \in L^p(\Omega), \text{ for } |\alpha| \leq m \text{ where } s = m \text{ is a nonnegative integer.}$$

Moreover we define the norm on $W^{s,p}(\mathbb{R}^n)$ by

$$\|u\|_{W^{s,p}(\Omega)} = \left\{ \sum_{|\alpha| \leq m} \int_{\Omega} |D^\alpha u|^p dx \right\}^{1/p}.$$

In general the space of all C^∞ functions with compact support in Ω is not dense in $W^{s,p}(\Omega)$.

Definition 14. (Grisvard 1.3.2.2)
For $s > 0$, we denote by $W_0^{s,p}(\Omega)$ the closure of $\mathcal{D}(\Omega)$ in $W^{s,p}(\Omega)$.

Definition 15. (Grisvard 1.3.2.4)

For every $s > 0$, we denote by $W^{s,p}(\overline{\Omega})$ the space of all distributions in Ω which are restrictions of elements of $W^{s,p}(\mathbb{R}^n)$.

Definition 16. (Grisvard 1.3.2.5)
For every positive s, we denote by $\tilde{W}^{s,p}(\Omega)$, the space of all $u \in W^{s,p}(\Omega)$, where $\tilde{u} \in W^{s,p}(\mathbb{R}^n)$.

Definition 17. (Grisvard 1.4.5.1)
Let Ω be a bounded open subset of $\mathbb{R}^2$. We say that the boundary Γ is a curvilinear polygon of class C^m, m integer ≥ 1(respectively $C^{k,\alpha}$, k integer ≥ 1, $0 < \alpha \leq 1$) if for every $x \in \gamma$ there exists a neighborhood V of x in $\mathbb{R}^2$ and a mapping ψ from V in $\mathbb{R}^2$ such that

- ψ is injective,
- ψ together with ψ^{-1} (defined on $\psi(V)$) belongs to the class C^m (respectively $C^{k,\alpha}$),
- $\Omega \cap V$ is either

$$\{y \in \Omega | \psi_2(y) < 0\}, \{y \in \Omega | \psi_1(y) < 0 \text{ and } \psi_2(y) < 0\}$$

or

$$\{y \in \Omega | \psi_1(y) < 0 \text{ or } \psi_2(y) < 0\}$$

where $\psi_i(y)$ denotes the ith component of ψ.

Definition 18. We denote the Sobolev spaces $W^{s,2}(\Omega)$ by $H^s(\Omega)$. Moreover we denote $W_0^{s,2}(\Omega)$ be $H_0^s(\Omega)$. Recall that $H^0(\Omega) = W^{0,2}(\Omega) = L^2(\Omega)$.

5.2 Problem Definition and Existence of Solutions

We begin by considering the Poisson problem:

$$\begin{cases} -\Delta u = f & \text{in } \Omega \\ u = 0 & \text{on } \partial\Omega \end{cases}. \tag{5.1}$$

Specifically we will consider the variational formulation of this problem

$$\begin{cases} \text{Find } u \in H_0^1(\Omega) \text{ such that:} \\ \int_\Omega \nabla u \nabla v dx = \int_\Omega v f \, dx \\ \text{for every } v \in H_0^1(\Omega). \end{cases} \tag{5.2}$$

For consistency in notation we rewrite the above problem setting $a(u,v) = \int_\Omega \nabla u \nabla v dx$ and $f(v) = \int_\Omega v f \, dx$. Thus our problem becomes

$$\begin{cases} \text{Find } u \in H_0^1(\Omega) \text{ such that:} \\ a(u,v) = f(v) \\ \text{for every } v \in H_0^1(\Omega). \end{cases} \tag{5.3}$$

It can be shown that the bilinear form a is both continuous and coercive. With this knowledge the Lax-Milgram Theorem provides both existence and uniqueness of a solution to our given problem. For reference, the Lax-Milgram Theorem is stated below

Theorem 5.2.1. *Lax-Milgram Theorem*
Let $a(u,v)$ be a continuous, coercive, bilinear form. Then for every $\phi \in H'$ there exists $u \in H$ such that

$$a(u,v) = \langle \phi, v \rangle \quad \forall v \in H.$$

Although the Lax-Milgram theorem guarantees existence and uniqueness of the solution of the variational problem, it provides no means for actually determining the solution. For difficult problems, we are often forced to determine the solution numerically, one such way is the finite element method. In this method we approximate the solution by solving the problem exactly in the subspace V_h of V, i.e.

$$\begin{cases} \text{Find } u_h \in V_h(\Omega) \text{ such that:} \\ a(u_h, v_h) = f(v_h) \\ \text{for every } v_h \in V_h(\Omega). \end{cases} \tag{5.4}$$

The subspace V_h must be chosen carefully to balance ease of solution with accuracy of the solution.

We begin our quest for a solution with the first abstract result, Céa's Lemma, which provides an understanding of the error incured by solving the problem on a subspace. We state (and prove) this well known result for the special space H^1 below

Lemma 5.2.2. *Céa's Lemma*
Suppose the bilinear form $a(u,v)$ is coercive and that $H_0^1 \hookrightarrow V \hookrightarrow H^1$. Moreover $V \hookrightarrow V_h$. Suppose u is the solution to the variational problem (5.3) and u_h is the solution to the variational problem (5.4). Then

$$\|u - u_h\|_{H^1(\Omega)} < \frac{C}{\alpha} \inf_{v_h \in V_h} \|u - v_h\|_{H^1(\Omega)} .$$

Proof. Since u and u_h are solutions to the variational problem, this implies that

$$a(u,v) = f(v) \quad \forall v \in V$$

and

$$a(u_h,v) = f(v) \quad \forall v \in V_h.$$

Moreover since $V_h \subset V$, this means that

$$a(u - u_h, v) = 0 \quad \forall v \in V_h.$$

Define $v_h - u_h \in V_h$. By coerciveness

$$\begin{aligned}
\alpha \|u - u_h\|^2_{H^1(\Omega)} &\leq a(u - u_h, u - u_h) \\
&= a(u - u_h, u - u_h) + a(u - u_h, v_h - u_h) \\
&= a(u - u_h, u - v_h) \\
&\leq C \|u - u_h\|_{H^1(\Omega)} \|u - v_h\|_{H^1(\Omega)} \qquad \text{(by continuity)}.
\end{aligned}$$

We divide both sides by $\|u - u_h\|_{H^1(\Omega)}$ and α, then take infimum to get the desired result. □

5.3 Mesh Considerations

When using the finite element method, the subspace of our problem V_h is determined by the mesh used. Until now no restrictions have been made on the domain Ω however,

since the mesh created is highly dependent on Ω we place a few restrictions on Ω now.

First, we will assume that $\Omega \subset \mathbb{R}^2$ is a polygon, and that its boundary Γ is continuous. Second, we assume that the finite element mesh is composed only of triangles (although this assumption can be relaxed to include quadrilaterals). Third, we assume that the mesh consists of only a finite number of triangles.

Moreover we make the following definitions:

Definition 19. Let $\mathcal{T}$ and $\hat{\mathcal{T}}$ be two subsets of $\mathbb{R}^n$. We say that $\mathcal{T}$ and $\hat{\mathcal{T}}$ are *affine equivalent* if there exists an invertible affine mapping $F_{\mathcal{T}} : \mathbb{R}^n \to \mathbb{R}^n$ defined by $F_{\mathcal{T}}(\hat{X}) = B_{\mathcal{T}}\hat{X} + a$ such that $\mathcal{T} = F_{\mathcal{T}}(\hat{\mathcal{T}})$.

In general we will consider $\mathcal{T}$ and $\hat{\mathcal{T}}$ to be two triangles in our domain with $\hat{\mathcal{T}}$ defined as the model triangle, where $\hat{\mathcal{T}} \in \mathbb{R}^2$ and the vertices of $\hat{\mathcal{T}}$ are located at $(0,0)$, $(1,0)$, and $(0,1)$.

Finally we define some terms to help quantify the differences between triangles in the mesh.

Definition 20. For any triangle, $\mathcal{T}$ define

$$h_{\mathcal{T}} = \text{the length of the largest side of } \mathcal{T}$$
$$\rho_{\mathcal{T}} = \text{the diameter of the largest ball inscribed in } \mathcal{T}$$

Moreover we define the shape regularity constant σ (sometimes called the aspect ratio or chunkiness ratio) as $h_{\mathcal{T}}/\rho_{\mathcal{T}}$.

Finally we give a precise definition of what is meant when we say the domain is conformally triangulated

Definition 21. A **(conformal) triangulation** T_h is a finite set of closed triangles ($\mathcal{T}$) on a domain Ω (recall Ω is a polygon in $\mathbb{R}^2$) with the following properties:

1. $\bar{\Omega} = \bigcup_{\mathcal{T} \in T_h} \mathcal{T}$
2. For any $\mathcal{T} \in T_h$, $\mathcal{T}$ is affine equivalent to $\hat{\mathcal{T}}$.

3. $\mathring{\mathcal{T}}_i \cap \mathring{\mathcal{T}}_j = \emptyset$ if $i \neq j$.

4. Any edge of a triangle $\mathcal{T}_1 \in T_h$ is either a subset of Γ or the edge of another triangle $\mathcal{T}_2 \in T_h$. (Note that this disallows the occurrence of "hanging nodes.")

5. $h = \max_{\mathcal{T} \in \mathcal{K}_H} h_{\mathcal{T}}$

Once the domain has been discretized, it is necessary to create a subspace V_h correspondent to our discretization T_h. The subspace we will use (recall that we have not yet relaxed the assumption that the discretization be only triangles) is the special space that is linear on every triangle, and continuous on the larger domain $\overline{\Omega}$. We denote this space by $P_h^1(\Omega)$. We construct the basis for this space by defining a set of functions $\phi_i : \overline{\Omega} \to \mathbb{R}$ (here $1 \leq i \leq N$ where N is the number of triangle vertices in T_h) by making ϕ_i the unique function that is linear on each $\mathcal{T} \in T_h$ and has the property that $\phi_i(x_j) = \delta_{ij}$ for every vertex $x_j \in T_h$. Now we define a linear interpolation operator that takes functions from $H^2(\Omega)$ to this special space of piecewise linear functions.

Definition 22. Let $\mathcal{T}$ be a triangle with vertices x_1, x_2, x_3 that is affine equivalent to the reference triangle $\hat{\mathcal{T}}$. We define the linear interpolation map $\Pi_{\mathcal{T}} : C^0(\overline{\mathcal{T}}) \to P_1(\mathcal{T})$ by setting $\Pi_{\mathcal{T}}(v)$ be the unique linear function $\overline{v} \in P_1(\mathcal{T})$ such that $\overline{v}(x_i) = v(x_i)$ for $i = 1, 2, 3$. By the Sobolev imbedding theorem, $H^2(K) \hookrightarrow C^0(\bar{K})$. Thus every $v \in H^2(\mathcal{T})$ has a continuous representative $\tilde{v}$, so we may define $\Pi_{\mathcal{T}} : H^2(\mathcal{T}) \to P_1(\mathcal{T})$ by $\Pi_{\mathcal{T}}(v) = \Pi_{\mathcal{T}}(\tilde{v})$. If T_h is a discretization of Ω as above, then we define $\Pi_h : H^2(\Omega) \to P_h^1(\Omega) \subset H^1(\Omega)$ to be the map satisfying $\Pi_h(v) = \Pi_K(v)$ for all $v \in H^2(\Omega)$ and for all $\mathcal{T} \in T_h$.

5.4 Transformation of Triangles

The goal of this section is to study the transformation of triangles so that we might be able to estimate the error in the finite element approach. For an arbitrary triangle $\mathcal{T}$ recall the definition of the transformation function $F_{\mathcal{T}}$ as the function that maps the model triangle $\hat{\mathcal{T}}$ to our triangle $\mathcal{T}$.

$$F_{\mathcal{T}} : x \leftarrow a + B_{\mathcal{T}} x$$

where

$$a := \begin{bmatrix} a_1 \\ a_2 \end{bmatrix} \text{ and } B_{\mathcal{T}} := \begin{bmatrix} b_1 & c_1 \\ b_2 & c_2 \end{bmatrix}$$

The following theorem and its associated proof is proved with greater generality in [7]

Theorem 5.4.1. *Let Ω and $\hat{\Omega}$ be two affine-equivalent subsets of $\mathbb{R}^2$. if a function v belongs to the space $H^m(\Omega)$ for some integer $m \geq 0$, the function $\hat{v} = v \circ F$ belongs to the space $H^m(\hat{\Omega})$, and in addition there exists a constant $C_{\mathcal{T}} = C(m)$ such that*

$$\forall v \in H^m(\Omega),\ \hat{v}_{H^m(\hat{\Omega})} \leq C_{\mathcal{T}} \left\| B_{\mathcal{T}} \right\|^m \left| det\left(B_{\mathcal{T}}\right) \right|^{-1/2} |v|_{H^m(\Omega)} \tag{5.5}$$

Analogously one has

$$\forall \hat{v} \in H^m(\hat{\Omega}),\ \ |v|_{H^m(\Omega)} \leq C_{\mathcal{T}} \left\| B_{\mathcal{T}}^{-1} \right\|^m \left| det\left(B_{\mathcal{T}}\right) \right|^{1/2} |\hat{v}|_{H^m(\hat{\Omega})} \tag{5.6}$$

Proof. First assume the function v belongs to the space $\mathcal{C}^m\left(\bar{\Omega}\right)$, so the function $\hat{v}$ belongs to the space $\mathcal{C}^m(\bar{\hat{\Omega}})$. For any multi-

$$\partial^\beta \hat{v}(\hat{x}) = D^m \hat{v}(\hat{x}) \left(e_{\beta_1}, e_{\beta_2}, \ldots, e_{\beta_m}\right)$$

where the vectors $e_{\beta_i}, 1 \leq i \leq m$ are some of the basis vectors of $\mathbb{R}^2$, we deduce that

$$\left|\partial^\beta \hat{v}(\hat{x})\right| \leq \left\| D^m \hat{v}(\hat{x}) \right\| = \sup_{\substack{\|\zeta_i\| \leq 1 \\ 1 \leq i \leq m}} \left| D^m \hat{v}(\hat{x})\right) \left(\zeta_1, \zeta_2 \ldots \zeta_m\right) | .$$

Consequently,

$$|\hat{v}|_{H^m(\hat{\Omega})} = \left(\int_{\hat{\Omega}} \sum_{|\beta|=m} \left|\partial^\beta \hat{v}\left(\hat{x}\right)\right|^2 d\hat{x} \right)^{1/2} \leq C_{T1} \left(\int_{\hat{\Omega}} \left\| D^m \hat{v}\left(\hat{x}\right) \right\|^2 d\hat{x} \right)^{1/2} \tag{5.7}$$

where C_{T1} is defined as

$$C_{T1}(m) = \sum_{i \leq 2} \left(\text{card}\left\{ \beta \in \mathbb{N}^m; |\beta| = m \right\} \right)^{1/2} .$$

(For $\mathbb{R}^2$, $C_{T1} = 2^m$ see [2].) Using the chain rule, we know for any vector $\zeta_i \in \mathbb{R}^2, 1 \leq i \leq m$,

$$D^m\hat{v}\left(\hat{x}\right)\left(\zeta_1,\zeta_2,\ldots\zeta_m\right)=D^m v\left(x\right)\left(B_{\mathcal{T}}\zeta_1,B_{\mathcal{T}}\zeta_2,\ldots,B_{\mathcal{T}}\zeta_m\right)$$

so that

$$\left\|D^m\hat{v}\left(\hat{x}\right)\right\|\leq\left\|D^m v\left(x\right)\right\|\left\|B_{\mathcal{T}}\right\|^m$$

and therefore

$$\int_{\hat{\Omega}}\left\|D^m\hat{v}\left(\hat{x}\right)\right\|^2 d\hat{x}\leq\left\|B_{\mathcal{T}}\right\|^{2m}\int_{\Omega}\left\|D^m v\left(F\left(\hat{x}\right)\right)\right\|^2 d\hat{x} \tag{5.8}$$

Using the formula for change of variables for integrals we get

$$\int_{\hat{\Omega}}\left\|D^m v\left(F\left(\hat{x}\right)\right)\right\|^2 d\hat{x}\leq\left|\det\left(B_{\mathcal{T}}^{-1}\right)\right|\int_{\Omega}\left\|D^m v\left(x\right)\right\|^2 dx. \tag{5.9}$$

Since there exists a constant C_{T2} (also dependent on cardinality) such that

$$\left\|D^m v\left(x\right)\right\|\leq C_{T2}\max_{|\beta|=m}\left|\partial^\beta v\left(x\right)\right|,$$

one obtains

$$\left(\int_{\Omega}\left\|D^m v\left(x\right)\right\|^2 dx\right)^{1/2}\leq C_{T2}\left|v\right|_{H^m(\Omega)}. \tag{5.10}$$

As above $C_{T2}=2^m$. To complete the proof we must use the continuity of the linear operator $w:v\in\mathcal{C}^m\left(\bar{\Omega}\right)\rightarrow\hat{v}\in H^m\left(\hat{\Omega}\right)$ with respect to the norms $\left\|\cdot\right\|_{H^m(\Omega)}$ and $\left\|\cdot\right\|_{H^m\left(\hat{\Omega}\right)}$, the denseness of the space $\mathcal{C}^m\left(\bar{\Omega}\right)$ in the space $H^m\left(\Omega\right)$, and the definition of the unique extension of the mapping w to the space $H^m\left(\Omega\right)$.
Inequality (5.5) is a consequence of (5.7),(5.8), (5.9), and (5.10). Inequality (5.6) is shown in a similar manner. □

Key to equations (5.5) and (5.6) are the appearance of the terms $\left\|B_{\mathcal{T}}\right\|,\left\|B_{\mathcal{T}}^{-1}\right\|$ and $\left|\det\left(B_{\mathcal{T}}\right)\right|$. To more easily use these equations we wish to convert the norms into simpler, geometric based equalities.

Lemma 5.4.2. *Let $\hat{\Omega}$ and $\Omega=F_{\mathcal{T}}\left(\hat{\Omega}\right)$ be two affine-equivalent open subsets of R^2 where $F_{\mathcal{T}}:\hat{x}\rightarrow B_{\mathcal{T}}\hat{X}+a$ is an invertible affine mapping. Then the following upper bounds hold*

$$\left\|B_{\mathcal{T}}\right\|\leq\frac{h_{\mathcal{T}}}{\rho_{\hat{\mathcal{T}}}}\ \textit{and}\ \left\|B_{\mathcal{T}}^{-1}\right\|\leq\frac{h_{\hat{\mathcal{T}}}}{\rho_{\mathcal{T}}}.$$

Proof. We recall that

$$\|B_{\mathcal{T}}\| = \frac{1}{\rho_{\hat{\mathcal{T}}}} \sup_{\|\zeta\|=\rho_{\hat{\mathcal{T}}}} \|B_{\mathcal{T}}\zeta\|.$$

If ζ satisfies $\|\zeta\| = 2\rho_{\hat{\mathcal{T}}}$, there exists two points $\hat{y}, \hat{z} \in \bar{\hat{\Omega}}$ such that $\hat{y} - \hat{z} = \zeta$ by the definition of $\rho_{\hat{\mathcal{T}}}$. Since $B_{\mathcal{T}} = F_{\mathcal{T}}(\hat{y}) - F_{\mathcal{T}}(\hat{z})$ with $F_{\mathcal{T}}(\hat{y}), F_{\mathcal{T}}(\hat{z}) \in \bar{\Omega}$, it is clear that $\|B_{\mathcal{T}}\zeta\| \leq 2h_K$, and the first inequality is proved. The second inequality follow in a similar manner. □

We remark that for our model triangle $\hat{\mathcal{T}}$ the values for $h_{\hat{\mathcal{T}}}$ and $\rho_{\hat{\mathcal{T}}}$ are easily calculated to be $2^{1/2}$ and $2\left(2+\sqrt{2}\right)^{-1}$ respectively. We also note that

$$|\det(B_{\mathcal{T}})| = \frac{\text{meas}(\Omega)}{\text{meas}(\hat{\Omega})}.$$

Before we may apply the above transformation formula to a given discretization of a domain it is important to define the notion of a shape-regular domain.

Definition 23. A triangulation T_h is shape-regular if there exists σ such that $\frac{h_{\mathcal{T}}}{\rho_{\mathcal{T}}} \leq \sigma$ for all $\mathcal{T} \in T_h$. A family of triangulations $\{T_h\}$, indexed by $h := \max_{\mathcal{T}\in T_h} h_{\mathcal{T}}$, is regular if T_h is shape-regular for each h, and $h \to 0$.

5.5 Interpolation Results

With the linear interpolation operator $\Pi_{\mathcal{T}}$ defined we consider the error of approximating a function $u \in H^2(\Omega)$ with a linear function. First we bound this error on a model triangle, and then consider convex polygonal domains. Our first result, often referred to as the Bramble Hilbert lemma, shows that the error is bounded by the H^2 seminorm of u.

Lemma 5.5.1. *Let $\hat{\mathcal{T}}$ be the reference triangle with vertices $z_1 = (0,0)$, $z_2 = (0,1)$ and $z_3 = (1,0)$. Let $\Pi_{\hat{\mathcal{T}}} : H^2(\hat{\mathcal{T}}) \to P_1(\hat{\mathcal{T}})$ be the linear interpolation operator defined as above (see Definition 22). Then there exists a constant $C_S = C_S(\Omega, z_1, z_2, z_3)$ such that*

$$\|u - \Pi_{\hat{\mathcal{T}}} u\|_{H^2(\hat{\mathcal{T}})} \leq C_S |u|_{H^2(\hat{\mathcal{T}})} \quad \forall u \in H^2(\hat{\mathcal{T}}). \tag{5.11}$$

Proof. Outline: Endow $H^2(\hat{\mathcal{T}})$ with the norm $\|v\|^* := |v|_{H^2(\hat{\mathcal{T}})} + \sum_{i=1}^{3} |v(z_i)|$ and show that the norms $\|\cdot\|^*$ and $\|\cdot\|_{H^2(\hat{\mathcal{T}})}$ are equivalent. Then the result follows from using the

definitions of $\|\cdot\|^*$ and $\Pi_{\hat{\mathcal{T}}}$:

$$\begin{aligned}\|u - \Pi_{\hat{\mathcal{T}}} u\|_{H^2(\hat{\mathcal{T}})} &\leq C_S \|u - \Pi_{\hat{\mathcal{T}}} u\|^* \\ &= C_S \left[|u - \Pi_{\hat{\mathcal{T}}} u|_{H^2(\hat{\mathcal{T}})} + \sum_{i=1}^{3} |(u - \Pi_{\hat{\mathcal{T}}} u)(z_i)| \right] \\ &= C_S |u - \Pi_{\hat{\mathcal{T}}} u|_{H^2(\hat{\mathcal{T}})} \\ &= C_S |u|_{H^2(\hat{\mathcal{T}})}.\end{aligned}$$

So, we will begin by showing that $\|\cdot\|^* \leq C_S \|\cdot\|_{H^2(\hat{\mathcal{T}})}$. As noted before, by the Sobolev Embedding Theorem, we have $H^2(\hat{\mathcal{T}}) \hookrightarrow C^0(\overline{\hat{\mathcal{T}}})$. Thus, there exists $C > 0$ such that $\max_{i=1,2,3} |v(z_i)| \leq \|v\|_{C^0(\overline{\hat{\mathcal{T}}})} \leq C \|v\|_{H^2(\hat{\mathcal{T}})}$ for every $v \in H^2(\hat{\mathcal{T}})$. So, $\|v\|^* = |v|_{H^2(\hat{\mathcal{T}})} + \sum_{i=1}^{3} |v(z_i)| \leq (1 + 3C) \|v\|_{H^2(\hat{\mathcal{T}})}$.

Now, we will show that $\|\cdot\|_{H^2(\hat{\mathcal{T}})} \leq C_S \|\cdot\|^*$ by contradiction. Suppose such a C_S does not exist. Then there exists a sequence $\{v_k\} \in H^2(\hat{K})$ with $\|v_k\|_{H^2(\hat{\mathcal{T}})} = 1$ and $\|v_k\|^* = \frac{1}{k}$ for each k. Since $H^2(\hat{\mathcal{T}}) \hookrightarrow\hookrightarrow H^1(\hat{\mathcal{T}})$, (by the Rellich-Kondrashov theorem) a subsequence of $\{v_k\}$ converges in $H^1(\hat{\mathcal{T}})$. Now, using the definition of $\|u\|_{H^2(\hat{\mathcal{T}})}$ as $\|u\|_{H^1(\hat{\mathcal{T}})} + |u|_{H^2(\hat{\mathcal{T}})}$ for every $u \in H^2(\hat{\mathcal{T}})$, we note that for each $k, l \in \mathbb{N}$,

$$\|v_k - v_l\|^2_{H^2(\hat{\mathcal{T}})} \leq \|v_k - v_l\|^2_{H^1(\hat{\mathcal{T}})} + (|v_k|_{H^2(\hat{\mathcal{T}})} + |v_l|_{H^2(\hat{\mathcal{T}})})^2. \tag{5.12}$$

Then, since $\{v_k\}$ is a Cauchy sequence in $H^1(\hat{\mathcal{T}})$, the first term on the right hand side goes to 0 as $k, l \to \infty$. By design, $\|v_k\|^* \to 0$ as $k \to \infty$, and since $|v_k|_{H^2(\hat{\mathcal{T}})} \leq \|v_k\|^*$, the second term on the right hand side of (5.12) also goes to 0 as $k, l \to \infty$. Thus $\{v_k\}$ is a Cauchy sequence in $H^2(\hat{\mathcal{T}})$, as well. Since $H^2(\hat{\mathcal{T}})$ is complete, there exists $v^* \in H^2(\hat{\mathcal{T}})$ such that $\|v_k - v^*\|_{H^2(\hat{K})} \to 0$ as $k \to \infty$. By continuity of norms, $\|v^*\|_{H^2(\hat{\mathcal{T}})} = 1$ and $\|v^*\|^* = 0$. Since $\|v^*\|^* = 0$, we have that both $|v^*|_{H^2(\hat{\mathcal{T}})} = 0$ and $v^*(z_i) = 0$ for $i = 1, 2, 3$. Since $|v^*|_{H^2(\hat{\mathcal{T}})} = 0$ implies $v^* \in P_1(\hat{\mathcal{T}})$ we must have $v^* = 0$ contradicting $\|v^*\|_{H^2(\hat{\mathcal{T}})} = 1$. □

Now we combine the above Lemma with the definition of a shape-regular triangulation given previously, to give the following result.

Theorem 5.5.2. *Let $\Omega \subset \mathbb{R}^2$ with a polygonal boundary, and introduce T_h a shape-*

regular triangulation of the domain. Then the following inequality holds for some C_M

$$\|u - \Pi_h u\|_{H^1(\Omega)} \leq C_M h \, |u|_{H^2(\Omega)} \tag{5.13}$$

where Π_h is the linear interpolation operator defined previously.

Proof. It suffices to establish the inequality

$$\|u - \Pi_h u\|_{H^1(\mathcal{T})} \leq Ch|u|_{H^2(\mathcal{T})} \quad \forall u \in H^2(\mathcal{T})$$

for each $\mathcal{T} \in T_h$ since $\|\cdot\|_{H^m(\Omega)} = \sum_{\mathcal{T}\in T_h} \|\cdot\|_{H^m(\mathcal{T})}$. So, let $\mathcal{T} \in T_h$ be given. Then by assumption, $\mathcal{T}$ is affine equivalent to $\hat{\mathcal{T}}$, so there exists a bijective affine map $F_{\mathcal{T}} : \hat{\mathcal{T}} \to \mathcal{T}$ defined by $F_{\mathcal{T}}(\hat{x}) = B_{\mathcal{T}}\hat{x} + a$. Then by Lemma 5.5.1 and Theorem 5.4.1, and using the fact that $(\det B^{-1}) = (\det B)^{-1}$, we have:

$$\begin{aligned}
|u - \Pi_h u|_{H^1(\mathcal{T})} &\leq C_{\mathcal{T}} \left\|B_{\mathcal{T}}^{-1}\right\|^1 |\det B_{\mathcal{T}}^{-1}|^{-\frac{1}{2}} |\hat{u} - \Pi_h \hat{u}|_{H^1(\hat{\mathcal{T}})} \\
&\leq C_{\mathcal{T}} \left\|B_{\mathcal{T}}^{-1}\right\|^1 |\det B_{\mathcal{T}}|^{\frac{1}{2}} \|\hat{u} - \Pi_h \hat{u}\|_{H^2(\hat{\mathcal{T}})} \\
&\leq C_{\mathcal{T}} \left\|B_{\mathcal{T}}^{-1}\right\|^1 |\det B_{\mathcal{T}}|^{\frac{1}{2}} C_S |\hat{u}|_{H^2(\hat{\mathcal{T}})} \\
&\leq C_{\mathcal{T}} \left\|B_{\mathcal{T}}^{-1}\right\|^1 |\det B_{\mathcal{T}}|^{\frac{1}{2}} C_S C_{\mathcal{T}} (\|B_{\mathcal{T}}\|^2 |\det B|^{-\frac{1}{2}} |u|_{H^2(\mathcal{T})}) \\
&= C(\|B_{\mathcal{T}}\| \left\|B_{\mathcal{T}}^{-1}\right\|)^t \|B_{\mathcal{T}}\|^1 |u|_{H^2(\mathcal{T})}.
\end{aligned}$$

□

From what we have already stated about the bounds of $\|B_{\mathcal{T}}\|$ and $\left\|B_{\mathcal{T}}^{-1}\right\|$ we can state that $\|B_{\mathcal{T}}\| \cdot \left\|B_{\mathcal{T}}^{-1}\right\| \leq \frac{\hat{h}}{\hat{\rho}}\sigma$, and $\|B_{\mathcal{T}}\| \leq h/\hat{\rho} = (2+\sqrt{2})h$. Thus in the inequality

$$\|u - \Pi_h u\|_{H^1(\Omega)} \leq C_M h \, |u|_{H^2(\Omega)} \,,$$

C_M is dependent on σ, $C_{\mathcal{T}}$, and C_S.

We notice that the previous results require a very important assumption, that is $u \in H^2(\Omega)$. This assumption is not automatic and is dependent on the characteristics of the domain. Formally stated the assumption is:

Definition 24. Let $m \geq 1$, $H_0^m(\Omega) \subset V \subset H^m(\Omega)$ and suppose that $a(\cdot,\cdot)$ is a V-elliptic

bilinear form . Then the variational problem

$$a(u,v) = (f,v)_0 \ \ \forall v \in V$$

is called H^s- regular if there exists a constant C such that for every $f \in H^{s-2m}$ there is a solution $u \in H^s(\Omega)$ with

$$\|u\|_{H^s(\Omega)} \leq C \|f\|_{H^{s-2m}(\Omega)}.$$

Remark 21. If a is an $H_0^1(\Omega)$-elliptic bilinear form with sufficiently smooth coefficient functions functions, and Ω is convex or has C^2 boundary, then the Dirichlet problem is H^2-regular.[2]

So if we have a *convex* polygonal domain we will be able to solve our variational problem. If the polygonal domain is not convex we will need to work in the weighted space $H^{2,\lambda}(\Omega)$ which will be considered in the next section. We return now to the original variational problem and introduce the requirement that the domain Ω be a convex polygon. We now wish to establish an estimate of the error by approximating the solution to problem 5.2 by the solution to the variational problem

$$\begin{cases} \text{Find } u_h \in P_h^1(\Omega) \cap H_0^1(\Omega) \text{ such that:} \\ \int_\Omega \nabla u_h \nabla v_h dx = \int_\Omega v_h f \ dx \\ \text{for every } v_h \in P_h^1(\Omega). \end{cases} \tag{5.14}$$

Theorem 5.5.3. *Suppose T_h is a family of regular triangulations of Ω satisfying the conditions of Definition 21. Let u and u_h be the solutions of the abstract variational problems*

$$a(u,v) = f(v) \quad \forall v \in H_0^1(\Omega) \tag{5.15}$$

and

$$a(u_h,v_h) = f(v_h) \quad \forall v_h \in P_h^1(\Omega) \tag{5.16}$$

respectively, where $a(\cdot,\cdot)$ is a continuous, elliptic bilinear form on $H_0^1(\Omega)$, $f \in L^2(\Omega)$, and $P_1^h(\Omega)$ is the space of piecewise linear functions on Ω defined earlier. Then if the variational problem 5.15 is H^2-regular, the finite element approximation $u_h \in P_1^h(\Omega) \cap$

$H_0^1(\Omega)$ *satisfies:*

$$\begin{aligned} \|u - u_h\|_{H^(\Omega)} &\leq Ch \|u\|_{H^2(\Omega)} \\ &\leq Ch \|f\|_{L^2(\Omega)} . \end{aligned} \tag{5.17}$$

Proof. By Theorem 5.5.2, there exist $v_h \in P_h^1(\Omega)$ such that $\|u - v_h\|_{H^1(\Omega)} \leq C_M h \|u\|_{H^2(\Omega)}$. Combining with Céa's Lemma (Lemma 5.2.2), we have

$$\|u - u_h\|_{H^1(\Omega)} \leq \|u - v_h\|_{H^1(\Omega)} \leq C_M h \|u\|_{H^2(\Omega)} .$$

By definition of H^2-regular, there exists a constant C such that for every $f \in L^2(\Omega)$, $\|u\|_{H^2(\Omega)} \leq C \|f\|_{L^2(\Omega)}$. Therefore we have

$$\|u - u_h\|_{H^1(\Omega)} \leq Ch \|f\|_{L^2(\Omega)} .$$

□

Before giving a second estimate of the error between the solution of the variational problem in the finite element space and the solution in the whole space we need an additional abstract result.

Lemma 5.5.4. *Aubin-Nitsche Lemma*
Let H be a Hilbert Space with inner product $(\cdot, \cdot)$ and norm $|\cdot|$ and let V be a subspace of H also a Hilbert space with a different norm $\|\cdot\|$. Let the imbedding $V \hookrightarrow H$ be continuous. Moreover let u and u_h be solutions to the variational problems

$$a(u, v) = f(v) \quad \forall v \in V$$

and

$$a(u_h, v_h) = f(v_h) \quad \forall v_h \in V_h \subset V,$$

in V and V_h respectively. Moreover let φ_g be the unique (weak) solution to the variational problem

$$a(w, \varphi_g) = (g, w) \quad \forall w \in H.$$

Then the finite element solution in $V_h \subset V$ satisfies,

$$|u - u_h| \leq C \|u - u_h\| \sup_{g \in H} \left\{ \frac{1}{|g|} \inf_{v \in V_h} \|\varphi_g - v\| \right\}.$$

Proof. By duality arguments

$$|w| = \sup_{g \in H} \frac{(g, w)}{|g|}. \tag{5.18}$$

Since $u - u_h \in H$, we set $w = u - u_h$, giving

$$a(u - u_h, \varphi_g) = (g, u - u_h).$$

Moreover since u and u_h are solutions to the stated variational problems we know that

$$a(u - u_h, v) = 0 \quad \forall v \in V_h.$$

Thus by subtraction we have

$$a(u - u_h, \varphi_g - v) = (g, u - u_h) \quad \forall v \in V_h.$$

Using continuity arguments we can therefore say

$$\begin{aligned} |(g, u - u_h)| &= |a(u - u_h, \varphi_g - v)| \\ &\leq C \|u - u_h\| \|\varphi_g - v\|. \end{aligned}$$

Hence

$$|(g, u - u_h)| \leq C \|u - u_h\| \inf_{v \in V_h} \|\varphi_g - v\|.$$

Now using (5.18), it follows that

$$|u - u_h| \leq C \|u - u_h\| \sup_{g \in H} \left\{ \frac{1}{|g|} \inf_{v \in V_h} \|\varphi_g - v\| \right\}.$$

□

We now use Céas Lemma and the Aubin-Nitsche Lemma to show the error estimate

$$\|u - u_h\|_{L^2(\Omega)} \leq Ch^2 \|u\|_{H^2(\Omega)}. \tag{5.19}$$

Proof. We will first show that

$$\|u - u_h\|_{L^2(\Omega)} \leq Ch \|u - u_h\|_{H^1(\Omega)}.$$

We set H equal to $L^2(\Omega) = H^0(\Omega)$, and V equal to $H_0^1(\Omega)$. Clearly $V \subset H$, and since $\|\cdot\|_{L^2(\Omega)} \leq \|\cdot\|_{H^1(\Omega)}$, V is compactly imbedded in H. If we let $V_h := P_1^h(\Omega) \cap H_0^1(\Omega)$, the Aubin-Nitsche Lemma implies that

$$\|u - u_h\|_{L^2(\Omega)} \leq C \|u - u_h\|_{H^1(\Omega)} \sup_{g \in L^2(\Omega)} \left\{ \frac{1}{\|g\|_{L^2(\Omega)}} \inf_{\varphi_h \in V_h} \|\varphi_g - \varphi_h\|_{H^1(\Omega)} \right\}.$$

Now by Cea's Lemma the quantity in the curly brackets is less then or equal to $C_2 h$. Combining this result with Theorem 5.5.3 the desired inequality is immediate.

□

5.6 The Presence of Singular Corners

Thus far we have only considered convex domains in $\mathbb{R}^2$. We now wish to consider how to minimize the finite element error in domains with one or more singular corners. Recall that a singular corner is one whose angle is greater then π. To simplify our results we will consider a polygonal domain Ω whose boundary is made up of linear segments $\Gamma_1 \ldots \Gamma_N$, and contains only one singular point. This is equivalent to the statement that all of the angles between Γ_j and Γ_{j+1} are less then π for all j except for $j = N$. Denote the angle between Γ_N and Γ_1 as θ, and the point of intersection as S_N. For simplicity assume that S_N is at the origin (if it is not, simply translate the domain until it is).

Remark 22. For the remainder of this document we will use the term reentrant to describe angles that are more then π. An equivalent definition is: an angle θ is reentrant if $\frac{\pi}{\theta} < 1$

Consider now that solution $u \in H^1(\Omega)$ which for $f \in L^2(\Omega)$ satisfies

$$-\Delta u = f \text{ in } \Omega.$$

From the study of singular points we know that there is a unique solution u and a unique

number η such that

$$u - \eta r^{\pi/\theta} \sin \frac{\pi\omega}{\theta} \in H^2(\Omega) \tag{5.20}$$

This property prevents u from belonging to $H^2(\Omega)$ except when η vanishes. However it does allow u to belong to the following weighted space.

Definition 25. Let λ be a nonnegative real number and for each λ we define a weighted Sobolev space (denoted by $H^{2,\lambda}(\Omega)$) as

$$H^{2,\lambda}(\Omega) = \left\{ u \in H^1(\Omega) : r^\lambda \cdot D^\beta u \in L^2(\Omega), \beta = (\beta_1, \beta_2) \text{ s.t. } |\beta| = 2 \right\},$$

equipped with the norm

$$\|u\|_{H^{2,\lambda}(\Omega)} := \left\{ \|u\|^2_{H^1(\Omega)} + \sum_{|\beta|=2} \left\| r^\lambda \cdot D^\beta u \right\|^2_{H^0(\Omega)} \right\}^{1/2}.$$

Remark 23. It is shown in [14] (Lemma 8.4.1.2) that the natural imbedding of $H^{2,\lambda}(\Omega)$ is compact for $\lambda < 1$. Moreover $H^{2,\lambda}(\Omega)$ is continuously imbedded in $C^0\left(\overline{\Omega}\right)$.

Remark 24. Note that if $\lambda = 0$, the space $H^{2,\lambda}(\Omega)$ is the space $H^2(\Omega)$ and the norms are also equal.

Here r is a function such that $r : \Omega \to \mathbb{R}^+$, $r \in C(\overline{\Omega})$ and that $r(x) = |x - P|$ if x is in a small neighborhood of a reentrant point P. We will more precisely define r when we consider specific domains in Chapter 7. The following lemma is presented in [14] and its proof is given here for completeness.

Lemma 5.6.1. *Let $P_1(\Omega)$ be the space of the first-order polynomial (linear polynomials) restricted to Ω. Then there exists a constant C_G such that*

$$\inf_{p \in P_1(\Omega)} \|u - p\|^2_{H^{2,\lambda}(\Omega)} \leq C_G^2 \sum_{|\beta|=2} \left\| r^\lambda D^\beta u \right\|^2_{L^2(\Omega)} \tag{5.21}$$

for every $u \in H^{2,\lambda}(\Omega)$.

Proof. To begin the following inequality must be shown:

$$\|v\|^2_{H^{2,\lambda}(\Omega)} \leq C_1^2 \sum_{|\beta|=2} \left\| r^\lambda D^\beta u \right\|^2_{L^2(\Omega)} \tag{5.22}$$

for every $v \in P_1^{\perp}(\Omega)$, the orthogonal of $P_1(\Omega)$ in $H^{2,\lambda}(\Omega)$.
Similar to Lemma 5.5.1, we will shown this by contradiction. Assume (5.22) does not hold, this

$$\|v_n\|_{H^{2,\lambda}(\Omega)} = 1 \tag{5.23}$$

for every n, while

$$r^{\lambda} D^{\beta} v_n \to 0, \ |\beta| = 2 \tag{5.24}$$

in $L^2(\Omega)$ as $n \to +\infty$.

The compactness of the imbedding of $H^{2,\lambda}(\Omega)$ into $H^1(\Omega)$ implies the existence of a strongly convergent subsequence in $H^1(\Omega)$. Denote this sequence, again, by v_n, $n = 1, 2, ...$ and thusly there exists $v \in H^1(\Omega)$ such that

$$v_n \to v$$

in $H^1(\Omega)$ as $n \to +\infty$.

By the definition of the norm in $H^{2,\lambda}(\Omega)$, the sequence v_n is Cauchy in $H^{2,\lambda}(\Omega)$. Thus

$$\|v_n - v_m\|^2_{H^{2,\lambda}(\Omega)} = \|v_n - v_m\|^2_{H^1(\Omega)} + \sum_{|\beta|=2} \left\|r^{\lambda} D^{\beta}(v_n - v_m)\right\|^2_{L^2(\Omega)}$$

with both of the terms on the right converging to zero as $n, m \to +\infty$. Accordingly we have

$$v \in H^{2,\lambda}(\Omega)$$

and

$$v_n \to v$$

in the norm of $H^{2,\lambda}(\Omega)$. Hence $v \in P_1(\Omega)^{\perp}$ since $v_n \in P_1(\Omega)^{\perp}$ for every n, and (5.24) implies that

$$D^{\beta} v = 0, \ |\beta| = 2$$

which implies $v \in P_1(\Omega)$. Hence, $v \in P_1(\Omega) \cap P_1(\Omega)^{\perp}$, which implies $v = 0$, contradicting (5.23).

To complete the proof we set $v = u - p$ in Equation (5.22) where p is the orthogonal

projection of u onto $P_1(\Omega)$. $\square$

Let us now consider a model triangle $(\hat{\mathcal{T}})$ with vertices located at (0,0), (0,1) and (1,0). If we denote by $\hat{\Pi}u$ the linear interpolating polynomial for any function $u \in H^{2,\lambda}\left(\hat{\mathcal{T}}\right)$ then

$$\hat{\Pi}u \in P_1\left(\hat{\mathcal{T}}\right)$$

and

$$\hat{\Pi}u = u$$

at the vertices of the model triangle. Then for every $p \in P_1\left(\hat{\mathcal{T}}\right)$ we have

$$u - \hat{\Pi}u = \left(1 - \hat{\Pi}\right)(u - p).$$

Since both the identity operator and $\hat{\Pi}$ are continuous from $H^{2,\lambda}\left(\hat{\mathcal{T}}\right)$ into $H^1\left(\hat{\mathcal{T}}\right)$ then there exists a constant $\hat{C}$ such that

$$\left\|1 - \hat{\Pi}\right\|_{H^{2,\lambda}(\hat{\mathcal{T}}) \to H^1(\hat{\mathcal{T}})} \leq \hat{C}$$

thus

$$\left\|u - \hat{\Pi}u\right\|_{H^1(\hat{\mathcal{T}})} = \left\|(1 - \hat{\Pi})(u - p)\right\|_{H^1(\hat{\mathcal{T}})} \leq \hat{C}\,\|u - p\|_{H^{2,\lambda}(\Omega)}.$$

Taking the infimum over p it follows from Lemma 5.6.1 that

$$\left\|u - \hat{\Pi}u\right\|^2_{H^1(\hat{\mathcal{T}})} \leq \hat{C}^2 \sum_{|\beta|=2} \left\|r^\lambda D^\beta u\right\|^2_{L^2(\hat{\mathcal{T}})} \tag{5.25}$$

Finally we recall the affine mapping introduced earlier, $F_{\mathcal{T}}(x) = B_{\mathcal{T}}x + a$ where x is a point in the model triangle and $B_{\mathcal{T}}$ is a non-singular 2x2 matrix and a is a vector in $\mathbb{R}^2$. By $\Pi_{\mathcal{T}}u$ we denote the first-order interpolating polynomial which is equal to u at the vertices of the triangle. The following estimate is proved in [14] (Lemma 8.4.1.4), and the proof is similar to that of Theorem 5.5.2, for the transformation of triangles.

Lemma 5.6.2. *Let b be the point represented by the vector a (i.e. b is the vertex with the reentrant angles). There exists a constant C independent of the triangle $\mathcal{T}$ such that*

$$\|u - \Pi_{\mathcal{T}}u\|^2_{H^1(\mathcal{T})} \leq C \cdot \left\|B_{\mathcal{T}}^{-1}\right\|^{2+2\lambda} \cdot \|B_{\mathcal{T}}\|^4 \sum_{|\beta|=2} \int_{\mathcal{T}} d(x,b)^{2\lambda} \left|D^\beta u(x)\right|^2 dx \tag{5.26}$$

for every $u \in H^{2,\lambda}(\mathcal{T})$.

Remark 25. When the triangle $\mathcal{T}$ does not have a vertex which coincides with a singular point, i.e. $\lambda = 0$ the above inequality becomes

$$\|u - \Pi_{\mathcal{T}} u\|^2_{H^1(\mathcal{T})} \leq C \cdot \left\|B_{\mathcal{T}}^{-1}\right\|^2 \cdot \|B_{\mathcal{T}}\|^4 \sum_{|\beta|=2} \left\|D^\beta u\right\|^2_{L^2(\mathcal{T})} = C \cdot \left\|B_{\mathcal{T}}^{-1}\right\|^2 \cdot \|B_{\mathcal{T}}\|^4 |u|^2_{H^2(\mathcal{T})}. \tag{5.27}$$

which is equivalent to the inequality (5.13) shown earlier.

When one of the vertices of the triangle coincide with a singular point, i.e. $\lambda > 0$ then we get the following weighted inequality

$$\|u - \Pi_{\mathcal{T}} u\|^2_{H^1(\mathcal{T})} \leq C \cdot \left\|B_{\mathcal{T}}^{-1}\right\|^{2+2\lambda} \cdot \|B_{\mathcal{T}}\|^4 \sum_{|\beta|=2} \left\|r^\lambda D^\beta u\right\|^2_{L^2(\mathcal{T})} \tag{5.28}$$

Remark 26. The constant C in Lemma 5.6.2 and equations (5.27) and (5.28) is dependent only on the model triangle and the space $H^1(\mathcal{T})$, in the same manner that C_M is dependent on the C_S and $C_{\mathcal{T}}$ in Theorem 5.5.2.

The following important theorem is presented in Grisvard[14]

Theorem 5.6.3. *Let* Ω *be a nonconvex polygonal domain and* T_h *a family of shape regular meshes on* Ω. *Let* h *be the global mesh size,* $h_{\mathcal{T}}$ *the local mesh size, and for a fixed real number* $\lambda > 0$ *then there exists a* $\sigma > 0$ *(*$\sigma \geq h_{\mathcal{T}}/\rho_{\mathcal{T}}$*) such that*

- $h_{\mathcal{T}} \leq \sigma h^{1/(1-\lambda)}$ *for every* $\mathcal{T} \in T_h$ *such that at least one vertex coincides with the vertex of a reentrant corner of* Ω;
- $h_{\mathcal{T}} \leq h \inf_{\mathcal{T}} r^\lambda$ *for every* $\mathcal{T} \in T_h$ *with no vertex of any reentrant corner of* Ω, *but in a small neighborhood of at least one of them*

Then there exists a constant C *such that*

$$\|u - \Pi_h u\|_{H^1(\Omega)} \leq Ch \|u\|_{H^{2,\lambda}(\Omega)} \tag{5.29}$$

for every $h > 0$ *and every* $u \in H^{2,\lambda}(\Omega)$, *provided* $\lambda < 1$

This theorem shows that the same asymptotic rate of convergence can be expected as for smooth functions if the mesh is refined in a suitable manner near the offending corner.

Proof. Since for every $k \in T_h$ the restriction $\Pi_h u|_k$ of $\Pi_h u$ to $\mathcal{T}$ is just $\Pi_{\mathcal{T}}(u|\mathcal{T})$, the two inequalities (5.27) and (5.28) can be applied to $u|_{\mathcal{T}}$.
If one of the vertices of the triangle corresponds to a singular point, then we use (5.28), thus yielding

$$\|u - \Pi_h u\|^2_{H^1(\mathcal{T})} \leq C^2 \left\|B_{\mathcal{T}}^{-1}\right\|^{2+2\lambda} \cdot \|B_{\mathcal{T}}\|^4 \sum_{|\beta|=2} \left\|r^\lambda D^\beta\right\|^2_{L^2(\mathcal{T})}$$

If, in contrast, $\mathcal{T}$ contains no vertices which are also singular points then we use (5.27), yielding

$$\begin{aligned}\|u - \Pi_h u\|^2_{H^1(\mathcal{T})} &\leq C^2 \left\|B_{\mathcal{T}}^{-1}\right\|^2 \cdot \|B_{\mathcal{T}}\|^4 \sum_{|\beta|=2} \left\|D^\beta u\right\|^2_{L^2(\mathcal{T})} \\ &\leq C^2 \left\|B_{\mathcal{T}}^{-1}\right\|^2 \cdot \|B_{\mathcal{T}}\|^4 \left(\inf_{\mathcal{T}} r^{2\lambda}\right)^{-1} \sum_{|\beta|=2} \left\|D^\beta u\right\|^2_{L^2(\mathcal{T})}.\end{aligned}$$

Note that the values for $\|B_{\mathcal{T}}\|$ and $\left\|B_{\mathcal{T}}^{-1}\right\|$ are known (see previous section). Combining these values with the assumptions of the theorem, the following inequality is implied

$$\|u - \Pi_h u\|^2_{H^1(\mathcal{T})} \leq C^2 h^2 \sum_{|\beta|=2} \left\|r^\lambda D^\beta\right\|^2_{L^2(\mathcal{T})}$$

with the value of C dependent on the value of $\|B_{\mathcal{T}}\|$, $\left\|B_{\mathcal{T}}^{-1}\right\|$, and the value of C determined in Lemma 5.6.1. The inequality follows by addition and Poincaré's inequality. □

Corollary 5.6.4. *If a triangulation T_h of domain Ω fulfills the conditions of Theorem 5.6.3, then there exists a constant C which is independent of both u and h such that*

$$\|u - u_h\|_{H^1\Omega} \leq Ch \|u\|_{H^{2,\lambda}(\Omega)}. \tag{5.30}$$

Proof. Similar to the proof of equation 5.17 we use inequality 5.29 and Céa's Lemma (Lemma 5.2.2). □

5.7 Remarks on the Constant C

Key to the error estimates 5.17 and 5.30 is the presence of a constant C. We wish to determine the maximal amount of information about this constant. We will begin by

considering the constant in Equation 5.17 and then consider the constant in Equation 5.30.

Reviewing the proofs leading to the creation of Equation 5.17, we can glean some data on this constant given a triangulation. This constant is an amalgamation of constants appearing in several different Theorems, we can say that $C = C(C_c, C_{\mathcal{T}}, C_S, \sigma)$ where C_c is the constant from Céa's Lemma (Lemma 5.2.2), $C_{\mathcal{T}}$ is the constant from Theorem 5.4.1, C_S is from the Bramble-Hilbert Lemma (Lemma 5.5.1) and σ is the shape regularity constant. Brenner and Scott [3] give a direct proof of the Bramble-Hilbert Lemma and from this proof we discover that the constant C_S is dependent on the Sobolev space, the dimension of the problem space, and shape regularity constant σ.

In a similar manner the constant in Equation 5.17 can also be studied. Again this constant is a combination of several previous constants, namely constants from Céa's Lemma, Lemma 5.6.1 and Lemma 5.6.2. We note that similar to the Bramble-Hilbert Lemma the constant in Lemma 5.6.1 is dependent on a proof by contradiction. However, unlike the previous case no work has been done to determine the value of the constant. With additional work it may be possible to adapt the proof in [3] to handle the case with singularities, so that further information can be extracted. We do not, however that the constant in Equation 5.17 is dependent on the shape regularity constant σ since the constant in Lemma 5.6.2 is dependent on this value.

Chapter 6

An Adaptive Mesh

Thus far in the dissertation we have restricted ourselves to the special case of the standard Koch curve (and the standard Sierpinski gasket). We wish, however, to be able to consider a whole family of Koch curves (i.e. with differing values of α), so that we can have greater control over the dimension of our boundary. Although there is a large number of tools designed to create finite element meshes for nearly any shaped object, we want to create one that will take advantage of the self-similarity inherent in the prefractal. In particular can we design a mesh that is valid not only for the nth iteration of the prefractal, but all of the previous m iterations? For the classic Koch curve, ($\alpha = 3$) the solution to this problem is trivial, as the classic Koch curve lends itself easily to a mesh containing only equilateral triangles (as seen in Chapters 2 and 3). For all rational values of α we provide a mesh with the following characteristics:

1. The mesh can be created for all rational values of α.
2. The mesh is valid for all previous iterations of the prefractal. That is to say the mesh created for the nth iteration also holds true for all iterations m where $m \leq n$.
3. The mesh is shape regular, and the number of triangle types is finite and fixed.

We will term such a mesh an adaptive mesh and will denote it by $\mathcal{M}(\alpha, n)$. The mesh can be considered doubly adaptive because not only can it be adapted to any rational value of α, it is also adapted to the problem of studying nested sequences of prefractals. The main result of this chapter is the following theorem that will be shown via a constructive proof.

Theorem 6.0.1. *For every rational α and every n there exists an adaptive mesh $\mathcal{M}(\alpha, n)$.*

We will also present the following theorem.

Theorem 6.0.2. *Our adaptive mesh is regular with shape regularity constant $\kappa(\alpha)$ dependent only on α, and independent of the prefractal iteration number n. Moreover the value of $\kappa(\alpha)$ diverges as $\alpha \to 2$ and $\alpha \to 4$ with the following limits*

$$\lim_{\alpha \to 2} \frac{\kappa(\alpha)}{\alpha - 2} \leq +\infty$$

and

$$\lim_{\alpha \to 4} \frac{\kappa(\alpha)}{4 - \alpha} \leq +\infty.$$

We structure this chapter as follows. First we will introduce a closely related problem of dividing a line segment in a Cantor like manner, based on a parameter α. Second we recall the Koch curve and relate the problem addressed in the first section to the problem of filling the area underneath the fractal curve with a regular mesh. We will then transition the Koch curves to the four sides of a unit square, and will provide a methodology for filling the entire curve with elements. We will conclude by summarizing the shape regularity of the elements.

6.1 A Cantor Like Construction

Consider the following Cantor like construction on a set of segments. Fix α such that $2 < \alpha \leq 4$. For each iteration, divide each segment into three pieces in the following manner. If l is the length of the segment, the first segment will have length l/α, with its end points located at $(0, l/\alpha)$. The second segment will have end points at l/α and $l - l/\alpha$, and will have length $l\,(\alpha - 2)\,/\alpha$. Lastly the third piece will have length l/α and have end points located at $(l - l/\alpha, l)$. See Figure 6.1.

Subsequently these segments will be referred to as "Cantor segments", with the first and third pieces referred to as the "Cantor wings" and the second piece being referred to as the "Cantor center." We will use the number t to refer to the Cantor iteration.

Suppose now that we consider an isosceles triangle with each of the three sides subject to the Cantor like construction detailed above. Without loss of generality orient the triangle such that the two sides of equal length form the sides of the triangle and the

Figure 6.1: A Cantor like construction with $\alpha = 2.5$. The green pieces are the "Cantor wings" and the red piece is the "Cantor center"

side with odd length, forms the base. We will refer to the initial segment as the "base" of this triangle. This motivates the introduction of finite element triangles (henceforth referred to as FET), which will fill our original triangle (referred to as the main triangle).

We now impose the following restriction on α and will extend the results from this restriction. Let $2 < \alpha \leq 3$ and require α such that

$$length(\text{Cantor wing})/length(\text{Cantor Side}) = \text{an integer}.$$

This implies $\alpha = 2 + 1/m$ where $m \in \mathbb{Z}^+$. If $\alpha = 2 + 1/m$ then

$$length(\text{Cantor wing})/length(\text{Cantor Side}) = m.$$

This brings us to the main idea. Create a FET that is similar to the main triangle, with base of width $l\,(\alpha - 2)\,/\alpha$ (the Cantor center width). We can place $2m+1$ of these triangles on the base (as referred to above), with m being placed on each Cantor wing, and 1 in the Cantor center. Let $T = 2m + 1$ be the total number of FET triangles that will fill the base. If we consider the main triangle (the term "base" will correspond to the base of this triangle) it will be filled with T^2 identical FET triangles. Moreover, the nodes of these triangles will coincide exactly with the nodes of the Cantor like iterations on the sides. (See Figure 6.2)

We then repeat the Cantor iteration on each of the elements of the Cantor segment set. The smallest new Cantor segment will correspond to the Cantor center of the smallest element of the previous set. It is easy to see that the smallest element at any iteration will be the Cantor center located in the exact center of the original segment.

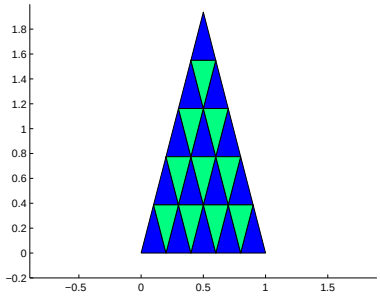

Figure 6.2: The triangle filled with T^2 identical FET triangles

By construction the width of this segment for the second iteration is:

$$\frac{l\,(\alpha-2)}{\alpha}-\frac{2l\,(\alpha-2)}{\alpha^2}=l\left(\frac{\alpha-2}{\alpha}\right)^2$$

By induction it is easy to show that for iteration t of the Cantor iteration the smallest segment width will be equal to

$$l\left(\frac{\alpha-2}{\alpha}\right)^t$$

where l is the original segment length. Since the FET width is dependent on the smallest segment width, the FET width for iteration t will be

$$l\left(\frac{\alpha-2}{\alpha}\right)^n.$$

We note that since the width of the triangles in the FET is dependent of the Cantor iteration it makes sense to use the same index t to refer to both the Cantor iteration and the FET. A useful relation can be determined by comparing the FET width between iteration t and iteration $t+1$:

$$\frac{l\left(\frac{\alpha-2}{\alpha}\right)^t}{l\left(\frac{\alpha-2}{\alpha}\right)^{t+1}}=\frac{\alpha}{\alpha-2}=2m+1=T.$$

Hence T triangles from iteration t will be placed on the base of a FET element from iteration $n-1$.

One final consideration is whether the finite element triangulation created by nth

step will correspond to the Cantor iteration for step t, that is, will the new nodes introduced in Cantor step t correspond to nodes of the FET. By construction, it is clear that the FET nodes will correspond for the Cantor centers, but it remains to be shown for the Cantor wings. Consider a Cantor wing from the first iteration. It will be covered by m FET triangles from the first iteration and $m \times T$ FET triangles from the second iteration. If the width of the new Cantor center created on the Cantor wing is l_{wc} then the length of the parent wing was $(2m+1)\, l_{wc}$. This implies that the new Cantor center will be covered by m triangles in the second iteration, and by induction will be covered by m^{t-1} triangles in iteration t.

Having shown certain properties for the simpler case, $(\alpha = 2 + 1/m)$ we now extend our results to the more general case of $\alpha = 2 + p/q$ where $0 < p/q \leq 2$ and $p, q \in \mathbb{Z}$. For these values of α, the ratio

$$length(\text{Cantor wing})/length(\text{Cantor Side}) = \frac{q}{p},$$

which is not an integer, rather a positive rational number. For this more general case we now create a FET similar to the original triangle, but in this case the base has a width of $l\,(\alpha - 2)\,/(p\alpha)$. We place q of these triangles on each of the Cantor wings, and p of these triangles on the Cantor center, with a total $T = 2q + p$ triangles being placed. It is easily shown that the original length l is equal to $(2q+p) \times l\,(\alpha - 2)\,/(p\alpha)$. Following the methodology introduced earlier one can show that the FET width is dependent on α and the iteration number t and is equal to

$$l\left(\frac{\alpha - 2}{p\alpha}\right)^t.$$

Additional results (such as verification of correspondence between the triangulation and the Cantor iteration) are easily reproduced for this more general case.

6.2 Filling the Area Under a Koch Curve

Now that we have illustrated a manner of filling a larger triangle with smaller, similar triangles, we will relate our work to a prefractal Koch curve, and provide an algorithm for filling the area under the curve with suitable triangles. The Koch curve is a *self-*

similar fractal by the definition given by Hutchinson in [16]. We refer to the reader to the definition of the Koch curve given in Chapter 1

In order to use Cantor like construction we have developed, we restrict our choice of α to $2 + p/q$. An important distinction must be made between the Cantor iteration number t and the prefractal iteration number n. In order for the nodes of the Koch curve to correspond to nodes in the Cantor like construction t must be greater then or equal to n. There is no requirement however that the two be equal, in fact we may wish to fix the prefractal iteration at n and continue to iterate the Cantor like construction in order to increase the accuracy of approximation. For this purpose we continue to use separate indices, n and t.

An algorithm to fill the area under the prefractal curve with triangles is as follows: Begin with the initial curve S^0, iterate the Koch curve to the curve S^1, and fill the area under the curve with a single triangle. (The area covered by this triangle is the reference area, and the size of triangles in this area will be the reference size for any other triangles under the curve.) For each subsequent iteration, do the following:

1. Refine any existing standard size triangles (i.e. those that were not created by the stitching process detailed below), by dividing them into T^2 similar triangles, subject to the manner described above. (Recall $T = 2q + p$.)

2. Refine any triangles and quadrilaterals created in the stitching process. This is done by first recalling the original triangles, and dividing these triangles into T^2 triangles, while maintaining any edges and nodes created in the stitching process. (See figures 6.3, 6.4, and 6.5)

3. Iterate the Koch curve, and fill any newly created areas with as many triangles as needed with size equal to that of the triangles in the reference area.

4. Remove any hanging nodes by "stitching" the wings to the body.

5. Repeat steps 1-4 until desired prefractal curve is reached.

6.2.1 Stitching the Wings to the Body

Each time the Koch curve is iterated, new "wings" occur at the location of the Cantor centers. Due to the requirement that the triangles in these newly created wings must

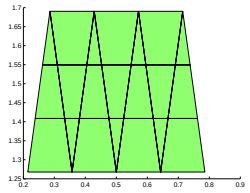

Figure 6.3: An area created by the stitching process

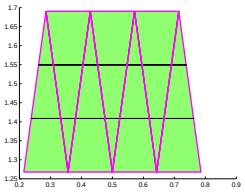

Figure 6.4: The same area with original triangles emphasized

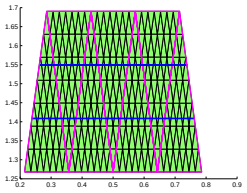

Figure 6.5: After the triangle division

be equal to the size of the triangles in the reference area, hanging nodes appear on the boundary between the wing and the body. Once again for simplicity we will consider the case $\alpha = 2 + 1/m$ and then consider the more general case of $\alpha = 2 + p/q$.

For the case $\alpha = 2+1/m$, it is easy to show that the number of reference triangles on the base of the wing is $W = m^{c_w - 1}$, ,where c_w is the iteration number where the Cantor wing first appears. Hence the number of reference triangles to fill the wing is W^2. There exists a simple relationship between the sides of the reference triangle and the base, i.e.

$$\frac{\text{side}}{\text{base}} = \frac{1/\alpha}{1 - 2/\alpha} = m$$

Thus, there will be $m^{c_w - 2}$ new hanging nodes and exactly $m - 1$ hanging nodes on each triangle. To stitch the Koch wings to the base, one simply connects each of these hanging nodes to the node opposite it on the Koch body (See Figure 6.6.) This action creates $m - 1$ types of quadrilaterals, however these quadrilaterals are similar to those created in previous iterations.

We now consider the more general case of $\alpha = 2 + p/q$. When we consider the intersection between the wings and the body, we must take into consideration that there will be hanging nodes on both the triangles that are part of the body and the triangles that are part of the wing. Just as in the simple case, one can show that the number of reference triangles on the wing in the general case is $W = pq^{c_w - 1}$, where c_w is defined as before. As before the relationship between the sides of the reference triangle and the

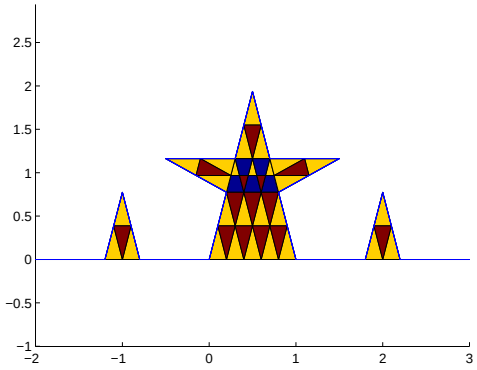

Figure 6.6: Stitching the wings to the body in the case $\alpha = 2 + 1/m$

base, is given by

$$\frac{\text{side}}{\text{base}} = \frac{1/\alpha}{1 - 2/\alpha} = \frac{q}{p}.$$

Unlike the previous case, unless p divides q, this number is a fraction instead of an integer. The number of triangles occurring in the body between the edges of the Cantor wing is therefore $W \times p/q$. We will divide the triangles occurring along the base of the wing into W/q similar groups. Each of these groups will have exactly $p-1$ hanging nodes. If $p-1$ is odd, then combine the groups pair wise, so that there are $W/2q$ similar groups with $2\,(p-1)$ hanging nodes in each. To handle the hanging nodes in the wing triangles we do an outer stitch, which is accomplished by connecting two of these nodes thus creating additional similar triangles and quadrilaterals. This methodology is illustrated below for two values of α. The hanging nodes which occur in the triangles inside the

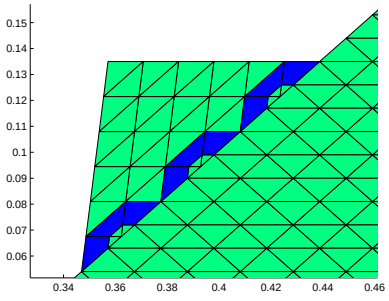

Figure 6.7: Outer stitch for α=3/2

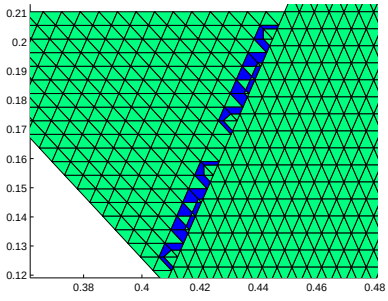

Figure 6.8: Outer stitch for α=4/5

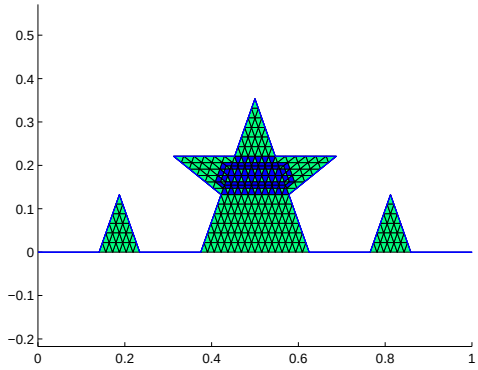

Figure 6.9: Stitching the wings to the body in the case $\alpha = 2 + 2/3$

"body" are handled in a similar manner to the simple case, i.e., they are simply stitched across the body. The number of these hanging nodes is equal to $W - 1 - W/q$. A final stitch is shown below (Figure 6.9).

6.3 Filling a Square Domain

We now consider filling a square domain, which has an interior fractal boundary, with finite elements. This scenario may arise in transmission problems, where we study the transmission from an exterior domain to an interior domain along a prefractal boundary. (See Figure 6.10.) We will fill the domain in a symmetric manner by placing curves in a square domain in the manner of Cesàro as illustrated in [24].

Filling this domain is a three-step process. First we will consider the smallest isosceles triangle that contains the prefractal boundary (of a fixed iteration n), and fill it with elements. Using symmetry, this triangle will then be placed on the other three sides of the square domain. Next we consider the slivers in between the isosceles triangles. The vertices of these slivers are the top vertices of two isosceles triangles, and one of the corners of the square. Finally we will consider the square in the center of the domain, created by joining the top vertices of the four isosceles triangles. A graphical representation of these three areas is seen in Figure 6.11.

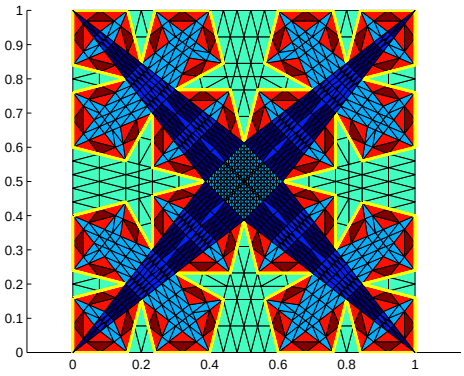

Figure 6.10: A sample domain with an internal fractal transmission boundary. Here green is the external domain, yellow indicates the transmission boundary and the blue and red shades are in the interior of the domain.

6.3.1 Filling the Isosceles Triangles

To fill an isosceles triangle we will make use of the methodology described in Section 3. We consider the base of the triangle to be the edge of the triangle that shares an edge with the domain, and the "top" of the triangle to be vertex of the triangle located near the center of the domain. Let us consider the triangle that contains the Koch boundary of a given fixed iteration n. This curve is located along the base of triangle, and will be considered the *primary* Koch curve. We then place Koch curves (with the same α and the same iteration number n) along the other two sides of the triangles. These *secondary* curves must be oriented so that they invade the triangle, that is, the curves are contained in the closure of the triangle. Now using the methodology section 3, fill the area under these curves with triangles and quadrilaterals. See Figure 6.12.

Next consider the area of the triangle not covered by the curves. This area will be referred to as the matching area in the triangle, and has the following characteristics:

- The matching area consists of a collection of triangles (referred to as matching triangles) which are all similar to both each other and the original isosceles triangle under consideration.
- The number of triangles is related to the iteration n of the prefractal and is equal to $4n$

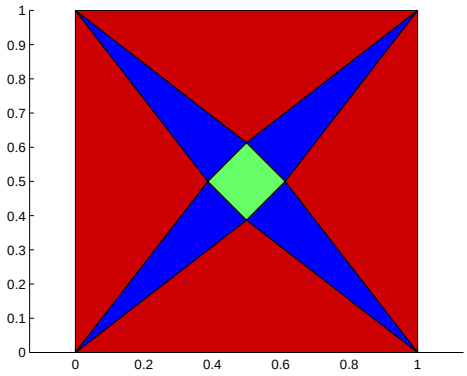

Figure 6.11: This illustrates the three areas. Step 1 will handle the blue areas (isosceles triangles), Step 2 will handle the green areas (slivers) and Step 3 will handle the red area (center square)

- A map (similar to the map for the Koch curve) brings the triangles from one iteration to the next.
- The area of the triangle is also related to the iteration and is equal to $A/(\alpha^{2n})$ where A is the area of the isosceles triangle.
- The total area covered by the matching triangles at each iteration is $(4^n)/(\alpha^{2n})A$, and it is clear that as $n \to \infty$ then the area approaches zero for all fixed $\alpha > 2$.

Figures 6.13-6.15, show the iteration of the triangles in the matching area.

We observe that the triangles in matching area, have at least one hanging nodes along they sides share with either the primary or secondary Koch curves. The portion of the Koch curve shared by this triangle is equal to the portion referred to as a "Cantor wing" in the proceeding section, or is equal to the entire side of a Koch wing. We recall that the number of hanging nodes will be equal to pq^{t-1} where p and q are as defined previously, and t is the iteration number of the Cantor iteration with $t \geq n$. Since the number of hanging nodes is equal on each side (or not specified if the edge of the triangle lies on the boundary of our isosceles triangle), a Sierpinski like division with $\beta = p * q^{t-1}$ will remove the hanging nodes. Here β is the homothey factor, that is each new triangle has sides that are $1/\beta$ the original length. Moreover, the Sierpinski division does not introduce any new *types* of triangles, but instead creates β^2 new similar triangles as

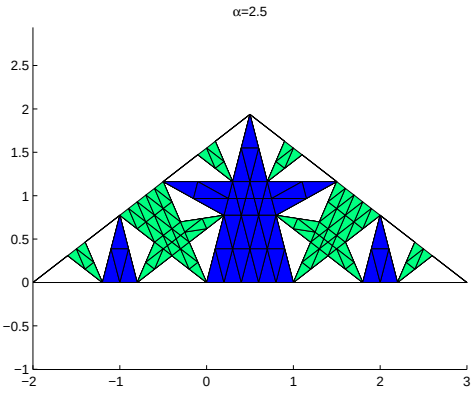

Figure 6.12: Filling the area under the primary and secondary curves. The area under the primary curve is blue, and the area under the secondary curve is green.

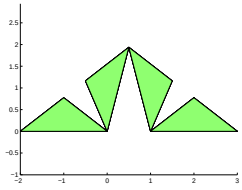

Figure 6.13: $t = 1$

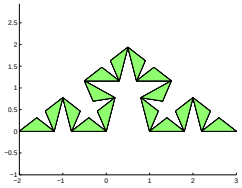

Figure 6.14: $t = 2$

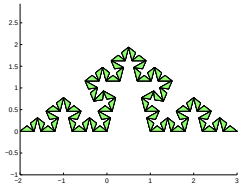

Figure 6.15: $t = 3$

illustrated in Figures 6.16 and 6.17.

By filling the Koch curves and matching triangles as detailed above, the isosceles triangle under consideration is now completely filled with elements appropriate for the finite element method as seen in Figure 6.18. We then rotate the isosceles triangles and place a copy on each of the four side of the square. (See Figure 6.19).

6.3.2 Filling the Slivers

We now consider the area bounded by a triangle of which two vertices are the top vertices of adjacent isosceles triangles, and the third vertex is the point common to the adjacent isosceles triangles. Similar to the case for the isosceles triangles, we will fill a single sliver and through rotation fill the other three slivers. Moreover, the filling of this area will be a multi-step process. For reference, the base of the sliver will be considered to be the side which has the two tops of the isosceles triangles as end points, and the

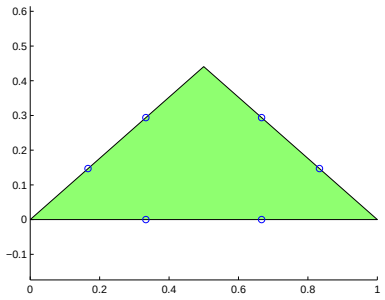

Figure 6.16: The hanging nodes for a matching area triangle

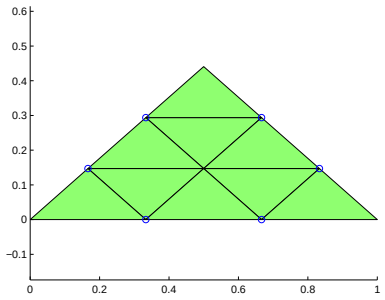

Figure 6.17: A Sierpinski like division into β^2 triangles (here $\beta = 3$).

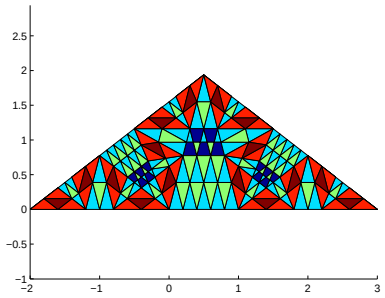

Figure 6.18: A single filled isosceles triangle

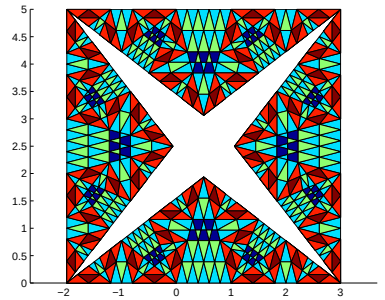

Figure 6.19: Four isosceles triangles located on each of the sides of the square

"head" of the sliver will be vertex that is common to the square.

The first step in filling the sliver is to examine the triangle created by connecting the head of the sliver to the first two hanging nodes (one on each side). It is worth noting that this is an isosceles triangle, and the length of the equal sides is equal to that of the sides of the Sierpinski triangles created in the matching area in the previous step. Define

$$W = \lfloor \frac{p(2q+p)^t}{q} \rfloor.$$

We will place

$$\left(\left(pT^{t-1} - 1 \right) / q + 2T^{t-1} \right)^2 = W^2$$

triangles inside the sliver (see Figure 6.20). Note first that these triangles do not com-

pletely fill the sliver, and the nodes of these triangles only line up with about half of the preexisting nodes for the sliver.

To remedy the situation we start by fix the first (counting from the head down), $(\lfloor W/2 \rfloor)^2$ triangles. (This corresponds to the first $\lfloor W/2 \rfloor$ rows). Next, slide the remaining triangles down one side of the sliver, so that their nodes line up with the nodes of the sliver. Then we split the group of triangles down the middle and push half of them to the other side of the sliver, as shown in Figure 6.21. Thus far the construction leaves

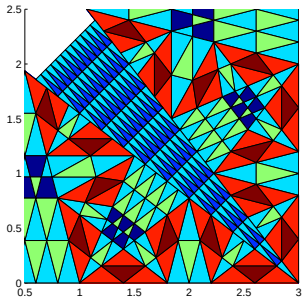

Figure 6.20: A single sliver, prior to sliding and splitting the triangles

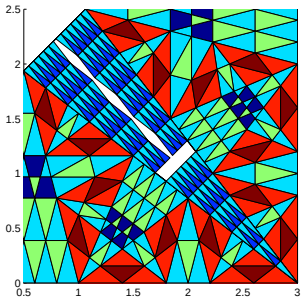

Figure 6.21: The same sliver, after sliding and splitting the triangles

us with a "T" shaped area that remains unfilled with elements. To fill this area with elements, connect each hanging node to another hanging node, using only lines parallel to the original sliver. In the upper portion of the "T" this will result in the creation of $\lfloor W/2 \rfloor$ parallelograms all of which are similar, and one triangle which is similar to the sliver. In the bottom portion of the "T ", $\lfloor W/2 \rfloor$ similar isosceles trapezoids are created. The resulting sliver is shown in Figure 6.22.

Finally we handle the remaining hanging nodes on the sides of the sliver. We handle these nodes in the same manner as the Koch wings were handled when filling the area under the Koch curve. To remove the hanging nodes, stitch across the sliver body. Once again this construction creates a finite number of quadrilateral types, however, provided that the Cantor iteration number t is at least 2 the number of quadrilateral types remains fixed regardless of the Cantor iteration number. Also it is worth noting that when $p \neq 1$, both the matching triangles as well as the interior Koch triangles create hanging nodes. For readability only illustrations using the simple case are shown. The final subdivision

of the sliver into elements is shown in Figure 6.23.

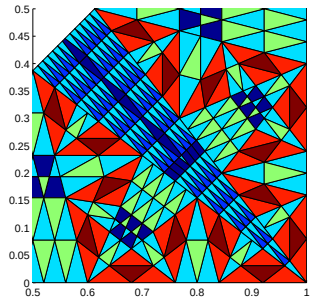

Figure 6.22: A sliver with the addition of quadrilaterals

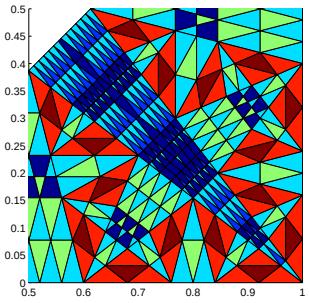

Figure 6.23: The final subdivision of a sliver

6.3.3 Filling the Center Square

To fill the center square with elements simply connect each node on a given side with the node on the opposite side of the square. Each of the resulting rectangles is then converted into two similar triangles by connecting two opposite vertices. Figure 6.24 shows the division of the center square.

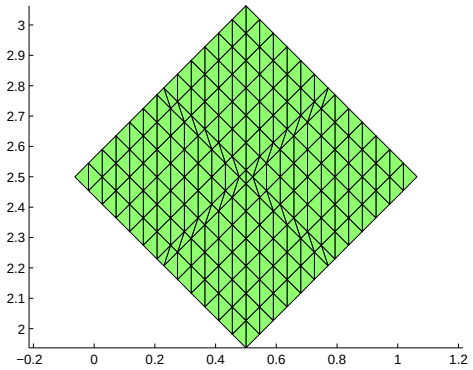

Figure 6.24: The center square broken into elements

Lastly the entire square is pieced together. First the four isosceles triangles are placed, then the four slivers, and finally the center square. The final division is illustrated in Figure 6.25.

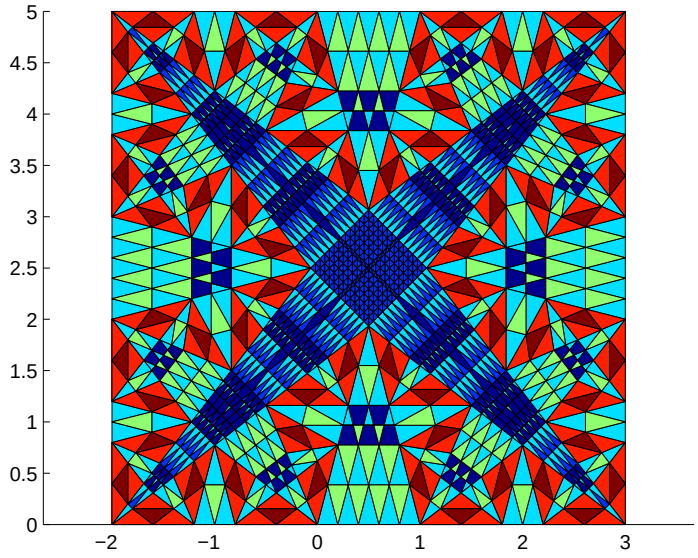

Figure 6.25: The final discretization of the square domain

Proof. (of Theorem 6.0.1)
Thus far we have described a methodology valid for all rational values of α to create a finite element mesh specific to the given value of α. Moreover the design of the mesh guarantees that the mesh will be valid for all previous iteration values m. (In fact the greater the difference between the iteration number n and the curve considered S^m the more accurate the finite element approximation for the curve S^m will be since the mesh for curve S^n represents a refinement of the curve S^m.) □

6.4 Shape Regularity of the Elements

In order to obtain an error estimate for any finite element calculations it is necessary to consider the regularity of the elements that fill the square domain. The described discretization is dependent on the choice of α and the Cantor iteration number t. Recall that a fixed prefractal curve has two variables α and n. The value α dictates the shapes of the elements in our discretization. The value of n dictates a minimum value of t, the Cantor iteration number, or in other words the value of n dictates the maximal size of the elements. Because the discretization creates a limited number of elements we will

address each element individually to understand both the aspect ratio of the element and to show that the element remains regular under further iteration (i.e. $n \to \infty$.) The elements which we will consider are

- The triangles created when filling the area under the Koch curve
- The triangles created in the matching areas of the isosceles triangles
- The triangles created in the slivers
- The triangles created in the center square
- The quadrilaterals created by stitching under the Koch curve
- The quadrilaterals created in the slivers

The triangles and quadrilaterals created when an outer stitch is performed will be considered separately. We first consider each of the triangle types, then the quadrilaterals, and finally the elements generated by the outer stitch.

6.4.1 Shape Regularity of Triangular Elements

We introduce some notation and define shape regularity for the triangular elements

$$r_{\mathcal{T}} = \text{the radius of the smallest ball containing a triangle } \mathcal{T}$$
$$p_{\mathcal{T}} = \text{the radius of the largest ball inscribed in a triangle } \mathcal{T}.$$

We recall the definition of a regular triangulation Definition 23 as: A triangulation T_h is shape-regular if there exists κ such that $r_{\mathcal{T}}/p_{\mathcal{T}} \leq \kappa$ for all $\mathcal{T} \in T_h$. A family of triangulations $\{T_h\}$, indexed by $h := \max_{\mathcal{T} \in T_h} r_{\mathcal{T}}$, is regular if T_h is shape-regular for each h, and $h \to 0$. (We emphasize that the shape regularity constant κ is independent of the size, h, of the mesh).

For each triangle we will compute the values of $r_{\mathcal{T}}$ and $p_{\mathcal{T}}$ using Equations (6.1) and (6.2) based on the length of the sides of the triangles s_1, s_2 and s_3. In these equations, S_P refers to the semiperimeter of the triangle (i.e. $S_P = (s_1 + s_2 + s_3)/2$),

$$r_{\mathcal{T}} = \frac{s_1 s_2 s_3}{4\sqrt{S_P\left(S_P - s_1\right)\left(S_P - s_2\right)\left(S_P - s_3\right)}}, \tag{6.1}$$

$$p_{\mathcal{T}} = \sqrt{\frac{(S - s_1)(S - s_2)(S_P - s_3)}{S_P}}. \tag{6.2}$$

We will then calculate the value for $\kappa = r_{\mathcal{T}}/p_{\mathcal{T}}$. Using equations (6.1) and (6.2) and simplifying we determine

$$\kappa = \frac{s_1 s_2 s_3}{4(S_P - s_1)(S_P - s_2)(S_P - s_3)}. \tag{6.3}$$

We observe that the value of κ is independent of the size of the triangle since it is the aspect ratio, and thus only depends on the choice of α. For the triangles created underneath the Koch curve, each is similar to the reference triangle (see Section 6.2), so it suffices to show the aspect ratio $\kappa = r_{\mathcal{T}}/p_{\mathcal{T}}$ for this triangle. Algebraic manipulation shows that for a given α, these triangles have the value

$$\kappa = \frac{2}{(4 - \alpha)(\alpha - 2)}.$$

The triangles created in the matching areas of the isosceles triangle, are similar to the original isosceles triangle, so for these triangles we calculate the aspect ratio $r_{\mathcal{T}}/p_{\mathcal{T}}$ for the isosceles triangle. For this triangle

$$\kappa = \frac{2}{2\sqrt{\alpha} - \alpha}.$$

Now we consider the triangles located in the sliver. Each of these triangles is similar to the sliver itself, so it suffices to calculate κ for this triangle alone. Then

$$\kappa = \frac{\sqrt{\alpha} - \sqrt{4 - \alpha}}{(2)^{5/2}(\alpha)^{3/2}(S_P - 1/\sqrt{\alpha})^2\left(S_P - \frac{\sqrt{\alpha} - \sqrt{4-\alpha}}{\sqrt{2\alpha}}\right)}.$$

(Here S_P is still the semi-perimeter of the triangle, but unlike the cases of the triangles underneath the Koch curve and matching triangles, S_P is left in the equation for simplicity. For the sliver triangles S_P is equal to $(4 + \sqrt{2\alpha} - \sqrt{8 - 2\alpha})/(4\sqrt{\alpha})$.)

Lastly we consider the two triangle types created in the center square. It is important to note that some of the triangles in this area are independent of the choice of α. The majority of the triangles are right isosceles triangles (and hence independent of the choice

of α) with

$$\kappa = 1 + \sqrt{2}.$$

The remainder of the triangles are dependent on the choice of α, and are right triangles with height 1 and width p/q where p and q is as defined before. Once again we leave the equation for κ in terms of the semi-perimeter S_P but note that for these triangles $S_P = (1 + p/q + \sqrt{(p/q)^2 + 1})/2$. Thus, the aspect ratio κ is

$$\kappa = \frac{p\sqrt{(p/q)^2 + 1}}{4q\left(S_P - p/q\right)\left(S_P - 1\right)\left(S_P - \sqrt{(p/q)^2 + 1}\right)}$$

6.4.2 Shape Regularity of Quadrilateral Elements

We start with the definition of a shape regular quadrilateral taken from [2].

Definition 26. Quadrilaterals are considered *shape regular* provided there is a constant κ such that the following are true

- For every quadrilateral, the ratio between maximal and minimal edge length is bounded by κ.
- Every quadrilateral contains an inscribed circle with radius $p_Q \geq h_Q/\kappa$ where h_Q is the diameter of the quadrilateral
- All angles are smaller then $\pi - \phi_0$ with some $\phi_0 > 0$.

We will first consider the quadrilaterals created beneath the Koch curve by the inner stitch when the wings are stitched to the body. For these quadrilaterals our construction guarantees the last of the conditions is satisfied with $\phi_0 = \theta$, where $\theta = \cos^{-1}(\alpha/2 - 1)$ as before. The first condition is easy to show for the quadrilaterals under consideration, and we will only show it is true for the "worst" quadrilateral created. In this case the longest side of the quadrilateral is $p/(2q + p)$ and the shortest side is $l/(2q + p)$ In this case $\kappa = p$. It is clear that every quadrilateral satisfies the second condition.

Next the quadrilaterals created in the slivers are considered. In the slivers two types of quadrilaterals, isosceles trapezoids and parallelograms may exist. We will first consider the isosceles trapezoids. For these quadrilaterals, the last condition for shape regularity is guaranteed by construction and $\phi_0 = \pi/4 + \theta/2$. The value for ϕ_0 is also valid for the

parallelograms. When calculating the value for κ for the isosceles trapezoids we again consider the worst trapezoid created by our methodology. The worst trapezoids created are those lying in the center of the sliver that do not get stitched. For these trapezoids the value of κ is

$$\kappa = \frac{q}{p^2}.$$

All of the parallelograms are similar and the value of κ is

$$\kappa = \frac{(p^{n+1} \mod q)\sqrt{2}}{q\left(\sqrt{\alpha} - \sqrt{4-\alpha}\right)}.$$

For these quadrilaterals the second condition can also be proved, but is left to the reader.

6.4.3 Shape Regularity in the Case of an Outer Stitch

Recall that an outer stitch is created whenever $p > 1$, and this stitch corrects hanging nodes in the cantor wing. The shape of the triangles and quadrilaterals generated are specific to the choice of p and q. For example when $p = 2$ and $q = 3$ (i.e. $\alpha = 2+2/3$) all of the triangles created are similar to the base triangle, and only two new quadrilaterals are created. However when $\alpha = 2+4/3$, new triangle types and several new quadrilateral types are created. Rather then investigating each individual triangle and quadrilateral type created, we will instead make some general observations.

1. We observe that no new quadrilateral types are created in moving from iteration (either Cantor or Koch) n to $n+1$ for $n \geq 2$.

2. The number of newly created element types is finite, and hence for a given α the appropriate shape regularity analysis can be done.

These observations assure us of a shape regular mesh for a given α.

6.4.4 Asymptotic Analysis of Shape Regularity

In order to gain information about the regularity of the elements and hence the accuracy of our any finite element estimation, we study the limit of the shape regularity parameter $\kappa(\alpha)$ as α approaches 2 and 4.

Proof. (of Theorem 6.0.2)
In Section 6.4, the shape regularity parameter $\kappa(\alpha) = r_{\mathcal{T}}/p_{\mathcal{T}}$, was calculated for each of

the four triangle types. From these calculations it is clear that $\kappa(\alpha)$ is dependent only on α and not on the iteration number of the prefractal n. We now study the limit of $\kappa(\alpha)$ as α tends toward either of its two extremes. Table 1 summarizes the behavior of $\kappa(\alpha)$ as α approaches both of these limits. Note that in the table each of the divergent cases diverge with speed $1/x$. This divergence in shown in graphical form in Figure 4 which plots $\kappa(\alpha)$ with respect to α. Note that in the table each of the divergent cases diverge with speed $1/x$. This behavior in shown in graphical form in Figure 6.26 which plots κ with respect to α. □

Triangle Type	Value of κ as $\alpha \to 2$	Value of κ as $\alpha \to 4$
Inner Koch	Divergent (as $1/(\alpha-2)$)	Divergent (as $1/(4-\alpha)$)
Matching	Constant	Divergent (as $1/(4-\alpha)$)
Sliver	Divergent (as $1/(\alpha-2)$)	Constant
Center (Type 1)	Constant	Constant
Center (Type 2)	Constant	Constant

Table 6.1: Asymptotic Analysis of κ

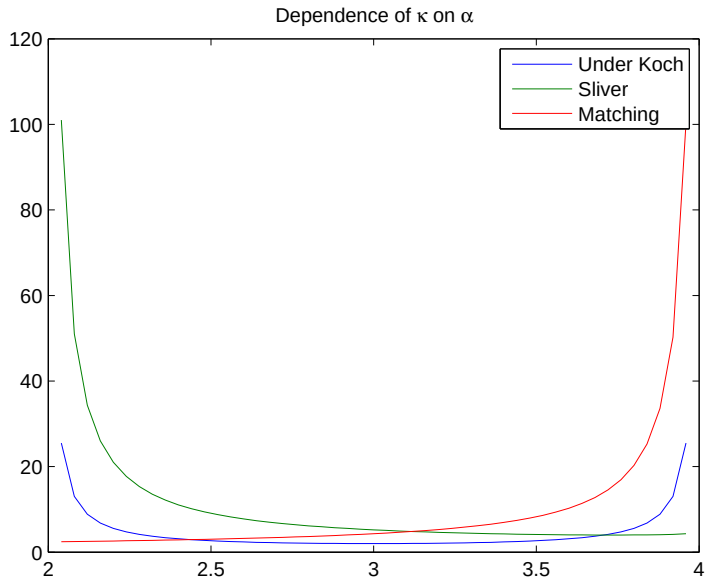

Figure 6.26: Dependence of κ on α

We notice that when $\alpha \to 2$ the triangles of greatest concern are the interior Koch

triangles, and the sliver triangles. However when we consider the domain encompassed by either of these triangles, we see that as $\alpha \to 2$ the measure of the domain goes to zero, and the majority of the domain is filled with "good" matching triangles. Likewise when $\alpha \to 4$ the area of the domain encompassed by either interior Koch triangles or matching triangles shrinks to measure zero and the majority of the domain is covered by center triangles and slivers. See Figure 6.27 for a visualization of this concept.

Figure 6.27: A classification of the domain into triangle types as $\alpha \to 2$ (left) and as $\alpha \to 4$ (right). The red toned area is the area covered by the matching triangles, whereas the blue toned areas are those covered by the slivers and center triangles.

Chapter 7

Numerical Considerations for the Adaptive Mesh

In Vacca [30] numerical solutions of transmission problems across a prefractal boundary were first studied. In her dissertation Vacca restricted her work only to the special case when $\alpha = 3$. This case is unique in that it easily lends itself to a mesh composed only of equilateral triangles. Since the publication of her work, Vacca's work has been extended to problems with a time variable (such as heat problems), but this work retains the requirement that $\alpha = 3$ or the use of an automatic mesh generator. A previous WPI student, Rebecca Wasyk, also considered the numerical solution of transmission problems across prefractal boundaries. In [31] Wasyk allows α to vary between 2 and 4 but relied on an automatic mesh generator to create a mesh for the domain. Wasyk then proved certain approximation results using the automatically generated mesh coupled with a refinement methodology to account for the singularities.

Our work differs from previous work in several key ways. For our numerical work we will use the adaptive mesh detailed in Chapter 6. Unlike the work of Vacca, this mesh allows us to consider both the transmission problem and the heat problem for domains with non-standard Koch boundaries. Our work differs from Wasyk's in that we do not rely on an automatic mesh generator and we will use a different refinement methodology to account for the singularities. In our dissertation, we will address the error estimates inherent in numerical approximation in the context of the fractal. We will show how the approximation error depends on the value of the contraction factor α and on the iteration n.

7.1 The Presence of Singular Corners

An additional important consideration when working with domains with either an internal prefractal curve or an external prefractal boundary, is the presence of singular corners. We will address the presence of these corners in this chapter of this dissertation. In this section we will consider three types of domains with prefractal boundaries. For each domain type we investigate the singular points of the domain and introduce a weight dependent on the measure of the angle of the singular corners. Then we introduce a refinement process, dependent on the weight calculated, to create a refined adaptive mesh $\mathcal{M}_R(\alpha, n, j)$ (here j refers to the number of times the mesh must be refined).

We begin by recalling the definition of a singular point and a reentrant angle found in Chapter 5. An angle is reentrant if it measures more the π, and singular points are those located at the vertex of a reentrant angle. The presence of singular corners (i.e. corners that have a reentrant angle) will necessitate a further refinement of our adaptive mesh, so that the error in any finite element estimates will remain bounded. With a plan of modifying our adaptive mesh to allow for singular points we now consider three domains with such points.

The first domain we consider is the Koch island domain (Ω_{KI}.) This domain is created by placing a Koch curve along each side of a square, and allowing the curve to "invade" into the square. When α is close to 4, the Koch island closely resembles the original square domain. As α approaches 2, the domain has many sharp inlets. We illustrate three examples of Koch islands in Figure 7.1. The boundaries of this domain correspond to the boundaries of elements in the adaptive mesh, making $\mathcal{M}(\alpha, n)$ a suitable starting mesh for the domain. We notice that although this domain has many singular corners (dependent on the iteration number n), each singular corner has the same reentrant angle measure. For the domain Ω_{KI} the reentrant angle has measure $\tau = \pi + 2\theta$ where $\theta = \cos^{-1}\left(\frac{\alpha}{2} - 1\right)$, which we use to define a weight (λ), that will be used when refining the domain. This weight is related to the solution space $H^{2,\lambda}$ that was introduced in Section 5.6, and will be used as an input variable when further refining the mesh. For the Koch island domain this weight is bounded from below by:

$$\lambda_{KI} > 1 - \frac{\pi}{\tau} = 1 - \frac{\pi}{\pi + 2\theta}. \tag{7.1}$$

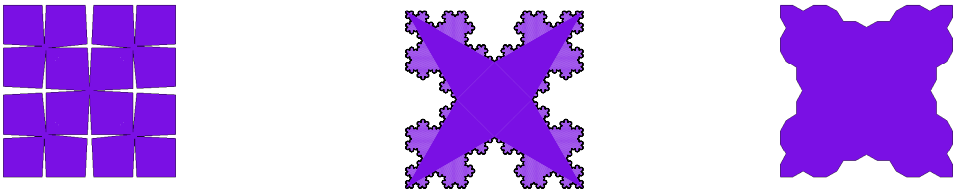

Figure 7.1: Three sample Koch island domains with $\alpha = 2.1, n = 2$, $\alpha = 3, n = 3$, and $\alpha = 3.75, n = 2$ respectively.

The second domain we consider is the external Koch island domain (Ω_{KE}.) This domain is created by placing a Koch curve along each side of a square, but allowing the curve to expand the domain. When α is close to 4, both the Koch island and the external Koch island closely resembles the original square domain. As α approaches 2, Ω_{KE} has very many sharp points, and as the iteration number n approaches infinity this domain becomes filling. We illustrate three examples of external Koch islands in Figure 7.2. Again, the boundaries of the external Koch island domain correspond to boundaries of $\mathcal{M}(\alpha, n)$. We notice that this domain, like the Koch island domain, has many singular corners (dependent on the iteration number n), and that each singular corner shares the same reentrant angle measure (different from that of the Koch island). For the domain Ω_{KE} the reentrant angle has measure $\gamma = \pi + \theta$, where $\theta = \cos^{-1}\left(\frac{\alpha}{2} - 1\right)$.

For this domain the weight λ is bounded by

$$\lambda_{KE} > 1 - \frac{\pi}{\gamma} = 1 - \frac{\pi}{\pi + \theta} \tag{7.2}$$

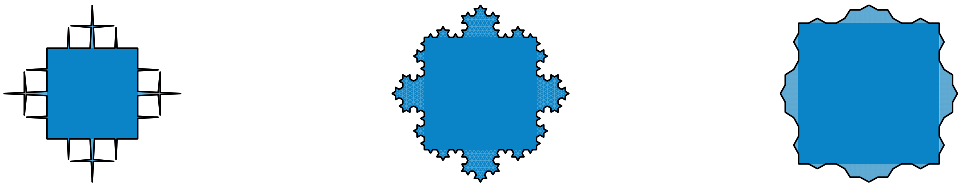

Figure 7.2: Three sample external Koch island domains with $\alpha = 2.1, n = 2$, $\alpha = 3, n = 3$, and $\alpha = 3.75, n = 2$ respectively.

The third and final domain considered is a domain with an internal Koch boundary (Ω_{TR}). One application of such a domain is the study of transmission problems of the first and second order. (See Figure 7.3.) Again our mesh is especially suited for studying this kind of problem. One distinguishing feature of this domain from the preceding two domains is that this domain has two different measures for the reentrant angles. In this case we must consider the values of both of the angles and bound λ by the larger of the two.

$$\lambda_{TR} > max(1 - \frac{\pi}{\pi + 2\theta}, 1 - \frac{\pi}{\pi + \theta}.) \tag{7.3}$$

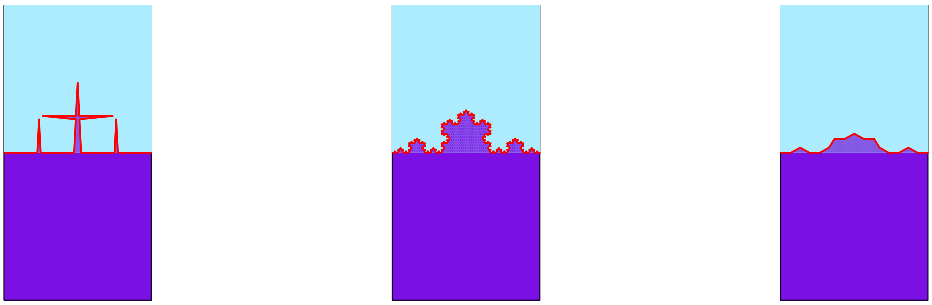

Figure 7.3: Three sample domains with an internal prefractal transmission boundary with values $\alpha = 2.1, n = 2$, $\alpha = 3, n = 3$, and $\alpha = 3.75, n = 2$ respectively.

Remark 27. We note that regardless of the domain the weight λ is always dependent on the parameter α of the Koch curve.

7.1.1 Refining the Domain

Our goal is to modify our mesh such that the conditions of Theorem 5.6.3 can be met. These conditions are:

(G1) $h_{\mathcal{T}} \leq \sigma h^{1/(1-\lambda)}$ for every $\mathcal{T} \in T_h$ if $\mathcal{T}$ has vertex at a reentrant corner of Ω;

(G2) $h_{\mathcal{T}} \leq C\sigma h \inf_{x \in \mathcal{T}} r_n(x)^{\lambda}$ otherwise

Here Ω is one of the three domains defined above, λ is the weight associated with the domain, σ is the regularity constant of the mesh, h is the global mesh size, and $h_{\mathcal{T}}$ is

the diameter of the triangle $\mathcal{T}$. Moreover we define

$$\eta_n = \frac{1}{4}\alpha^{-n}\min\{\alpha - 2, 1\},$$

and R the set of reentrant vertices in Ω. Then for $x \in \Omega$, define

$$r_n(x) = \begin{cases} |x - p| & \text{if } x \in B(P, \eta_n) \text{ for some } P \in R \\ 1 & \text{if } x \notin \bigcup_{P \in R} B(P, 2\eta_n) \\ \frac{1-\eta_n}{\eta_n}(|x - P| - \eta_n) + \eta_n & \text{otherwise} \end{cases}.$$

Th process presented is a modification of the one presented in [14], [30] and [31], adapted to $\mathcal{M}(\alpha, n)$.

We begin by defining a region of our domain which will contain those triangles which will need to be refined such that the two Grisvard conditions can be met. We define F as

$$F = \{\mathcal{T} \in \mathcal{M}(\alpha, n) | \inf_{\substack{x \in \mathcal{T} \\ P \in R}} |x - P| < 2\eta_n\}. \tag{7.4}$$

Refinement of the mesh is a four-step process

1. *Subdivide the quadrilaterals*
   The given results will only be true for finite element meshes that contain only triangular shaped elements. To account for this, we convert any quadrilaterals into two triangles. Special care must be made if the quadrilateral has a singular point as a vertex. In this case we connect the two vertices adjacent to the singular vertex.

2. *Identify the singular points and the associated set F*
   Before any refinement can be done we must first identify the singular points in our domain. After identifying the singular points we also identify every element that has one of these points as a vertex. We also identify all the triangles in F that do not have a singular vertex.

3. *Subdividing the triangles with singular points*
   In order to describe this subdivision in the simplest manner we will temporarily switch to using barycentric coordinates. Let T be any triangle in our mesh with

vertices V_1, V_2, and V_3 having barycentric coordinates $(1,0,0)$, $(0,1,0)$ and $(0,0,1)$ respectively. We can then describe a point with barycentric coordinates (c_1, c_2, c_3) as $c_1V_1 + c_2V_2 + c_3V_3$. Moreover, we will number the vertex with the singularity as V_1. We set $\varphi = \left(\frac{1}{3}\right)^{1/(1-\lambda)}$. We refine the triangle by introducing the following new nodes with the specified barycentric coordinates. (See also Figure 7.4)

$$N_1 = (1-\varphi, 0, \varphi) \qquad N_4 = \left(\frac{1}{2}, \frac{1}{4}, \frac{1}{4}\right)$$

$$N_2 = (1-\varphi, \varphi, 0) \qquad N_5 = \left(\frac{1}{2}, \frac{1}{2}, 0\right)$$

$$N_3 = \left(\frac{1}{2}, 0, \frac{1}{2}\right) \qquad N_6 = \left(0, \frac{1}{2}, \frac{1}{2}\right)$$

4. *Subdivide the remaining triangles in F*
   For those triangles in $\mathcal{T} \in F$ that do not have a vertex which is a singular point, we subdivide $\mathcal{T}$ into four congruent subtriangles.

5. *Removing the hanging nodes*
   Subdividing the triangles with singular points results in the creation of a hanging node on the side of the triangle opposite the singular point. Because of the specific manner in which these nodes are created we are guaranteed that the hanging nodes are located at the midpoint of the side of the triangle. We remove these hanging nodes in a three-step process.

   - First - We remove the hanging nodes for any triangle that has three hanging nodes by creating four equally sized similar triangles.
   - Second - We remove the hanging nodes for any triangle with two hanging nodes, by introducing a third hanging node, and proceeding in the manner for three hangings nodes.
   - Last - We handle all the triangles with a single hanging node by bisecting the angle opposite the hanging node, creating two new triangles. We color these new edges green as they may be removed in subsequent refinements.

Subsequent Refinements

Dependent on the value of α it may be necessary to refine the mesh $\mathcal{M}(\alpha, n)$ more than once so that the Grisvard conditions can be met. To avoid repeatedly bisecting the

same angle of a triangle, (which would increase the shape regularity constant), before performing steps 1-5 we remove all of those edges which are green. We refer to the refined mesh after j refinements as $\mathcal{M}_R(\alpha, n, j)$.

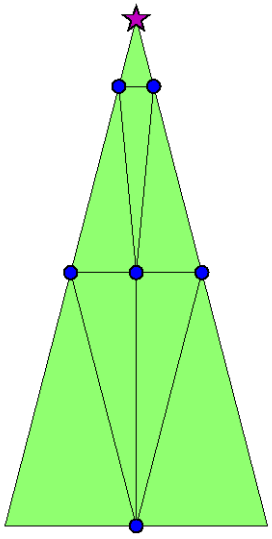

Figure 7.4: Subdivision of a triangle with a singular point. The singular point is marked by a star, and the newly introduced nodes are marked by circles.

Remark 28. The aspect ratio of the newly created triangles can easily be computed. What is important to note is that a *finite* number of new triangle types are created, and the total number of triangle types is still independent of the choice of n. Moreover, the additional refinement, does not change the adaptability of our mesh to previous iterations of the prefractal.

7.2 Proof of Grisvard Condition

Proposition 7.2.1. *The refined adaptive mesh $\mathcal{M}_R(\alpha, n, j)$, with the refinement given above satisfies the following two conditions:*

- $h_{\mathcal{T}} \leq \sigma h^{1/(1-\lambda)}$ *for every* $\mathcal{T} \in T_h$ *such that at least one vertex coincides with the vertex of a reentrant corner of* Ω;
- $h_{\mathcal{T}} \leq h \inf_{\mathcal{T}} r^{\lambda}$ *for every* $\mathcal{T} \in T_h$ *with no vertex of any reentrant corner of* Ω, *but in a small neighborhood of at least one of them*

Here h is the global mesh size, $h_{\mathcal{T}}$ is the local mesh size, σ is the shape regularity constant of the mesh and λ defined above.

Before showing this proposition it will be necessary to show a few preliminary Lemmas and introduce some new notation. We begin by defining $d(A, B)$ to be

$$d(A, B) := \inf_{\substack{x \in A \\ y \in B}} |x - y|.$$

Lemma 7.2.2. *Let $\mathcal{T}$ be a triangle in $\mathcal{M}(\alpha, n)$ with vertices V_1, V_2, and V_3 and shape regularity constant σ. Moreover use s_i to denote the side of $\mathcal{T}$ opposite V_i for each $i \in \{1, 2, 3\}$ and let $|\mathcal{T}|$ denote the area of $\mathcal{T}$. Then*

$$d(\{V_i\}, s_i) \geq \rho_{\mathcal{T}} \tag{7.5}$$

and

$$|\mathcal{T}| > \frac{h_{\mathcal{T}}^2}{2\rho_{\mathcal{T}}}. \tag{7.6}$$

Proof. Since $\rho_{\mathcal{T}}$ is defined as the diameter of the largest circle that can be inscribed in a triangle it is clear that 7.5 holds. Recall from Chapter 6 that $\rho_{\mathcal{T}}$ can be calculated as $\frac{2|\mathcal{T}|}{S_P}$, where S_P is the semi-perimeter of $\mathcal{T}$. Since $\frac{h_{\mathcal{T}}}{\rho_{\mathcal{T}}} \leq \sigma$ by assumption (and the definition of the shape regularity constant) we have

$$|\mathcal{T}| \geq \frac{S_P h_{\mathcal{T}}}{2\sigma}. \tag{7.7}$$

Since $h_{\mathcal{T}}$ is the length of the longest side of $\mathcal{T}$, and by the triangle inequality $S_P > h_{\mathcal{T}}$. Therefore 7.6 follows from 7.7. □

The next lemma will be critical to showing that the refinement satisfies the Grisvard conditions. The lemma puts into mathematical notation that the creation of $\mathcal{M}_R(\alpha, n, j)$ should result in smaller triangles near the reentrant corners and larger triangles farther away.

Lemma 7.2.3. *Let $\alpha \in (2, 4)$ and n be given. Let $\mathcal{M}(\alpha, n)$ be the adaptive mesh determined by α and n, and let the domain Ω be defined as either $\Omega := \Omega_{KE}$ or $\Omega := \Omega_{TR}$. Moreover, let*

$$h_0 := \max_{\mathcal{T} \in \mathcal{M}(\alpha, n)} h_{\mathcal{T}} \leq \frac{1}{\alpha(p + 2q)^n}$$

, $\mathcal{M}_R(\alpha, n, j)$ denote the mesh produced by j refinements using the methodology of Section 7.1.1 and let $\mathcal{A}$ be the set

$$\{\mathcal{T} \in \mathcal{M}(\alpha, n) | \textit{if } \mathcal{T}' \in \mathcal{M}(\alpha, n) \textit{ and } \mathcal{T}' \cap \mathcal{T} \neq \emptyset \textit{ then } \mathcal{T}' \cap \overline{F} = \emptyset\}. \tag{7.8}$$

Then $\mathcal{A}$, is non-empty, and for each $j \in \mathbb{N}$:

$$\max_{\substack{\mathcal{T} \in \mathcal{M}_R(\alpha,n,j) \\ \mathcal{T} \cap \overline{F} \neq \emptyset}} h_{\mathcal{T}} \leq 2^{-j} h_0 \tag{7.9}$$

and

$$h_j := \max_{\mathcal{T} \in \mathcal{M}_R(\alpha,n,j)} h_{\mathcal{T}} \geq 2^{-\lfloor j/2 \rfloor} \max_{\mathcal{T} \in \mathcal{A}} h_{\mathcal{T}} \tag{7.10}$$

where F is the fractal region defined in Section 7.1.1.

Proof. We begin by showing $\mathcal{A}$ is nonempty. Assume that $\Omega_{TR} = (0,1) \times (-1,1)$ and that Ω_{KE} has corners at $(0,0)$, $(0,1)$, $(1,1)$ and $(1,0)$ (if not simply scale and rotate the domains such that this is true). Choose $\mathcal{T} \in \mathcal{M}(\alpha, n)$ such that $d_M = \sup_{\substack{A \in \mathcal{T} \\ B \in R}} |A - B|$ is maximal. Moreover for the domains in question $d_M > 1/2$. Since h_0 represents the length of the longest edge of any triangle in $\mathcal{M}(\alpha, n)$, $d(\mathcal{T}, R) > 1/2 - h_0$. So if $\mathcal{T}'$ is a triangle in $\mathcal{M}(\alpha, n)$ sharing a vertex with $\mathcal{T}$, then $d(\mathcal{T}', R) > 1/2 - 2h_0$. Since $h_0 < \frac{1}{\alpha(p+2q)^n}$, we therefore have $d(\mathcal{T}', R) > 2\eta_n$ and by definition $x \in \overline{F}$ if and only if $d(R, x) \leq 2\eta_n$ for all R.

Now to show 7.9, suppose $\mathcal{T} \in \mathcal{M}(\alpha, n)$ such that $\mathcal{T} \cap \overline{F} \neq \emptyset$. Then $\mathcal{T}$ has at least one vertex in the fractal region and $\mathcal{T}$ is refined into either four or eight triangles according to the refinement in Section 7.1.1. We notice that regardless of the refinement chosen after refinement there exists a triangle $\mathcal{T}'$ such that $\mathcal{T}' \subset \mathcal{T}$, $h_{\mathcal{T}'} \leq \frac{1}{2} h_{\mathcal{T}}$ and $\mathcal{T}'$ has a vertex in F. Applying the same argument to $\mathcal{T}'$ any subtriangle of $\mathcal{T}'$ created by refining $\mathcal{T}'$ has no edge longer than $2^{-2} h_{\mathcal{T}}$. Continuing this argument for an arbitrary number of refinements and making use of the definition of h_0, 7.9 holds.

The proof of 7.10 is more difficult. We choose $\mathcal{T}_1 \in \mathcal{A}$ and will consider how this triangle is refined. Let $\mathcal{K}^1$ be the set $\{\mathcal{T} \in \mathcal{M}(\alpha, n) | \mathcal{T} \cap \mathcal{T}_1 \neq \emptyset\}$. Thus $\mathcal{K}$ is a polygon in Ω with boundary Γ. Suppose now that we refine $\mathcal{M}(\alpha, n)$ according to the procedure in Section 7.1.1. In the scenario that will create the most refinement of $\mathcal{K}^1$, every triangle

that has an edge on Γ will be have a hanging node. Thus, by the refinement methodology, each of these triangles will be refined by adding an edge. In particular, $\mathcal{T}_1$ is not refined.

Suppose that another refinement is needed, and again we have the scenario with maximal refinement of the triangles bordering $\mathcal{K}^1$. After the previous refinement each triangle in $\mathcal{K}^1$ with an edge in Γ had a hanging node and was refined by bisection. According to the procedure of our mesh refinement, the first step of any subsequent refinement is removal of these bisection edges. Then each triangle with these four hanging nodes will be divided into four congruent subtriangles (and then two of these triangles bisected). Unlike the previous iteration, new hanging nodes are created, and other triangles (including $\mathcal{T}_1$) must be refined. This refinement subdivides $\mathcal{T}_1$ into 4 congruent of triangles, hence $h_2 \geq \frac{1}{2} h_{\mathcal{T}_1}$.

We continue this argument by setting $\mathcal{T}_2$ to be the triangle in the center of the refined $\mathcal{T}_1$ and create the set $\mathcal{K}^2$ in a similar manner. Repeating the previous chain of reasoning, we see $h_3 \geq \frac{1}{2} h_{\mathcal{T}_1}$ and $h_4 \geq \frac{1}{4} h_{\mathcal{T}_1}$. Since $\mathcal{T}_1 \in \mathcal{A}$ was arbitrary, 7.10 follows. □

The following Theorem contains much of the work required to show that (G1)-(G2) hold for the mesh $\mathcal{M}_R(\alpha, n, j)$.

Theorem 7.2.4. *Let $\alpha \in (2,4)$, n and λ be given. Let $\mathcal{M}(\alpha, n)$ be the adaptive mesh determined by α and n, and let h_0 be defined as before. Let $\mathcal{M}_R(\alpha, n, j)$ denote the mesh produced by j refinements using the methodology of Section 7.1.1. Then there exists a $j^* \in \mathbb{N}$ such that each $\mathcal{T} \in \mathcal{M}_R(\alpha, n, j^*)$ satisfies :*

(G1)* $h_{\mathcal{T}} \leq \sigma h_*^{1/(1-\lambda)}$ *if* $\mathcal{T} \cap R \neq \emptyset$

(G2)* $h_{\mathcal{T}} \leq \sigma h_* d(\mathcal{T}, R)^{\lambda}$ *if* $\mathcal{T} \cap R = \emptyset$.

where $h_* = \max_{\mathcal{T} \in \mathcal{M}(\alpha,n,j)} h_{\mathcal{T}}$.

Proof. We begin by defining

$$\rho_0 := \min_{\substack{\mathcal{T} \in \mathcal{M}(\alpha,n) \\ \mathcal{T} \cap R \neq \emptyset}} \rho_{\mathcal{T}}, \tag{7.11}$$

$$h_{\mathcal{A}} = \max_{\mathcal{T} \in \mathcal{A}} h_{\mathcal{T}}, \tag{7.12}$$

and let $C_0 = h_{\mathcal{A}}/h_0$. We then choose $j^* \in \mathbb{N}$ such that

$$2^{\lfloor j^*/2 \rfloor} 3^{-j^*} \leq \sigma^{1-\lambda} C_0 h_{\mathcal{A}}^{\lambda} \tag{7.13}$$

and

$$2^{\lfloor j^*/2 \rfloor} 2^{-j^*} \leq \sigma C_0 \rho_0^{\lambda}. \tag{7.14}$$

We split the proof into two parts according to conditions (G1*)-(G2*).

Case 1: $\mathcal{T} \in \mathcal{M}(\alpha, n, j^*)$ with $\mathcal{T} \cap R \neq \emptyset$
Since $\mathcal{M}_R(\alpha, n, j^*)$ is a refinement of $\mathcal{M}(\alpha, n)$ there exists a $\mathcal{T}_0 \in \mathcal{M}(\alpha, n)$ such that $\mathcal{T}$ is created by refining $\mathcal{T}_0$ and $\mathcal{T}_0 \cap R \neq \emptyset$. We use P to denote this vertex and recall $P \in V^n$.

When $\mathcal{T}_0$ is refined as specified in 7.1.1 one subtriangle will be created with vertex P, we label this triangle $\mathcal{T}_1$ and observe $\mathcal{T}_0$ and $\mathcal{T}_1$ are similar. Moreover $h_{\mathcal{T}_1} = \varphi h_{\mathcal{T}_0}$. If $j^* = 1$ we are done refining but otherwise we refine triangle $\mathcal{T}_1$ creating triangle $\mathcal{T}_2$ and so forth. Thus $h_{\mathcal{T}} = \varphi^{j^*} h_{\mathcal{T}_0}$. By Lemma 7.2.3 we know that $h_* \geq 2^{-\lfloor j^*/2 \rfloor} h_0$. Thus using inequality 7.13 and recalling $\varphi = \left(\frac{1}{3}\right)^{1/(1-\lambda)}$, we have

$$\begin{aligned}
\sigma h_*^{1/(1-\lambda)} &\geq \sigma (2^{-\lfloor j^*/2 \rfloor} h_{\mathcal{A}}^{1/(1-\lambda)} \\
&\geq \sigma [(\sigma^{1-\lambda} C_0 h_0^{\lambda} 3^{j^*})^{-1} h_{\mathcal{A}}]^{1/(1-\lambda)} \\
&= \left[\left(\frac{1}{3} \right)^{1/(1-\lambda)} \right]^{j^*} h_0 \\
&= \varphi^{j^*} h_0 \geq h_{\mathcal{T}}.
\end{aligned}$$

So (G1*) is satisfied.

Case 2: $\mathcal{T} \in \mathcal{M}_R(\alpha, n, j^*)$ with $\mathcal{T} \cap R = \emptyset$ and $\mathcal{T} \in \overline{F}$
Here we consider two separate cases dependent on the characteristics of the triangle $\mathcal{T}_0 \in \mathcal{M}(\alpha, n)$ such that $\mathcal{T} \subset \mathcal{T}_0$.

Case 2a: $\mathcal{T} \subset \mathcal{T}_0 \in \mathcal{M}(\alpha, n)$ with $\mathcal{T}_0 \cap R = \emptyset$
At the first stage of refinement, $\mathcal{T}_0$ is refined into four congruent subtriangles, label the triangle that contains $\mathcal{T}$ as $\mathcal{T}_1$ and $h_{\mathcal{T}_1} = \frac{1}{2} h_{\mathcal{T}_0}$. If $j^* = 1$ we are done, otherwise, proceed in a similar manner until subdivision j^* is reached, creating a sequence of triangles

$\mathcal{T}_0 \subset \mathcal{T}_1 \subset \mathcal{T}_2 \subset \cdots \subset \mathcal{T}_{j^*-1} \subset \mathcal{T}$. Therefore $h_{\mathcal{T}} = 2^{-j*} h_{\mathcal{T}_0}$.

To test (G2*), we need to estimate $\sigma h_* d(\mathcal{T}, R)^\lambda$. From Lemma 7.2.2 and the definition of ρ_0, the distance from any vertex in R to an edge opposite it is greater than ρ_0. Since $\mathcal{T}_0 \cap R = \emptyset$, the $d(\mathcal{T}, R) > \rho$. Thus, using 7.14 and Lemma 7.2.3 we have

$$\begin{aligned}\sigma h_* d(\mathcal{T}, R)^\lambda &> (2^{-\lfloor j^*/2 \rfloor} h_{\mathcal{A}}) \rho_0^\lambda \\ &\sigma (\sigma C_0 \rho_0^\lambda 2^{j^*})^{-1} h_{\mathcal{A}} \rho_0^\lambda \\ &= 2^{-j^*} h_0.\end{aligned}$$

Combining this result with the earlier observation that $h_{\mathcal{T}} = 2^{-j^*} h_{\mathcal{T}_0}$, and the fact that $h_0 \geq h_{\mathcal{T}_0}$, (G2*) is satisfied.

Case 2b: $\mathcal{T} \subset \mathcal{T}_0 \in \mathcal{M}(\alpha, n)$ with $\mathcal{T}_0 \cap R \neq \emptyset$
As in the previous case, there exists a sequence of triangles (created by refinements of $\mathcal{T}_0$ such that for every $j < j^*$, $\mathcal{T}_j \cap \overline{F} \neq \emptyset$ and $\mathcal{T}_0 \subset \mathcal{T}_1 \subset \cdots \subset \mathcal{T}_{j^*-j} \subset \mathcal{T}$. By assumption the original triangle, $\mathcal{T}_0$ had a vertex which was a reentrant point, but $\mathcal{T}$ does not, therefore there exists an integer $\hat{j} \in [0, j^*)$ such that $\mathcal{T}_j \cap R \neq \emptyset$ for all $j \leq \hat{j}$, but $\mathcal{T}_j \cap R = \emptyset$ if $j > \hat{j}$. From the argument for case 1, we have

$$h_{\mathcal{T}_{\hat{j}}} = \varphi^{\hat{j}} h_{\mathcal{T}_0} \tag{7.15}$$

Now when $\mathcal{T}_{\hat{j}}$ is refined according to the methodology in Section 7.1.1 any subtriangle of $\mathcal{T}_{\hat{j}}$ has length less then or equal to $\frac{1}{2} h_{\mathcal{T}_{\hat{j}}}$. Combining with 7.15 we thus have

$$h_{\mathcal{T}_{\hat{j}+1}} \leq \frac{1}{2} \varphi^{\hat{j}} h_{\mathcal{T}_0} \tag{7.16}$$

For $j \geq \hat{j} + 1$, $\mathcal{T}_j$ has no vertices in R, but $\mathcal{T}_j \cap \overline{F} \neq 0$. Therefore further refinement of $\mathcal{T}_j$ will result in four congruent triangles being created. Combining this with 7.16 we thus have

$$h_{\mathcal{T}} \leq 2^{-(j^* - \hat{j})} \varphi^{\hat{j}} h_{\mathcal{T}_0} \tag{7.17}$$

Again, in order to verify (G2*), we must approximate $d(\mathcal{T}, R)$. Since the sequence of triangles $\mathcal{T}_j$ is a nested sequence, for any $j \in [1, j^*)$ we have $d(\mathcal{T}_j, R) \geq d(\mathcal{T}_{j-1}, R)$. By the definition of $\hat{j}$, if $j \leq \hat{j}$, $\mathcal{T}_j$ has a vertex in R and $d(\mathcal{T}_j, R) = 0$. Since the

given methodology guarantees that $\mathcal{T}_j$ is similar to $\mathcal{T}_0$ with proportionality constant φ^j if $j \leq \hat{j}$, for $j > \hat{j}$, $d(\mathcal{T}_j, R \cap \mathcal{T}_0) > \varphi^{\hat{j}} \rho_{\mathcal{T}_0} \geq \varphi^{\hat{j}} \rho_0$. By Lemma 7.2.2 we verify that $d(\mathcal{T}_j, R) > \rho_0$. Thus we can say $d(\mathcal{T}_j, R) \varphi^{\hat{j}} \rho_0$. Using this along with 7.17, Lemma 7.2.3, and the definition of φ, we have:

$$\begin{aligned}
\sigma h_* d(\mathcal{T}, R)^\lambda &> (2^{-\lfloor j^*/2 \rfloor} h_{\mathcal{A}})(\varphi^{\hat{j}} \rho_0)^\lambda \\
&\geq \sigma(\sigma C_0 \rho_0^\lambda 2^{j^*})^{-1} h_{\mathcal{A}} (\varphi^{\hat{j}} \rho_0)^\lambda \\
&= 2^{-j^*} h_0 (\varphi^\lambda)^{\hat{j}} \\
&= 2^{-(j^* - \hat{j})} 2^{-\hat{j}} \varphi^{\hat{j}} (\varphi^{\lambda - 1})^{\hat{j}} h_0 \\
&= \left(\frac{3}{2}\right)^{\hat{j}} 2^{-(j^* - \hat{j})} \varphi^{\hat{j}} h_0 \geq h_{\mathcal{T}}.
\end{aligned}$$

Thus (G2*) holds in this subcase as well. □

Theorem 7.2.5. *Let $\alpha \in (2, 4)$ and $n \in \mathbb{N}$ be given. Let $\Omega = \Omega_{TR}$, $\lambda > \lambda_{TR}$ and $\mathcal{M}(\alpha, n)$ be the triangulation of Ω. Then there exists a $j \in \mathbb{N}$ such that $\mathcal{M}(\alpha, n, j)$ can be created according to the methodology of Section 7.1.1 such that $\mathcal{M}(\alpha, n, j)$ has the following characteristics:*

1. *$\mathcal{M}(\alpha, n, j)$ is shape-regular with aspect ratio σ*
2. *$h_n := \max_{\mathcal{T} \in \mathcal{M}(\alpha, n, j)} h_{\mathcal{T}}$*
3. *$\mathcal{M}(\alpha, n, j)$ is a triangulation of Ω satisfying:*

$$h_{\mathcal{T}} \leq \sigma h_n^{1/(1-\lambda)} \qquad \text{if } \mathcal{T} \text{ has a vertex at a reentrant corner} \tag{7.18}$$

$$h_{\mathcal{T}} \leq 3^{\lambda/(1-\lambda)} \sigma h_n \left[\inf_{x \in \mathcal{T}} r_n(x)\right]^\lambda \qquad \text{otherwise} \tag{7.19}$$

for every $\mathcal{T} \in \mathcal{M}(\alpha, n, j)$.

Proof. By Theorem 7.2.4, there exists a $j \in \mathbb{N}$ such that $\mathcal{M}(\alpha, n, j)$ satisfies (G1*) and (G2*). Since $\mathcal{M}(\alpha, n)$ is a shape regular mesh by Theorem 6.0.2, so we need only show that $\mathcal{M}(\alpha, n, j)$ is shape-regular. In order to do this we must consider the refinement procedures used. According to the methodology in Section 7.1.1 triangles are only refined in three ways (or they are not refined at all). It is clear that if the triangle is not

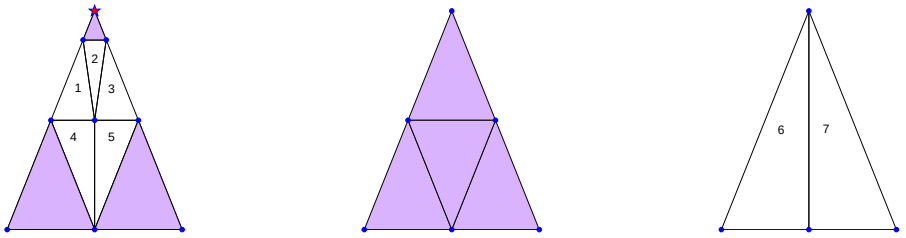

(a) Vertex in R (b) Equal Subdivision (c) Subdivision by bisection

Figure 7.5: Refinements with similarity classes labeled.

refined the shape regularity does not change. Moreover, since the shape regularity is unaffected by size, similar triangles have the same aspect ratio. We now show that there is a limited number of similarity classes created by our refinement.

Let $\mathcal{T}$ be a triangle with vertices V_1, V_2 and V_3 and suppose $\mathcal{T}$ is refined according to the methodology of Section 7.1.1. In Figure 7.5 the refinements of Section 7.1.1 are shown with the similarity classes of each triangle labeled. (Shaded triangles with no labels are similar to $\mathcal{T}$) The similarity classes of the triangle are easily identified by the description of the refinement and the barycentric coordinates found in Section 7.1.1. From Figure 7.5, we see that only 7 similarity classes are created. If only one refinement of $\mathcal{M}(\alpha, n)$ was needed (i.e. $j = 1$) this would be sufficient to show shape regularity.

Let us now consider the case where $j \geq 2$. From Figure 7.5 it is clear that if $\mathcal{T}'$ is a triangle in $\mathcal{M}(\alpha, n, 1)$ created by refining $\mathcal{T}$ and $\mathcal{T}' \cap R \neq \emptyset$ then $\mathcal{T}'$ is similar to triangle $\mathcal{T}$, and the subsequent refinement will create no new similarity classes. Now suppose $\mathcal{T}' \cap R = \emptyset$ and $\mathcal{T}' \in \overline{F}$. Then $\mathcal{T}'$ will be subdivided into four congruent triangles. If $\mathcal{T}'$ is not part of the fractal region, then $\mathcal{T}'$ will be refined according to the methodology in Section 7.1.1 which guarantees that no angle will be bisected more than once, thus limiting the aspect ratio.

It now remains to show 7.18 and 7.19. Recall that R is the set of all singular points in the domain and for Ω_{TR}, $R = V^n \setminus \{(0,0),(1,0)\}$. We also recall that Ω is divided into two subdomains Ω^1 and Ω^2 by the prefractal Koch curve. We denote by R^i the reentrant vertices of Ω^i and by $(\mathcal{M}(\alpha, n, j))^i$ the triangulation of Ω^i. Equation 7.18 holds by (G1*)

in Theorem 7.2.4.

We now show 7.19. Suppose $\mathcal{T} \in (\mathcal{M}(\alpha, n, j))^i$ and does not have a vertex in R^i. Then, since $R^i \subset R$, $\mathcal{T}$ may or may not have a vertex in R. If $\mathcal{T}$ does have a vertex in $R \setminus R^i$ we show $h_{\mathcal{T}} \leq 3^{\lambda/(1-\lambda)} \sigma h_n d(\mathcal{T}, R^i)^\lambda$. From Case 1 of Theorem 7.2.4, there exists a $\mathcal{T}_0$ such that $\mathcal{T}$ is refinement of $\mathcal{T}_0$. Moreover $h_{\mathcal{T}} = \varphi^j h_{\mathcal{T}_0} \leq 2^{-j} h_{\mathcal{T}_0}$. Therefore (G2*) holds and we use the fact that $r_n(x) \geq d(\{x\}, R)$ for any $x \in \Omega$ so 7.19 holds. If $\mathcal{T}$ does not have a vertex in R, then $\mathcal{T}$ may or may not have a vertex in F. If $\mathcal{T}$ has a vertex in F the (G2*) holds and we again use the fact that $r_n(x) \geq d(\{x\}, R)$ and 7.19 holds. The final case is when $\mathcal{T} \cap \overline{F} = \emptyset$. This implies $r_n(x) = 1$, so in this case equation 7.19 reduces to $h_{\mathcal{T}} \leq 3^{\lambda/(1-\lambda)} \sigma h_n$. This is true since $h_n \geq h_{\mathcal{T}}$ by definition, $\sigma > 1$ and $3^{\lambda/(1-\lambda)}$ when $\lambda \in (0, 1)$. □

Theorem 7.2.6. *Let $\alpha \in (2, 4)$ and $n \in \mathbb{N}$ be given. Let $\Omega = \Omega_{KE}$, $\lambda > \lambda_{KE}$ and $\mathcal{M}(\alpha, n)$ be the triangulation of Ω. Then there exists a $j \in \mathbb{N}$ such that $\mathcal{M}(\alpha, n, j)$ can be created according to the methodology of Section 7.1.1 such that $\mathcal{M}(\alpha, n, j)$ has the following characteristics:*

1. *$\mathcal{M}(\alpha, n, j)$ is shape-regular with aspect ratio σ*
2. *$h_n := \max_{\mathcal{T} \in \mathcal{M}(\alpha, n, j)} h_{\mathcal{T}}$*
3. *$\mathcal{M}(\alpha, n, j)$ is a triangulation of Ω satisfying:*

$$h_{\mathcal{T}} \leq \sigma h_n^{1/(1-\lambda)} \qquad \text{if } \mathcal{T} \text{ has a vertex at a reentrant corner} \tag{7.20}$$

$$h_{\mathcal{T}} \leq 3^{\lambda/(1-\lambda)} \sigma h_n \left[\inf_{x \in \mathcal{T}} r_n(x) \right]^\lambda \qquad \text{otherwise} \tag{7.21}$$

for every $\mathcal{T} \in \mathcal{M}(\alpha, n, j)$.

Proof. The proof of this theorem proceeds with little modification in the same manner as the proof of Theorem 7.2.5. □

7.3 Implementation and Sample Problems

In this section we show sample Grisvard refinements on two of the domains (Ω_{KE}, and Ω_{TR} introduced at the beginning of the chapter. We also introduce the transmission

problem, previously numerically considered by Vacca and Wasyk, that the refined mesh will be used to solve.

7.3.1 Sample Mesh Refinements

The adaptive mesh generation was accomplished in the MATLAB environment. Future work includes porting the adaptive mesh generation code to C++ to make it more efficient and better suited for use in other environments. The original mesh generation code produced multiple files which described the nodes, the elements, and the singularities. In addition for the domain Ω_{TR} a file was generated that identified the transmission boundary. These files from the original mesh generator were then given as inputs into the refinement code. The splitting of the original mesh generation from the refinement was done intentionally to allow future work to be done to either improve the refinement algorithm, the mesh generation algorithm, or the mesh itself. The splitting of the two functions also allows an external mesh generator to be used (such as in the case of [31]) if desired. We now present Grisvard refinements of the domains Ω_{KE} and Ω_{TR}. For the external Koch island we present two different values of n (but the same value of α). For the transmission domain we modify α, but again consider $n = 2$. We have intentionally chosen small values of n so that the mesh (and the associated refinements) can be seen clearly.

7.3.2 Sample Transmission Problem Calculations

We now consider the following transmission problem studied by both Vacca [30] and Wasyk [31]:

$$\begin{cases} -\Delta u = f & \text{in } \Omega_i,\ i = 1, 2 \\ -c\Delta_t u = \left[\frac{\partial u}{\partial \nu}\right] & \text{on } S^n \\ [u] = 0 & \text{across } S^n \\ u = 0 & \text{on } \partial\Omega. \end{cases}$$

When solving the problem numerically we will make use of the following weak formulation

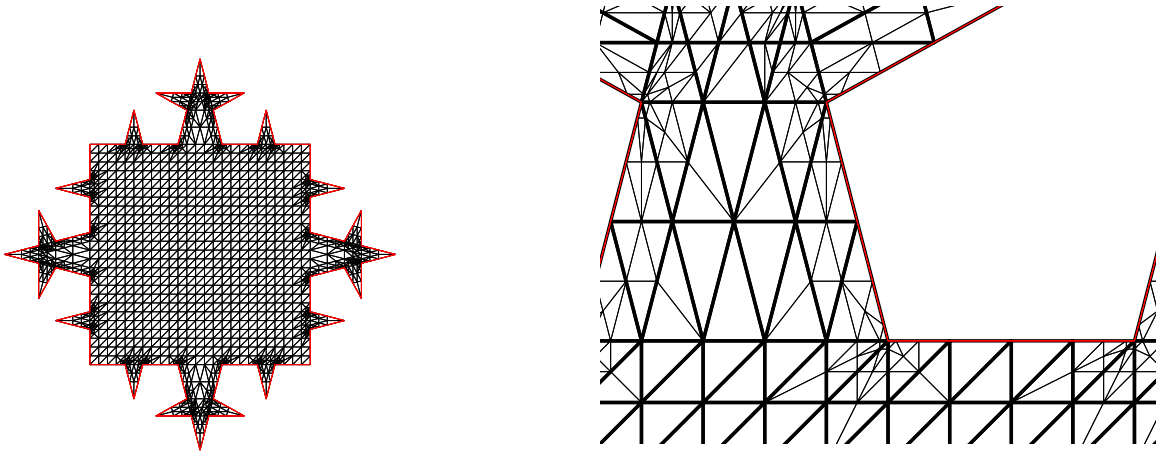

(a) Refined mesh

(b) Magnification of Mesh

Figure 7.6: A sample external Koch island domain with $\alpha = 2.5, n = 2$, with its associated Grisvard refinement.

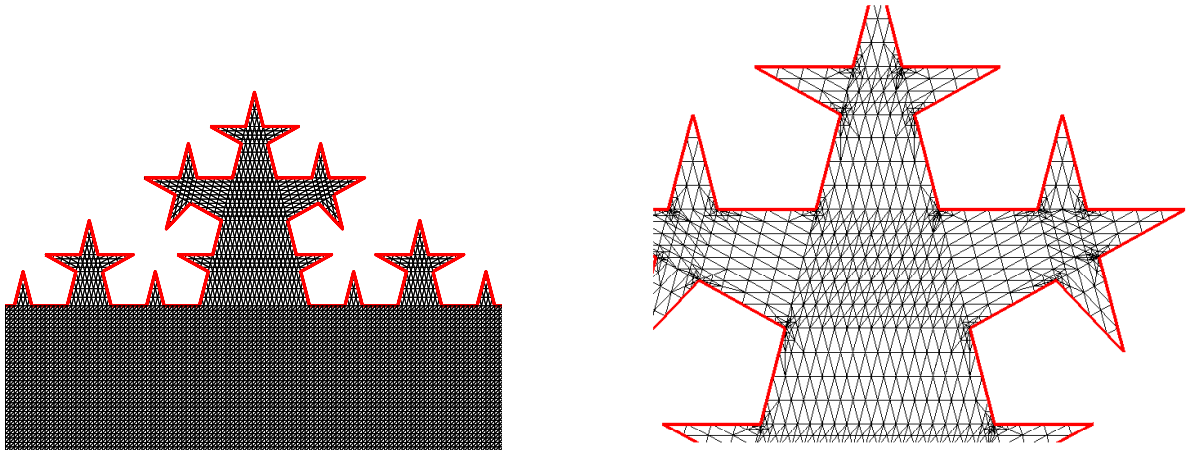

(a) Refined mesh

(b) Magnification of Mesh

Figure 7.7: A sample external Koch island domain with $\alpha = 2.5, n = 3$, with its associated Grisvard refinement.

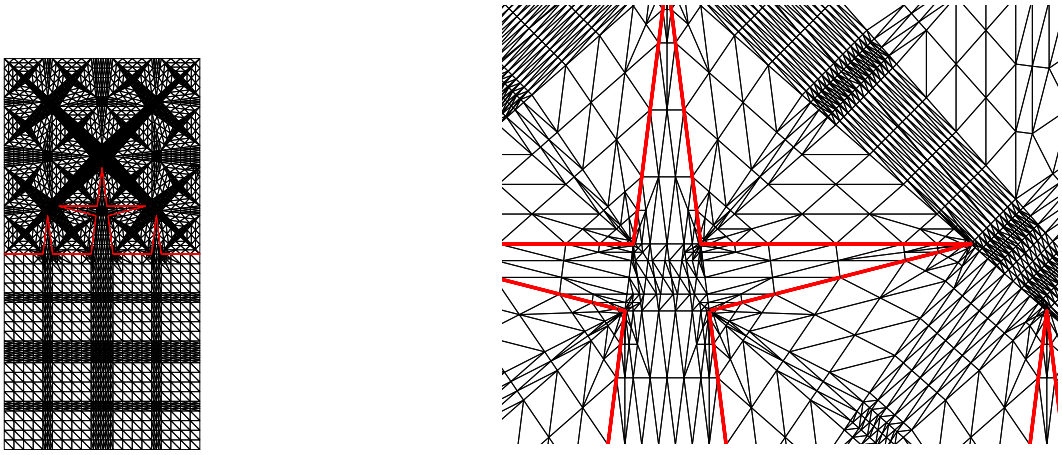

(a) Refined mesh

(b) Magnification of Mesh

Figure 7.8: A sample transmission domain with $\alpha = 2.25, n = 2$, with its associated Grisvard refinement.

$$\begin{cases} \text{Find } u \in V(\Omega, S^n) \text{ such that:} \\ \int\int_\Omega \nabla u \nabla v dx\, dy + c \int_{S^n} \nabla_l u \nabla_l v\, ds = \int\int_\Omega v f\, dx\, dy \\ \text{for every } v \in V(\Omega, S^n), \end{cases}$$

where V is the space defined as

$$V(\Omega, S^n) := \left\{ v \in H_0^1(\Omega) : v|_{S^n} \in H_0^1(S^n) \right\},$$

and $\int_{S^n} |\nabla_l u|^2 ds$ is defined piecewise on the prefractal curve S^n.

As mentioned in the introduction to this chapter Vacca restricted her studies to the special case of $\alpha = 3$. Wasyk used an automated mesh generator to create the mesh before then apply Grisvard refinements. Although the results presented below are not unique to this paper, the problems were solved using a refinement of the adaptive mesh. We show results for both multiple values of α and multiple values of the iteration number n. In these problems we set $f = 1$ which corresponds, physically to the problem of an elastic sheet reinforced along the fractal curve with a stronger thread.

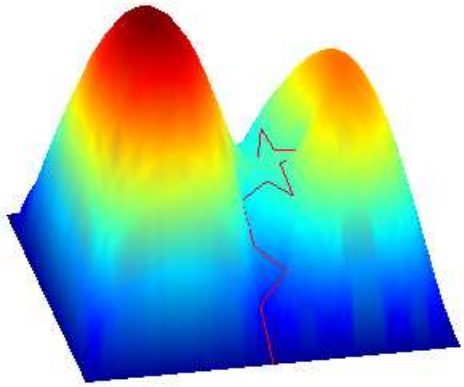

Figure 7.9: $n = 2, \qquad \alpha = 2.5.$

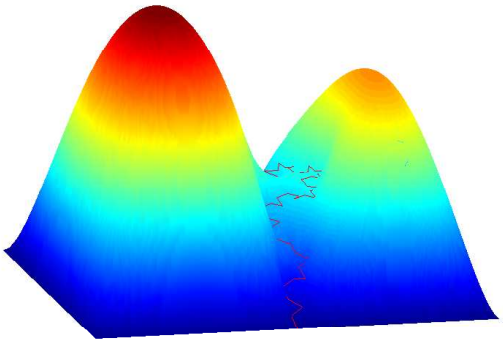

Figure 7.10: $n = 3, \qquad \alpha = 2.5.$

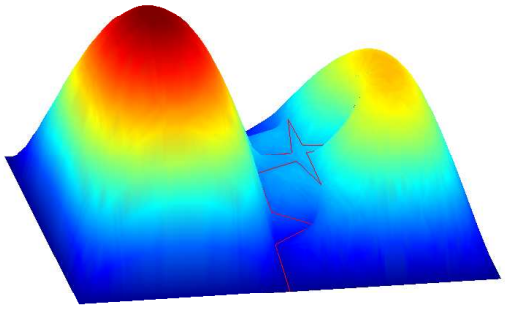

Figure 7.11: $n = 2, \qquad \alpha = 2.25.$

Appendix A

List of Notation

Fractal		
S	either the Koch curve or the Sierpinski gasket	6
α	the contraction factor	5
ψ_i	a contractive similitude	5
V_0	the vertices of the initial prefractal	6
V^n	the vertcies of the nth prefractal	6
V^∞	The closure of this set is the fractal S	6
S^n	the (polygonal prefractal curve of iteration n	6
μ	an invariant measure	6
d	the Hausdorf dimension of the fractal	7
ρ	the renormailization factor	8
d	the Hausdorf dimension of the fractal	7

Extension

Π	the linear extension operator from a fractal set S to a larger domain Ω	20
Π_n	the linear extension operator from a prefractal set V^n to a larger domain Ω	21
Ω	an open domain in $\mathbb{R}^2$ such that $S \subset \Omega$.	21
ω	a special polygonal domain used in the first step of function extension	23
β	the Hölder exponent	22
u_n	the restriction u to the prefractal vertices V^n	22
$\mathcal{A}_{T_{V^n}}(\Omega)$	the set of piecewise affine functions on T_{V^n}.	22
T_{V^n}	the traingulation of ω induced by the prefractal set V^n	23
T^n_{SC}	the sidecar triangles of the inducted triangulation T_{V^n}	24
T^n_{TR}	the transition triangles of the inducted triangulation T_{V^n}	24
T^n_{EX}	the external triangles of the inducted triangulation T_{V^n}	24

General

$\overline{A}$	closure of the set A	143
$A \subset\subset B$	A is compactly contained in B	144
$A \hookrightarrow B$	A compactly imbedded in B	144
$\|\cdot\|_X$	norm on X	144
supp$\{f\}$	support of f	143
$D^\alpha\phi$	$\frac{\partial^{\alpha_1}}{\partial x_1^{\alpha_1}} \cdots \frac{\partial^{\alpha_n}}{\partial x_1^{\alpha_n}}\phi$	144
$h_{\mathcal{T}}$	the length of the largest side of a triangle $\mathcal{T}$	149
$\rho_{\mathcal{T}}$	the diameter of the largest ball inscribed in $\mathcal{T}$	149
σ	the shape regularity constant which is equal to $h_{\mathcal{T}}/\rho_{\mathcal{T}}$	149
T_h	a conformal triangulation of a domain Ω	149
$F_{\mathcal{T}}$	the transformation function from $\mathcal{T}$ to $\hat{\mathcal{T}}$	150
$\Pi_{\mathcal{T}}$	the linear interpolation map	150
r	the distance to the singular point	149

Function spaces

$C^n(\Omega)$	n-times continuously differentiable functions on Ω	144
$C_0^n(\Omega)$	functions in $C^n(\Omega)$ with compact support	144
$L^p(\Omega)$	p-integrable functions on Ω	144
$L^p_{\text{loc}}(\Omega)$	$\{f \mid \|f\|_{L^p(K)} < \infty\}$ for every compact set $K \subset \Omega$	144
$W^{s,p}(\Omega)$	the Sobolev space	145
$W_0^{s,p}(\Omega)$	the closure of $C_0^\infty(\Omega)$ in $W^{k,p}(\Omega)$.	145
$W^{s,p}(\overline{\Omega})$	all distributions in Ω which are restrictions of elements of $W^{s,p}(\mathbb{R}^n)$	146
$\tilde{W}^{s,p}(\Omega)$	the space of all $u \in W^{s,p}(\Omega)$, where $\tilde{u} \in W^{s,p}(\mathbb{R}^n)$	146
$H^0(\Omega)$	$L^2(\Omega)$	146
$H^1(\Omega)$	Hilbert space equal to $W^{1,2}(\Omega)$	146
$H^2(\Omega)$	Hilbert space equal to $W^{2,2}(\Omega)$	146
$P_h^1(\Omega)$	the subspace that is piecewise linear on every triangle	150
$H^{2,\lambda}(\Omega)$	the weighted Sobolev Space	160
T	a Distribution	144
$\mathcal{D}'(\Omega)$	the space of all distributions	144
$\mathcal{D}(\Omega)$	the space of all C^∞ functions with compact support in Ω	144

Domains

Ω	a polygon in $\mathbb{R}^2$	149
$\hat{\mathcal{T}}$	the model triangle	149
$\mathcal{T}$	an arbitrary triangle in $\mathbb{R}^2$	149

Bibliography

[1] H. Attouch. *Variational convergence for functions and operators*. Applicable Mathematics Series. Pitman (Advanced Publishing Program), Boston, MA, 1984.

[2] Dietrich Braess. *Finite elements*. Cambridge University Press, Cambridge, second edition, 2001. Theory, fast solvers, and applications in solid mechanics, Translated from the 1992 German edition by Larry L. Schumaker.

[3] Susanne C. Brenner and L. Ridgway Scott. *The mathematical theory of finite element methods*, volume 15 of *Texts in Applied Mathematics*. Springer, New York, third edition, 2008.

[4] Yuri Brudnyi and Pavel Shvartsman. Generalizations of Whitney's extension theorem. *Internat. Math. Res. Notices*, (3):129 ff., approx. 11 pp. (electronic), 1994.

[5] Yuri Brudnyi and Pavel Shvartsman. The Whitney problem of existence of a linear extension operator. *J. Geom. Anal.*, 7(4):515–574, 1997.

[6] J. R. Cannon and G. H. Meyer. On diffusion in a fractured medium. *SIAM Journal on Applied Mathematics*, 20(3):434–448, 1971.

[7] Philippe G. Ciarlet. *The finite element method for elliptic problems*. North-Holland Publishing Co., Amsterdam, 1978. Studies in Mathematics and its Applications, Vol. 4.

[8] Emily Evans. A finite element approach to C^β extension using prefractals. Technical Report MS-3-1-47, WPI Mathematical Sciences Department, 2011.

[9] Emily Evans. Hölder extension of a function defined on a Sierpinski gasket. Technical Report MS-3-4-47, WPI Mathematical Sciences Department, 2011.

[10] Charles Fefferman. C^m extension by linear operators. *Ann. of Math. (2)*, 166(3):779–835, 2007.

[11] Charles Fefferman. Extension of $C^{m,\omega}$-smooth functions by linear operators. *Rev. Mat. Iberoam.*, 25(1):1–48, 2009.

[12] Charles Fefferman. Whitney's extension problems and interpolation of data. *Bull. Amer. Math. Soc. (N.S.)*, 46(2):207–220, 2009.

[13] Charles Fefferman and Bo'az Klartag. An example related to Whitney extension with almost minimal C^m norm. *Rev. Mat. Iberoam.*, 25(2):423–446, 2009.

[14] P. Grisvard. *Elliptic problems in nonsmooth domains*, volume 24 of *Monographs and Studies in Mathematics*. Pitman (Advanced Publishing Program), Boston, MA, 1985.

[15] Pham Huy Hung and Enrique Sánchez-Palencia. Phénomènes de transmission à travers des couches minces de conductivité élevée. *J. Math. Anal. Appl.*, 47:284–309, 1974.

[16] John E. Hutchinson. Fractals and self-similarity. *Indiana Univ. Math. J.*, 30(5):713–747, 1981.

[17] Alf Jonsson. Besov spaces on closed subsets of $\mathbf{R}^n$. *Trans. Amer. Math. Soc.*, 341(1):355–370, 1994.

[18] Alf Jonsson and Hans Wallin. Function spaces on subsets of $\mathbf{R}^n$. *Math. Rep.*, 2(1):xiv+221, 1984.

[19] Alf Jonsson and Hans Wallin. The dual of Besov spaces on fractals. *Studia Math.*, 112(3):285–300, 1995.

[20] Serguei M. Kozlov. Harmonization and homogenization on fractals. *Comm. Math. Phys.*, 153(2):339–357, 1993.

[21] M. R. Lancia and M. A. Vivaldi. Asymptotic convergence of transmission energy forms. *Adv. Math. Sci. Appl.*, 13(1):315–341, 2003.

[22] Maria Rosaria Lancia, Umberto Mosco, and Maria Agostina Vivaldi. Homogenization for conductive thin layers of pre-fractal type. *J. Math. Anal. Appl.*, 347(1):354–369, 2008.

[23] Elliott H. Lieb and Michael Loss. *Analysis*, volume 14 of *Graduate Studies in Mathematics*. American Mathematical Society, Providence, RI, second edition, 2001.

[24] Benoit B. Mandelbrot. *The fractal geometry of nature*. W. H. Freeman and Co., San Francisco, Calif., 1982. Schriftenreihe für den Referenten. [Series for the Referee].

[25] Umberto Mosco. Convergence of convex sets and of solutions of variational inequalities. *Advances in Math.*, 3:510–585, 1969.

[26] Umberto Mosco. Composite media and asymptotic Dirichlet forms. *J. Funct. Anal.*, 123(2):368–421, 1994.

[27] Umberto Mosco and Maria Agostina Vivaldi. An example of fractal singular homogenization. *Georgian Math. J.*, 14(1):169–193, 2007.

[28] Umberto Mosco and Maria Agostina Vivaldi. Fractal reinforcement of elastic membranes. *Arch. Ration. Mech. Anal.*, 194(1):49–74, 2009.

[29] Gilbert Strang and George J. Fix. *An analysis of the finite element method*. Prentice-Hall Inc., Englewood Cliffs, N. J., 1973. Prentice-Hall Series in Automatic Computation.

[30] Elisa Vacca. *Galerkin Approximation for Highly Conductive Layers.* PhD thesis, Universita degli Studi di Roma "LaSapienza", 2005.

[31] Rebecca D. Wasyk. *Numerical Solution of a Transmission Problem with a Prefractal Interface*. PhD thesis, Worcester Polytechnic Institute, 2007.

[32] Hassler Whitney. Analytic extensions of differentiable functions defined in closed sets. *Trans. Amer. Math. Soc.*, 36(1):63–89, 1934.

[33] Hassler Whitney. Differentiable functions defined in closed sets. I. *Trans. Amer. Math. Soc.*, 36(2):369–387, 1934.

[34] Hassler Whitney. Functions differentiable on the boundaries of regions. *Ann. of Math. (2)*, 35(3):482–485, 1934.